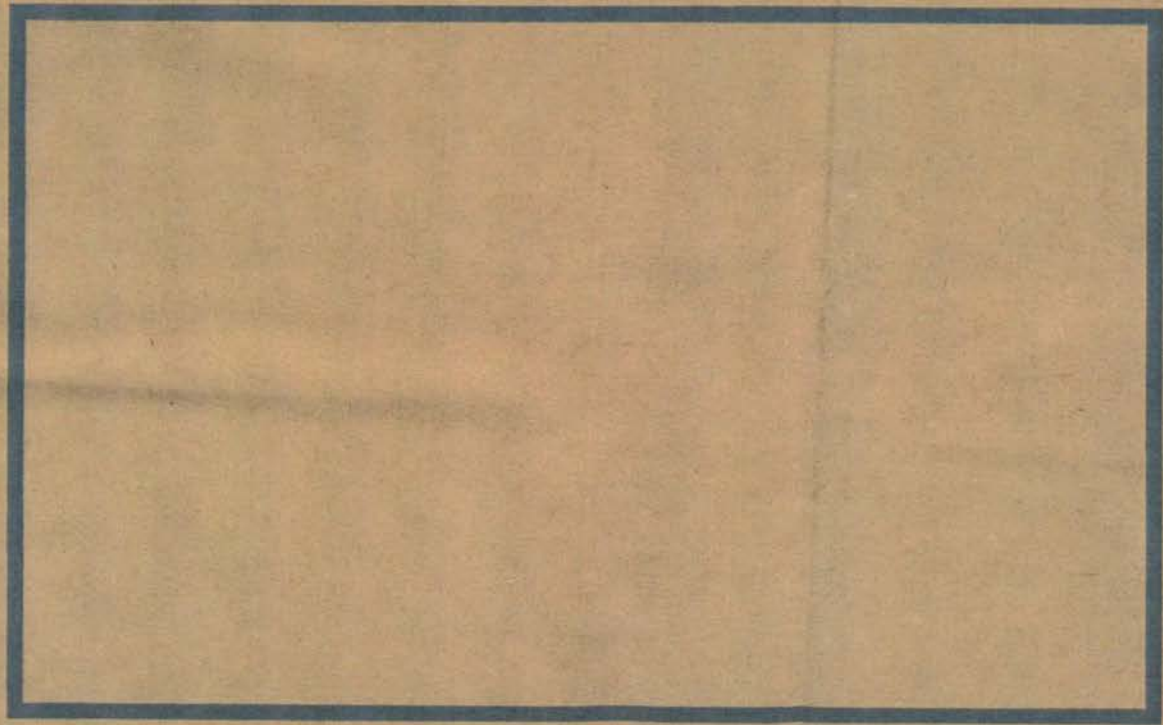
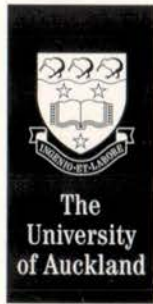


ENG 308-(EQC 1999/424)

Retrofit of seismically isolated buildings for near field ground motion using additional damping

Lyle Philip Carden, supervised by B J Davidson, T J Larkin, I G Buckle





Department of
Civil and
Resource
Engineering

**RETROFIT OF SEISMICALLY
ISOLATED BUILDINGS FOR NEAR
FIELD GROUND MOTION USING
ADDITIONAL DAMPING**

by

Lyle Philip Carden

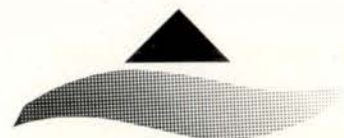
Dr. B. J. Davidson

Dr. T. J. Larkin

Prof. I. G. Buckle

School of Engineering
Report No. 602

March 2001



Civil and Resource Engineering

*Retrofit of Seismically Isolated Buildings for
Near Field Ground Motion Using Additional
Damping*

By

Lyle Philip Carden

Dr. B. J. Davidson

Dr. T. J. Larkin

Prof. I.G. Buckle

School of Engineering Report No. 602

Department of Civil and Resource Engineering

The University of Auckland

New Zealand.

March 2001

Abstract

Recently it has been observed that near field earthquakes containing forward directivity ground motion often causes a response in structures, particularly flexible structures, considerably larger than the design level response. As seismically isolated structures are designed with a flexible isolation layer, a number of these existing structures are now considered vulnerable to near field earthquakes. Such earthquakes are likely to cause the isolation systems of the seismically isolated buildings to exceed their maximum allowable displacements, resulting in failure at the bases or a large amount of damage in their superstructures.

In this thesis a number of generic seismically isolated buildings, designed using the requirements set out in the 1997 Uniform Building Code, have been retrofitted with additional damping. It was found that to control deformations at each level, in response to near field earthquakes, additional damping was required at the isolation layer and between at least the base and first floor of the superstructure. Additional viscous damping tended to be more effective than hysteretic and friction damping in limiting deformations, while maximising the reduction of forces in the superstructure.

Using concepts derived from analyses of the generic structures, a model of the seismically isolated William Clayton building located in Wellington was retrofitted. It was found that isolator deformations could be limited to maximum allowable levels in response to near field earthquakes using viscous dampers. Unlike the generic structures no additional damping was required in the superstructure to control inter-storey deformations, thus damping was only required at the isolation layer. The impact of additional damping in the William Clayton building, on the design level response and the accelerations at each floor, was found to be minimal.

Acknowledgements

The authors would like thank the primary sponsor, the New Zealand Earthquake Commission, for funding this project. They would also like to thank the School of Engineering and IPENZ for additional financial assistance.

This report is essentially the Master of Engineering thesis of the first author, and he would like to acknowledge the help and encouragement that he received from the other authors, his graduate student colleagues, his family and Abbey who spent many hours proof reading the initial drafts.

Table of Contents

ABSTRACT	I
ACKNOWLEDGEMENTS.....	III
TABLE OF CONTENTS.....	V
FIGURES AND TABLES.....	XI
NOMENCLATURE.....	XV
CHAPTER 1. INTRODUCTION.....	1
1.1 Seismic Isolation	1
1.1.1 Basic Concepts.....	1
1.1.2 Different Types of Isolation Systems.....	2
1.1.3 Seismically Isolated Structures in New Zealand.....	3
1.1.4 Past Design Criteria.....	4
1.2 Near Field Ground Motion	4
1.3 Effects of Near Field Ground Motion on Structures	6
1.4 Damping in Structures.....	7
1.5 Discussion of Past Attempts to Retrofit Seismically Isolated Structures for Near Field Ground Motion	10
1.5.1 Introduction.....	10
1.5.2 Substitution of the Seismic Isolation Mechanism with a New Mechanism.....	10
1.5.3 Modifications Requiring Removal or Replacement of Parts of the Existing Isolation System.....	11
1.5.4 Additional Passive Control Devices.....	12
1.5.5 Additional Active Control Devices.....	13
1.5.6 Summary	14
1.6 Thesis Objectives	14
1.7 Thesis Outline.....	15
CHAPTER 2. DESIGN OF GENERIC SEISMICALLY ISOLATED BUILDINGS	17
2.1 Design of Isolation Systems.....	17
2.1.1 Introduction.....	17

2.1.2	Linear Isolation Systems Designed to the 1997 Uniform Building Code	17
2.1.3	Design of Bilinear Isolation Systems	20
2.1.4	Maximum Displacement of the Isolation System.....	23
2.1.5	Response of Structures to the Near Field Hazard Spectrum	24
2.2	Design of Multi-Storey Superstructures for Seismically Isolated Buildings.....	26
2.2.1	Introduction	26
2.2.2	Calculation of Design Lateral Forces	27
2.2.3	Calculation of the Stiffness at each Level	28
2.2.3.1	<i>Introduction</i>	28
2.2.3.2	<i>Procedure for Calculating Storey Stiffness</i>	28
2.2.3.3	<i>Results</i>	31
2.2.4	Modal Damping.....	31
2.2.4.1	<i>Introduction</i>	31
2.2.4.2	<i>Procedure for Calculating Damping Constant</i>	31
2.2.4.3	<i>Results</i>	33
2.3	Summary.....	33

CHAPTER 3. RESPONSE OF RIGID SEISMICALLY ISOLATED BUILDINGS USING TIME HISTORY ANALYSES35

3.1	Introduction.....	35
3.2	SAP Model of the Seismically Isolated Buildings modelled with a Rigid Superstructure	35
3.3	Selection of Earthquake Records.....	36
3.3.1	Introduction	36
3.3.2	Design Level Earthquake Records	36
3.3.3	Near Field Earthquake Records.....	37
3.3.4	Comparisons between Design Level and Near Field Records	42
3.4	Scaling of the Earthquake Records.....	43
3.4.1	Scaling the Design and Near Field Earthquakes to Match the UBC Response.....	43
3.4.2	Scaling for Small Earthquakes	45
3.5	Time History Response of Unretrofitted Seismically Isolated Structures.....	45
3.6	Summary.....	46

CHAPTER 4. RETROFIT OF RIGID SEISMICALLY ISOLATED STRUCTURES49

4.1	Introduction.....	49
4.2	Initial Retrofit of Design 7.....	49

4.2.1	Introduction	49
4.2.2	Procedures for Addition of Damping	50
4.2.2.1	<i>Addition of Viscous Damping</i>	50
4.2.2.2	<i>Additional Friction Damping</i>	52
4.2.2.3	<i>An Additional Dual Level Hysteretic Buffer</i>	52
4.2.3	Average Results of Retrofit.....	53
4.2.4	Explanation of the Response for the Different Forms of Additional Damping	56
4.2.5	Variability Between Individual Earthquakes	57
4.2.6	Optimum Form of Additional Damping in the Structure.....	59
4.3	Mass Tuned Damping	60
4.3.1	Introduction	60
4.3.2	Application of Mass Tuned Damping to Seismically Isolated Structures.....	60
4.3.2.1	<i>Introduction</i>	60
4.3.2.2	<i>Calculation of Appropriate Masses</i>	61
4.3.2.3	<i>Calculation of Appropriate Spring Stiffness</i>	61
4.3.2.4	<i>Addition of Damping to Mass Tuned Damper</i>	62
4.3.3	Mass Tuned Damping Results	63
4.3.3.1	<i>Results of Mass Tuned Damping with Various Period Ratios</i>	63
4.3.3.2	<i>Results of Adding Damping to the Mass Tuned Damper</i>	65
4.3.4	Discussion of Mass Tuned Damping	66
4.4	Results of Retrofitting all of the Generic Seismically Isolated Structures with Additional Damping	68
4.4.1	Introduction	68
4.4.2	Retrofit Results	68
4.4.3	Optimum Solutions	69
4.4.3.1	<i>Optimum Near Field Response</i>	69
4.4.3.2	<i>Optimum Design Level Response</i>	74
4.4.3.3	<i>Discussion</i>	74
4.4.4	Comparison of Retrofits for Seismically Isolated Structures.....	75
4.4.4.1	<i>Introduction</i>	75
4.4.4.2	<i>Comparison of Structures with the Same Equivalent Linear Properties</i>	75
4.4.4.3	<i>Comparison of Structures with the Different Equivalent Linear Properties</i>	76
4.4.4.4	<i>Prediction of the Optimum Additional Damping Level for Retrofit of a Seismically Isolated Structure</i>	77
4.4.4.5	<i>Prediction of Other Responses</i>	79
4.5	Summary	80

CHAPTER 5. MODELLING OF MULTI-STOREY SEISMICALLY ISOLATED BUILDINGS.....	83
5.1 Introduction.....	83
5.2 SAP Models of Multi-storey Seismically Isolated Buildings.....	84
5.3 Earthquake Time Histories	85
5.4 Results from Analysis of Three Storey Seismically Isolated Buildings.....	85
5.4.1 Response of Unretrofitted Buildings at the Base	85
5.4.2 Comparisons with Rigid Seismically Isolated Structures.....	86
5.4.3 Displacements in the Superstructure	88
5.5 Results from Analysis of a Six Storey Seismically Isolated Building.....	88
5.6 System Identification for the Retrofit of the Superstructures	90
5.6.1 Proposed Retrofit for the Superstructure of each Seismically Isolated Building	90
5.6.2 Definition of Parameters and Variables	90
5.6.3 Development of a Quasi-Structural Model.....	91
5.6.4 Newton-Raphson Solution Procedure	93
5.7 Summary.....	95
CHAPTER 6. RETROFIT OF MULTI-STOREY SEISMICALLY ISOLATED BUILDINGS	97
6.1 Introduction.....	97
6.2 Response of the Three Storey Buildings Retrofitted at the Base.....	98
6.2.1 Deformations at Each Floor for Various Forms of Additional Damping.....	98
6.2.2 Acceleration Spectra at each Floor.....	99
6.3 Response of Fully Retrofitting the Three Storey Seismically Isolated Buildings	102
6.3.1 Introduction	102
6.3.2 Optimum Levels of Damping.....	103
6.3.3 Average Deformations at each Floor.....	104
6.3.4 Storey Shear Forces.....	104
6.3.5 Axial Forces due to Additional Damping.....	111
6.3.6 Variability between Individual Earthquake Responses	113
6.3.7 Acceleration Floor Spectra for Various Forms of Additional Damping	115
6.4 Response of the Six Storey Building Retrofitted at the Base	118
6.5 Retrofit of the Superstructure for the Six Storey Building	119
6.5.1 Optimum Levels of Damping.....	119
6.5.2 Average Deformations at each Floor.....	119
6.6 Comparison of Retrofits for the Multi-Storey Buildings.....	120
6.7 Effect of Retrofitting Multi-Storey Seismically Isolated Buildings on the Response to Small Earthquakes	121

6.7.1	Reduction in Acceleration Response	121
6.7.2	Acceleration Spectra at each Floor for Small Earthquakes	121
6.8	Summary of Results for Retrofitting of Multi-Storey Seismically Isolated Buildings	123
CHAPTER 7. RETROFIT OF THE WILLIAM CLAYTON BUILDING USING ADDITIONAL DAMPING.....		125
7.1	Introduction	125
7.2	Modelling of the William Clayton Building with a Rigid Superstructure	127
7.2.1	Description of the Rigid Model.....	127
7.2.2	Earthquakes Records and their Corresponding Scale Factors.....	128
7.2.3	Unretrofitted Response.....	131
7.2.4	Retrofit of William Clayton Building Modelled with a Rigid Superstructure	131
7.2.4.1	<i>Application of Additional Damping</i>	131
7.2.4.2	<i>Average Results of Retrofit</i>	132
7.2.5	Optimum Response and Comparisons with Generic Structures	132
7.3	Analysis and Retrofit of a Multi-Storey Model of the William Clayton Building.....	134
7.3.1	Overview	134
7.3.2	SAP Model.....	135
7.3.2.1	<i>Dimensions of the Structure</i>	135
7.3.2.2	<i>Modelling of Beams and Columns</i>	135
7.3.2.3	<i>Modelling of Isolation System</i>	137
7.3.2.4	<i>Seismic Weight</i>	137
7.3.2.5	<i>Damping</i>	137
7.3.3	Comparison of Drain 2DX and SAP	140
7.3.4	Response of Unretrofitted Building	143
7.3.5	Retrofit of the William Clayton Building	144
7.3.5.1	<i>Average Response at the Base</i>	144
7.3.5.2	<i>Average Displacement of the Superstructure with Optimal Retrofits</i>	145
7.3.5.3	<i>Variation in Response between Earthquakes</i>	147
7.3.5.4	<i>Individual Earthquake Response at the Base</i>	147
7.3.5.5	<i>Acceleration Floor Spectra</i>	150
7.3.6	Effect of Additional Damping in Response to Small Earthquakes	150
7.4	Optimal Retrofit for the William Clayton Building	153
7.5	Summary and Comparisons with the Generic Structures.....	155

CHAPTER 8. CONCLUSIONS	157
8.1 Design and Modelling of Seismically Isolated Buildings	157
8.2 Retrofit of the Generic Seismically Isolated Buildings for Near Field Earthquakes...	157
8.2.1 Identification of Suitable Passive Control Devices.....	157
8.2.2 Optimum Form of Additional Damping using Design Level Response	157
8.2.3 Optimum Form of Additional Damping using Near Field Response	158
8.2.4 Compromise Between Optimum Design Level and Near Field Responses	158
8.2.5 Effect of Additional Damping on Response to Small Earthquakes.....	159
8.3 Retrofit of William Clayton Building.....	159
8.4 Future Work.....	160
REFERENCES	161
APPENDICES	165
Appendix 1 Ground and Site Parameters for Design of Generic Seismically Isolated Structures.....	165
Appendix 2 Example for Design of a Bilinear Isolation System, Design 7, from an Effective Linear System.....	166
Appendix 3 Calculation of the Near Field Response for a Bilinear Isolation System, Design 7	167
Appendix 4 UBC Isolation System Properties in Response to the Near Field Spectrum.....	168
Appendix 5 Calculation of Column Stiffness for the Three Storey Superstructure.....	169
Appendix 6 Frequencies and Mode Shapes for Three and Six Storey Superstructures.....	170
Appendix 7 Calculation of Modal Damping in Three Storey Superstructure.....	171
Appendix 8 Modal Damping for Three and Six Storey Superstructures	172
Appendix 9 Effective Damping Check in SAP 2000 Models.....	173
Appendix 10 Example for Calculation of Optimum Levels of Damping using System Identification	175

Figures and Tables

Figure 1.1: Typical Design Acceleration and Displacement Spectra.....	2
Figure 1.2: Section of Lead Rubber Bearing.....	2
Figure 1.3: Diagram of Sliding Pendulum Bearing.....	3
Figure 1.4: Near Field Acceleration and Velocity Time Histories.....	5
Figure 1.5: 1940 El Centro NS Acceleration and Velocity Time Histories.....	6
Figure 1.6: Three Forms of Damping; (a) Viscous, (b) Hysteretic and (c) Coulomb.....	9
Figure 1.7: Lead Rubber Bearings with Sliding End Plates.....	11
Figure 1.8: Dual Level Hysteretic Isolation System.....	12
Figure 1.9: Schematic of Electrorheological Damper.....	14
Figure 2.1: Generic Seismically Isolated Structure Modelled with a Rigid Superstructure.....	17
Figure 2.2: UBC Design Acceleration Spectrum.....	18
Figure 2.3: Response of Generic Isolation Systems Designed to the UBC.....	20
Table 2.1: Bilinear Isolation System Properties.....	22
Figure 2.4: Bilinear Isolation Systems for Designs 7, 8 and 9.....	23
Figure 2.5: Design Level, Maximum Capable and Near Field UBC spectra.....	25
Table 2.2: Summary of Isolation System Responses to Various UBC Spectra.....	26
Figure 2.6: Generic Three Storey Seismically Isolated Building.....	27
Table 2.3: Design Storey Shear Forces for Three and Six Storey Superstructures.....	28
Figure 3.1: SAP Model of a Seismically Isolated Building Modelled with a Rigid Superstructure.....	36
Table 3.1: Design Level Earthquake Records.....	38
Table 3.2: Near Field Earthquake Records.....	38
Figure 3.2: Design Level Response Spectra.....	39
Figure 3.3: Near Field Response Spectra.....	39
Figure 3.4: Acceleration and Velocity Time Histories for the Design Level Earthquake Records.....	40
Figure 3.5: Acceleration and Velocity Time Histories for Northridge (Sim.), Rinaldi, Sylmar Hospital and Elysian Park.....	41
Figure 3.6: Acceleration and Velocity Time Histories for Lucerne and Imperial Valley.....	42
Table 3.3: Scale Factors for each Structure Calculated by Matching Structural Response.....	45
Table 3.4: Displacement Response of each Rigid Seismically Isolated Structures.....	47
Table 3.5: Base Shear Response of Rigid Seismically Isolated Structures.....	47

Figure 4.1: Seismically Isolated Building with Additional Viscous Damping at the Base.	50
Figure 4.2: Hysteresis Loops for Three Forms of Viscous Damping.....	51
Figure 4.3: Seismically Isolated Structure retrofitted with a Dual Level Hysteretic Buffer	53
Figure 4.4: Average Design and Near Field Response of Design 7 to a Different Forms of Retrofit .	54
Table 4.1: Response of Design 7 Retrofitted with Additional Damping.....	55
Figure 4.5: Design 7 Response of Individual Earthquakes Retrofitted using Viscous Damping, Velocity Exponent of 0.5.....	58
Figure 4.6: Design 7 Response of Individual Earthquakes Retrofitted with Friction Damping.	58
Figure 4.7: Seismically Isolated Building with a Rigid Superstructure Retrofitted with a Mass Tuned Damper.....	60
Figure 4.8: Normalised Near Field Displacement with Additional Mass Tuned Damping	64
Figure 4.9: Response of Design 7 Retrofitted with Mass Tuned Dampers of Different Masses	64
Figure 4.10: Time History Response of Mass Tuned Damper Additional Damping.....	65
Figure 4.11: Response of with Viscous Damping (a) and Friction Damping (b) in the Mass Tuned Damper.....	65
Figure 4.12: Displacement Response Time History for Sylmar Hospital (a) and Lucerne (b).....	67
Figure 4.13: Average Design and Near Field Response of $T = 1.5s$ Structure with Additional Damping	69
Figure 4.14: Average Design and Near Field Response of $T = 2.0s$ Structures with Additional Damping	70
Figure 4.15: Average Design and Near Field Response of $T = 2.5s$ Structures with Additional Damping	71
Figure 4.16: Average Design and Near Field Response of $T = 3.0s$ Structures with Additional Damping	72
Table 4.2: Optimum Retrofit of Seismically Isolated Structures in terms of Near Field Response.....	73
Table 4.3: Optimum Retrofit of All Seismically Isolated Structures in terms of Design Response	74
Figure 4.17: Optimum Level of Additional Viscous Damping for Isolated Structures at their Design Effective Period and Damping	78
Figure 4.18: Optimum Additional Viscous Damping Curves.....	79
Figure 5.1: SAP Model for Three Storey Seismically Isolated Building.....	84
Table 5.1: Maximum Displacements of Isolation Systems for the Three Storey Buildings	86
Table 5.2: Maximum Base Shear of Isolation Systems for the Three Storey Buildings	86
Figure 5.2: Average Unretrofitted Response of Three Storey Buildings.....	87
Table 5.3: Displacement Response of Isolation System for the Six Storey Building	89
Table 5.4: Base Shear Response of Isolation System for the Six Storey Building.....	89
Figure 5.3: Unretrofitted Response of the Six Storey Building	89

<i>Table 6.1: Optimum Levels of Damping at the Base from Rigid Superstructure Models</i>	98
<i>Figure 6.1: Base Retrofitted Response of Three Storey Seismically Isolated Structures</i>	100
<i>Figure 6.2: El Centro Acceleration Response Spectra at each Floor for Designs 3.1 and 3.7 Retrofitted at the Base</i>	101
<i>Table 6.2: Optimum Levels of Damping at each Floor for Three Storey Seismically Isolated Structures</i>	103
<i>Figure 6.3: Deformations of the Three Storey Seismically Isolated Structures after Retrofitting the Superstructure</i>	105
<i>Figure 6.4: Near Field Shear Forces in Three Storey Seismically Isolated Structures</i>	106
<i>Figure 6.5: Rinaldi Shear Force Time Histories for Design 3.7 with each Form of Damping</i>	108
<i>Figure 6.6: Sylmar Shear Force Time Histories for Design 3.7 with each Form of Damping</i>	109
<i>Figure 6.7: El Centro Shear Force Time Histories for Design 3.7 with each Form of Damping</i>	110
<i>Figure 6.8: Example of Three Storey Building with Additional Damping in the Superstructure.</i>	111
<i>Figure 6.9: Coefficient of Variation for Displacements of Three Storey Seismically Isolated Buildings</i>	114
<i>Figure 6.10: El Centro and Parkfield Acceleration Response Spectra at each Floor for Design 3.7</i>	116
<i>Figure 6.11: Bucharest and Joshua Tree Acceleration Response Spectra at each Floor for Design 3.7</i>	117
<i>Figure 6.12: Unretrofitted and Base Retrofitted Response of Six Storey Seismically Isolated Building</i>	118
<i>Table 6.3: Additional Damping for each Level of Six Storey Structure</i>	118
<i>Figure 6.13: Deformation of Six Storey Seismically Isolated Building</i>	119
<i>Table 6.4: Additional Damping Level at Base of Rigid and Three Storey Buildings</i>	120
<i>Figure 6.14: Acceleration Floor Spectra for the Small Earthquakes</i>	122
<i>Figure 7.1: William Clayton Building</i>	125
<i>Figure 7.2: Multi-Storey Model of the William Clayton Building</i>	126
<i>Figure 7.3: Design and Near Field Acceleration Spectra for the William Clayton Building</i>	129
<i>Table 7.1: Scale Factors for the William Clayton Building</i>	130
<i>Table 7.2: Displacement Response of William Clayton Modelled with a Rigid Superstructure</i>	131
<i>Table 7.3: Base Shear Response of William Clayton Modelled with a Rigid Superstructure</i>	131
<i>Figure 7.4: Average Design and Near Field Response of Isolation System Retrofitted with Three Forms of Damping</i>	133
<i>Table 7.4: Reduction in Average Response of Isolation System Using Optimal Damping Level Based on Maximum Displacement of 150 mm</i>	133

<i>Table 7.5: Reduction in Average Response of Isolation System Using Optimum Damping Level Based on a Maximum Displacement of 166 mm</i>	133
<i>Table 7.6: Beam and Column Properties</i>	136
<i>Table 7.7: Mass at each Floor</i>	137
<i>Figure 7.5: Mass and Stiffness Proportional Damping</i>	138
<i>Table 7.8: Modal Damping</i>	139
<i>Figure 7.6: Portal Frame used for Comparison of Drain 2DX and SAP</i>	140
<i>Figure 7.7: One Bay Portal Frame used to Verify SAP Model</i>	141
<i>Figure 7.8: El Centro Base Displacement Time History for William Clayton Building</i>	142
<i>Figure 7.9: El Centro Roof Displacement Time History for William Clayton Building</i>	142
<i>Table 7.9: Inter-storey Displacements for Unretrofitted William Clayton Building</i>	143
<i>Table 7.10: Reduction in Average Response of Isolation System Using Optimal Retrofit</i>	144
<i>Figure 7.10: Average Design and Near Field Response of Isolation System Retrofitted with Three Forms of Damping</i>	145
<i>Figure 7.11: Force Displacement Relationship for Pushover of William Clayton Building</i>	146
<i>Table 7.11: Results of Pushover Analysis for William Clayton Building</i>	146
<i>Figure 7.12: Average Displacement of Each Floor</i>	148
<i>Figure 7.13: Coefficients of Variation for Displacements of Each Floor</i>	148
<i>Figure 7.14: Individual Earthquake Response at the Base for Various Levels of Pure Viscous Damping</i>	149
<i>Figure 7.15: El Centro Floor Acceleration Spectra</i>	151
<i>Figure 7.16: Acceleration Spectra at the Base Level for Design Level Earthquakes</i>	152
<i>Figure 7.17: Small El Centro and Parkfield Accn. Floor Spectra Before and After Retrofit</i>	154

Nomenclature

Symbol Description

A	Amplitude of Vibration
A_k^i	Quadratic Constant for System Identification
B_D	Damping Coefficient
B_k^i	Quadratic Constant for System Identification
c_i	Generalised Simplified Damping
c_{MT}	Mass Tuned Damping Constant
[c]	Simplified Damping Matrix
C_{aD}	Design Seismic Coefficient
C^i	Quadratic Constant for System Identification
C_i	Generalised Damping
C_{vD}	Design Seismic Coefficient
[C]	Damping Matrix
D_i	Dynamic Amplification Factor for mode i
D_D	Design Displacement
E	Error in System Identification (Chapter 5)
E	Elastic Modulus (Chapter 7)
$f_i(x)$	Function to Minimise Error in System Identification for structural response parameter i
F_{MT}	Mass Tuned Damping Force
F_x	Force at a Floor x
$\underline{F}(x)$	Vector of Functions to Minimise Error in System Identification
g	Acceleration due to Gravity
h_x	Height of Floor x
I	Seismic Importance Factor (Chapter 2)
I	Moment of Inertia (Chapter 7)
[J](x)	Jacobian Matrix
k_D	Design Effective (secant) Stiffness
k_{eff}	Effective (secant) Stiffness

k_{dmin}	Minimum Effective (secant) Stiffness
k_{MT}	Stiffness of Mass Tuned Damper Spring
k_o	Initial Stiffness
k_θ	Rotational Stiffness
[k]	Simplified Stiffness Matrix
K_i	Generalised Stiffness
K_s	Stiffness Constant
[K]	Stiffness Matrix
l	Effective Length
L_i	As Defined in Appendix 9
m_{MT}	Mass of Mass Tuned Damper
M_i	Generalised Mass
M_n	Mass of nth Floor
[M]	Mass Matrix
N_a	Near Source Factor
N_v	Near Source Factor
P_i	Structural Response Parameter i
PM_i	Optimum Structural Response Parameter i
PQ_i	Quasi-Structural Response Parameter i
R_l	Lateral Force Resisting System Coefficient
R_A	Ratio of Hysteretic Area to Plastic Area
S_{aD}	Design Spectral Acceleration
S_{aNF}	Near Field Spectral Acceleration
T_D	Design Effective Period
\underline{u}	Vector of Displacements of each Floor
V_s	Design Base Shear above the Isolation System
w_x	Weight of Floor x
W	Total Seismic Weight of Structure
x_k	Significant Structural Parameters
Y	Vector of Modal Amplitudes at each Floor
Z	Seismic Zone Factor

α	Post Yield Stiffness Ratio (Chapter 2)
α	Mass Proportional Damping Constant (Chapter 7)
β	Stiffness Proportional Damping Constant
ϕ	Modeshape for Mode i
$[\phi]$	Matrix of Modeshapes
γ	Velocity Exponent
μ	Displacement Ductility (Chapter 2)
μ	Friction Coefficient (Chapter 4)
μ_{MT}	Friction Coefficient for Mass Tuned Damper
ω_i	Natural Frequency of Mode i
$\bar{\omega}$	Forced Natural Frequency
θ	Phase Angle
ξ_i	Fraction of Critical Viscous Damping for Mode i
ξ_{MT}	Fraction of Critical Viscous Damping for Mass Tuned Damper

Chapter 1.

Introduction

1.1 Seismic Isolation

1.1.1 Basic Concepts

Seismic isolation has been developed as a way of mitigating the effects of earthquakes on structures. The basic principle of seismic isolation is to decouple the superstructure from the ground using a flexible layer at the base of the structure. Consequently, the system is commonly referred to as “base isolation”. By providing a flexible base the dominant natural frequency of a seismically isolated structure tends to be outside the frequency range in which a large proportion of the earthquake energy is concentrated.

Typically a structure with a fixed base natural period of about half a second might be seismically isolated thereby increasing its natural period to approximately two seconds for example. Therefore the accelerations in the structure are reduced, as illustrated by the typical design acceleration response spectrum taken from the 1997 Uniform Building Code (UBC)¹² in Figure 1.1a. However, increasing the natural period of a building also increases the displacement response, as shown by the displacement spectrum in Figure 1.1b. Thus isolation systems tend to be designed with high levels of damping to prevent extremely large displacement responses and help further minimise the acceleration response. Figures 1.1a and 1.1b also illustrate the influence of increasing the damping in a structure, by comparing the response spectra for 5% and 20% damping, coupled with the effect of increasing the natural period from 0.5 to 2.0 seconds.

The most common methods for protection of structures from seismic actions are ductile moment resisting frames and shear walls. As accelerations and forces have been reduced by seismic isolation, this form of design can prevent structural damage during an earthquake. In contrast, ductile frames and shear walls are generally designed to prevent collapse but sustain some damage. Therefore, it is the intention that seismic isolation not only prevents loss of life

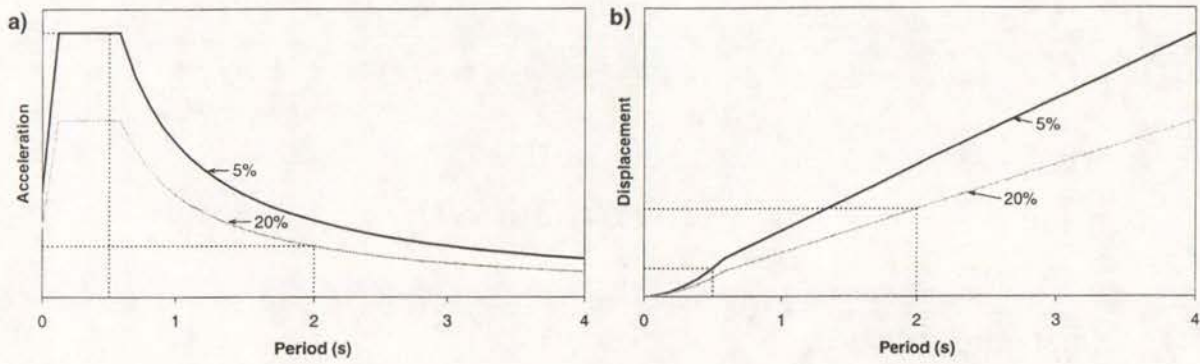


Figure 1.1: Typical Design Acceleration and Displacement Spectra¹².

but also reduces the cost of earthquake damage. Seismically isolated structures are generally designed to maintain functional capacity after an earthquake. This is important for buildings such as civil defence headquarters and hospitals, and structures such as motorway viaducts which provide essential access to highly populated areas.

1.1.2 Different Types of Isolation Systems

The most common type of isolation system used in buildings is “lead rubber bearings”(LRBs) described by Skinner et al.²⁶. The flexibility of lead rubbers bearings is provided by a laminated rubber bearing which deforms in shear, while damping is supplied by a lead plug at the centre of the bearing, as illustrated in Figure 1.2. Another increasingly common system is the use of sliding pendulum bearings³⁴, as illustrated in Figure 1.3. These consist of a curved bearing able to slide across a bowl with equal curvature. The friction resistance provides damping in the system. Roller bearings are similar to sliding friction bearings, the difference being that rollers have little inherent damping, therefore damping must be provided by additional devices.

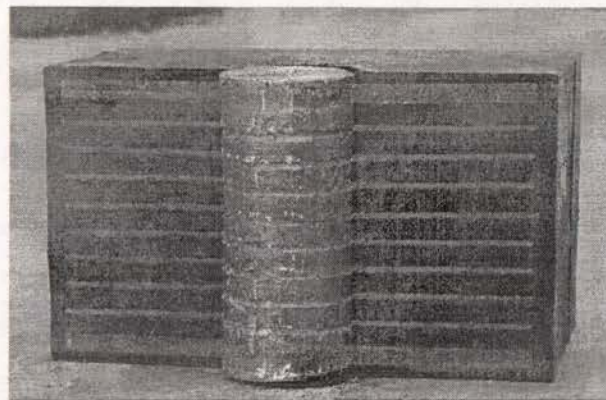


Figure 1.2: Section of Lead Rubber Bearing

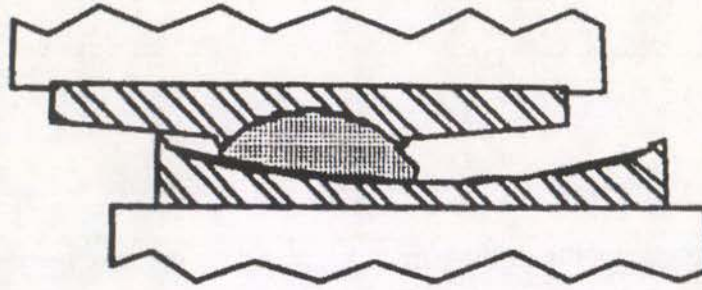


Figure 1.3: Diagram of Sliding Pendulum Bearing

The aforementioned systems are able to deform in shear but have limited capacity for axial tensile loads, thus are unable to prevent overturning in a building. Flexible piles, which consist of piles pinned at the top and bottom and able to move laterally within an oversized sleeve, are more appropriate for taller buildings as they can carry axial forces and thus prevent overturning moments in these buildings. Damping for this type of isolation system is supplied using additional damping devices. Rocking mechanisms have also been used for taller structures, where the columns rock on their foundations preventing damage to the structure. Supplementary devices again provide damping to the system²⁶. A brief review and references to other types of isolation systems is presented by Buckle³. Although there are many other forms of isolation systems and damping mechanisms, they adopt the same principles as those described in Section 1.1.1.

1.1.3 Seismically Isolated Structures in New Zealand

In 1999 there were ten seismically isolated buildings in New Zealand, which are listed by van de Vorstenbosch et al.³³. Six of these were isolated at the time of construction while the other four have been retrofitted with seismic isolation. Four of the ten buildings have been isolated exclusively with LRBs including the first seismically isolated building in New Zealand, the William Clayton Building, built in 1981. The other buildings are; the INL Press Hall built in 1990, Hutt Hospital emergency ward and operating theatres built in 1996, and the Wellington Maritime Museum retrofitted in 1999. Four other buildings have been isolated with LRBs and friction sliding systems. These are: New Zealand Parliament House and the General Assembly Library both retrofitted in 1994; the Museum of New Zealand – Te Papa Tongarewa built in 1997 and the Old Bank of New Zealand building retrofitted in 1999. Union House, built in 1984, and the Wellington Central Police Station, built in 1991, are both

isolated with flexible piles²⁶. Union House is damped with ductile steel plates while the Wellington Police Station is damped with lead extrusion damping devices.

1.1.4 Past Design Criteria

The early seismically isolated buildings in New Zealand were designed using conventional earthquake spectra. These structures were often designed conservatively due to uncertainty in the performance of seismically isolated structures. As the effects of near field ground motion became apparent, as described in following sections, isolation systems were designed with enough capacity to counter these effects. This is indicated by an increase in the displacement capacity of isolation systems over time³³. However there is concern over the performance of some existing structures that have an isolation system displacement capacity which is likely to be exceeded in a near field event.

1.2 Near Field Ground Motion

Near field ground motion, as the term suggests, describes the ground motion at a site close to the active fault during an earthquake. Some of the characteristics of near field ground motion have been known for some time. Bertero² discussed some of the features and design implications of near field earthquakes by analysing records from the 1971 San Fernando earthquake. In this work it was realised that a large magnitude, long duration pulse was responsible for much of the structural damage which occurred, including damage to the newly constructed Olive View Medical Centre. This pulse was also observed in the Pacoima Dam records. Damage to structures modelled using near field ground motions derived from this earthquake correlated closely to the observed damage. The damage caused by the San Fernando earthquake initiated advancement in the development of seismic design provisions for building codes in the United States but did not appear to initiate specific attention to near field ground motion in these design provisions.

The 1994 Northridge and 1995 Kobe earthquakes renewed studies into near field effects as they gave rise to extensive damage linked to near field ground motion. The damage from these two earthquakes is described in a number of sources^{7, 9, 10, 21}. As a result of Northridge in particular, the Structural Engineers Association of California recommended the inclusion of a near field factor in the 1997 version of the UBC to allow for near field ground motion^{12, 21}.

At a site close to the active fault during an earthquake, the close proximity to the source of the earthquake, results in the ground motion being at its largest. However the near field ground motion can also be amplified by what is described by Somerville²⁸ as two main effects:

1. Hanging wall effects.
2. Rupture directivity effects.

The hanging wall effects relate to sites on the hanging wall of a dipping fault which have a closer proximity to the fault as a whole than the sites on the foot wall of the fault²⁸. These sites experience large magnitude, short period ground motions, however they are not of particular concern in relation to seismically isolated structures due their long natural periods. Rupture directivity effects, particularly forward directivity effects, are more important in relation to seismic isolation. These effects tend to amplify the response of structures with a relatively long natural period. Forward directivity effects are caused by propagation of the fault rupture towards a site and often result in a large magnitude, long period pulse²⁷. Forward directivity near field ground motion is exemplified by the ground acceleration and velocity time histories for the Rinaldi site during the 1994 Northridge earthquake, as shown in Figure 1.4. The time histories exhibit a low frequency pulse between 2.0 and 3.0 seconds and feature a large magnitude acceleration of approximately 0.9g, and a particularly large magnitude velocity pulse of 1.8 m/s. This can be compared to the 1940 El Centro NS response in Figure 1.5, which exhibits no such pulse in either the acceleration or velocity histories, and lower magnitude ground motion.

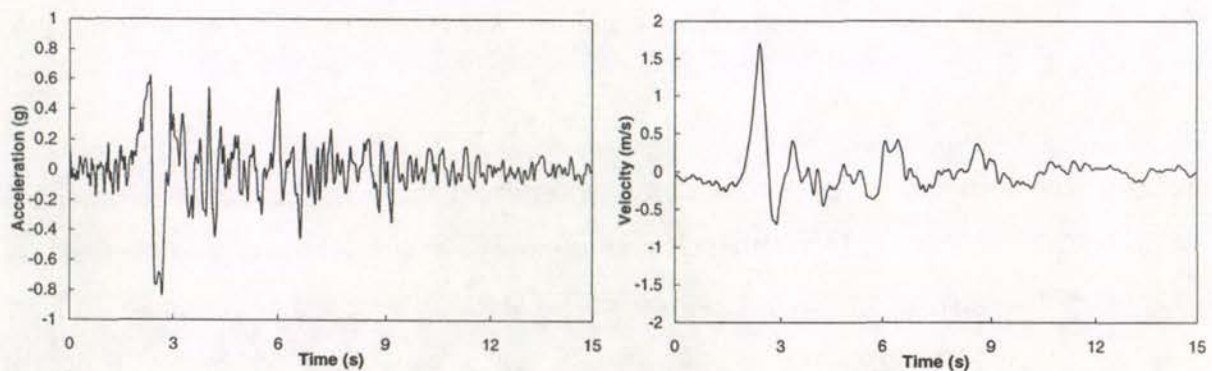


Figure 1.4: Near Field Acceleration and Velocity Time Histories

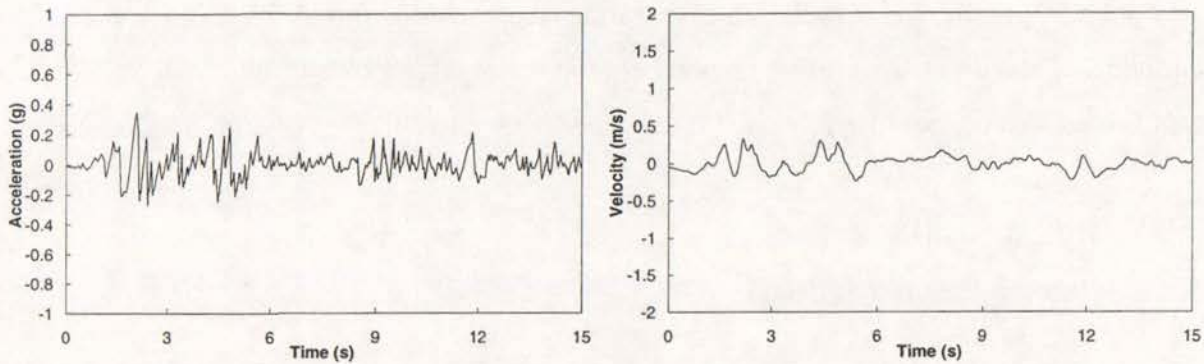


Figure 1.5: 1940 El Centro NS Acceleration and Velocity Time Histories

Forward directivity effects can occur in both dip-slip and strike-slip faulting mechanisms. They can be observed at sites within 50 kilometres of a fault. Their influence tends to be dependent on the distance to the fault, therefore the largest effects are observed within a few kilometres²⁸ of the fault. The largest forward directivity effects are prevalent at the surface projection of the fault and in a direction normal to the fault plane. Backward directivity, where the rupture propagates away from a site, is generally of little consequence to structures as it contains relatively low amplitude ground motion. Therefore, future reference to near field ground motion in this thesis implies forward directivity effects, unless expressly stated otherwise.

1.3 Effects of Near Field Ground Motion on Structures

As already mentioned, near field ground motion can contain a large amount of energy in a low frequency pulse. Potentially, this makes long period structures such as seismically isolated structures vulnerable. Until recently, large magnitude near field earthquakes have been overlooked in the design of many structures which are now known to be located in a near field region.

In recent years a number of studies have been performed using near field ground motion. In one such study by Hall et al.¹⁰, a ground motion model was used to illustrate the effects of near field earthquakes on a fixed base, twenty storey steel building and a seismically isolated building. By numerically modelling the twenty storey building, it showed evidence of connection failure, which prompted a later study⁹ in which the fracture of steel frame connections was modelled in buildings subject to near field ground motion. It was shown that structures designed to conventional Japanese and United States building codes were

vulnerable to the large displacements induced by long period ground motion, thus highlighting the need to investigate the effects on other flexible structures. A numerical model of a seismically isolated building was investigated with different limiting isolator displacements, and different levels of equivalent viscous damping¹⁰. The maximum allowable displacement was frequently exceeded by the isolation system due to near field earthquakes. As a result the isolation system and superstructure would have suffered considerable damage during an earthquake.

The William Clayton building in Wellington was analysed by Davidson et al⁷ to assess the impacts of near field ground motion using the Pacoima Dam record from the 1976 San Fernando earthquake and the Sylmar County Hospital record from the 1994 Northridge earthquake. It was found that the maximum isolator displacements were reached, causing the structure to pound on the adjacent retaining walls.

Based on previous work as mentioned above, retrofit procedures need to be developed to limit the isolation system displacements of some existing seismically isolated buildings. However, since near field events are less likely to occur than "design level" earthquakes, retrofits should not compromise the response of the buildings to a design level event.

1.4 Damping in Structures

There are a number of sources of energy dissipation in a structure that are apparent during an earthquake. For example material deformation such as cracking in concrete or yielding of steel or vibration of non structural items, such as furniture and partitions in a building, all provide energy dissipation. The many sources of energy dissipation are often grouped together and referred to as damping.

As damping in buildings is difficult to accurately predict or measure, it is often modelled as a nominal level of equivalent viscous damping to encompass all the various forms of energy dissipation. Fixed base structures tend to have damping distributed throughout the structure providing a relatively low level of energy dissipation. It is considered reasonable to model the damping in these structures as nominal equivalent viscous damping. In contrast, seismically isolated buildings have relatively high levels of damping that tend to be concentrated at the base to limit displacements of the isolation system. Kelly¹⁴ discusses how

the effect of large levels of damping influence the response of buildings by increasing the participation of modes other than the first mode. These higher modes tend to be more damaging to seismically isolated buildings. Therefore accurate modelling of a seismically isolated building requires modelling of the appropriate form, level and location of damping to accurately predict its response.

The main forms of damping used in the isolation systems of seismically isolated structures can be categorised into three groups:

1. Viscous damping.
2. Bilinear hysteretic damping.
3. Plastic hysteretic (Coulomb) damping.

Each form of damping is discussed because it is shown in the following sections that additional damping provides a potential means of retrofitting seismically isolated buildings for near field ground motion. Viscous damping is a velocity or frequency dependent form of damping⁵. The damping force in a viscous damper at any point in time is dependent on the velocity of the motion. As the amount of energy dissipated in any system is dependent on the area described by the force displacement relationship of the system, then the amount of energy dissipated in viscously damped system is dependent on the velocity of the system. The most common mechanism for providing viscous damping is in the form of a hydraulic damper, which absorbs energy by forcing a fluid through a small orifice. For harmonic oscillations of such a system the maximum velocity occurs when the displacement is zero. Thus the maximum viscous damping force occurs when the deformations in the system are zero. The hysteresis loop for a viscous damper is illustrated Figure 1.6a.

The amount of hysteretic damping, like viscous damping, is dependent on the area of the hysteresis loop described by the force displacement relationship of a system. Damping is provided by the inelastic stiffness properties of a system which describe the hysteretic area, as exemplified by Figure 1.6b. The level of energy dissipation in a hysteretic system is independent of velocity and frequency, but dependent on the stiffness properties in the system. Test results show that hysteretic energy dissipation is a more realistic way of modelling damping than equivalent viscous damping for many structural systems. This is true

for reinforced concrete structures and isolation systems with non-linear stiffness properties, as the damping in these systems has been found to be frequency independent⁵.

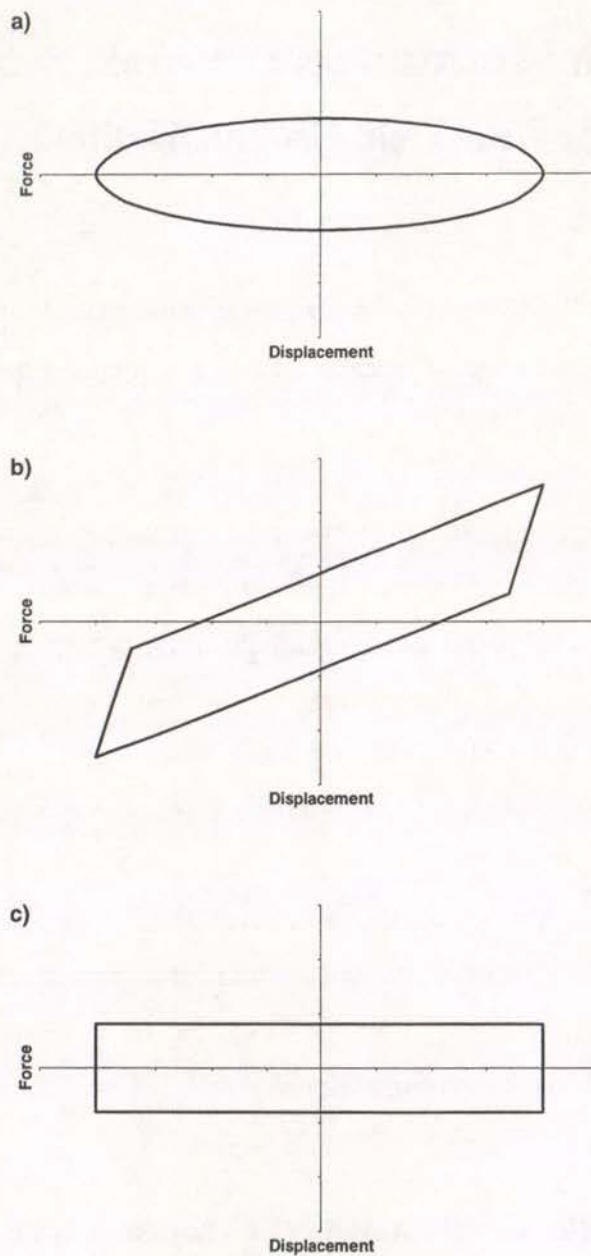


Figure 1.6: Three Forms of Damping; (a) Viscous, (b) Hysteretic and (c) Coulomb

Coulomb damping, illustrated typically in Figure 1.6c, is a special form of hysteretic damping where the force displacement relationship is approximately rectangular. Coulomb damping is normally associated with the friction energy dissipated by friction produced during the sliding of two surfaces across each other. However, dampers such as “Lead Extrusion Dampers”²³ also exhibit Coulomb damping by extruding a lead cylinder through an orifice of smaller diameter. It can provide excellent energy dissipation, as the area is large relative to the areas

of viscous and hysteretic systems with the same maximum force and displacement. However, this form of damping often results in permanent deformations in the system.

1.5 Discussion of Past Attempts to Retrofit Seismically Isolated Structures for Near Field Ground Motion

1.5.1 Introduction

As near field earthquakes are likely to cause the isolation system of many existing seismically isolated buildings to fail, a number of possible retrofit options have been proposed in the past to prevent failure. These include:

1. Substituting the existing isolation system with completely a new system.
2. Relative minor changes to the isolation system which require removing and replacement of certain parts of the existing isolation system.
3. Adding passive control devices such as various forms of additional damping devices to modify the properties of the existing isolation system.
4. Adding an active control device to the existing isolation system.

Each of these potential retrofits are discussed in terms of their ability to reduce the near field displacement response of isolation systems, while limiting the forces in structures to acceptable levels. The effect of any proposed modification on the design level response of seismically isolated structures is also considered.

1.5.2 Substitution of the Seismic Isolation Mechanism with a New Mechanism

It may be possible to replace the existing isolation system with a completely new system that has been found to be effective for mitigating the effects of near field earthquakes. However because such a replacement is likely to be difficult and expensive, an alternative which requires modification only to the existing isolation system is preferred.

1.5.3 Modifications Requiring Removal or Replacement of Parts of the Existing Isolation System

A number of possible ways of modifying the isolation system of seismically isolated buildings have been suggested by Skinner and McVerry²⁵. One proposed modification was to replace existing lead rubber bearings with oversized rubber bearings or segmented bearings²⁵. Although this would require changing each bearing, the new bearings would be similar in size and properties, thus the foundations and fittings of the building would require little modification. Oversized rubber bearings or segmented bearings are capable of withstanding large displacements while maintaining similar isolation system properties as the existing lead rubber bearings. However, replacing existing bearings with bearings of larger displacement capacity is only possible if the isolation system displacement is not limited by an adjacent structure such as a moat, wall or another building. Such constraints are likely to be found in the majority of seismically isolated buildings. Therefore it was considered unlikely that oversized or segmented bearings could be used to retrofit these buildings.

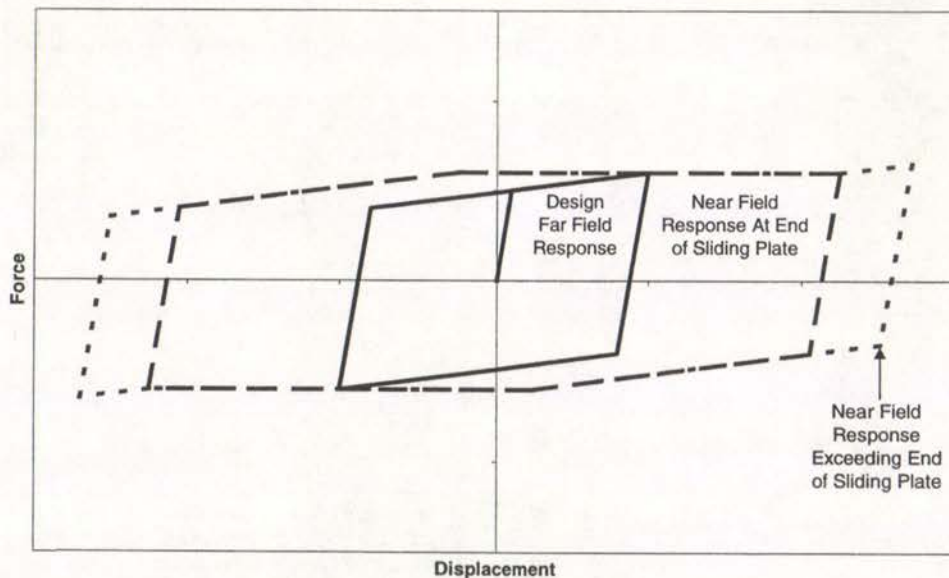


Figure 1.7: Lead Rubber Bearings with Sliding End Plates

Another proposed mechanism²⁵ is modifying an existing lead rubber bearing isolation system with sliding end plates placed in series with the components of the existing isolation system. This is a dual action system where a sliding plate is activated when the force in each lead rubber bearing reaches its limiting design value. A typical hysteresis loop for this system is given in Figure 1.7. Again however, it requires the capacity for large isolation system

displacements to be reached, which is generally not possible due to adjacent constraints. This was therefore considered an unlikely form of retrofit.

1.5.4 Additional Passive Control Devices

A number of passive control devices have been proposed to provide additional damping to a seismically isolated structure in order to control its near field response. A study performed by Makris and Chang¹⁶ considered a mathematical model of a seismically isolated structure with a rigid superstructure, that was subjected to a cyclical pulse representative of near field ground motion. It was concluded that a combination of viscous damping and a small level of friction damping was the most effective form of retrofit in terms of reducing displacements with a minimal increase in base shear.

A combination of additional hysteretic and viscous damping was used in an analysis of the William Clayton building to help control displacements while keeping inter-storey shears to a minimum⁷. Another investigation of the William Clayton building³⁵ found that hysteretic lead extrusion dampers were effective in reducing the displacements and minimising damage from a near field event. As explained in Section 1.4, the different forms of damping have quite different properties. Thus, a comparison of the various forms of damping is required to determine which form is the most effective when applied to the retrofit of seismically isolated buildings.

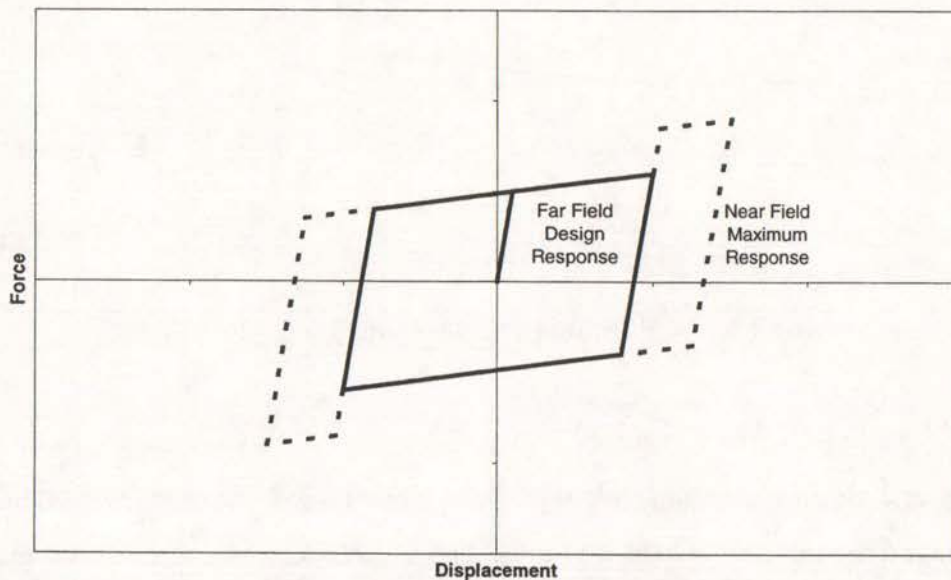


Figure 1.8: Dual Level Hysteretic Isolation System

Another additional passive control device, proposed by Skinner and McVerry²⁵, is a hysteretic buffer. This buffer creates a dual level hysteretic system, where a second level of hysteretic action is induced for displacements larger than the design displacement, as illustrated in Figure 1.8. The first level of hysteretic action is provided by the existing isolation system, which is assumed to be hysteretic. Placing a buffer adjacent to the existing isolation system could provide the second hysteretic level. This system remains effective for the design level response, as its properties remain unchanged. However the near field displacements of the isolation system are likely to be reduced at the expense of large forces in the superstructure.

One system used in the past to control vibrations in structures for various applications is mass tuned damping³². This is a system where a relatively small mass is attached to a structure using a spring and damper system. It has had little application to seismic design in the past, as mass tuned damping has only been found to be effective for reducing vibrations once a steady state response has been initiated and has little effect on reducing the transient response. It is hypothesised that it may be effective for mitigating the effects of near field ground motion as the response of a mass tuned damper could be initiated by earthquake motion prior to the occurrence of the near field pulse. If the damping provided prior to the occurrence of the pulse was sufficient, the effects of the near field pulse in a structure could be limited. The advantage of this system is that it could be applied to a structure at one point without it having to be attached to the ground or to another floor. Conceivably it could be placed within the ceiling of a given level of a building to reduce the response at that level.

1.5.5 Additional Active Control Devices

A number of active and semi-active control systems have been proposed for use in near field regions^{15, 29}. The advantage of these systems is their ability to change their properties depending on earthquake demands. One such system proposed, as an example, was electrorheological dampers¹⁵, which exploit the use of friction damping for large magnitude forces, then revert to viscous damping at lower forces to prevent permanent displacements. A schematic is shown in Figure 1.9.

Electrorheological dampers are semi-active, relying on a power supply to work effectively. The difficulty is maintaining a reliable power supply, in a situation where the dampers are left untouched for long periods of time, or in the disruptive event of an earthquake when the

external power supply can be disrupted. For this reason, passive control systems tend to be preferred over active systems, until proven reliable active control systems with superior performance are produced.

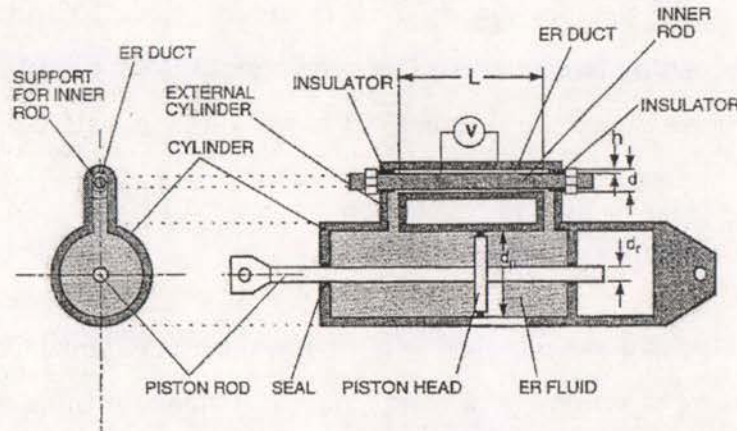


Figure 1.9: Schematic of Electrorheological Damper¹⁵.

1.5.6 Summary

Additional passive control devices appear to provide the most effective means of retrofitting existing seismically isolated buildings. They are considered relatively easy to add to an existing isolation system compared to complete replacement or replacement of parts of the existing system. For example, additional viscous damping could be provided by “Taylor Devices”³¹, which are large fluid dampers designed for seismic applications. Additional Coulomb damping could be provided by “Lead Extrusion Dampers”²³ or friction devices²². Many devices, such as inelastic steel devices for example, could provide other forms of hysteretic damping. Hysteretic damping is the form of damping most commonly provided by existing isolation systems. The background for these passive control devices is well proven compared to less robust active control systems.

1.6 Thesis Objectives

It is proposed that existing seismically isolated buildings that are vulnerable to near field earthquakes can be retrofitted using additional passive control devices. Therefore the objectives of this thesis are:

1. To design and model a range of generic seismically isolated buildings which represent typical seismically isolated buildings that are vulnerable to near field earthquakes.
2. To select near field earthquake records which are appropriate for modelling the effects of near field earthquakes on the generic buildings.
3. To identify additional passive control systems for the generic seismically isolated buildings which limit the near field displacement response of the isolation systems to maximum allowable levels.
4. To optimise possible proposed retrofits in order to minimise the impact of these retrofits on the design level response of each structure.
5. To optimise possible proposed retrofits in order to also minimise the damage in response to the near field earthquakes.
6. To calculate the impact of proposed retrofits on the response to small earthquakes.
7. To apply concepts developed using the generic structures to find an optimum retrofit for the William Clayton building in Wellington.

1.7 Thesis Outline

The design of various generic seismically isolated buildings is presented in Chapter 2. These designs are typical of buildings that have been designed in the past without consideration of the possible effects of near field earthquakes. Each building is assumed to have bilinear isolation system properties with the range of properties encompassing those typically found in seismically isolated structures. The design procedure was based on UBC¹² requirements using a UBC design spectrum to calculate appropriate design responses. The near field response of each building was then calculated using a UBC near field spectrum.

Models of each building were created in SAP 2000⁶. The objective was to calculate the effect of various retrofits on the response of the buildings to real design level and near field earthquakes. To this end a number of appropriate earthquake records were selected, as discussed in Chapter 3. Each record was scaled so that the unretrofitted design and near field response of each building matched the responses calculated using the UBC. In Chapter 4 possible retrofits for each generic building modelled with a rigid superstructure, were developed using different forms of additional passive control devices. These included:

1. Several forms of viscous damping.

2. Friction damping.
3. A dual level hysteretic buffer.
4. Mass tuned damping coupled with viscous and friction damping.

In Chapter 5 the design and near field response was calculated for models of generic multi-storey seismically isolated buildings. The concepts for retrofitting developed in Chapter 4 were applied in Chapter 6 to the multi-storey models. In this chapter the structural response is investigated in terms of deformations and forces in each storey and the effect of possible retrofitting is also investigated in terms of accelerations at each level. In addition an optimum retrofit was used to investigate the response to small earthquakes that did not cause the isolation system of a building to yield.

Concepts developed for retrofitting seismically isolated buildings using the generic structures were applied to a model of the William Clayton Building. An optimal retrofit is proposed for this building in Chapter 7. Conclusions are presented in Chapter 8.

Chapter 2.

Design of Generic Seismically Isolated Buildings

2.1 Design of Isolation Systems

2.1.1 Introduction

The first objective was to design a range of seismically isolated structures, which represent typical seismically isolated buildings found in regions where near field ground motion can be expected. The 1997 Uniform Building Code (UBC)¹² was used to design a number of such buildings. Using this code, isolation systems were designed almost independently of the superstructures. Consequently, the superstructure of each building was initially considered to be a rigid block above the isolation system as shown in Figure 2.1. Once design of the isolation systems was completed, multi-storey superstructures were designed using resulting base shears.

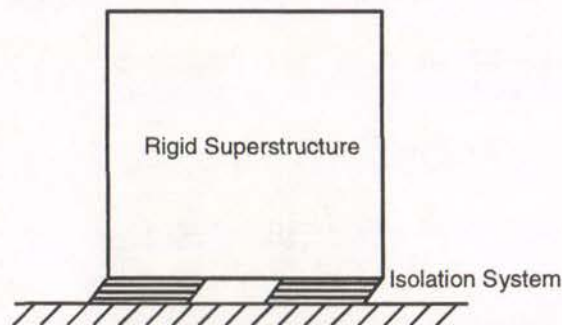


Figure 2.1: Generic Seismically Isolated Structure Modelled with a Rigid Superstructure

2.1.2 Linear Isolation Systems Designed to the 1997 Uniform Building Code

All structures were designed assuming that they were located in the highest seismic region given in the UBC. However they were initially assumed to be located outside a near field region. At a later stage it was assumed that they were found to be located in a near field

regime and appropriate retrofit options were explored. The ground and site parameters for the UBC design level event are given in Appendix 1. These parameters were used to describe the design hazard spectrum, as shown in Figure 2.2, which has a ten percent probability of exceedence in 50 years.

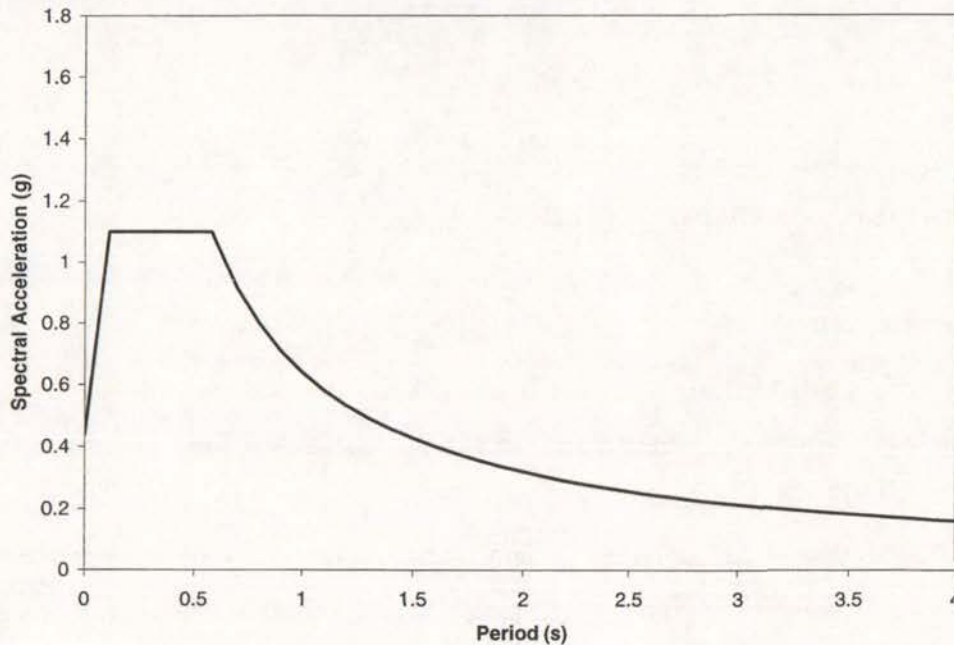


Figure 2.2: UBC Design Acceleration Spectrum

The action of these isolation systems is typically non-linear, however the UBC uses a design procedure based on effective linear stiffness and equivalent viscous damping, thus making the designs linear. The design procedure is set out in the Section 16 Appendix of the UBC¹².

Initially 12 linear isolation systems were designed using a combination of effective periods equal to 1.5, 2.0, 2.5 and 3.0 seconds and effective damping of 10, 20 and 30%. These values were considered to encompass the range which can typically be expected in seismically isolated buildings. Each of these 12 designs are shown by the intersection of the effective period and equivalent viscous damping curves shown in Figure 2.3.

By defining the design effective period, for example 1.5 seconds, the minimum effective stiffness can be calculated by rearranging Equation 2.1a¹² to make the stiffness the subject of the formula as in Equation 2.1b:

$$T_D = 2\pi \sqrt{\frac{W}{k_{D\min} g}} \quad \dots \text{Equation 2.1a}$$

rearranging gives:

$$k_{D\min} = 4\pi^2 \frac{W}{T_D^2 g} \quad \dots \text{Equation 2.1b}$$

where: T_D = design effective period of the isolation system

$k_{D\min}$ = minimum effective (secant) stiffness of the isolation system

W = the total weight of the superstructure

g = acceleration due to gravity

Then, defining the effective damping, for example 10%, gives the damping coefficient from Table A-16-C in the UBC. As the seismic coefficient was defined in calculating the design hazard spectrum the design displacement for the isolation system can be calculated using Equation 2.2:

$$D_D = \frac{g}{4\pi^2} \frac{C_{vD} T_D}{B_D} \quad \dots \text{Equation 2.2}$$

where: D_D = design displacement

C_{vD} = design seismic coefficient

B_D = design damping coefficient

The design base shear can be calculated directly from the design displacement using Equation 2.3. Assuming the superstructure is going to be elastic, then the lateral force resisting system coefficient is equal to 1.0. The maximum stiffness is normally defined by the variability of the results from tests on a proposed isolation system to be used in the design. In this study the maximum effective stiffness is assumed to be equal to the minimum effective stiffness due to the assumption that there is no variation in test results for the generic isolation systems.

$$V_s = \frac{k_D D_D}{R_l} \quad \dots \text{Equation 2.3}$$

where: V_s = design base shear above the isolation system

k_D = effective (secant) stiffness of the isolation system

R_l = lateral force resisting system coefficient

The 12 linear isolation system designs were plotted in Figure 2.3 to illustrate the relationships between effective period, effective damping, design displacement and base shear. As discussed above, these 12 designs are located at each intersection of the effective period and damping curves. From this plot 7 designs, considered realistic, were selected using three levels of design base shear, 0.25, 0.20 and 0.15 W; and the four effective periods, 1.5, 2.0, 2.5 and 3.0 seconds. The 7 designs are represented by the triangular points on Figure 2.3. Precise levels of damping and design displacements, for each of the 7 designs, were calculated using Equations 2.1, 2.2 and 2.3.

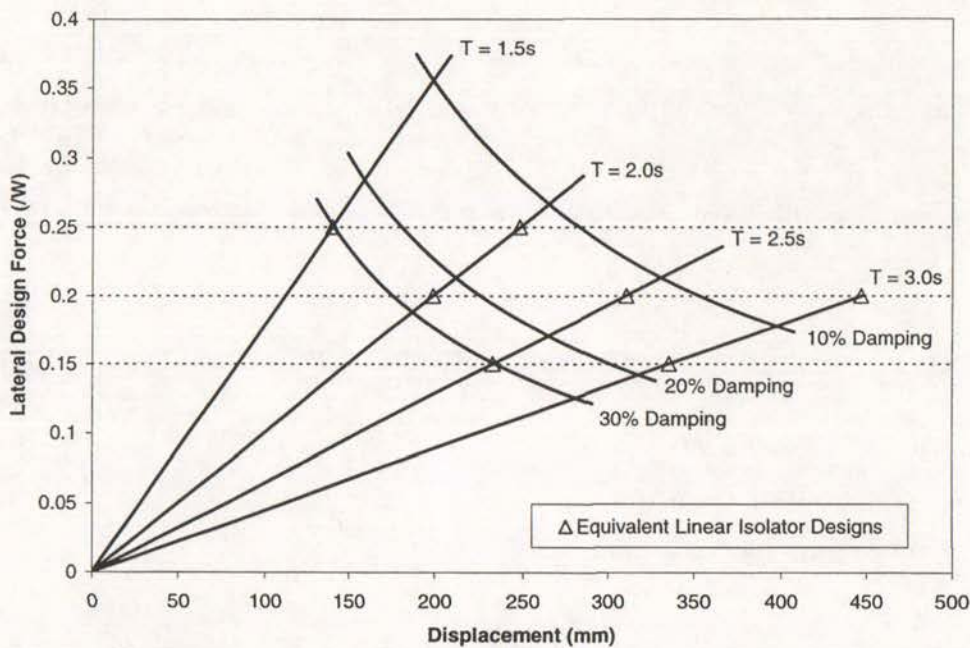


Figure 2.3: Response of Generic Isolation Systems Designed to the UBC

2.1.3 Design of Bilinear Isolation Systems

In reality, isolation systems such as lead rubber bearings, tend to have stiffness properties which can be closely approximated by bilinear properties. Therefore bilinear stiffness properties were calculated for each of the effective linear isolation systems described above. The procedure for assigning bilinear stiffness properties to a linearly designed UBC system is described below. It is similar to that set out by Andriano and Carr¹.

The design displacement of an equivalent bilinear system is equal to the UBC design displacement. To calculate appropriate bilinear properties, initially a post yield stiffness ratio

(for example 0.02) was assumed, then an initial stiffness and isolator yield force were also estimated. As a guide, the initial stiffness divided by the total weight of the structure was estimated as 10 (/m) and the yield force divided by the total weight as 0.05. Using the above variables, the yield displacement and design ductility can be calculated, and consequently, the design effective stiffness of the bilinear system was calculated using Equation 2.4¹.

$$k_D = k_0 \left(\frac{1-\alpha}{\mu} + \alpha \right) \quad \dots \text{Equation 2.4}$$

where: k_0 = initial stiffness of the isolation system

α = post yield stiffness ratio

μ = design ductility of the isolation system

To calculate the damping, firstly the ratio between the area under the bilinear curve and the area of a perfectly plastic system of equal design force and displacement was calculated using Equation 2.5¹.

$$R_A = (1-\alpha) \left(\frac{\mu-1}{\mu^2} \right) \frac{k_0}{k_{eff}} \quad \dots \text{Equation 2.5}$$

where: R_A = ratio of bilinear hysteretic area to area of plastic system

This ratio was converted to a fraction of critical viscous damping using Equation 2.6¹.

$$\xi = \frac{2}{\pi} R_A \quad \dots \text{Equation 2.6}$$

where: ξ = fraction of critical viscous damping

Knowing the fraction of effective viscous damping allowed the UBC damping coefficient to be calculated¹² and thus the effective stiffness and damping coefficient could be checked. These quantities needed to match those for the linear designs. New estimates of the initial stiffness and yield force were made and an iteration performed using Equations 2.4 and 2.5 until the effective period and damping converged to the linear design values. This procedure is illustrated using an example in Appendix 2. The design shear force and displacement for the bilinear designs were found to equal to those calculated for the linear designs.

Three sets of bilinear properties were attempted for each linear design with post-yield stiffness ratios of 0.02, 0.1 and 0.2. Not all these systems were possible because in order for all the stiffness and damping criteria to match the linear values, for highly damped short period systems, the high post-yield stiffness ratios could not be achieved. From 21 attempted designs 17 bilinear designs were achievable.

The differentiating properties for each of the 17 designs are listed in Table 2.1, where they are subdivided into their various effective linear designs. The design numbers are used to refer to each of the generic buildings. Design 7 has been used throughout the thesis as a representative isolation system when only one seismically isolated structure as required. It was selected because:

1. Its effective period, equal to 2.5 seconds, was considered typical.
2. Its design shear force of 0.20 times the total weight of the superstructure is the median of all of the structures.
3. Its post yield stiffness of 0.02 is the most common used in the 17 isolation systems.

Table 2.1: Bilinear Isolation System Properties.

Design	Effective Period (s)	Post Yield Stiffness Ratio	Equivalent Viscous Damping (%)	Initial Stiffness / Weight (/m)	Post Yield Stiffness / Weight (/m)	Yield Force / Weight	Design Displacement (mm)	Design Force / Weight
1	1.50	0.02	30.3	46.00	0.92	0.1240	140	0.250
2	2.00	0.02	12.7	40.20	0.80	0.0512	248	0.250
3	2.00	0.10	12.7	7.99	0.80	0.0571	248	0.250
4	2.00	0.20	12.7	3.95	0.79	0.0670	248	0.250
5	2.00	0.02	25.0	30.30	0.61	0.0812	199	0.200
6	2.00	0.10	25.0	5.76	0.58	0.0952	199	0.200
7	2.50	0.02	12.7	25.75	0.52	0.0409	311	0.200
8	2.50	0.10	12.7	5.12	0.51	0.0455	311	0.200
9	2.50	0.20	12.7	2.53	0.51	0.0536	311	0.200
10	2.50	0.02	30.4	16.50	0.33	0.0746	233	0.150
11	2.50	0.10	30.4	2.87	0.29	0.0924	233	0.150
12	3.00	0.02	6.7	20.00	0.40	0.0215	447	0.200
13	3.00	0.10	6.7	4.00	0.40	0.0237	447	0.200
14	3.00	0.20	6.7	1.99	0.40	0.0271	447	0.200
15	3.00	0.02	17.4	16.20	0.32	0.0422	336	0.150
16	3.00	0.10	17.4	3.19	0.32	0.0478	336	0.150
17	3.00	0.20	17.4	1.55	0.31	0.0576	336	0.150

Graphically the bilinear properties of the isolation system for design numbers 7, 8 and 9, are shown on Figure 2.4. The design effective stiffness for each of these designs are equal, due to equal design displacements and base shear forces. The effective viscous damping is also equal, which is graphically represented by equal areas under the bilinear plot resulting in equal hysteretic areas. Therefore each of the three bilinear designs are equivalent to the UBC linear design, with an effective period of 2.5 seconds and design base shear of 0.2 times the weight of the superstructure.

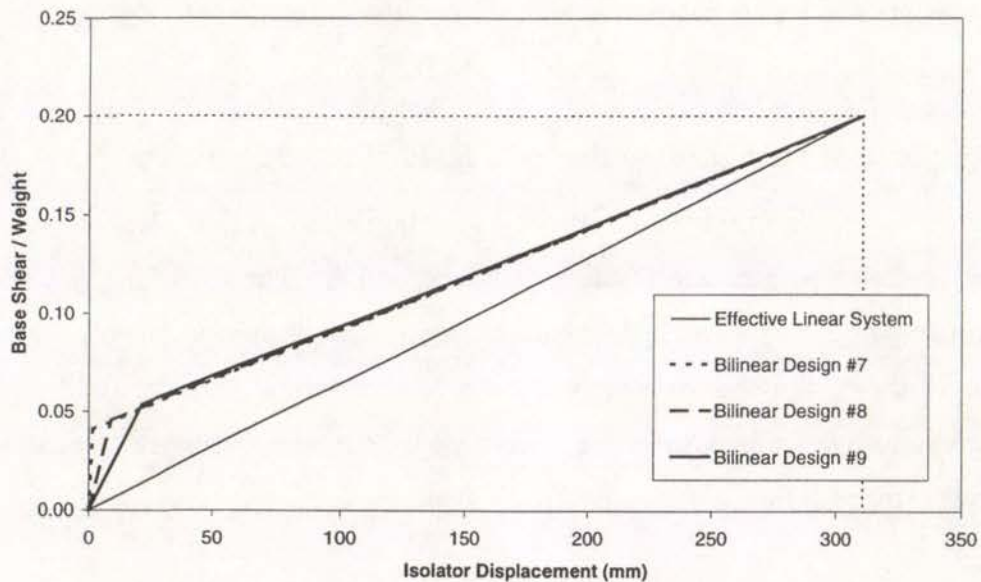


Figure 2.4: Bilinear Isolation Systems for Designs 7, 8 and 9.

2.1.4 Maximum Displacement of the Isolation System

The UBC states that the isolation system of a seismically isolated building should still perform during a maximum credible event, which is an event that has a ten percent probability of exceedence in one hundred years. Therefore, it has been assumed that the maximum isolation system displacement, which a typical seismically isolated building can reach without failure, corresponds to the displacement of the isolation system in response to this maximum credible earthquake. The parameters for the maximum event, as outlined by the UBC, are given in Appendix 1. These parameters define the maximum capable hazard spectrum, which is shown in Figure 2.5.

For each of the bilinear isolation systems the maximum credible displacement was calculated by assuming the post yield stiffness was equal for displacements larger than the design

displacement. By first estimating the maximum isolator displacement, the maximum ductility, effective stiffness and effective damping of each system was calculated. As a result, substituting the design parameters, C_{VD} , T_D and B_D in Equations 2.1 and 2.2 for the maximum values gave a new estimate of the maximum displacement. By repeatedly modifying the initial estimate using iteration, the maximum displacement was found.

The displacement of each isolation system in response to the maximum capable earthquake is listed in Table 2.2, along with the design displacement and base shear. As shown, the maximum displacements are approximately 1.4 times the design displacements.

2.1.5 Response of Structures to the Near Field Hazard Spectrum

The structures were designed for the highest seismic region in the UBC, however, it was assumed that they were located outside a near field region. The 1997 UBC includes a near field factor to account for near field ground motion, which is used to change the magnitude and shape of the design spectrum for structures located within the near field region. The generic structures were now assumed to be located within two kilometres of a fault, thus the near field spectrum for this region is defined by Equation 2.7.

$$\begin{aligned} S_{aNF} &= 1.5S_{aD}, \quad T < 0.58s \\ S_{aNF} &= 2.0S_{aD}, \quad T > 0.78s \end{aligned} \quad \dots \text{Equation 2.7}$$

where: S_{aNF} = near field spectral acceleration

S_{aD} = design spectral acceleration

There is a non linear increase in the ratio of the design spectral acceleration and the near field spectral acceleration between periods of 0.58 and 0.78 seconds, such that the spectral acceleration is at a constant level up to 0.78 seconds. The near field spectrum is illustrated in Figure 2.5, compared with the design and maximum capable earthquake spectra.

Using the near field spectrum, the near field displacement response of a given isolation system was calculated in the same way that the maximum displacement was calculated. It was again assumed that the bilinear isolator properties did not change for displacements in excess of the design and maximum isolator displacements. The near field displacement was

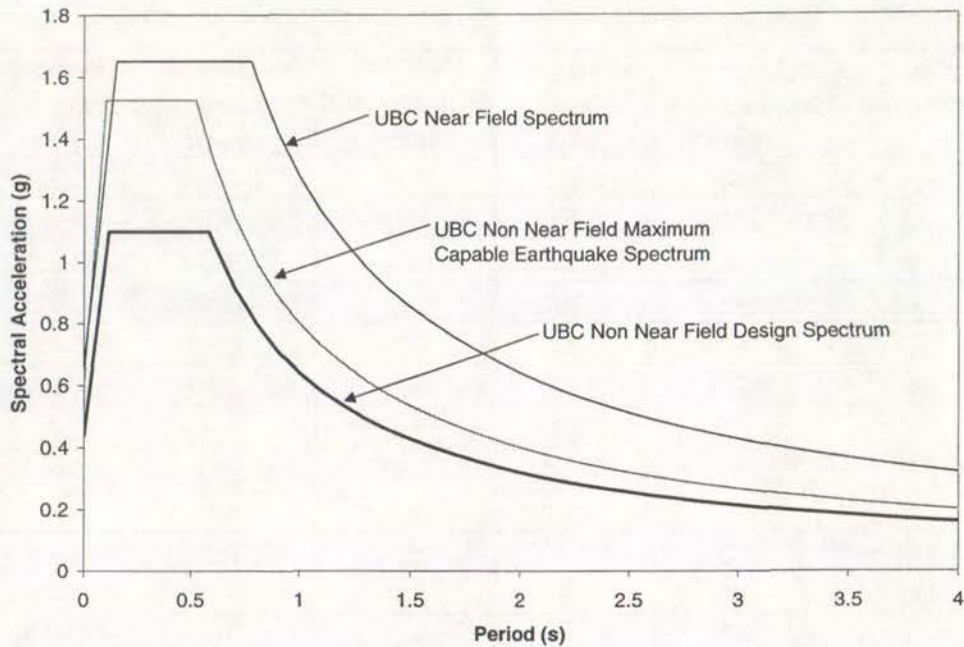


Figure 2.5: Design Level, Maximum Capable and Near Field UBC spectra

first estimated in order to calculate the near field ductility, effective period and effective damping. The near field value for C_{VD} was calculated as 1.28^{12} , which enabled the near field displacement response to be calculated using Equation 2.2. This displacement was compared to the original estimate and, if not equal to the original estimate, it was used as a new estimate. The procedure was repeated until the displacements converged. Once the near field displacement was known, the near field base shear could be calculated using Equation 2.3. An example of this procedure is given in Appendix 3.

The design, maximum and near field displacement along with the design and near field base shear for each isolation system is presented in Table 2.2. A full table of the near field properties for each generic isolation system is given in Appendix 4. Table 2.2 illustrates that the near field isolation system displacements were generally 2.5 to 3.0 times greater than the design values. Therefore, it was apparent that the structures needed to be retrofitted in order to reduce the near field displacements, as the maximum allowable displacement of each isolation system was only approximately 1.4 times the design values. The near field base shear was approximately 2.0 to 2.5 times the design base shear, thus this also needed to be reduced to prevent excessive damage in the superstructure.

Table 2.2: Summary of Isolation System Responses to Various UBC Spectra

Design Number	Design Displacement (mm)	Design Force (/W)	Maximum Displacement (mm)	Near Field Displacement (mm)	Near Field Force (/W)
1	140	0.250	204	435	0.521
2	248	0.250	344	667	0.587
3	248	0.250	344	668	0.585
4	248	0.250	342	664	0.578
5	199	0.200	282	593	0.439
6	199	0.200	282	587	0.424
7	311	0.200	430	834	0.469
8	311	0.200	430	835	0.469
9	311	0.200	427	830	0.463
10	233	0.150	337	719	0.311
11	233	0.150	334	700	0.284
12	447	0.200	605	1161	0.485
13	447	0.200	605	1161	0.485
14	447	0.200	605	1162	0.485
15	336	0.150	479	957	0.352
16	336	0.150	476	953	0.347
17	336	0.150	473	943	0.338

2.2 Design of Multi-Storey Superstructures for Seismically Isolated Buildings

2.2.1 Introduction

The isolation systems were designed using UBC requirements, assuming a rigid superstructure from which the design displacements and base shears were calculated. The UBC assumes that the superstructure above the isolation layer can be designed independently of the isolation system once the design base shear of the isolation system has been calculated. Therefore three and six storey “shear type” superstructures were designed using the three levels of design base shear, 0.25 W, 0.20 W and 0.15 W, from the isolation systems. A diagram of a three storey structure is shown in Figure 2.6.

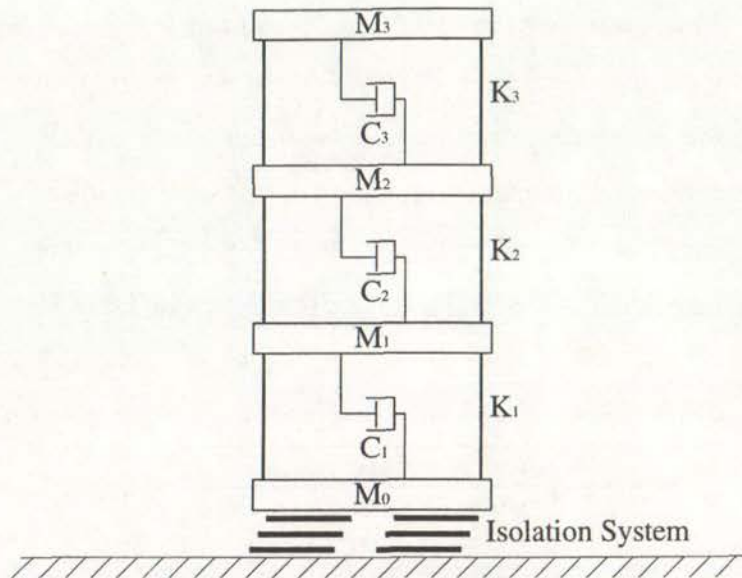


Figure 2.6: Generic Three Storey Seismically Isolated Building

2.2.2 Calculation of Design Lateral Forces

The total weight of the building was distributed evenly between each of the floors and the base level in the multi-storey superstructure. The weight of each floor, in the three storey seismically isolated structure, was equal to the total weight of the superstructure divided by four. Similarly, the weight of the each floor, in the six storey building, was equal to the total weight divided by seven. The inter-storey height between each floor was also equal.

To calculate the strength of each floor level, the base shear from the isolation system was distributed vertically up the building in accordance with the UBC. The force at each level, x , was calculated using Equation 2.8¹², from which the design shear strength of each level was calculated.

$$F_x = \frac{V_s w_x h_x}{\sum_{i=1}^n w_i h_i} \quad \dots \text{Equation 2.8}$$

where: F_x = lateral force at a given floor x

V_s = total base shear above the isolation layer

w_x = weight of a given floor x

h_x = height of a given floor x

The storey shears at each level were used as yield forces for numerical modelling of the multi-storey structures. During a design level event it was assumed that the maximum storey shears would not exceed these forces and the superstructure would act elastically. For an earthquake that exceeds the design level event, damage was expected, thus the buildings were modelled to yield at the design shear force. The shear forces at each level, for the three and six storey superstructures and the three levels of design base shear, are given in Table 2.3.

Table 2.3: Design Storey Shear Forces for Three and Six Storey Superstructures

Three Storey Superstructure			
Level	Design Shear Force / Weight		
Base	0.250	0.200	0.150
1	0.250	0.200	0.150
2	0.208	0.167	0.125
3	0.125	0.100	0.075

Six Storey Superstructure	
Level	Design Shear Force / Weight
Base	0.200
1	0.200
2	0.190
3	0.171
4	0.143
5	0.105
6	0.057

2.2.3 Calculation of the Stiffness at each Level

2.2.3.1 Introduction

In the design of the generic multi-storey superstructures, it was assumed that typical first mode effective periods for a three storey and six storey structure were 0.4 and 0.8 seconds respectively. A second assumption was that the stiffness of each level was equal, which is based on the supposition that the cross sections of the columns are the same all the way up the buildings. Therefore K_1 , K_2 , and K_3 in Figure 2.6 are equal. The procedure for calculating the stiffness is described in the following section.

2.2.3.2 Procedure for Calculating Storey Stiffness

The mass matrix for n floors above the isolation system, excluding the base, is represented by:

$$[M] = \begin{bmatrix} M_1 & 0 & 0 & \dots & 0 \\ 0 & M_2 & 0 & \dots & 0 \\ 0 & 0 & M_3 & \dots & 0 \\ \vdots & \vdots & \vdots & \ddots & \vdots \\ 0 & 0 & 0 & \dots & M_n \end{bmatrix} \quad \dots \text{Equation 2.8}$$

where: $M_n =$ mass of n th floor

and the stiffness matrix is:

$$[K] = K_s [k] \quad \dots \text{Equation 2.9}$$

where: $K_s =$ stiffness constant

and:

$$[k] = \begin{bmatrix} 2 & -1 & 0 & \dots & 0 \\ -1 & 2 & -1 & \dots & 0 \\ 0 & -1 & 2 & \dots & 0 \\ \vdots & \vdots & \vdots & \ddots & \vdots \\ 0 & 0 & 0 & \dots & 1 \end{bmatrix}_{n \times n} \quad \dots \text{Equation 2.10}$$

To solve for the undamped natural mode shapes and frequencies of the building:

$$[M] \ddot{\underline{u}} + [K] \underline{u} = 0 \quad \dots \text{Equation 2.11}$$

where: $\ddot{\underline{u}} =$ acceleration vector for the building

$\underline{u} =$ displacement vector for the building

and the vector describing the floor displacements, \underline{u} , for n floors above the isolation system is:

$$\underline{u} = \begin{bmatrix} u_1 \\ u_2 \\ u_3 \\ \vdots \\ u_n \end{bmatrix} \quad \dots \text{Equation 2.12}$$

The actual displacement of the structure, can be described in terms of modeshapes and modal amplitudes by:

$$\underline{u} = [\phi] \underline{Y} \quad \dots \text{Equation 2.13}$$

where: \underline{Y} = vector of modal amplitudes at each floor

where the modeshape $[\phi]$ for n modes and n floors is:

$$[\phi] = \begin{bmatrix} \phi_1^1 & \phi_1^2 & \phi_1^n \\ \phi_2^1 & \phi_2^2 & \phi_2^n \\ \phi_3^1 & \phi_3^2 & \phi_3^n \\ \vdots & \vdots & \vdots \\ \phi_n^1 & \phi_n^2 & \phi_n^n \end{bmatrix} \quad \dots \text{Equation 2.14}$$

Using the mode shapes and modal amplitudes, Equation 2.11 can be rearranged to:

$$([K] - \omega^2 [M])\phi = 0 \quad \dots \text{Equation 2.15}$$

where: ω = natural frequency of a given mode

therefore:

$$\det([K] - \omega^2 [M]) = 0 \quad \dots \text{Equation 2.16}$$

Substituting Equation 2.9 into Equation 2.16 and rearranging gives:

$$\det\left([k] - \frac{\omega^2}{K_s} [M]\right) = 0 \quad \dots \text{Equation 2.17}$$

By solving the eigen problem in Equation 2.17, n solutions for ω^2 divided by K_s can be calculated. For example, a three storey superstructure, assumed to be rigidly fixed to the ground, has three natural modes of vibration and consequently three solutions. The first mode had the lowest natural frequency and corresponded to the smallest solution. As the desired first mode natural period of the system was known, then the stiffness constant, K_s , could be calculated. The eigen solution also gave the other natural frequencies and mode shapes for each mode.

2.2.3.3 Results

The calculation of inter-storey stiffness for the three storey superstructure is given in Appendix 5 as an example. For the three storey superstructure the stiffness divided by the total weight of the structure was equal to 31.767 (/m), and for the six storey building the stiffness divided by the weight was equal to 15.466 (/m). Using these stiffness', the natural frequencies and modeshapes are given in Appendix 6 for both the three and six storey superstructures.

2.2.4 Modal Damping

2.2.4.1 Introduction

It has been assumed that there is five percent equivalent viscous damping in the first mode for both the three and six storey superstructures. Like the stiffness, it was assumed that there is an equal amount of damping available in each level, therefore the damping constants, C_1 , C_2 and C_3 in Figure 2.6 are equal. The damping constant was required for modelling in SAP.

2.2.4.2 Procedure for Calculating Damping Constant

For free vibration of a system which is no longer undamped, Equation 2.11 is modified to:

$$[M]\ddot{u} + [C]\dot{u} + [K]u = 0 \quad \dots\text{Equation 2.15}$$

where: $[C]$ = damping matrix

\dot{u} = velocity of the system

The damping matrix can be written in terms of the damping constant by:

$$[C] = \beta[c] \quad \dots\text{Equation 2.16}$$

where: β = damping constant

and where $[c]$ takes the same form as the stiffness matrix:

$$[c] = \begin{bmatrix} 2 & -1 & 0 & \cdot & 0 \\ -1 & 2 & -1 & \cdot & 0 \\ 0 & -1 & 2 & \cdot & 0 \\ \cdot & \cdot & \cdot & \cdot & \cdot \\ 0 & 0 & 0 & \cdot & 1 \end{bmatrix}_{n \times n} \quad \dots \text{Equation 2.17}$$

Converting actual displacements to modal shapes and modal amplitudes using Equation 2.12 and premultiplying by the transpose of $[\phi]$, Equation 2.15 becomes:

$$[\phi]^T [M][\phi] \ddot{Y} + [\phi]^T [C][\phi] \dot{Y} + [\phi]^T [K][\phi] Y = 0 \quad \dots \text{Equation 2.18}$$

where $[\phi]$ is an $n \times n$ matrix containing modeshapes for n modes and Y is a vector of modal amplitudes for each mode. For a given mode, i , Equation 2.18 can be written as:

$$M_i \ddot{Y}_i + C_i \dot{Y}_i + K_i Y_i = 0 \quad \dots \text{Equation 2.19}$$

M_i , C_i and K_i are the generalised mass, damping and stiffness respectively for mode i . From Equation 2.20 these quantities are:

$$M_i = \phi_i^T [M] \phi_i \quad \dots \text{Equation 2.21}$$

$$K_i = \phi_i^T [K] \phi_i \quad \dots \text{Equation 2.23}$$

and as in Equation 2.16:

$$C_i = \beta c_i \quad \dots \text{Equation 2.24}$$

where:

$$c_i = \phi_i^T [c] \phi_i \quad \dots \text{Equation 2.25}$$

The damping in a system for a given mode can be described in terms of a fraction of critical damping by:

$$C_i = 2\xi_i M_i \omega_i \quad \dots \text{Equation 2.26}$$

Therefore the damping constant, β , in a system can be calculated by:

$$\beta = \frac{2\xi_i \omega_i M_i}{c_i} \quad \dots \text{Equation 2.27}$$

Using the modeshapes and natural frequencies calculated in Section 2.2.3, the damping constant for 5% effective viscous damping in the first mode was calculated for the three and six storey superstructures. By rearranging Equation 2.27, this was used to calculate the effective viscous damping in each of the other modes.

2.2.4.3 Results

The damping constants calculated for the models of the three and six storey superstructures were 0.2022 W (s/m) and 0.1969 W (s/m) times the total weight of the structure respectively. The damping constant is the same for all superstructures regardless of the base shear in the structures. These damping constants describe the modal damping in the structures while they remain elastic. Once the superstructure yields hysteretic damping is added to the system.

Appendix 7 shows a complete calculation of the damping constant for a three storey superstructure. The effective damping for the other modes has been calculated and listed in Appendix 8.

Once the SAP models were constructed the level of damping was checked by applying a cyclic load at a frequency close to the natural frequency of each mode. The steady state dynamic amplification factor was calculated consequently allowing the damping in the system to be calculated. The level of damping for each mode found using this method was within 1% of the expected level. An example of this calculation procedure is presented in Appendix 9.

2.3 Summary

A number of generic isolation systems have been designed to represent a range of isolation systems found in areas of high seismic activity. They have been assumed to be designed to UBC requirements without regard to near field earthquakes, as have many buildings in the past. When the near field response was calculated it was found that the displacements of their

isolation systems in response to the UBC near field spectrum exceeded their design displacements by 2.5 to 3.0 times and their maximum displacements by typically 2.0 times.

Three and six storey superstructures were designed for each of the isolation systems. Each superstructure was designed with columns of equal stiffness at each level and yield forces at each level as defined by the UBC. Each superstructure has been designed with five percent effective damping in the first mode of its fixed base response.

In the following chapters the generic seismically isolated buildings modelled with a rigid superstructure are referred to as for example "Design 7". The number refers to the reference number for the design of the isolation system. The seismically isolated buildings modelled with a three storey superstructure are referred to as for example "Design 3.7". Where the "7" refers to the reference number of the isolation system and the "3" refers to the three storey superstructure. Similarly, the six storey building investigated is referred to as "Design 6.7".

Chapter 3.

Response of Rigid Seismically Isolated Buildings Using Time History Analyses

3.1 Introduction

In order to retrofit the previously designed generic seismically isolated buildings for near field ground motion, they needed to be modelled in such a way that their structural response to real earthquakes matched their design response. Numerical models of the isolation systems were constructed and analysed using SAP⁶. These models were initially assumed to each have a rigid superstructure in order to focus on the properties of the isolation systems. The seismically isolated structures modelled with a rigid superstructure are discussed exclusively in this chapter and are commonly referred to as “rigid seismically isolated structures”. A number of earthquakes were selected for modelling both design and near field events and were scaled so that the response of each rigid seismically isolated structure to these earthquakes was equal to the respective UBC design and near field response.

3.2 SAP Model of the Seismically Isolated Buildings modelled with a Rigid Superstructure

Initially the seismically isolated structures were modelled in SAP as a rigid mass located above isolation systems with a range of bilinear properties as designed in Chapter 2. The isolation systems were modelled as non-linear shear links between a node at the ground, Node 1, and an upper node, Node 2, as illustrated in Figure 3.1. The distance between the two nodes is inconsequential as the element was modelled to deform only in shear. The bilinear properties of the non-linear link are prescribed by an initial stiffness, post yield stiffness ratio, yield force and a yielding exponent. All of these properties have been calculated for each of the isolation systems and are listed in Table 2.1, except the yielding exponent which describes the transition between the initial stiffness and the post yield stiffness. As a sharp transition has been assumed, a high value (equal to 100) was used.

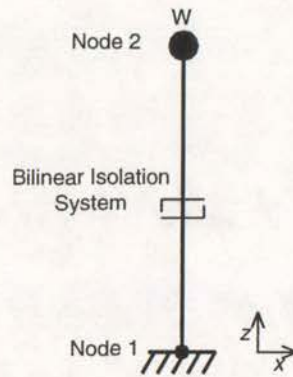


Figure 3.1: SAP Model of a Seismically Isolated Building Modelled with a Rigid Superstructure

Node 1 was constrained from moving in any direction, while node 2 was constrained from moving in all directions except the global “x” direction. Node 2 contained the total mass of the system which acts in the global “x” direction. The earthquake accelerations were applied at ground level and also orientated in the “x” direction.

3.3 Selection of Earthquake Records

3.3.1 Introduction

Various design level and near field records were selected in order to model the UBC response of the generic isolation systems in SAP using time history analysis. This would later enable the response of the structures to be determined after retrofitting. Factors for selection of appropriate design level and near field records are discussed in Sections 3.3.2 and 3.3.3. The various records are compared in Section 3.3.4.

3.3.2 Design Level Earthquake Records

Four design level earthquake records were used for modelling in SAP. Information about each record and the earthquake from which it was obtained is presented in Table 3.1. A number of records were considered for analysis, but only records with an acceleration spectrum of approximately the same magnitude as the UBC response spectrum were used. This is illustrated in Figure 3.2.

Two of the design level records used, El Centro and Bucharest were obtained from sources at the University of Auckland, while Parkfield and Joshua Tree were obtained from the Strong

Motion Database¹¹. El Centro and Parkfield were selected because of their extensive use for design in the past. The record taken from the Bucharest earthquake was recorded at a soft soil site and was included to assess the variation between a soft soil site and the other sites. The other record, Joshua Tree, has been reported²⁷ to contain backward directivity motion and was included to determine the effect of retrofitting on the response to this type of ground motion. A structure located in the near field is just as likely to experience backward directivity ground motion and, although its effects are not likely to be as hazardous as forward directivity effects its response is important. Acceleration and velocity time histories for each design level earthquake are presented in Figure 3.4.

The primary reason for having the design level earthquakes was to check modifications made to the seismically isolated structures to counter the effects of near field ground motion. It was important that these modifications did not adversely affect the response of the structure during a design level event.

3.3.3 Near Field Earthquake Records

Six near field earthquake records were selected to model the seismically isolated buildings in response to a near field event. Requirements for selection of these records were similar to those for the design level records. The acceleration spectra for the selected records are shown to be similar in magnitude to the UBC near field spectrum. These spectra are illustrated in Figure 3.3.

For the records used, either Somerville²⁷ or McVerry¹⁸ has reported that they are approximately fault normal components containing forward directivity effects. A second feature of the selected near field records is the occurrence of a long period, large magnitude pulse which is visible in the acceleration time history, but more clearly visible in the velocity time history, as exemplified in Figures 3.5 and 3.6. General information for the selected near field records and the earthquake from which they were sourced is given in Table 3.2.

Four of the near field earthquake records are taken from real earthquakes in California. The Rinaldi and Sylmar County Hospital records are both taken from the 1994 Northridge earthquake. The Lucerne ground motion was recorded in the 1992 Landers earthquake. The Imperial Valley record was taken from the 1979 Imperial Valley earthquake. The other two

listed near field records are artificial records derived by Hall et al¹⁰. The first is from a simulation of the fault rupture during the 1994 Northridge earthquake. From a number of sites on a grid of the area, the record with the largest peak ground velocity was used in this thesis. The second artificial record is from a simulation predicting the rupture of the Elysian Park fault in the Los Angeles region. This models a magnitude 7.0 earthquake resulting in extremely large ground motions. Again the site with the largest magnitude ground motions was selected.

Table 3.1: Design Level Earthquake Records

Year	Reference	Earthquake	Station	Comp.	Mag.	Epicentral Distance (km)	Focal Depth (km)	Soil Type	Peak Accn (g)	Peak Vel (m/s)	v/a (s)
1940	El Centro¹	Imperial Valley	El Centro Array #9	NS	6.9	8	9	Soil	0.35	0.32	0.09
1966	Parkfield¹	Parkfield	California Array #2	N65E	6.1	36	7	Soil	0.50	0.78	0.16
1977	Bucharest²	Bucharest	Building Res. Inst.	NS	7.2	n/a	94	Soft Soil	0.20	0.72	0.37
1992	Joshua Tree¹	Landers	Joshua Tree	EW	7.3	14	5	Soil	0.28	0.43	0.15
Average					6.9	19	29		0.33	0.56	0.19

1. Acceleration and velocity taken from source data.
2. Acceleration taken from source data. Velocity calculated by SAP.

Table 3.2: Near Field Earthquake Records

Year	Reference	Earthquake	Station	Comp.	Mag.	Epicentral Distance (km)	Focal Depth (km)	Soil Type	Peak Accn (g)	Peak Vel (m/s)	v/a (s)
1994	Northridge (Sim.)³	Northridge	Artificial E04		6.7	25	19	Soil	0.77	1.76	0.23
	Rinaldi¹		Rinaldi	S49W	6.7	10	19	Soil	0.84	1.70	0.21
	Sylmar⁴		Sylmar Hospital	360	6.7	16	19	Soil	0.84	1.29	0.16
Pred.	Elysian Park²	Elysian Park	Artificial E05		7.0	9	9	Rock	0.93	1.76	0.19
1992	Lucerne¹	Landers	Lucerne	N90E	7.3	42	5	n/a	0.73	1.46	0.20
1979	Imperial Valley¹	Imperial Valley	Array #7	230	6.4	29	12	Soil	0.46	1.13	0.25
Average					6.8	22	14		0.76	1.52	0.21

1. Acceleration and velocity taken from source data.
2. Acceleration taken from source data. Velocity calculated by SAP.
3. Acceleration taken from source data. Velocity as published by Somerville²⁷.
4. Acceleration taken from source data. Velocity as published by McVerry¹⁸.

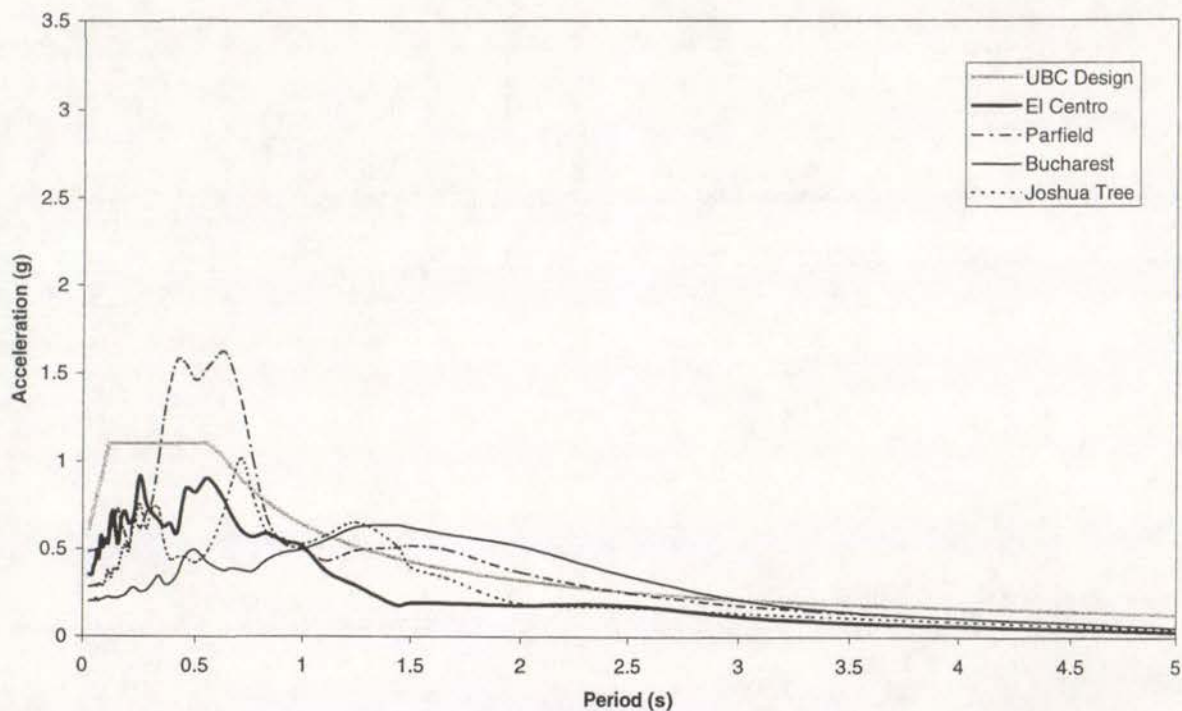


Figure 3.2: Design Level Response Spectra

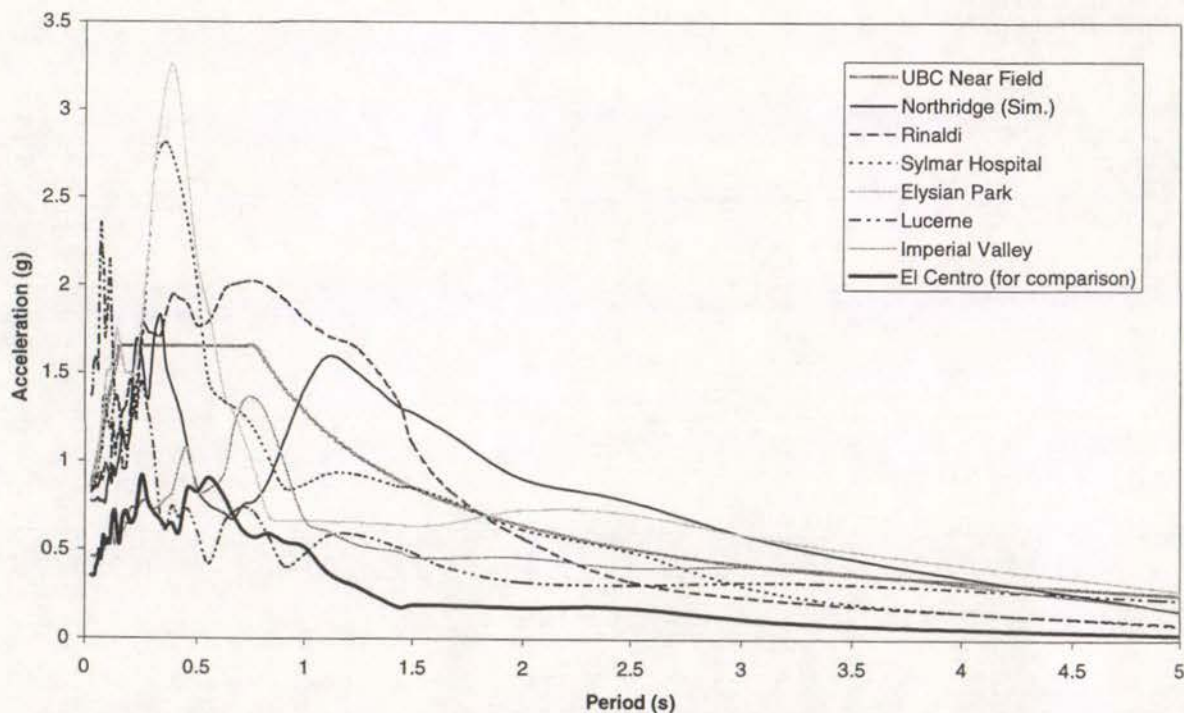
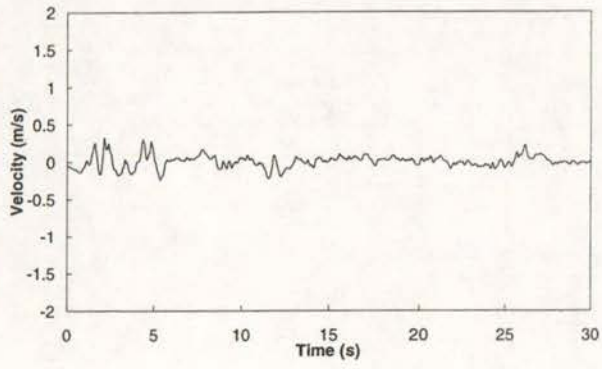
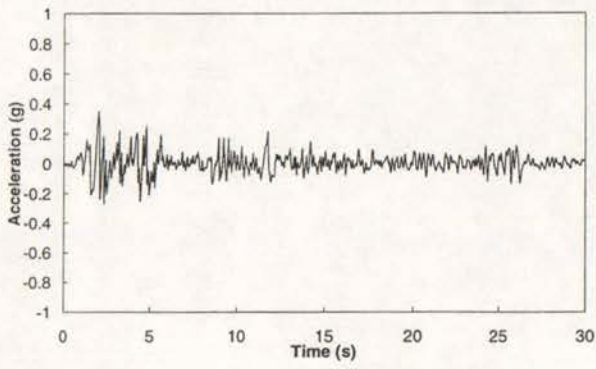
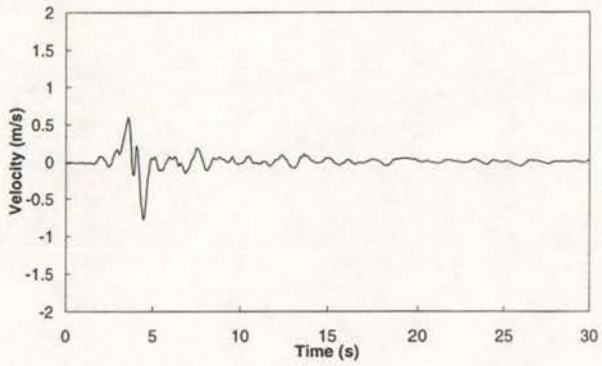
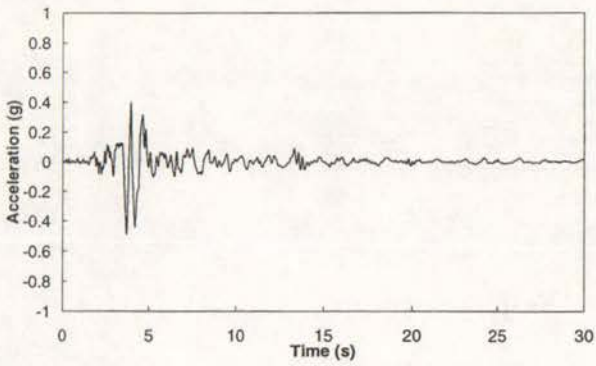


Figure 3.3: Near Field Response Spectra

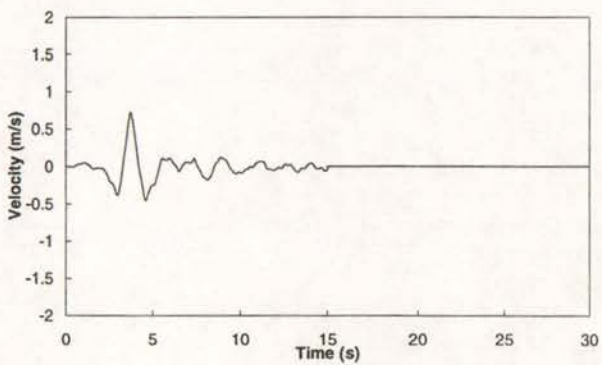
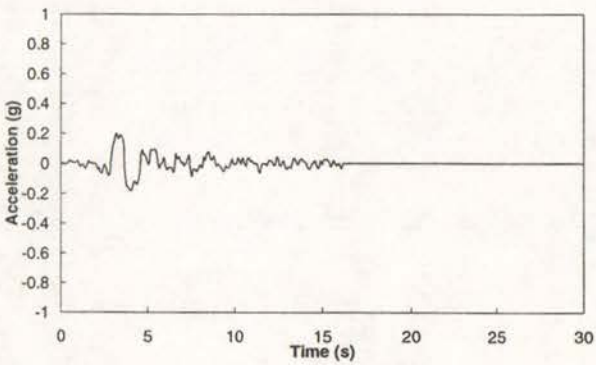
El Centro



Parkfield



Bucharest



Joshua Tree

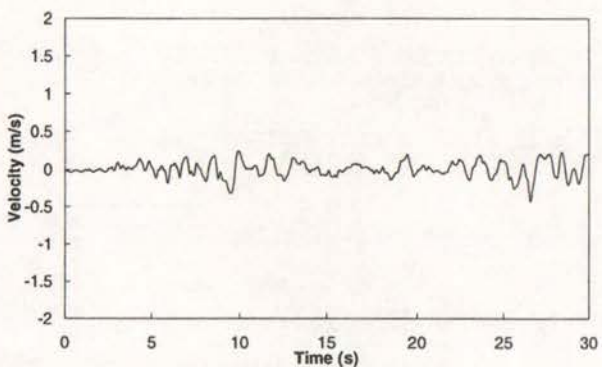
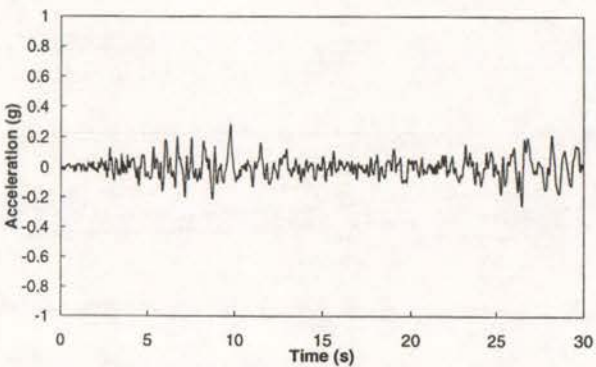
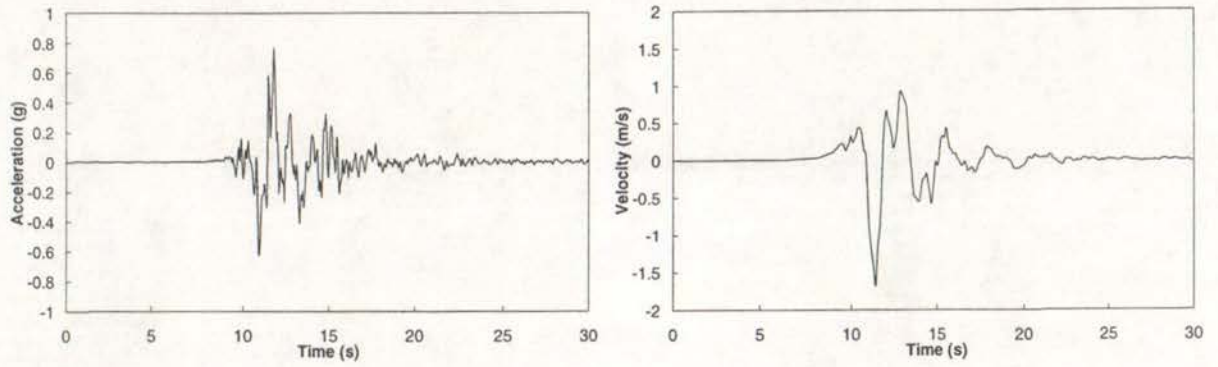
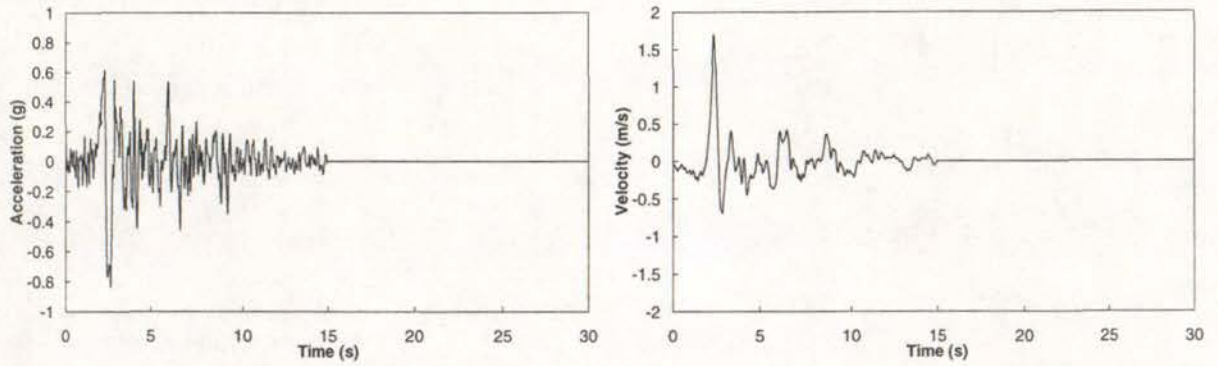


Figure 3.4: Acceleration and Velocity Time Histories for the Design Level Earthquake Records

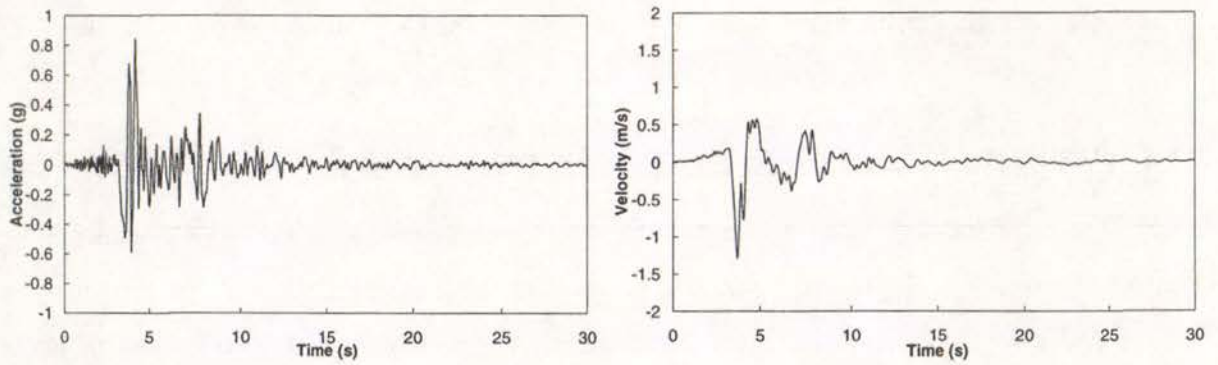
Northridge (Simulated)



Rinaldi



Sylmar Hospital



Elysian Park (Hypothetical)

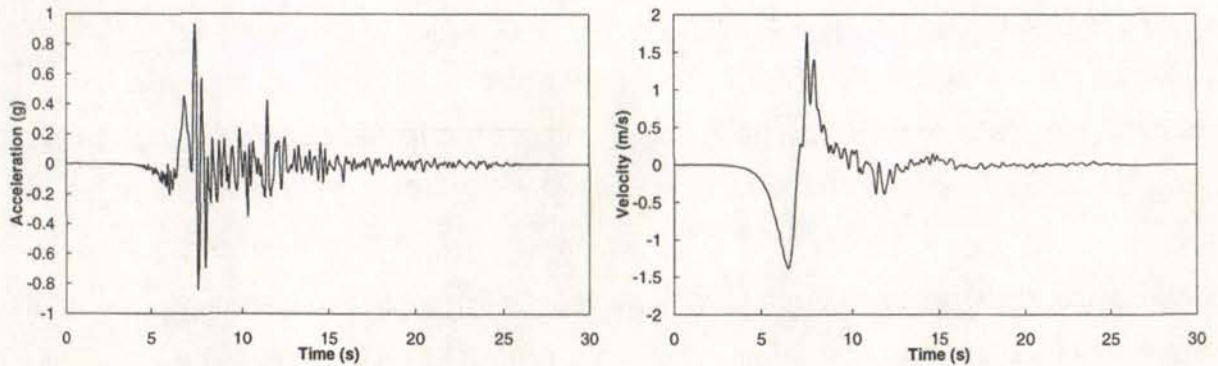


Figure 3.5: Acceleration and Velocity Time Histories for Northridge (Sim.), Rinaldi, Sylmar Hospital and Elysian Park

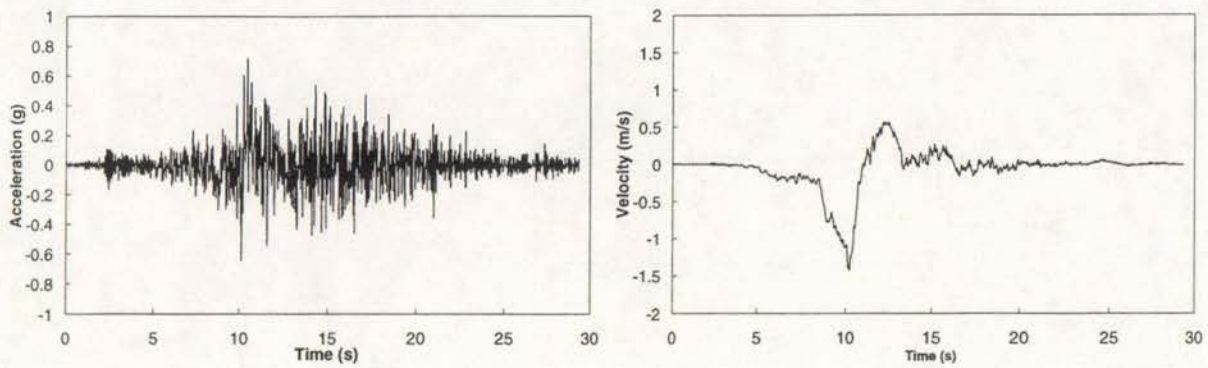
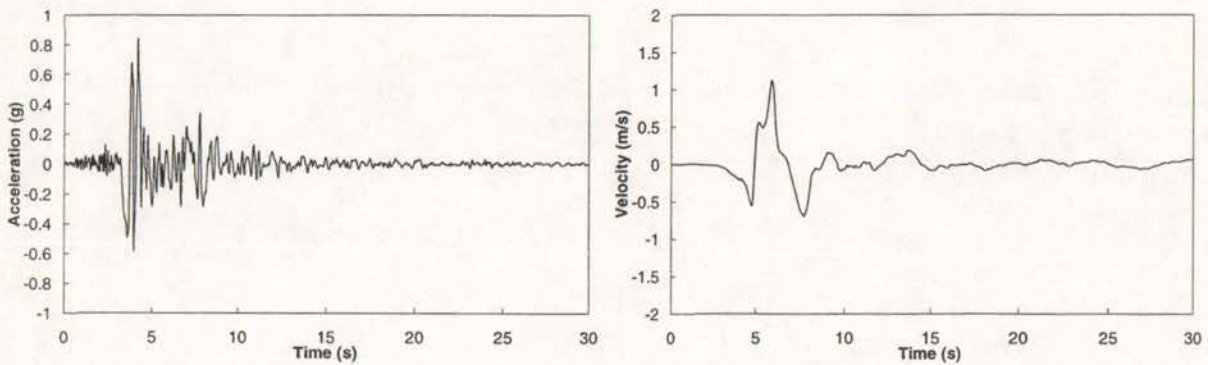
Lucerne**Imperial Valley**

Figure 3.6: Acceleration and Velocity Time Histories for Lucerne and Imperial Valley

3.3.4 Comparisons between Design Level and Near Field Records

Comparing the data in Tables 3.1 and 3.2 show that the near field records generally have considerably larger peak ground accelerations and even larger peak ground velocities than the design level events, particularly if the comparatively large velocity of the soft soil Bucharest earthquake is disregarded. However, the average magnitude of the design level earthquakes is identical to the average magnitude of the near field earthquakes. The average focal depths are also similar if the large depth of the Bucharest earthquake is again disregarded. Furthermore, the average distance to the epicentre is actually smaller for the design level earthquakes than the near field earthquakes, demonstrating that the directivity effects have a large impact on the magnitude and frequency content of the ground motion for the near field earthquakes. It is apparent that the large ground motions in the near field records are more dependent on the proximity of a site, not to the epicentre, but to the fault. The design level records, El Centro, Parkfield, and Joshua Tree, are located in the same region and have similar ground conditions to the Californian near field records. Parkfield is interesting because its source is a relatively

small earthquake, magnitude 6.1, yet it has a relatively large peak ground acceleration and also a large peak ground velocity. This suggests that it also shows evidence of forward rupture directivity effects, although the effects are not as pronounced as the effects in the near field records.

3.4 Scaling of the Earthquake Records

3.4.1 Scaling the Design and Near Field Earthquakes to Match the UBC Response

A number of appropriate design level and near field earthquake records were chosen so that the seismically isolated structures could be modelled using real seismic events. The unscaled responses of each structure to these records tend to approximate the UBC design and near field responses respectively. However there is still significant variation for each structure between the response to each earthquake. Some form of scaling was necessary to reduce this variation. Because the isolation systems are non-linear, it was difficult to derive a simple scaling procedure that resulted in a response to each earthquake within five percent of the calculated UBC responses. It was important that the variation in response for the unretrofitted structures was small as a large variation would have made it difficult to compare the various earthquakes when different forms of retrofit were attempted in the buildings.

A number of scaling techniques was considered in an effort to find an appropriate scaling procedure. It was considered inappropriate to scale the earthquakes in the frequency domain to directly match the UBC spectra as this would distort the frequency content of the earthquakes, consequently distorting the near field pulses. Therefore scaling was restricted to changing the magnitude of the earthquake records. It was also considered inappropriate to scale the magnitude of the records outside the range of 0.5 to 2.0, as the frequency content is likely to become unrealistic with large levels of scaling.

A number of magnitude scaling techniques were attempted, including:

1. Scaling peak ground accelerations to a common value.
2. Scaling peak ground velocities to a common value.
3. Scaling the earthquake response spectra to the UBC, five percent damped, design and near field spectra respectively at a period of 1.0s.

4. Response spectrum scaling at periods equal to the design effective periods of the isolation systems.

None of these attempts resulted in design and near field responses consistently within five percent of the responses calculated for each structure using the UBC. Therefore it was decided to calculate the unscaled response to each earthquake using SAP, then modify the response by adjusting the scale factors until the responses were within five percent of the calculated UBC response. An appropriate scale factor for each earthquake was found by performing several analyses until the required response was obtained. Using this procedure a different set of scale factors was obtained for each generic rigid seismically isolated structure. The scale factors were all within the range of 0.5 to 2.0 for each structure, with the exception of El Centro which had a scale factor of up to 2.2. This was considered acceptable due to historical importance of El Centro for the basis of design in the past.

The response of each of structure has been matched to the UBC design and near field spectra, therefore comparisons between structures can be made with reference to the UBC response. This form of scaling enabled good comparison between the various earthquake records when each of the structures was retrofitted with different levels and types of damping in the isolation systems. A list of the scale factors for each structure is included in Table 3.3.

Table 3.3 demonstrates that the average near field scale factor for each structure has a range of approximately 1.1 to 1.3, implying that the UBC near field response spectrum is 10 to 30% larger than the average response expected from this set of earthquakes. This is considered a realistic and conservative level for the near field response. The range of average design level scale factors is approximately 1.2 to 1.5, therefore the design level earthquakes needed to be scaled by a larger amount than the near field earthquakes. This implies that the difference between the design level and near field earthquakes was actually larger than the UBC suggests. This conclusion is dependent on the given selection of earthquake records.

As illustrated, the design level earthquakes were scaled to the UBC design spectrum and the near field earthquakes were scaled to the UBC near field spectrum with comparable scale factors. Hence it was confirmed that near field ground motion can be expected to increase the response of the seismically isolated buildings.

Table 3.3: Scale Factors for each Structure Calculated by Matching Structural Response

Design	1	2	3	4	5	6	7	8	9	10	11	12	13	14	15	16	17
Design Level Earthquakes																	
El Centro	2.15	2.00	2.10	2.20	2.00	2.10	2.00	2.05	1.95	2.20	1.80	2.05	2.05	2.00	2.15	2.20	2.10
Parkfield	0.90	0.95	0.88	0.85	0.88	0.88	0.92	0.90	0.85	0.90	0.75	1.12	1.12	1.12	0.95	0.95	0.92
Bucharest	1.00	0.75	0.68	0.68	0.81	0.73	0.75	0.75	0.70	0.88	0.70	0.92	0.92	0.92	0.88	0.88	0.84
Joshua Tree	1.60	1.75	1.70	1.60	1.60	1.35	1.90	1.90	1.85	1.70	1.30	1.80	1.80	1.75	2.00	2.00	1.95
Average	1.41	1.36	1.34	1.33	1.32	1.27	1.39	1.40	1.34	1.42	1.14	1.47	1.47	1.45	1.50	1.51	1.45
Near Field Earthquakes																	
Northridge (Sim.)	0.78	0.77	0.77	0.73	0.76	0.76	0.70	0.68	0.68	0.82	0.80	0.71	0.71	0.71	0.80	0.80	0.80
Rinaldi	1.00	1.30	1.30	1.30	1.40	1.40	1.70	1.65	1.70	1.60	1.40	2.00	2.00	2.00	1.80	1.80	1.70
Sylmar Hospital	1.15	1.15	1.10	1.15	1.20	1.15	1.15	1.20	1.18	1.37	1.30	1.42	1.40	1.40	1.60	1.60	1.60
Elysian Park	1.10	0.88	0.88	0.89	0.90	0.90	0.80	0.79	0.79	0.83	0.75	0.80	0.80	0.80	0.80	0.79	0.78
Luceme	1.50	1.50	1.55	1.50	1.35	1.30	1.40	1.40	1.50	1.25	1.20	1.55	1.55	1.55	1.30	1.30	1.30
Imperial Valley	1.50	1.40	1.40	1.40	1.30	1.30	1.20	1.20	1.20	1.15	1.10	1.10	1.10	1.10	1.05	1.05	1.05
Average	1.17	1.17	1.17	1.16	1.15	1.14	1.16	1.15	1.18	1.17	1.09	1.26	1.26	1.26	1.23	1.22	1.21

3.4.2 Scaling for Small Earthquakes

One of the disadvantages of seismic isolation is its amplification of small earthquakes that can cause noticeable vibrations which would not normally be observed in a fixed base structure. Two earthquakes have been developed to investigate the effects of retrofits on the response of a seismically isolated building to relatively small earthquakes. The magnitude of El Centro and Parkfield was scaled down by as much as 50 times so that the maximum base shear response divided by the weight of the structure was 0.04, which is below the yield force for the isolation system of the building investigated. This response contains accelerations at a level, approximately equal to 0.04 g, therefore occupants of a building would tend to be aware of this level earthquake. Although a large amount of scaling was necessary, it is considered an appropriate way of representing the vibrations from a small earthquake of this magnitude.

3.5 Time History Response of Unretrofitted Seismically Isolated Structures

Tables 3.4 and 3.5 give the displacement and base shear divided by the total weight of the structure for each of the bilinear seismically isolated structures modelled with a rigid

superstructure, to a number of design level and near field earthquakes. The tables show the average design level and near field earthquake responses, with their coefficients of variation, and comparisons to the UBC responses. As calculated by the UBC, the near field displacement was typically 2.0 times the maximum displacement for each structure. At a maximum of 4% of the average response, the coefficient of variation between the displacements and base shears is small for both design level and near field earthquakes.

3.6 Summary

The maximum displacement and base shear, calculated for each of the rigid generic isolation systems modelled in SAP, matched the UBC design and near field responses respectively. The earthquake records selected to represent design and near field events were found to be appropriate records. The near field records in particular were found to be appropriate by considering four particular factors:

1. It has been stated^{10, 18, 27} that each selected record contains forward directivity near field ground motion.
2. The selected near field records were derived from similar magnitude earthquakes and have similar focal depths and epicentral distances to the design level earthquakes used in this thesis. However the near field records have considerably larger peak ground accelerations and velocities than the design records. Thus it is apparent that forward directivity effects have caused an increase in the magnitude of the ground motion.
3. A low frequency pulse is evident in the time histories of the near field records.
4. After scaling to the UBC design and near field responses respectively, the scale factors for the design and near field records were similar in size even though the magnitude of near field acceleration spectrum was two times that of the design spectrum. Thus it was reasonable that the response of each seismically isolated building to the selected near field records is expected to be considerably larger than the design level response.

The maximum near field displacements of the generic isolation systems were typically 2.0 times their maximum allowable displacements. Therefore it was apparent that the isolation systems need to be retrofitted in order to control isolator deformations for a near field event.

Table 3.4: Displacement Response of each Rigid Seismically Isolated Structures

Design	Design Displacement (mm)			Near Field Displacement (mm)		
	UBC Displacement	Average Earthquake Displacement	Coefficient of Variation	UBC Displacement	Average Earthquake Displacement	Coefficient of Variation
1	140	142	0.019	435	436	0.016
2	248	251	0.029	667	666	0.020
3	248	246	0.015	668	666	0.016
4	248	254	0.014	664	670	0.017
5	199	198	0.031	593	592	0.012
6	199	196	0.018	587	578	0.020
7	311	303	0.010	834	833	0.025
8	311	314	0.024	835	832	0.022
9	311	309	0.020	830	848	0.013
10	233	231	0.014	719	720	0.010
11	233	233	0.037	700	693	0.016
12	447	444	0.007	1161	1148	0.029
13	447	449	0.019	1161	1148	0.017
14	447	450	0.009	1162	1147	0.014
15	336	332	0.030	957	950	0.010
16	336	334	0.028	953	962	0.016
17	336	340	0.016	943	956	0.028

Table 3.5: Base Shear Response of Rigid Seismically Isolated Structures

Design	Design Base Shear / Weight			Near Field Base Shear / Weight		
	UBC Base Shear	Average Earthquake Base Shear	Coefficient of Variation	UBC Base Shear	Average Earthquake Base Shear	Coefficient of Variation
1	0.250	0.252	0.010	0.521	0.522	0.012
2	0.250	0.252	0.023	0.587	0.585	0.019
3	0.250	0.248	0.012	0.585	0.583	0.015
4	0.250	0.255	0.011	0.578	0.583	0.015
5	0.200	0.200	0.019	0.439	0.438	0.010
6	0.200	0.198	0.010	0.424	0.418	0.016
7	0.200	0.196	0.008	0.469	0.469	0.023
8	0.200	0.202	0.019	0.469	0.467	0.020
9	0.200	0.199	0.016	0.463	0.472	0.011
10	0.150	0.149	0.007	0.311	0.311	0.008
11	0.150	0.150	0.017	0.284	0.282	0.012
12	0.200	0.199	0.007	0.485	0.480	0.028
13	0.200	0.201	0.017	0.485	0.480	0.017
14	0.200	0.201	0.008	0.485	0.479	0.013
15	0.150	0.149	0.022	0.352	0.349	0.009
16	0.150	0.150	0.020	0.347	0.350	0.014
17	0.150	0.152	0.011	0.338	0.342	0.024

Chapter 4.

Retrofit of the Rigid Seismically Isolated Structures

4.1 Introduction

As the displacements and base shears of the structures discussed in Chapter 3 exceed their maximum allowable levels, retrofit of the structures was necessary in order to reduce the near field responses. This had to be achieved without adversely affecting the performance of their superstructures. The retrofitted structures must also perform well in response to the design level earthquakes. Attempts to retrofit each of the generic seismically isolated structures modelled with a rigid superstructure are discussed in this chapter using different forms of additional damping.

4.2 Initial Retrofit of Design 7

4.2.1 Introduction

One of the generic seismically isolated structures, Design 7 chosen as the typical structure in Section 2.1.3, was retrofitted with six forms of additional damping devices. These included:

1. Four forms of additional viscous damping,
2. Additional friction damping, and
3. A dual level hysteretic buffer as proposed by Skinner²⁵.

The addition of each of these forms of damping to the rigid seismically isolated structure is discussed in this section.

4.2.2 Procedures for Addition of Damping

4.2.2.1 Addition of Viscous Damping

In one attempt to retrofit the typical seismically isolated structure, a viscous damper was added to the isolation system between the structure and the ground as shown in Figure 4.1.

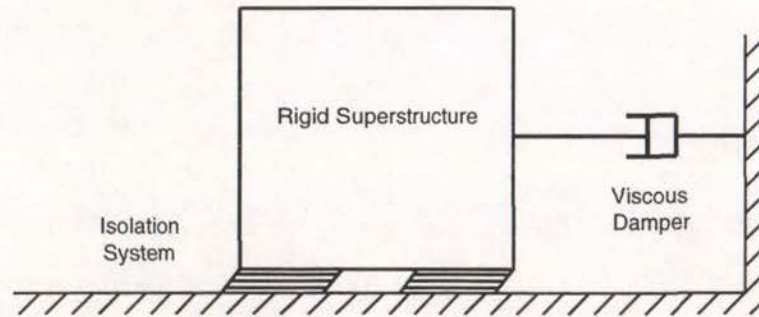


Figure 4.1: Seismically Isolated Building with Additional Viscous Damping at the Base.

The force in a viscous damper is given by Equation 4.1³¹.

$$F_{Damp} = c\dot{u}^\gamma \quad \dots\text{Equation 4.1}$$

where: F_{Damp} = damping force

c = damping constant

\dot{u} = velocity of the system

γ = velocity exponent

For pure viscous damping the velocity exponent in the above equation is equal to 1.0. Reducing the velocity exponent changes the shape of the force displacement curve and increases the area enclosed by the curve assuming the same maximum damping force and displacement, as illustrated in Figure 4.2. For a velocity exponent greater than 1.0 the area is reduced. If the velocity exponent was equal to zero then the damping force would be equal to the damping constant and the shape of the hysteresis loop would be the same as that for friction or Coulomb damping.

Taylor Devices³¹, as described in Section 1.5, can be designed with velocity exponents between 1.0 and 0.3. Therefore viscous dampers with three velocity exponents equal to 1.0, 0.5 and 0.3, each of which are commercially available, were tested as a possible form of

retrofit. A fourth type, with an exponent equal to 1.5 was also tested to determine whether it may be more effective, even though it might not be currently commercially available.

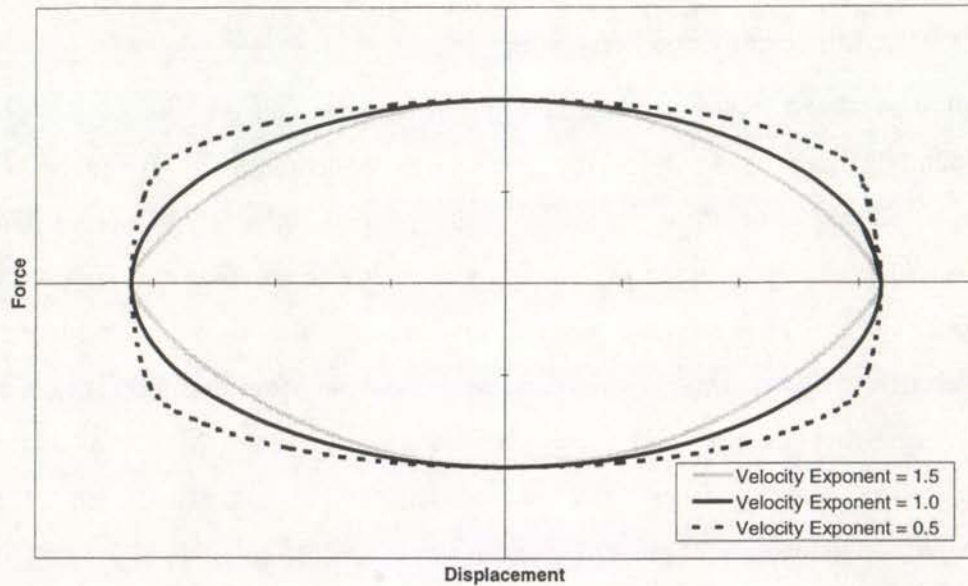


Figure 4.2: Hysteresis Loops for Three Forms of Viscous Damping

Each form of damping was tested at a range of damping levels determined by the damping constant. The damping constant was described in terms of the fraction of critical damping for pure viscous damping, and also the mass and design effective stiffness of the system using Equation 4.2⁵. This equation assumes a single degree of freedom system, an assumption which is valid for seismically isolated structures modelled with a rigid superstructure. For velocity exponents not equal to 1.0, the damping constant must change in order to get the same level of effective damping. For simplicity this distinction was disregarded, therefore, the level of damping given for any form of viscous damping in terms of a percentage of critical damping, refers to the corresponding damping constant for the given level of pure viscous damping.

$$c = 2\xi \sqrt{\frac{Wk_D}{g}} \quad \dots \text{Equation 4.2}$$

Additional damping levels were tested using each of the four velocity exponents for damping constants which correspond to 5, 10, 20, 30 and 40% of critical pure viscous damping. The damping constants vary for each structure depending on the design effective stiffness of its

isolation system. For Design 7 the damping constants divided by the total weight of the structure are 0.026, 0.051, 0.106, 0.154 and 0.205 s/m respectively.

4.2.2.2 Additional Friction Damping

The structure shown in Figure 4.1 was also tested by replacing the viscous damping device with a Coulomb damping device in the form of friction damping. A number of friction dampers have recently been designed for seismic applications^{4, 22, 30}. Friction damping has plastic properties, therefore once the force in the damper exceeds the friction force, the damper is activated, with a constant force. This form of damping was considered to be the most effective form of hysteretic damping, as the area of the hysteresis loop is maximum for a given maximum displacement and force, thus no other forms of hysteretic damping were considered. The damping force in a friction damper is written in terms of a friction coefficient, μ , and the weight of the system as in Equation 4.3.

$$F_{Damp} = \mu W \quad \dots \text{Equation 4.3}$$

The friction damper was modelled as a bilinear system with a high initial stiffness divided by the total weight of the structure (100 /m), zero post yield stiffness and a yield force which corresponds to the damping force. As the weight of the superstructure is fixed, the only variable in the application of friction damping is the friction coefficient. The range of friction coefficients tested were 0.02, 0.05, 0.10 and 0.15. This system could have been modelled using viscous damping with a velocity exponent equal to zero, however the plastic element was considered a more precise representation of a friction damped system and more suitable for modelling in SAP.

4.2.2.3 An Additional Dual Level Hysteretic Buffer

One retrofit suggested by Skinner and McVerry²⁵ was to use a hysteretic buffer. This buffer is activated when an isolation system exceeds its design displacement creating a dual level hysteretic system, the details of which are given in Section 1.5. It was modelled in SAP using a gap and hook element which was activated at the design displacement of the isolation system as illustrated in Figure 4.3.

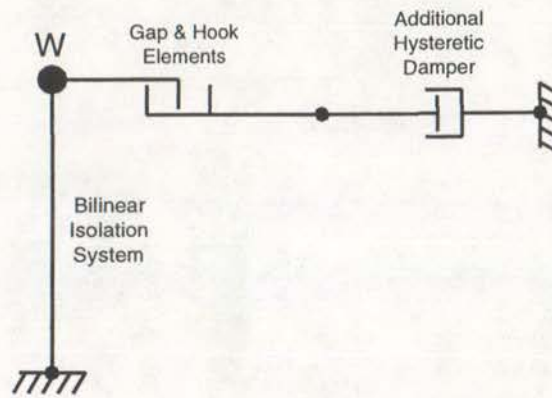


Figure 4.3: Seismically Isolated Structure retrofitted with a Dual Level Hysteretic Buffer

The buffer was assumed to be a friction damper as this is the most efficient form of hysteretic system. The properties of the hysteretic buffer, once the buffer was activated, were similar to the properties of the friction damper discussed in Section 4.2.2.2. The initial stiffness divided by the total weight of the structure was equal to 100 (/m) and the various friction coefficients used were 0.05, 0.10, 0.20, 0.30 and 0.40. These were higher than those used for simple additional friction damping as the hysteretic buffer was activated for a shorter duration than the friction damper.

4.2.3 Average Results of Retrofit

The maximum response after retrofitting Design 7 using the six different damping devices, averaged over the various design and near field earthquakes respectively, is presented in Figure 4.4. Both design level and near field responses are shown. The average design response is described by the set of curves on the left while the near field response is shown by the curves on the right. Each curve represents a different form of damping. The points on each curve indicate different levels of damping, increasing from the right to left. The levels of additional damping used are given in Sections 4.2.2.1 to 4.2.2.3.

Using Figure 4.4 each form of damping was able to be compared graphically. The maximum allowable displacement for this generic isolation system was 430 mm, as given in Table 2.2. By interpolating between the points, the optimal level of damping was found which was able to limit the average near field displacement to the maximum allowable displacement, for each form of additional damping. Dashed lines in Figure 4.4 show how the damping level,

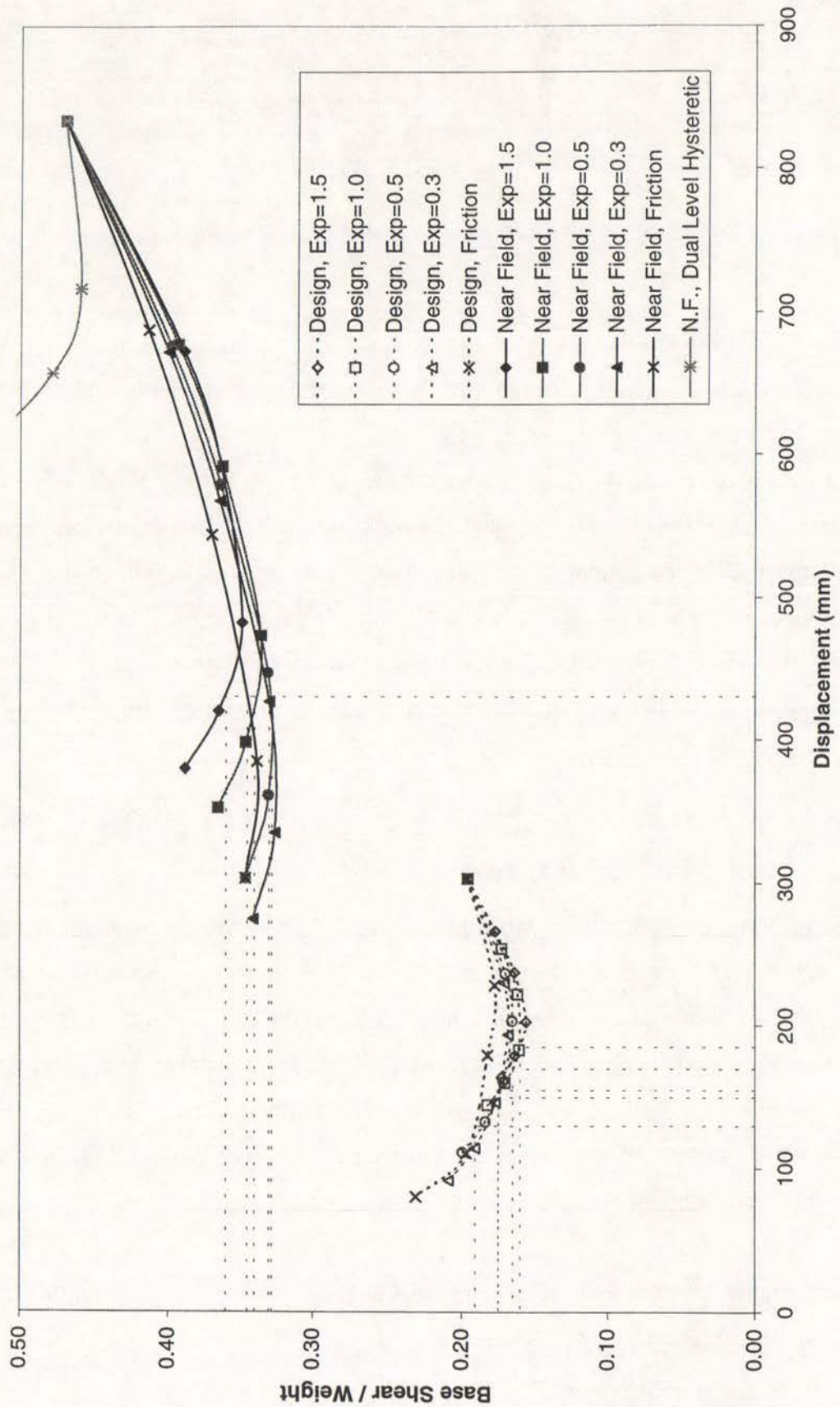


Figure 4.4: Average Design and Near Field Response of Design 7 to a Different Forms of Retrofit

displacements and base shears were interpolated at the optimum level of damping for each form of damping. Using the optimum damping levels the average design response was also estimated from Figure 4.4.

The optimum levels of damping, and the design and near field responses are presented in Table 4.1. The levels of viscous damping are defined in terms of the damping constants divided by the total weight of the structure, while the optimum level of friction damping is defined in terms of the friction coefficient. No retrofit was possible for the dual level hysteretic system because, as shown in Figure 4.4, it was not able to limit the near field displacement response to the maximum allowable displacement.

Table 4.1: Response of Design 7 Retrofitted with Additional Damping

Damping Type	Damping Level c/W (s/m) or μ ()	Design Level		Near Field	
		Displacement (mm)	Base Shear (/W)	Displacement (mm)	Base Shear (/W)
Viscous, Exp. = 1.5	0.143	185	0.160	430	0.360
Viscous, Exp. = 1.0	0.128	170	0.165	430	0.330
Viscous, Exp. = 0.5	0.113	155	0.175	430	0.325
Viscous, Exp. = 0.3	0.097	150	0.175	430	0.325
Friction	0.080	130	0.190	430	0.345
Dual Level Hysteretic	Not Possible				

It can be seen in Table 4.1 that additional viscous damping with a velocity exponents of 0.5 and 0.3 have the lowest near field base shear response. Thus these forms of additional damping were considered to be the most effective for reducing the near field response.

If the maximum allowable displacement was different, the form of damping found to be optimum is also likely to be different. For discussion, the maximum allowable displacement was considered to be at various displacements between the near field displacement and design displacement. The maximum allowable displacement of Design 7 was initially considered to be not much smaller than the near field displacement response, for example at 700 mm. At this displacement, Figure 4.4 shows that the most effective form of damping would have been viscous damping with a velocity exponent of 1.5 as the near field base shear response was smallest for this form of damping. If the maximum allowable displacement was at 500 mm then pure viscous damping would have been the most effective form of damping. The trend

continues until at some point friction damping, although not shown on Figure 4.4, would have been most effective.

The design level response for each form of additional damping at the optimum damping levels is given in Table 4.1. In terms of the design level response, the most effective forms of damping have the smallest design level base shear. It can be seen that these also corresponded to the smallest reduction in design displacement. Therefore, in terms of the design level response, viscous damping with a velocity exponent of 1.5 was the most effective form of retrofit. Each form of additional damping was less effective as its velocity exponent was decreased. At the optimum levels for each form of additional damping, the design base shear was less than the original unretrofitted base shear, suggesting that the response of the structure was improved, however this needed further investigation.

As different forms of damping were found to be most effective using the design and near field base shears, finding the optimum form of damping required some trade off between the optimum design response and optimum near field response. This is discussed further in Section 4.4.3.

4.2.4 Explanation of the Response for the Different Forms of Additional Damping

As explained in Chapter 1, the amount of damping in a system is defined by the area enclosed by the hysteresis loop from the force displacement characteristics of the damper. Viscous damping with a high velocity exponent has a smaller hysteretic area than viscous damping with a low velocity exponent based on the same maximum force and displacement. In turn friction damping has the largest hysteretic area. Therefore in order to achieve the same amount of damping and with the same maximum displacement, the force in a pure viscous damper, for example, must be larger than the force using friction damping. However, the viscous damping force is zero when the velocity of the system is zero, which tends to be when deformations in the isolation system are maximum. In contrast the force in a friction damper is maximum at all times. It can be shown that with low levels of additional damping, the base shear is equal to the sum of the forces in the isolation system at the maximum displacement. Therefore at low levels, pure viscous damping is more effective than friction damping as the viscous damping force is zero while the friction damping force is non-zero at the maximum

displacement. However, at higher levels of damping, the damping force using viscous damping becomes large enough so the maximum base shear no longer occurs when the displacement of the system is also maximum. If the combination of damping, inertia and elastic forces is larger than the combination using friction damping, then friction damping becomes more effective. Various forms of viscous damping with velocity exponents less than 1.0 have responses between those for additional pure viscous damping and friction damping.

As the maximum base shear contains the largest combination of forces in a structure, it was considered to be a good way of measuring the effectiveness of the various forms of additional damping. This is confirmed in later analyses of multi-storey seismically isolated buildings.

4.2.5 Variability Between Individual Earthquakes

As mentioned previously, the earthquakes were scaled so that the maximum unretrofitted design and near field displacement respectively, were within five percent of the UBC design responses. This enabled a measure of the variability between the individual earthquakes in response to various retrofit procedures to be determined. The individual earthquake responses were compared at the optimum levels using additional viscous damping with a velocity exponent of 0.5, and friction damping.

Figure 4.5 illustrates the response to the various design level and near field earthquakes when a viscous damper, with a velocity exponent equal to 0.5, was added. The design level response was quite variable, which is indicative of the wide variation in properties of these earthquakes. The base shear of Joshua Tree, the design level earthquake with the least favourable response, only just exceeds the unretrofitted design base shear at high levels of additional damping. Using this response it appears that while additional damping is able to control forward directivity effects it is less effective for backward directivity ground motion.

The near field response has relatively small variation between the different earthquakes and is close to the average response. The only exception is the Rinaldi response, which results in a smaller reduction in maximum displacements and base shears than the other earthquakes when additional damping is added. The Rinaldi record is taken from the same earthquake as the Sylmar Hospital record suggesting that it is not the type of earthquake that has caused the

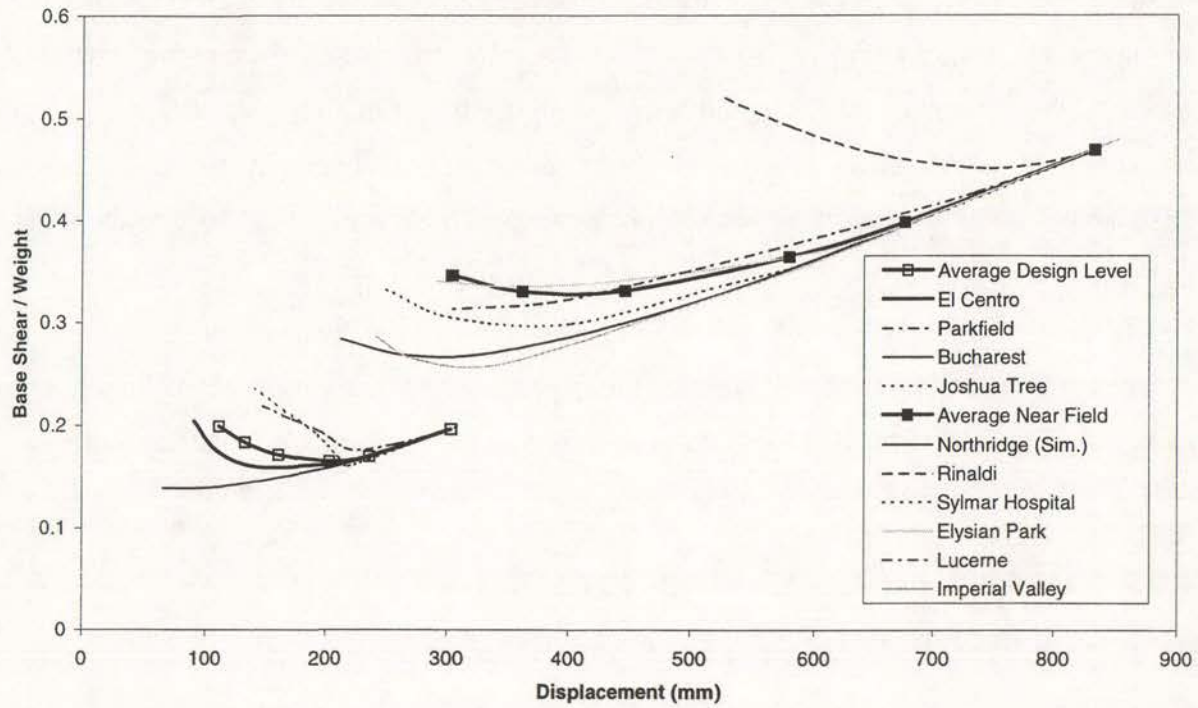


Figure 4.5: Design 7 Response of Individual Earthquakes Retrofitted using Viscous Damping, Velocity Exponent of 0.5.

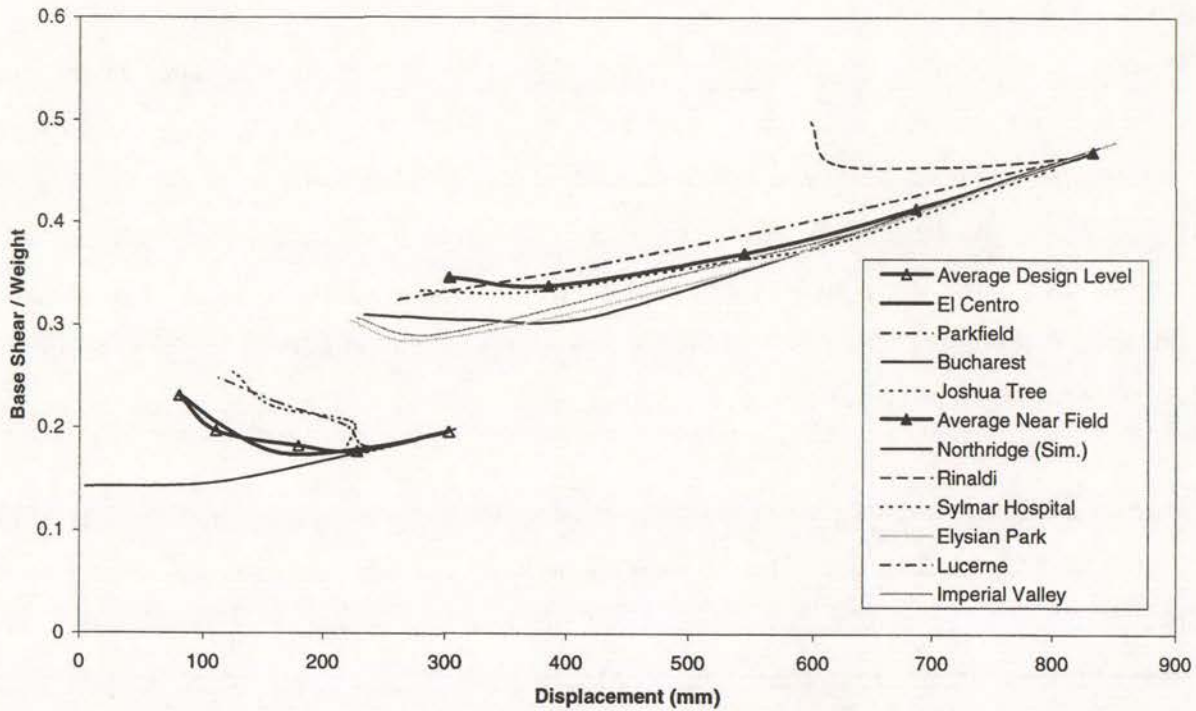


Figure 4.6: Design 7 Response of Individual Earthquakes Retrofitted with Friction Damping.

variation between this record and the other near field earthquake records. A detailed analysis of the site and frequency content of the ground accelerations would need to be undertaken in order to determine the true cause of such a large variation.

The response of the individual earthquakes retrofitted with friction damping is shown in Figure 4.6, which is similar to Figure 4.5. One difference compared to Figure 4.5 is that the soft soil Bucharest response is reduced to the extent that the response at high levels of friction damping appears to be elastic. Although such high levels of damping would not be required, it highlights a possibly greater sensitivity of friction damping over viscous damping to different earthquakes. This sensitivity is particularly apparent for the design level earthquakes. The variation between earthquakes is investigated further in Chapter 6.

4.2.6 Optimum Form of Additional Damping in the Structure

Comparing the average responses and investigating the variability between the individual earthquake responses for each of the various forms of additional damping enabled the most effective form of damping for Design 7 to be determined. In terms of minimising near field response, the most effective form of damping was viscous damping with a velocity exponent of around 0.3 to 0.5. In terms of the design level earthquakes viscous damping with larger velocity exponents of 1.0 to 1.5 were more effective. Therefore a compromise has to be made between the two responses. This is investigated using the other generic seismically isolated structures.

Of the six forms of additional damping modelled in Section 4.2, the other seismically isolated structures were investigated with two forms of additional viscous damping, one with a velocity exponent of 0.5 and another with a velocity exponent of 1.0. Additional friction damping was also investigated. Viscous damping with a velocity exponent of 1.5, although effective for the design level earthquakes, was ineffective for the near field earthquakes. There was also doubt over its commercial availability, thus it was excluded in following analyses. Viscous damping with a velocity exponent equal to 0.3 was not used in further analyses as its response was similar to the response using viscous damping with an exponent of 0.5.

4.3 Mass Tuned Damping

4.3.1 Introduction

Although Section 4.2 has found forms of additional viscous damping and friction damping to be effective for retrofitting a generic seismically isolated structure, it was hypothesised that mass tuned damping may also be effective. There is no apparent record of an investigation using mass tuned damping for mitigating the effects of near field ground motion, thus an attempt to implement it is discussed. The application of mass tuned damping is tested on Design 7.

In brief, mass tuned damping is a system where a mass, for example, five percent of a given structure's mass, is attached to the structure through a spring and damper. The system works by transferring the energy of vibration from the structure into the additional mass which is free to vibrate, thus reducing the amplitude of vibration in the structure. The vibration of the added mass is reduced over time with damping provided by an additional damper.

4.3.2 Application of Mass Tuned Damping to Seismically Isolated Structures

4.3.2.1 Introduction

It was proposed that a mass tuned damper tuned to the natural frequency of a given structure at its predicted response, could mitigate the effects of the near field earthquakes. Mass tuned damping is not able to reduce the amplitude for the first oscillation of a harmonic system, but tends to reduce the amplitude of later vibrations⁸. Therefore, it was theorised that earthquake

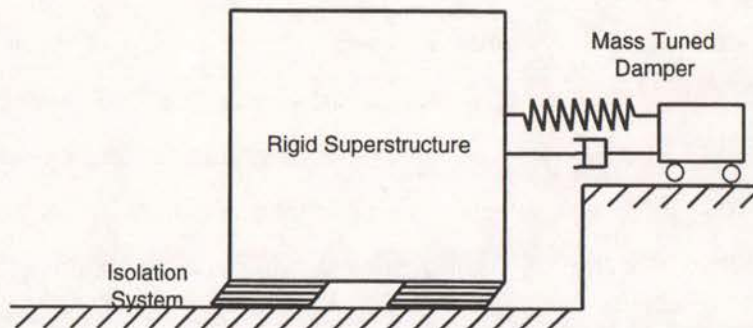


Figure 4.7: Seismically Isolated Building with a Rigid Superstructure Retrofitted with a Mass Tuned Damper.

energy from ground motion which reaches the site prior to the near field pulse reaching the site, would be able to transfer enough energy into the mass tuned damper to limit the near field response to an acceptable level. Consequently, an additional mass attached to the rigid superstructure using a spring and damper, as shown in Figure 4.7, was tested with a range of stiffness and damping properties.

4.3.2.2 Calculation of Appropriate Masses

Davidson⁸ has found that an appropriate mass for the added damper is approximately 0.05 times the mass of the structure. A range of masses was tested from 0.0125 times the mass of the structure, at one quarter of that suggested, to 0.05. The masses used were 0.0125, 0.025, 0.0375 and 0.050 times the total weight of the structure.

4.3.2.3 Calculation of Appropriate Spring Stiffness

The period ratio, as the term suggests, is the ratio of the natural period of the mass tuned damper to the natural period of the structure. Mass tuned dampers with a range of period ratios were investigated. For a given mass the period of the mass tuned damper is dependent on the stiffness of the mass tuned damper spring. A range of spring stiffness' were calculated to give the mass tuned damper a range of natural periods using ratios of the design natural period equal to 2.5 seconds.

Davidson found that a staircase application⁸, a frequency ratio of 0.975 was the most effective for reducing the vibrations. This corresponds to a period ratio of 1.025. It was expected that the mass tuned damper would work most effectively at the natural period of the near field response as this is the response which it is trying to reduce. The near field effective period for Design 7 is 2.67 seconds from Appendix 4, therefore the ratio of the near field effective period to the design effective period is 1.069. Thus the period ratio expected to be most effective for controlling the near field response is 1.025×1.069 which is equal to 1.09.

To test this theory, a range of period ratios was used to calculate a range of spring stiffness' for the various mass tuned dampers. Initially a mass of 0.0125 times the mass of the seismically isolated structure was used. Once an optimum period ratio was found, a smaller

range of period ratios was used to calculate responses for the larger masses, as given in Section 4.3.2.2.

4.3.2.4 Addition of Damping to Mass Tuned Damper

Once the optimum level of stiffness was found for an undamped mass tuned damper, the effect of adding damping was calculated. Both pure viscous damping and friction damping were attempted. A range viscous damping constants were calculated, in terms of the percentage of critical damping using Equation 4.4, by again assuming the mass tuned damper was an independent single degree of freedom system.

$$c_{MT} = 2\xi_{MT}\sqrt{m_{MT}k_{MT}} \quad \dots\text{Equation 4.4}$$

where: c_{MT} = damping constant for mass tuned damping

ξ_{MT} = damping coefficient for mass tuned damping

m_{MT} = mass of tuned damper

k_{MT} = stiffness of mass tuned damper spring

The range of viscous damping tested, in terms of percentage of critical damping, was; 2%, 5%, 10% and 20%. The velocity exponent was assumed to be equal to 1.0 for all levels of damping.

Friction damping was modelled by replacing the viscous damper as shown in Figure 4.4 by a plastic non linear element. The properties of the plastic element were described by a large initial stiffness, 100 times the total weight of the damper (/m), zero post-yield stiffness and a yielding exponent assumed to be 100. The only other variable was the yield force, which was used to describe the level of friction damping. This was calculated in terms of the friction coefficient using Equation 4.5.

$$F_{MT} = \mu_{MT}m_{MT}g \quad \dots\text{Equation 4.5}$$

where: F_{MT} = Force in the damper of the mass tuned damper

μ_{MT} = friction coefficient for mass tuned damper

The friction coefficients tested were; 0.02, 0.05, 0.10 and 0.15.

4.3.3 Mass Tuned Damping Results

4.3.3.1 Results of Mass Tuned Damping with Various Period Ratios

The maximum displacement of the structure in response to each of the near field earthquakes using mass tuned dampers containing different period ratios, is shown in Figure 4.8. The mass of the damping device divided by the total mass of the seismically isolated structure is equal to 0.0125. At this stage there is no additional viscous or friction damping in the system. As the maximum base shear force is proportional to the maximum displacement, it was only necessary to consider displacements. The displacements have been normalised so that the response is equal to the mass tuned damped displacement divided by the unretrofitted displacement for each earthquake. The average displacement for all the earthquakes is indicated by the bold curve.

Using the average response, Figure 4.8 shows that the reduction in displacement is a maximum at a period ratio of around 1.15, which is close to the predicted ratio of 1.09. However, the maximum reduction in the average displacement response is only equal to 6%. Even the ground motion showing the largest maximum displacement reduction, Sylmar Hospital, only has a reduction of 11%. This is not effective for retrofitting the structure, as a 48% reduction is required to reduce the near field displacement response to the maximum allowable displacement response.

The mass of the mass tuned damper was increased to see if the effectiveness of the mass tuned damping could be improved. The reduction in displacements achieved using larger dampers is illustrated in Figure 4.9. The plot shows that the optimum period ratio for the average response of the structure the dampers of larger mass was close to 1.3, further from the expected value than for the smaller mass. This suggests that the method for predicting the optimum spring stiffness needs to be revised. The average reduction in maximum displacement response at the optimum period ratio, for the mass tuned damper with the largest mass was 11%. This was improved compared to the earlier response, but was still not effective in reducing the near field displacement response to the maximum allowable response. The practical implications of such a large mass would also make such a retrofit difficult.

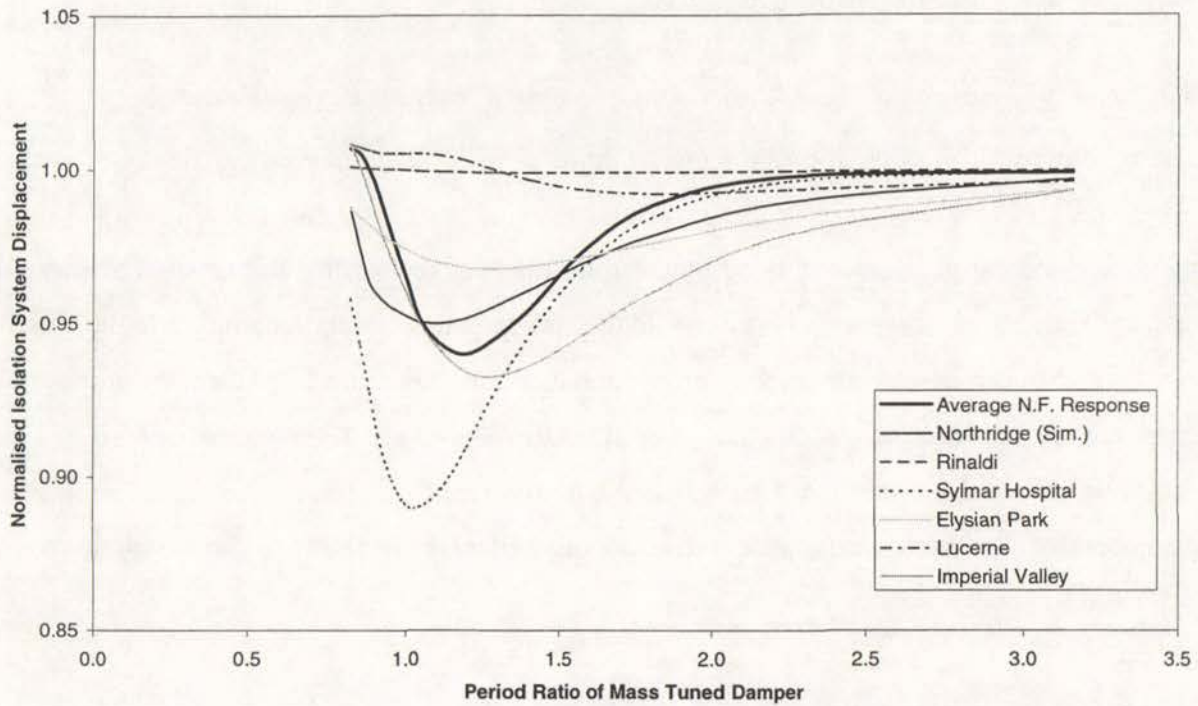


Figure 4.8: Normalised Near Field Displacement with Additional Mass Tuned Damping

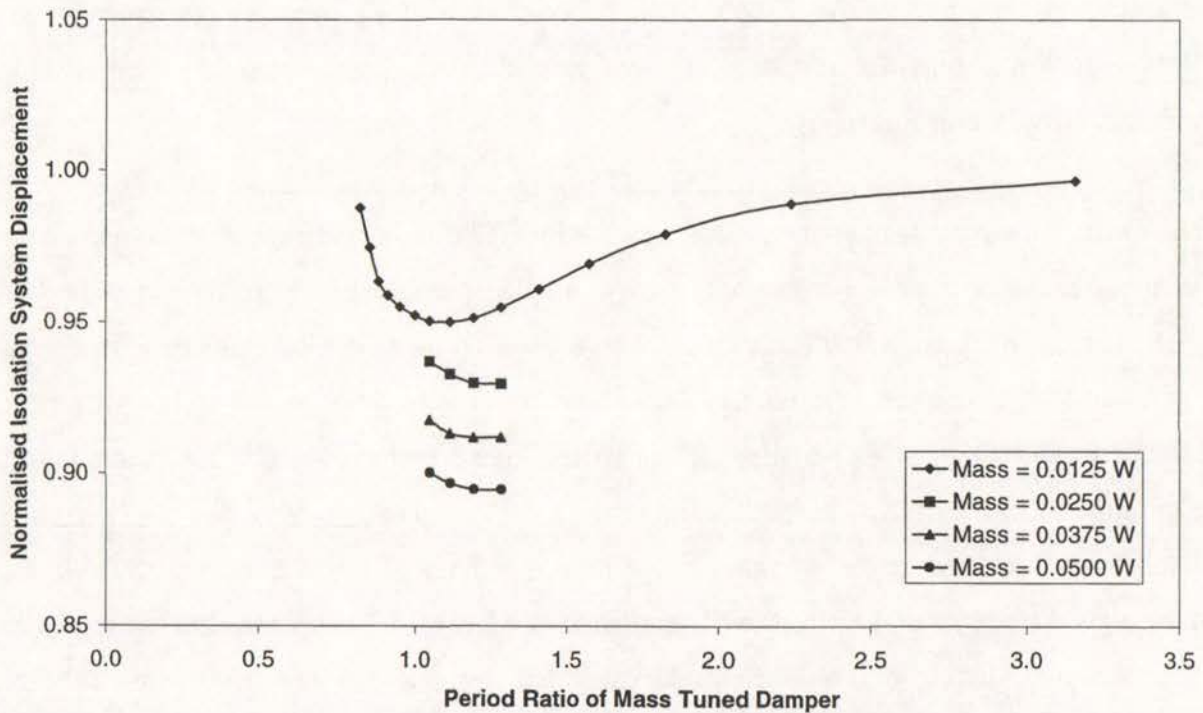


Figure 4.9: Response of Design 7 Retrofitted with Mass Tuned Dampers of Different Masses

4.3.3.2 Results of Adding Damping to the Mass Tuned Damper

The effect of adding both viscous and friction damping to the mass tuned damping system was investigated in a further attempt to improve the system. One mass tuned damping system with a mass of 0.0125 W and stiffness corresponding to a period ratio of 1.1 was analysed with four levels of viscous damping and four levels of friction damping as described in Section 4.3.2.4.

Time histories for the structure and the mass tuned damper in response to Sylmar Hospital, in Figure 4.10a, show that with no damping in the system the mass tuned damper oscillates continuously. Just a small level of damping, for example 2% as shown in Figure 4.10b will decrease the amplitude over a period of time and decrease the maximum displacement of the mass tuned damper.

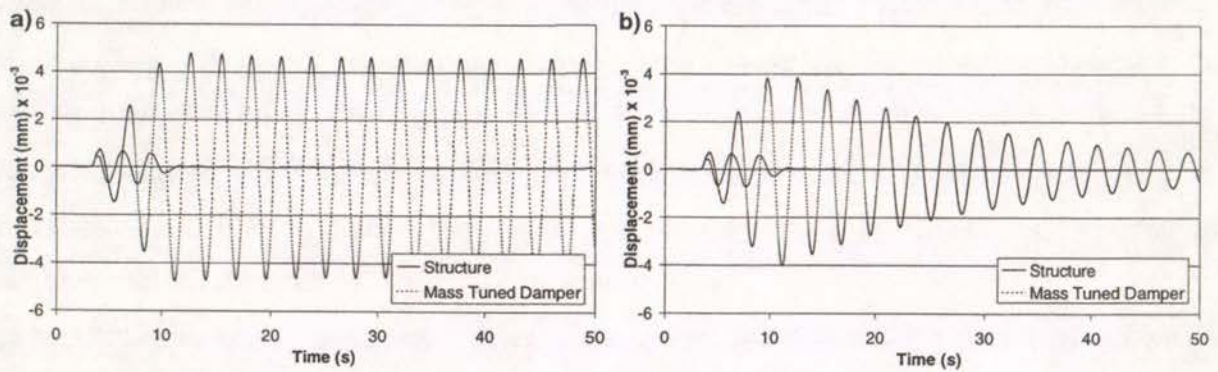


Figure 4.10: Time History Response of Mass Tuned Damper Additional Damping

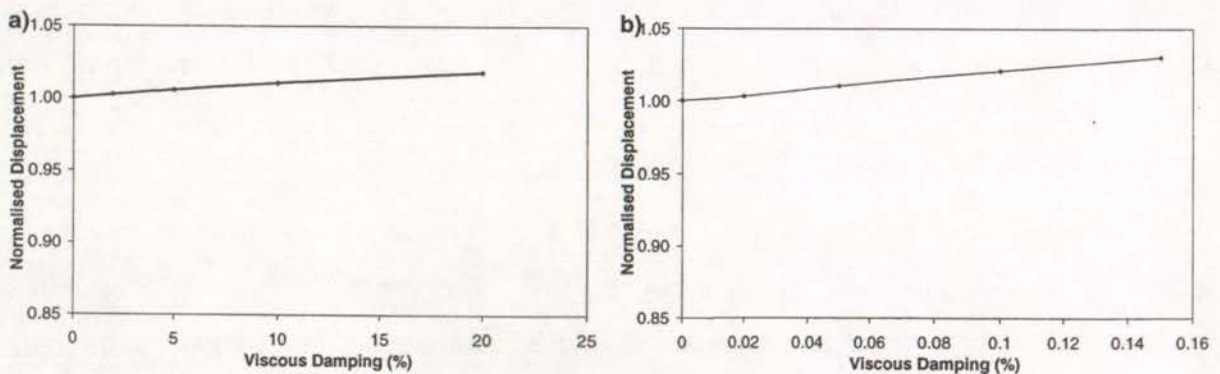


Figure 4.11: Response of with Viscous Damping (a) and Friction Damping (b) in the Mass Tuned Damper

The average maximum displacement of the structure using different levels of damping is shown in Figure 4.11 normalised to the undamped displacement. It shows that the effects of

adding viscous damping and friction damping are similar. However it also shows that adding damping is not able to further decrease the displacement response of the structure, thus unable to increase the effectiveness of the mass tuned damper. For maximum effectiveness, as little damping as possible is preferred in the mass tuned damper, although this is not effective in retrofitting the seismically isolated structure for near field ground motions.

4.3.4 Discussion of Mass Tuned Damping

It has been shown that mass tuned damping is largely ineffective for reducing the response of a structure in response to the near field earthquakes. The magnitude of the average reduction in displacement is too small and the variation between the various earthquakes is too large. A probable cause for the variation in response can be illustrated by comparing the unretrofitted time history for the Sylmar Hospital, which responded most favourably to mass tuned damping, to the Lucerne time history, which was least favourable. The maximum displacement in response to Sylmar Hospital ground motion was in the second oscillation of the isolation system while the maximum displacement in response to Lucerne ground motion was in the oscillation, as shown in Figure 4.12. Therefore during the Sylmar Hospital response energy had been transferred into the mass tuned damper prior to the maximum response being reached and reduced the maximum displacement. In contrast, for the response to the Lucerne record the earthquake energy remained in the seismically isolated structure at the maximum response. It appears the hypothesis that the initial earthquake vibration, which occurs before the near field pulse reaches the site, is not effective in transferring energy into the mass tuned damper to reduce the near field response. If there was more of a build-up in response before the near field pulse reached the site then mass tuned damping may have been effective.

It has been confirmed that mass tuned damping is able to reduce the steady state response of a system but has little effect on the transient response. Because the response to a near field earthquake appears to be largely transient, mass tuned damping has limited application in the retrofit of structures for near field earthquakes. If mass tuned damping was to be implemented in a given structure, the type of earthquake expected at a site should not contain a sudden pulse at the beginning of the time history. A more gradual build up is required. If the type of earthquake expected is known to be of this type, then mass tuned damping may be useful where only a relatively small modification to the response is necessary in order to

retrofit the structure. At this stage there is too much uncertainty in prediction of earthquakes for it to be used in such an application with confidence.

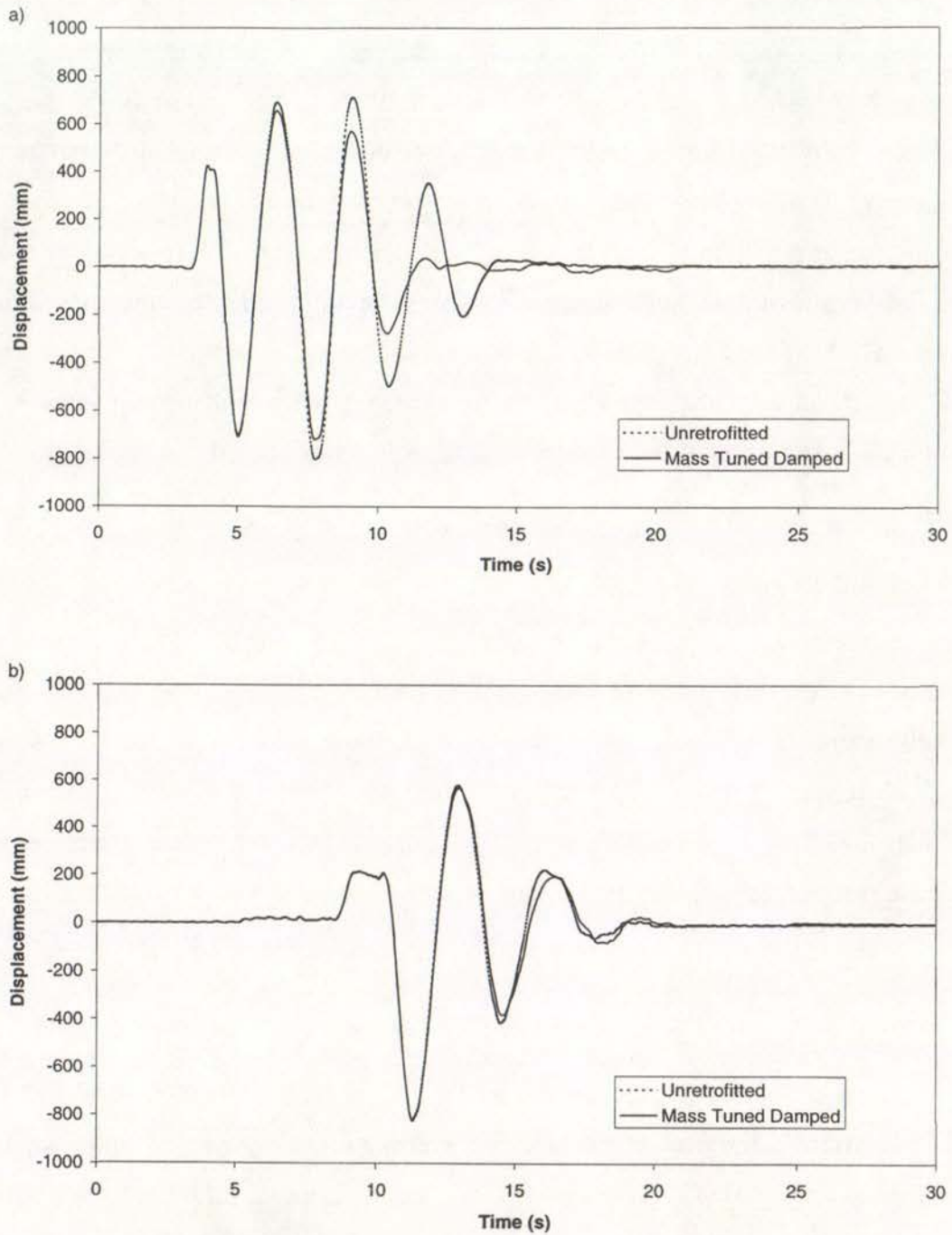


Figure 4.12: Displacement Response Time History for Sylmar Hospital (a) and Lucerne (b)

4.4 Results of Retrofitting all of the Generic Seismically Isolated Structures with Additional Damping

4.4.1 Introduction

It has been found that three forms additional damping; viscous damping with velocity exponents of 1.0 and 0.5, and friction damping are likely to be optimal for retrofitting the generic seismically isolated structures. Other forms of damping included hysteretic buffers and mass tuned damping have been discounted as possible forms of retrofit. Therefore, the 17 seismically isolated structures modelled with rigid superstructures, were analysed with each of these three forms of damping. From the results, the optimum form of damping and level of damping was calculated for each structure. Retrofitting a number of isolation systems allowed the structures to be compared, and relationships between their properties and the levels of additional damping required for an appropriate retrofit could be established.

4.4.2 Retrofit Results

The response of each structure is presented in Figures 4.13 to 4.16. These show results of retrofitting with varying levels of each form of additional damping in terms of isolation system displacements and base shears. Figure 4.13 illustrates the response of the structure with a design effective period of 1.5 seconds. Similarly, Figure 4.14 shows the response of each structure with an effective stiffness of 2.0 seconds, Figure 4.15 shows structures with an effective stiffness of 2.5 seconds, and Figure 4.16 shows structures with an effective stiffness of 3.0 seconds. The design base shear, design equivalent viscous damping and post yield stiffness of each structure is listed in Table 2.1.

As in Figure 4.4, the set of three curves on the left of each plot in Figures 4.13 to 4.16 represent the average design level response of each structure and the set of curves on the right represent the average near field response. Each curve describes a different form of damping; two forms of viscous damping and friction damping. The unretrofitted design and near field response is represented by the point with the largest displacement in each of the two sets of curves respectively. Therefore, the points on each of the curves represent increasing levels of damping as the displacement response of the isolation system decreases.

The dashed line on each of the plots represents the maximum allowable displacement of the isolation system. This is the limiting displacement for retrofitting in response to the near field earthquakes. It was used to find the level of damping required for the optimum retrofits.

4.4.3 Optimum Solutions

4.4.3.1 Optimum Near Field Response

The optimum level of damping was calculated by interpolating to find the level of additional damping for which the average near field displacement was equal to the maximum displacement for each form of damping in each structure. The optimum form of damping was selected from the form of damping with smallest near field base shear between the various forms of damping at the maximum allowable displacement. For certain structures, such as Design 12 in Figure 4.16, the average near field base shear is actually smaller at a larger level of damping than that required to limit the displacement to the maximum allowable displacement. However, if any, there is only a small difference in near field base shears between the minimum base shear and that at the level of damping which limited the near field displacement to the maximum allowable displacement. It was beneficial to use as little damping as possible for minimal impacts to the design level response and floor accelerations, as will be illustrated in following sections. Therefore, the optimum level of damping was taken as that at the maximum allowable displacement.

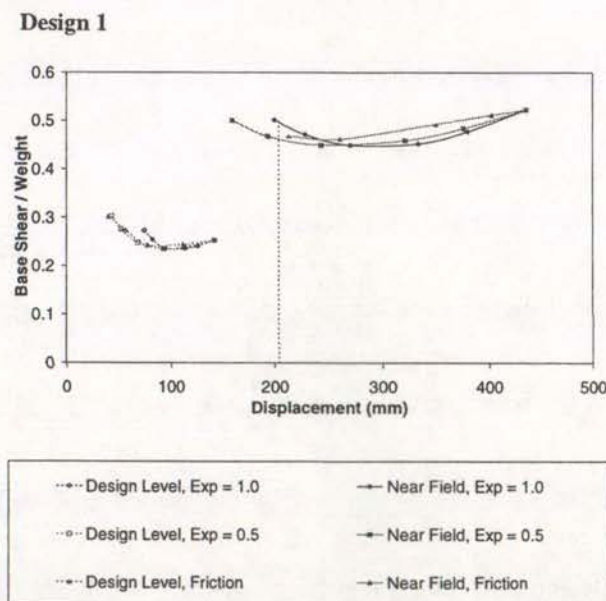
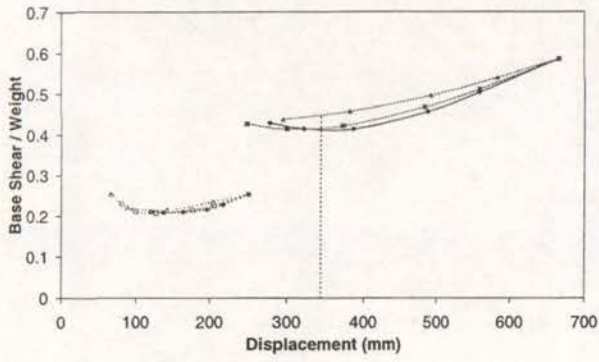
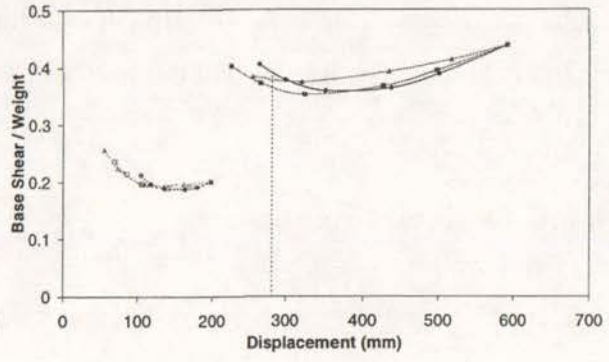


Figure 4.13: Average Design and Near Field Response of T = 1.5s Structure with Additional Damping

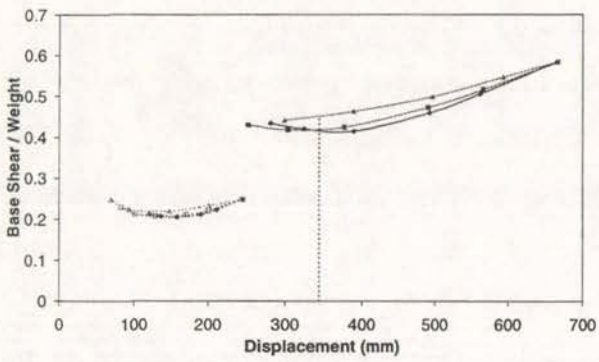
Design 2



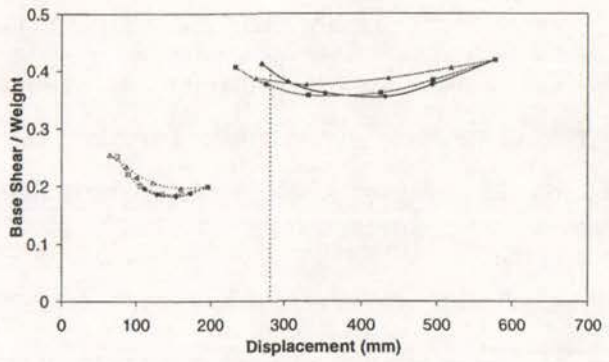
Design 5



Design 3



Design 6



Design 4

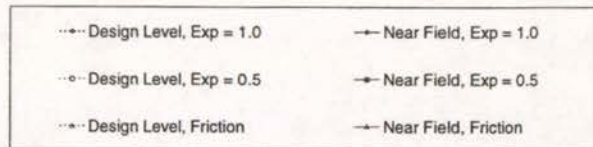
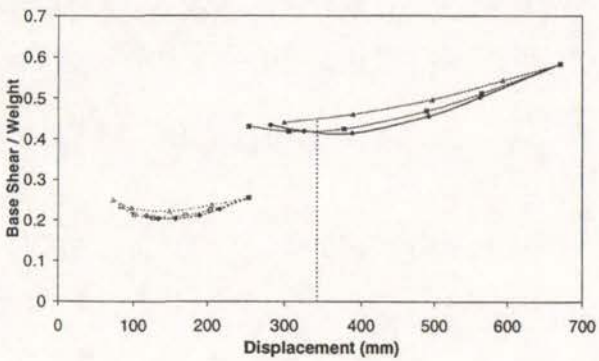
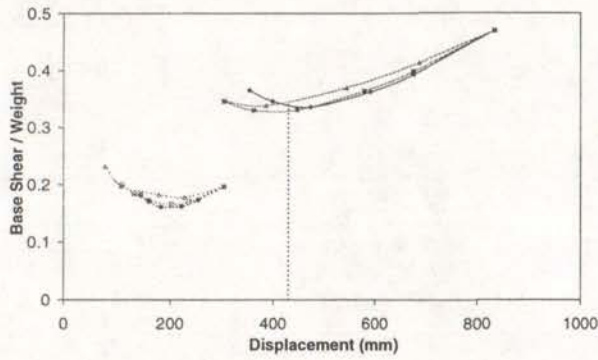
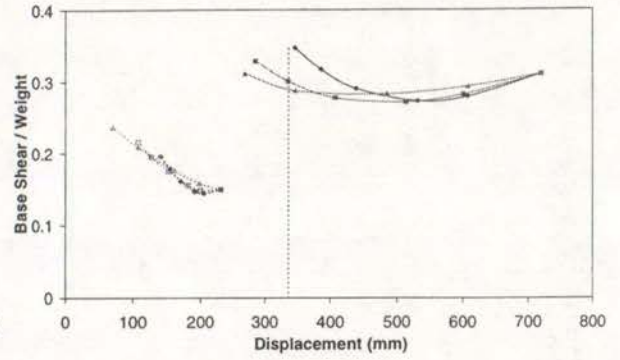


Figure 4.14: Average Design and Near Field Response of T = 2.0s Structures with Additional Damping

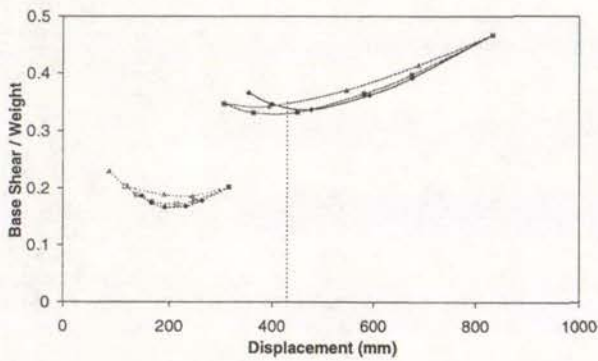
Design 7



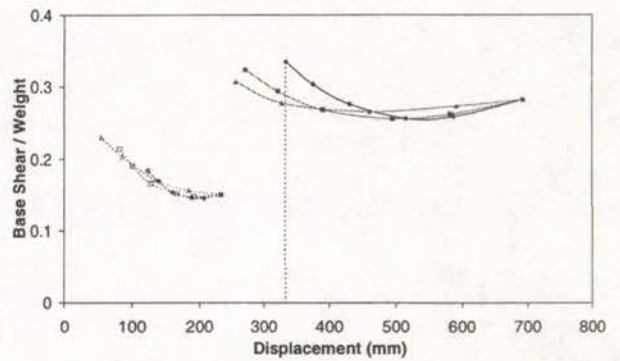
Design 11



Design 8



Design 10



Design 9

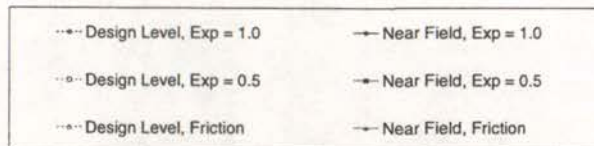
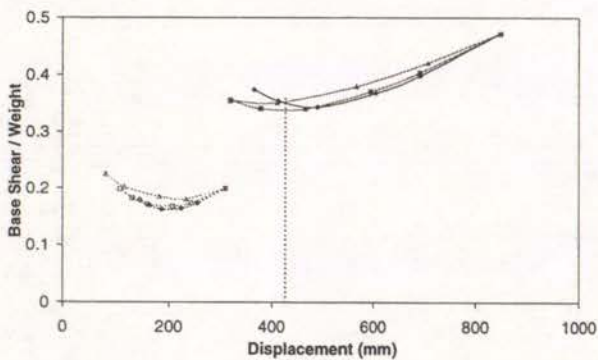
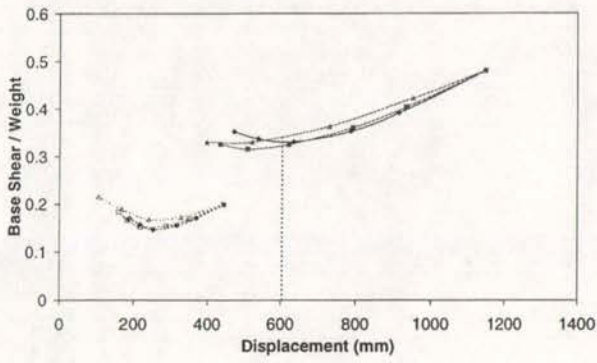
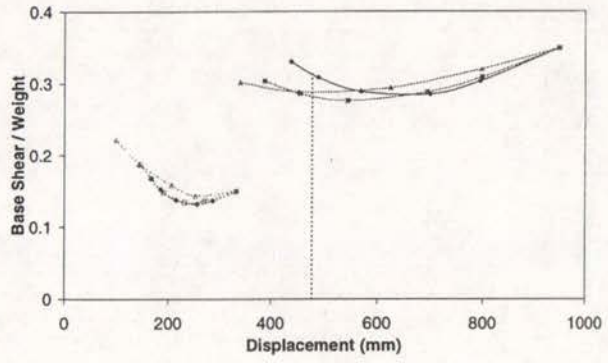


Figure 4.15: Average Design and Near Field Response of T = 2.5s Structures with Additional Damping

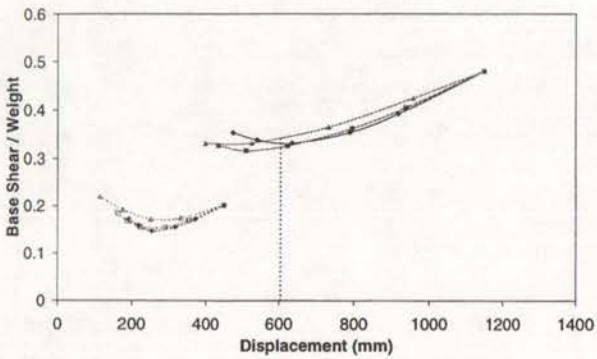
Design 12



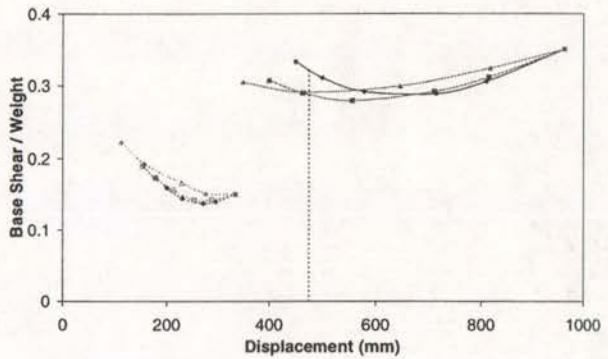
Design 15



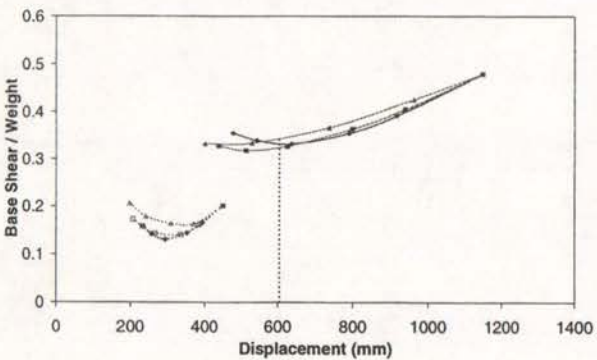
Design 13



Design 16



Design 14



Design 17

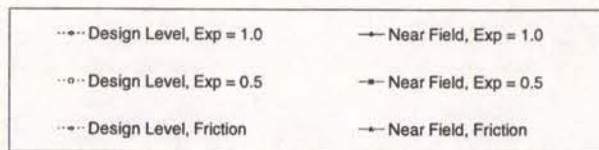
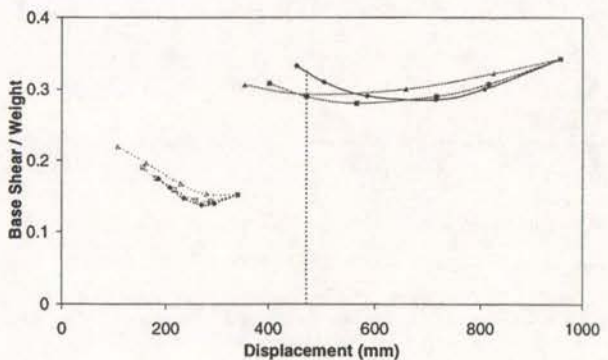


Figure 4.16: Average Design and Near Field Response of $T = 3.0s$ Structures with Additional Damping

The form of additional damping, optimum level of damping, and the reduction in the near field displacement and base shear response for each structure is given in Table 4.2. Viscous damping levels have been calculated in terms of the damping constant divided by the total weight of the structure, while friction damping is given in terms of the friction coefficient. Negative values for the design base shears imply an increase in response. Subdivisions have been made between structures with different equivalent linear properties.

Table 4.2 shows that 12 of the 17 structures have been optimally retrofitted using viscous damping with a velocity exponent of 0.5. Two structures were optimally retrofitted with friction damping, and the remaining three used viscous damping with a velocity exponent of 1.0, for optimum retrofits. Therefore it was apparent that viscous damping with a velocity exponent of 0.5 was generally the better form of damping in terms of reducing the near field displacement with a minimum level of near field base shear. It can be shown that using this form of damping, for those structures where it was not the optimal form of retrofit, results in a small increase in base shear.

Table 4.2: Optimum Retrofit of Seismically Isolated Structures in terms of Near Field Response

Design	Damping Type	Damping Level c/W (s/m) $\mu()$	Reduction of Unretrofitted Near Field Response using Optimal Retrofit (%)	
			Displacement	Base Shear
1	Visc. Exp. = 0.5	0.239	53	12
2	Visc. Exp. = 1.0	0.173	48	30
3	Visc. Exp. = 1.0	0.173	48	29
4	Visc. Exp. = 1.0	0.179	49	29
5	Visc. Exp.= 0.5	0.173	52	17
6	Visc. Exp.= 0.5	0.186	51	10
7	Visc. Exp.= 0.5	0.113	48	31
8	Visc. Exp.= 0.5	0.113	48	29
9	Visc. Exp.= 0.5	0.123	50	29
10	Friction	0.105	53	7
11	Friction	0.095	52	1
12	Visc. Exp.= 0.5	0.090	47	32
13	Visc. Exp.= 0.5	0.090	47	32
14	Visc. Exp.= 0.5	0.094	47	32
15	Visc. Exp.= 0.5	0.120	50	20
16	Visc. Exp.= 0.5	0.124	51	19
17	Visc. Exp.= 0.5	0.128	51	15

Table 4.3: Optimum Retrofit of All Seismically Isolated Structures in terms of Design Response

Design	Damping Type	Damping Level c/W (s/m)	Reduction of Unretrofitted Design Response using Optimal Retrofit (%)	
			Displacement	Base Shear
1	Visc. Exp. = 0.5	0.239	58	-7
2	Visc. Exp. = 1.0	0.173	40	17
3	Visc. Exp. = 1.0	0.173	41	17
4	Visc. Exp. = 1.0	0.179	45	21
5	Visc. Exp.= 0.5	0.173	55	-5
6	Visc. Exp.= 1.0	0.237	46	-6
7	Visc. Exp.= 1.0	0.133	44	18
8	Visc. Exp.= 1.0	0.133	44	18
9	Visc. Exp.= 1.0	0.143	45	17
10	Visc. Exp.= 0.5	0.154	46	-31
11	Visc. Exp.= 0.5	0.143	53	-20
12	Visc. Exp.= 1.0	0.094	46	25
13	Visc. Exp.= 1.0	0.094	47	28
14	Visc. Exp.= 1.0	0.098	38	33
15	Visc. Exp.= 1.0	0.137	46	-4
16	Visc. Exp.= 1.0	0.145	43	-10
17	Visc. Exp.= 1.0	0.157	43	-12

4.4.3.2 Optimum Design Level Response

The optimal forms of damping were calculated in terms of design response by finding the form of damping which resulted in the smallest average design level base shears. The level of damping was still taken as that needed to limit the near field displacement response to the maximum allowable displacement. The results for each structure are presented in Table 4.3. This table shows that the optimum form of damping at the design response for 13 out of the 17 structures is additional pure viscous damping.

4.4.3.3 Discussion

When retrofitting a seismically isolated building and it is found that one particular form of additional damping is optimal for both design and near field earthquakes then naturally that form would be used. If the design and near field responses are optimal with different forms of damping then a decision as to which form is most appropriate has to be made. Consider a structure, which was retrofitted optimally using pure viscous damping in terms of design base shear, and viscous damping with a velocity exponent of 0.5 in terms of near field base shear.

This was common for the rigid generic seismically isolated structures. It can be shown that there is typically a five percent increase in the design base shear compared to the optimum value, when retrofitting the structure using viscous damping with a velocity exponent of 0.5. There is a similar increase in near field base shear when retrofitting the structure with pure viscous damping. Therefore it is difficult to determine which is most effective. However, a design level earthquake is considered more likely than a near field level earthquake. Therefore, it may be argued that it is better to use the optimum form of damping that has the least impact on the design level response and allow more damage in the superstructure during a near field earthquake. Using this reasoning pure viscous damping is generally the most effective form of damping. This compromise will be further discussed in the following chapters.

4.4.4 Comparison of Retrofits for Seismically Isolated Structures

4.4.4.1 Introduction

A number of generic seismically isolated structures were studied so that comparisons between structures could be made. This was hoped to enable the prediction of a suitable retrofit for any given structure designed using the same UBC provisions.

4.4.4.2 Comparison of Structures with the Same Equivalent Linear Properties

The response of the different seismically isolated structures with the same equivalent linear properties but different bilinear properties was compared using Figures 4.13 to 4.16. The structures compared had the same design effective stiffness, equivalent viscous damping, displacement and base shear force. Each of the plots on the left hand side and right hand side respectively, of Figures 4.13 to 4.16, represent seismically isolated structures with the same equivalent linear properties and different bilinear properties.

As Figures 4.13 to 4.16 show, the responses are similar for isolation systems with the same equivalent linear properties. This similarity is illustrated numerically in Table 4.2, where the different equivalent linear structures are separated to identify the structures with the same linear properties. The optimum form of damping in terms of both design and near field response is the same for each structure with the same equivalent linear properties, with one

exception. The range of optimum additional damping levels is within 10%. Typically there is a 2 to 3% increase in the additional damping level required between a structure with a post yield stiffness of 0.02 and one with a post yield stiffness of 0.1. Then again there is a 2 to 3% between post yield stiffness' of 0.1 and 0.2, assuming the structures have the same equivalent linear properties. This increase is reasonable, as the structures with a post yield stiffness of 0.02 have a lower yield force, therefore dissipate more energy at displacements lower than the design displacement, than the structure with the post yield stiffness of 0.2 for example. As a structures is vibrating at displacements lower than the design displacement for the majority of the duration of an earthquake, then a greater total energy is dissipated by the structure with the lower velocity exponent than the structure with a higher velocity exponent. Thus less additional damping is required.

The differences in the near field base shear responses between comparable linear structures are also small. The maximum difference is 6% between Designs 10 and 11, in terms of the percentage reduction in base shear compared to the unretrofitted base shear. Similar variations in response are found for the design level earthquakes.

4.4.4.3 Comparison of Structures with the Different Equivalent Linear Properties

It has been shown that all the isolation systems can be retrofitted optimally or close to optimally in terms of the near field response using viscous damping with a velocity exponent of 0.5. Similarly, pure viscous damping tends to be optimal for the design level responses.

Other than these trends other observations can be made. As briefly discussed in Section 4.2.4, the effectiveness of various forms of damping, in terms of near field response, is dependent on the size of the maximum displacement relative to the unretrofitted near field displacement. This can be illustrated in any one of the plots in Figures 4.13 to 4.16 by imagining the maximum displacement to be located at a number of different displacements between the unretrofitted design displacement and the unretrofitted near field displacement. It can be seen that if the unretrofitted near field response exceeds the maximum allowable displacement by a relatively small amount, then additional pure viscous damping tends to be the most effective form for reducing displacements, in terms of minimising the near field base shear response. If the difference between the unretrofitted near field response and maximum response is slightly larger, then viscous damping with a velocity exponent of 0.5 becomes more effective. If an

even larger reduction in the unretrofitted near field displacement is required to reach the maximum allowable displacement, then friction damping tends to be most effective.

One form of additional damping tended to be optimal in terms of the near field base shear and this was due to the magnitude of the unretrofitted near field displacement for each structure relative to the maximum allowable response. These relative responses were defined by the UBC and shown in Chapter 2 to be similar for each generic structure. In reality the relative magnitude of the maximum allowable and unretrofitted near field displacements would be defined by; the calculated near field hazard spectrum particular for a given building, and; the constraints which define the maximum allowable displacement. This relative displacement is likely to be different to those defined in the UBC. The most effective form of additional damping found for retrofitting the building, in terms of near field response, is largely dependent on this relative displacement. The design response showed a similar dependence, although for the earthquakes used, a form of damping with a higher velocity exponent tended to be optimal.

The properties of the isolation system also had some effect on which form of damping was found to be optimum. This is discussed in the following section in attempts to predict the optimum form of damping.

4.4.4.4 Prediction of the Optimum Additional Damping Level for Retrofit of a Seismically Isolated Structure

It was shown that structures with different bilinear properties but the same equivalent linear properties have similar responses. Structures with one type of bilinear post yield stiffness ratio has been focused on for comparison in this section. Each of structures with a post yield stiffness ratio of 0.02 were plotted in terms of their design effective period and design equivalent viscous damping, as shown on Figure 4.17. Next to each of the points the level of additional viscous damping required to retrofit the isolation system was noted. This was based on retrofits using additional viscous damping with a velocity exponent of 0.5. These damping levels were shown in an attempt to establish a relationship between the structural properties and the level of damping required. By interpolating between the points trend lines were plotted to show approximate levels of additional damping required to retrofit a structure

for near field earthquakes, as shown in Figure 4.18. Percentages of critical viscous damping were used to enable linear trend lines to be plotted in this figure.

Although, the trend lines are linear, the response of the seismically isolated structures to earthquakes is non-linear and the trend lines have also been based on relatively few points. Therefore, it is not expected that Figure 4.18 will give an exact prediction of an appropriate retrofit, however, it should be able to give a good estimate. The prediction is reliant on the relative unretrofitted design and near field response of a structure being proportional to those calculated by the UBC. The near field factor which defines the near field response relative to the design response was equal to 2.0, and the maximum capable earthquake coefficient was 1.25.

The use of Figure 4.18 will be demonstrated. For example, if a structure had a design effective period of 2.25 seconds and a design equivalent viscous damping of 20%, then the level of additional damping required would be approximately 25%. This implies the damping constant that corresponds to a percentage of critical pure viscous damping of 25%, but viscous

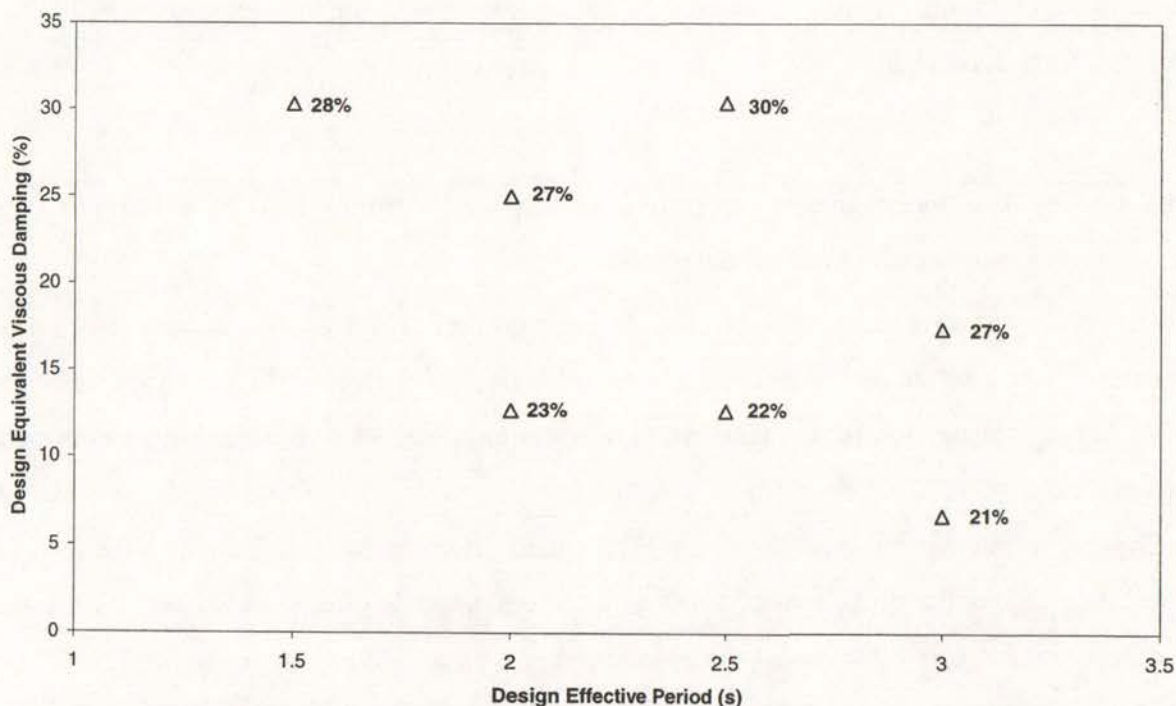


Figure 4.17: Optimum Level of Additional Viscous Damping for Isolated Structures at their Design Effective Period and Damping

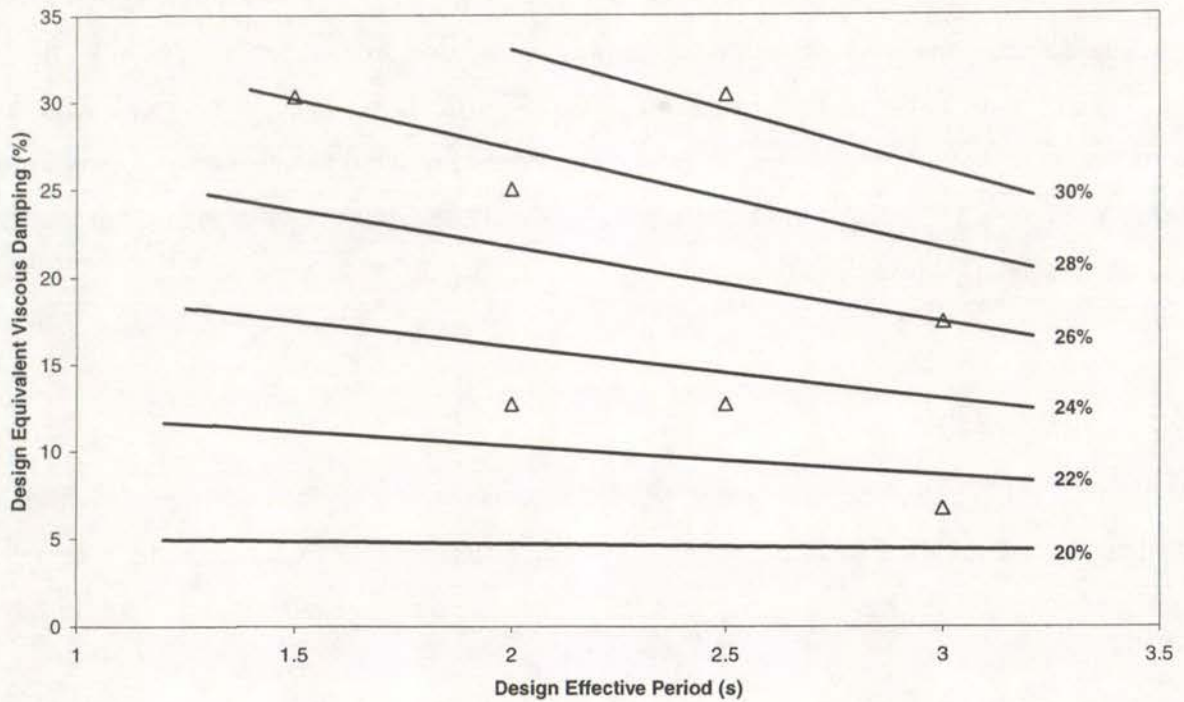


Figure 4.18: Optimum Additional Viscous Damping Curves

damping with a velocity exponent of 0.5 is actually used. It can be seen from Figure 4.18 that the additional damping curves are close to horizontal. Therefore the additional damping required in a structure, is approximately proportional to the level of initial equivalent viscous damping in the structure.

4.4.4.5 Prediction of Other Responses

Attempts were made to find trends which would enable the prediction of other responses, such as the near field base shear response, and the design displacement and base shear response. However it was found that, although there did appear to be certain trends, they were highly non-linear and using just seven points made it difficult to plot trend lines with any confidence.

Attempts to predict the optimum form of damping again found a large amount of non-linearity, therefore it was difficult to find relationships between the optimum form of damping and certain properties of the isolation system. In comparing the levels of additional damping and the forms of damping found optimal for each structure, it was shown that when high level of damping were required, a form of damping with a lower velocity exponent tended to be

optimal. The converse was also approximately true. As the level of additional damping was approximately proportional to the level of initial damping in a given isolation system, then this suggests that the form of additional damping is also approximately proportional to the level of additional damping in the structures. It was difficult to illustrate this trend with any certainty using this number of generic structures. Predicting the optimum form of damping is better considered in terms of the relative magnitude of the unretrofitted design displacement and the maximum allowable displacement.

4.5 Summary

The generic rigid superstructure models show that conceptually different forms of additional damping could be used to limit isolation system displacements in response to near field earthquakes. A hysteretic buffer and mass tuned damping were not effective.

The most effective form of additional damping for controlling the near field deformations was viscous damping with a velocity exponent of 0.5 for the majority of the structures, although friction damping and pure viscous damping respectively were most effective for a few structures. In terms of the design response pure viscous damping was generally most effective. The distinction must be made as to which is most important:

1. Optimally reducing the near field response allowing slightly more damage in response to the design level earthquakes, or
2. Using an additional form of damping which minimises the impact on the design level performance of a building but may not be optimal for the near field response.

It was accepted that, as design level earthquakes were more common, minimising the impact of retrofits on the design level response was most important. This issue is discussed further in following chapters.

It has been shown that for the range of properties considered, different bilinear properties had a minimal effect on the response of the structures with the same equivalent linear properties. For structures with different equivalent linear properties the optimum form of damping was difficult to relate to the properties of the different isolation systems. However, it was shown for each structure that the optimum form of damping was largely dependent on the relative

unretrofitted near field displacement and maximum allowable displacement. As this relative response was similar for each structure, the forms of damping found optimum were also similar. The generic structures have allowed the optimum level of damping to be predicted for a seismically isolated building, given the design effective period and equivalent viscous damping of the isolation system.

Chapter 5.

Modelling of Multi-Storey Seismically Isolated Buildings

5.1 Introduction

In Chapter 4 possible retrofit solutions were presented for generic seismically isolated structures modelled with a rigid superstructure. The results showed that although the displacement of the isolation systems in response to near field earthquakes could be reduced to maximum allowable levels, the near field base shears were still significantly larger than the design base shears. Consequently, it was expected that elastically designed superstructures of the buildings would become damaged during a near field event.

The results in Chapter 4 also showed that the structures with the same equivalent linear isolation system properties but different post yield stiffness ratios, had almost the same response. Therefore the seven seismically isolated structures, which have different equivalent linear isolation system properties and the same post yield stiffness ratio equal to 0.02, were modelled with multi-storey superstructures. These seven structures are defined in Table 2.1.

Each of the buildings were initially modelled with no additional retrofitting. These models were used to calculate the displacement ductility of the superstructures in response to the near field earthquakes. Although the superstructures have been designed to be elastic, in reality some damage would be permitted in an extreme event. Therefore it was decided that an average inter-storey ductility of two was acceptable in response to the near field earthquakes. These limits were used as a basis for finding an appropriate retrofit for the multi-storey seismically isolated buildings.

5.2 SAP Models of Multi-storey Seismically Isolated Buildings

The rigid superstructure, assumed in previous analyses, was replaced with a multi-storey superstructure for each of the seismically isolated structures. It was modelled with three or six additional nodes, for three and six storey superstructures respectively. As with the isolation system, the height of each storey is inconsequential as lateral deformations are modelled as shear deformations.

Two non-linear shear links were placed between the nodes at each level, as shown in Figure 5.1. Of the two non-linear shear links at each level, one was used to describe the bilinear stiffness properties of the columns. The initial stiffness was defined as calculated in Section 2.2.3 and the post yield stiffness ratio was equal to zero. The yield force was as calculated in Section 2.2.2. The yielding exponent was made equal to 100 for a sharp transition between the initial stiffness and post yield stiffness. The second non-linear link at each floor was used to describe the modal damping, with the damping constant as calculated in Section 2.2.4 and a damping exponent equal to 1.0. The automatic modal damping feature in SAP was not utilised so that the properties of the model were fully understood. The only other variable was the damping stiffness which had to be large enough, greater than 10 times the damping exponent divided by the timestep used in the analysis⁶, to promote pure viscous damping.

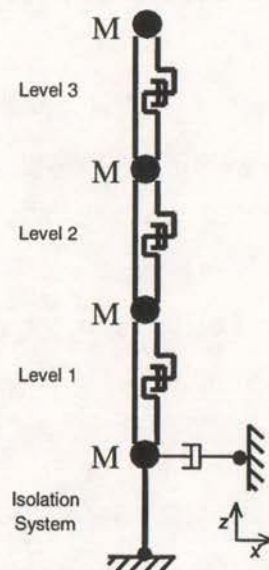


Figure 5.1: SAP Model for Three Storey Seismically Isolated Building.

All the nodes were constrained like node 2, to move in only the "x" direction. Each node not connected to the ground was assigned a mass corresponding to the mass of each floor from the weights calculated in Section 2.2.2.

The unretrofitted response of each structure was determined. When it was found that the superstructure would require retrofitting, extra non linear damping elements were placed in parallel with the existing modal damping elements between each of the levels.

5.3 Earthquake Time Histories

The same earthquake time histories were used for modelling the multi-storey seismically isolated buildings as those used for the rigid seismically isolated structures. It was assumed that the unretrofitted response of the isolation systems for each the multi-storey building would be similar to the respective response for the rigid superstructures. Therefore the same earthquake time history scale factors were used for a given multi-storey seismically isolated building as those used for the corresponding rigid structure. This allowed the responses of the isolation systems for both the rigid and multi-storey structures to be compared. The scale factors for each of the buildings are given in Table 3.4.

5.4 Results from Analysis of Three Storey Seismically Isolated Buildings

5.4.1 Response of Unretrofitted Buildings at the Base

The design level and near field displacement response of the isolation system for each of the seven seismically isolated buildings, modelled with a three storey superstructure, has been summarised in Table 5.1. The base shear divided by the total weight for each three storey building is given in Table 5.2. For comparison, displacements and base for the rigid seismically isolated structures are shown in small font after each of the responses for the three storey structures.

Table 5.1: Maximum Displacements of Isolation Systems for the Three Storey Buildings

Design	Design Displacement (mm)			Near Field Displacement (mm)		
	UBC Displacement	Average Earthquake Displacement	Coefficient of Variation	UBC Displacement	Average Earthquake Displacement	Coefficient of Variation
3.1	140	164 142	0.069 0.019	435	399 436	0.028 0.016
3.2	248	246 251	0.050 0.029	667	574 666	0.037 0.020
3.5	199	196 198	0.102 0.031	593	564 592	0.016 0.012
3.7	311	301 303	0.007 0.010	834	719 833	0.063 0.025
3.1	233	234 231	0.028 0.014	719	653 720	0.061 0.010
3.12	447	439 444	0.013 0.007	1161	976 1148	0.076 0.029
3.15	336	332 332	0.037 0.030	957	836 950	0.064 0.010

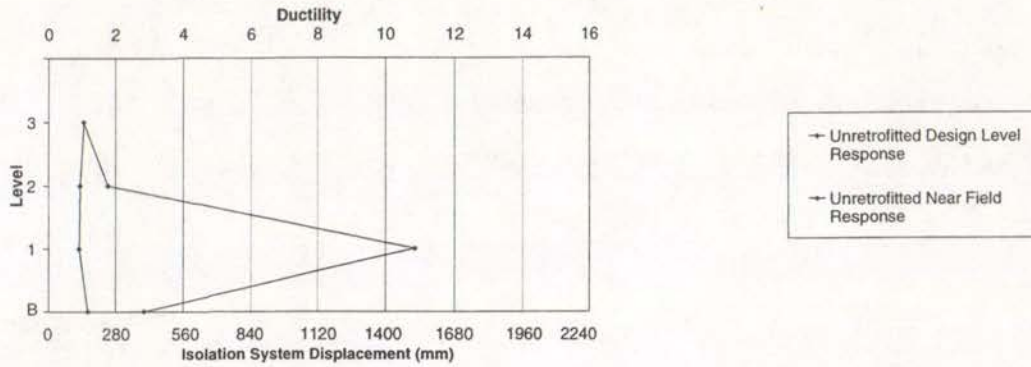
Table 5.2: Maximum Base Shear of Isolation Systems for the Three Storey Buildings

Design	Design Base Shear / Weight			Near Field Base Shear / Weight		
	UBC Base Shear	Average Earthquake Base Shear	Coefficient of Variation	UBC Base Shear	Average Earthquake Base Shear	Coefficient of Variation
3.1	0.250	0.272 0.252	0.038 0.010	0.521	0.488 0.522	0.021 0.012
3.2	0.250	0.248 0.252	0.040 0.023	0.587	0.511 0.585	0.034 0.019
3.5	0.200	0.198 0.200	0.061 0.019	0.439	0.422 0.438	0.013 0.010
3.7	0.200	0.195 0.196	0.005 0.008	0.469	0.411 0.469	0.057 0.023
3.1	0.150	0.150 0.149	0.014 0.007	0.311	0.289 0.311	0.046 0.008
3.12	0.200	0.197 0.199	0.012 0.007	0.485	0.411 0.480	0.072 0.028
3.15	0.150	0.149 0.149	0.027 0.022	0.352	0.312 0.349	0.054 0.009

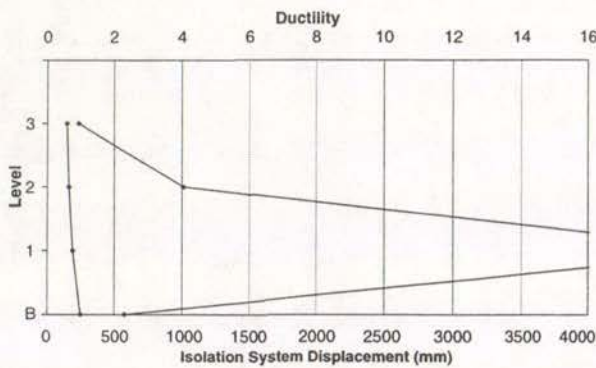
5.4.2 Comparisons with Rigid Seismically Isolated Structures

Comparisons show that the average design level displacements for the three storey buildings were almost identical to the rigid superstructures responses. With the exception of Design 1, which had a 15% larger response, the maximum difference was 2%. The average near field displacement of the isolation systems for each three storey building was smaller than the response with a rigid superstructure. This can be explained by the energy absorbed in damaging the superstructure of the three storey buildings, reducing the amount of hysteretic energy that needed to be dissipated by the isolation systems, This caused a reduction in the maximum displacement of the isolation systems. The variations between the earthquake responses, in terms of coefficients of variation for each of the structure, were increased in the three storey structures. However, they remained small, at a maximum of 0.1. Comparing the base shear responses between the three storey buildings and the structures modelled with a rigid superstructure gives similar results to the displacement comparisons.

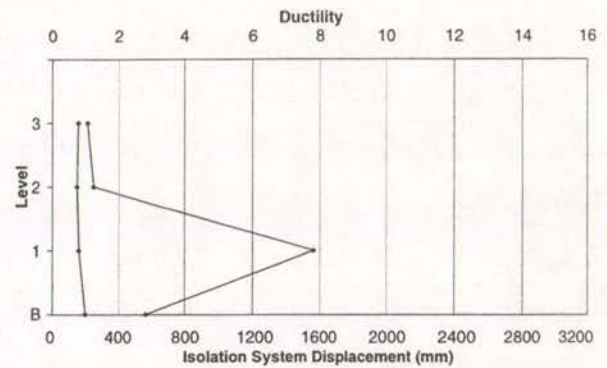
Design 3.1



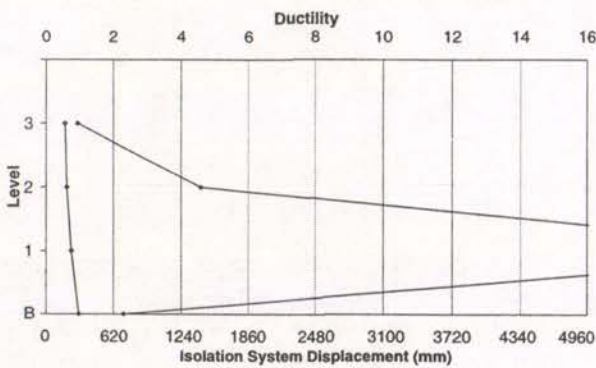
Design 3.2



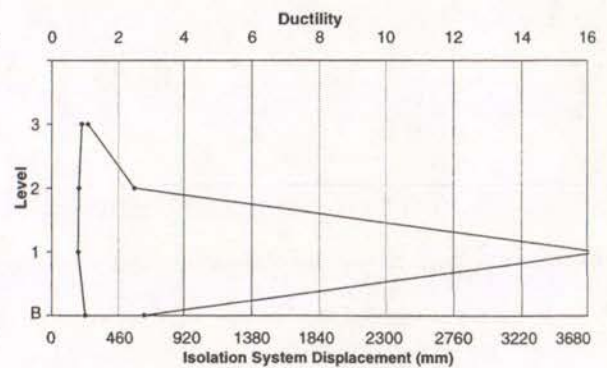
Design 3.5



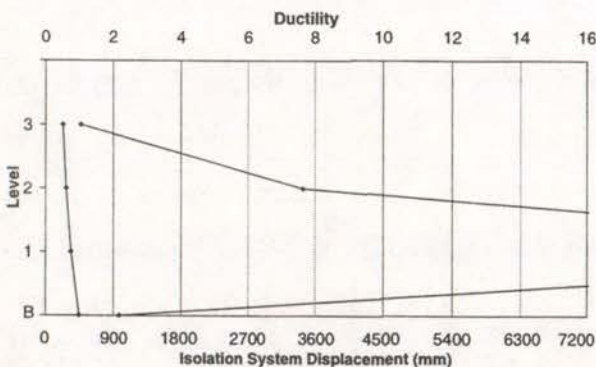
Design 3.7



Design 3.10



Design 3.12



Design 3.15

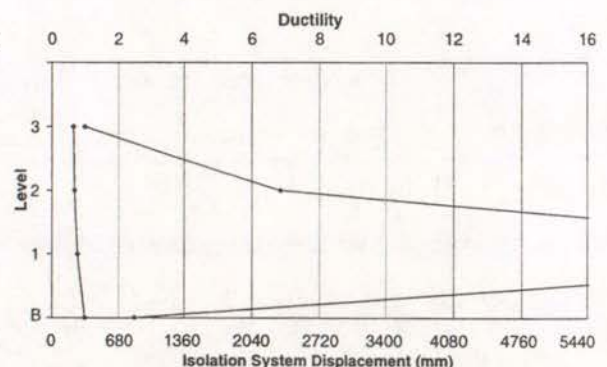


Figure 5.2: Average Unretrofitted Response of Three Storey Buildings

5.4.3 Displacements in the Superstructure

The average maximum design level and near field deformations at each level are shown in Figure 5.2 for each unretrofitted seismically isolated building. The deformations of the various floors are shown in terms of displacement ductilities using the axis at the top, while the displacement of the isolation system is given in millimetres on the bottom axis.

Chapter 2 described how in the UBC the multi-storey superstructures were designed independently of the isolation system, using just the design base shear of the isolation system to calculate the forces in the superstructure. This may appear to be an oversimplified procedure as it might be expected that there is more interaction between the response of the superstructure and the isolation system. However, Figure 5.2 shows that UBC designs have a good average response to the design level earthquakes. The ductility of each level is between around 0.6 and 1.0 indicating that the structures remained elastic, although some conservatism is apparent. The near field response of the unretrofitted structure, shown in Figure 5.2, illustrates that the displacement of the isolation system, not only exceeds the maximum allowable response, but that there is also a soft storey failure in the first level.

5.5 Results from Analysis of a Six Storey Seismically Isolated Building

It was clear that the superstructure the three storey buildings needed to be retrofitted. Thus a six storey building was also analysed to compare any retrofit found for the corresponding three storey building to the retrofit required for a six storey building. Design 6.7 was used, with isolation system properties given in Table 2.1 and superstructure properties defined in Table 2.3 and Sections 2.2.3 and 2.2.4.

The unretrofitted displacement response, and the base shear response divided by weight for Design 6.7 is given in Tables 5.3 and 5.4 respectively. These can be compared to the response of Design 3.7 in Tables 5.1 and 5.2. Comparing the displacement response of the six storey seismically isolated building to the response calculated by the UBC shows that the average design displacement has been reduced by 5%, however, the near field response has been reduced by 22%. This is 8% more than the response reduction of the three storey building, which suggests that there was more energy dissipated in the superstructure of the six

storey building. The variation between individual earthquakes for the three and six storey buildings are similar, so too is the base shear responses.

Table 5.3: Displacement Response of Isolation System for the Six Storey Building

Design	Design Displacement (mm)			Near Field Displacement (mm)		
	UBC Displacement	Average Earthquake Displacement	Coefficient of Variation	UBC Displacement	Average Earthquake Displacement	Coefficient of Variation
6.7	311	294	0.037	834	648	0.074

Table 5.4: Base Shear Response of Isolation System for the Six Storey Building

Design	Design Base Shear / Weight			Near Field Base Shear / Weight		
	UBC Base Shear	Average Earthquake Base Shear	Coefficient of Variation	UBC Base Shear	Average Earthquake Base Shear	Coefficient of Variation
6.7	0.200	0.191	0.029	0.469	0.374	0.067

The averaged deformations of the unretrofitted building in response to the design and near field earthquakes are shown in Figure 5.3. In this figure, the displacements of the various floors are given in terms of displacement ductilities along the top axis, while the displacement of the isolation system is given in millimetres on the bottom axis. Figure 5.3 shows a soft storey failure in the first floor similar to the soft storey failure in the three storey buildings.

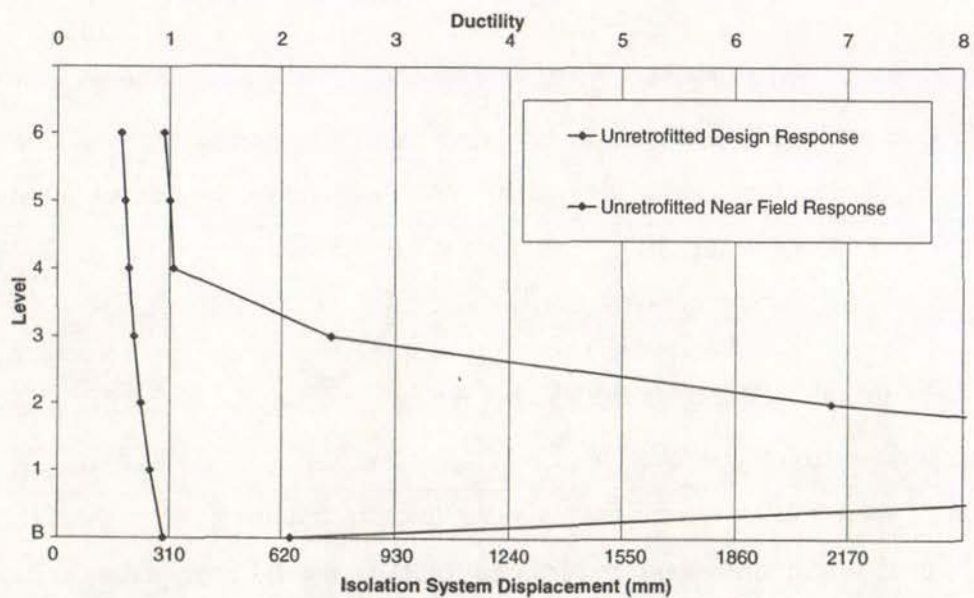


Figure 5.3: Unretrofitted Response of the Six Storey Building

5.6 System Identification for the Retrofit of the Superstructures

5.6.1 Proposed Retrofit for the Superstructure of each Seismically Isolated Building

It will be shown that additional viscous damping at the base of the multi-storey seismically isolated buildings alone is not reduce the displacements of the isolation system while also controlling the deformation of each floor. Thus, it was proposed that additional damping added between some if not all of the floors above the isolation system, could limit the inter-storey deformations to acceptable levels. In order to implement this, additional shear dampers were added to the SAP models in parallel to the existing modal dampers at each level, as illustrated in Figure 5.1.

Such a retrofit involves optimising the damping at each level. It is impractical to analyse a large number of combinations of additional damping particularly in the six storey structure where the number of combinations is potentially very large. Therefore, system identification was used to predict the optimum level of additional damping in each storey of a given structure. This technique required a relatively small number of analyses and converged well to the optimum solution which was checked using an additional analysis in SAP.

Scarry²⁴ outlined a system identification process for use in structural engineering applications and using this procedure he identified some of the structural stiffness properties of a bridge from a number of experimental tests. This procedure has been modified to find the optimum damping level at each floor of each multi-storey seismically isolated building using a limited number of SAP analyses. An example applying this procedure to the calculation of the optimum level of damping, using viscous damping with a velocity exponent of 0.5 for Design 3.7, is given in Appendix 10.

5.6.2 Definition of Parameters and Variables

In this method structural response parameters, P_i , were used to describe the average deformation of each level of a multi-storey superstructure requiring retrofit, and the average deformation of the isolation system, in response to the near field earthquakes. Floors which initial analyses found to require no retrofit were not included in the system identification

procedure. The optimum structural response parameters, PM_i , correspond to the optimum deformations of each floor. The first optimal structural response parameter, PM_1 , is defined as the maximum allowable displacement of the isolation system, calculated earlier using the UBC. The other optimum structural response parameters are defined by the inter-storey displacements equal to an inter-storey ductility of 2.0. Again only the floor requiring additional damping are included. For example for Design 3.7, the maximum displacement of the isolation system of 430 mm is equal to PM_1 , and the maximum deformation at the first floor of 12.59mm, which corresponds to the displacement equal to a ductility of 2.0, corresponds to PM_2 . The deformations at the second and third floors were not included, as initial analyses with approximately optimal levels of additional damping at each floor, showed that deformations of these floors had a ductility less than two. By adding damping to a given storey the deformation of the floor above tended to increase, therefore the number of storeys which require retrofitting is not immediately obvious. Thus preliminary analyses need to approximate the level of additional damping at each storey in order to determine how many storeys actually need retrofitting. The number of storeys requiring additional damping including the isolation layer, is equal to N . Therefore for the Design 3.7, N is equal to two as additional damping is required at the base and first floor only.

Using the system identification procedure, the structural response parameters were calculated in terms of the significant structural parameters, x_k , which correspond to the structural variables in the system. The variables used to retrofit the multi-storey seismically isolated structures were the levels of additional viscous damping between each floor. Again, there are a total of N optimal significant structural parameters, one for each structural response parameter.

5.6.3 Development of a Quasi-Structural Model

A quasi-structural model was developed so that the quasi-structural response parameters for each storey, PQ_i , can be considered a quadratic function of the significant structural parameters. The quasi-structural response parameters, can be calculated using Equation 5.1²⁴:

$$PQ_i = C^i + \sum_{k=1}^N (x_k A_k^i + x_k^2 B_k^i) \quad \dots \text{Equation 5.1}$$

where: N = number of storeys requiring additional damping, and $1 \leq i \leq N$

PQ^i = quasi structural response parameters

$x_k =$ significant structural parameters

A_k^i, B_k^i and C^i are quadratic constants

The quadratic constants A_k^i, B_k^i and C^i can be calculated by making a number of estimates of the significant structural parameters and using these estimates to perform analyses in SAP to find corresponding structural response parameters. To calculate these constants, $2N + 1$ preliminary analyses were used. The first analysis used an initial estimate of the optimum levels of damping at each floor, these estimates are defined as the base values. Upper and lower estimates of the levels of additional damping for each storey were then made. Therefore for two estimates at each floor excluding the base estimate, namely the upper and lower estimates, and N floors requiring additional damping, there were $2N$ upper and lower additional damping variables. These upper and lower estimates typically needed to be within approximately 25% of the optimal levels of additional damping for the procedure to eventually converge to the optimum solution.

$2N + 1$ analyses were performed to calculate the quadratic constants in the quasi-structural model, firstly using all the additional damping base estimates, then replacing each base estimate individually with the $2N$ upper and lower estimates. As a result, $2N + 1$ sets of quasi-structural response parameters were calculated from the average near field displacement response of each floor that required additional damping. These were calculated from SAP analyses for each of the above combinations of additional damping estimates. Knowing all the quasi-structural response parameters, Equation 5.1 can be rearranged to calculate the quadratic constants. Instead of having N quasi-structural response parameters corresponding to the optimum response at each level as in Equation 5.1, there are now $2N+1$ analyses with N quasi-structural response parameters to enable calculation of the quadratic constants. The calculation of the quadratic constants can be most easily illustrated in matrix form as in Equation 5.2. Each row of the quasi-structural response matrix, with PQ terms, represents the response to different analyses with a different set of damping levels at each floor. Each column represents the response of the different floors.

$$\begin{bmatrix} C^1 & C^2 & \dots & C^N \\ A_1^1 & A_1^2 & \dots & A_1^N \\ B_1^1 & B_1^2 & \dots & B_1^N \\ \dots & \dots & \dots & \dots \\ A_N^1 & A_N^2 & \dots & A_N^N \\ B_N^1 & B_N^2 & \dots & B_N^N \end{bmatrix} = \begin{bmatrix} 1 & x_1^b & (x_1^b)^2 & x_2^b & (x_2^b)^2 & \dots & (x_N^b)^2 \\ 1 & x_1^u & (x_1^u)^2 & x_2^b & (x_2^b)^2 & \dots & (x_N^b)^2 \\ 1 & x_1^l & (x_1^l)^2 & x_2^b & (x_2^b)^2 & \dots & (x_N^b)^2 \\ \dots & \dots & \dots & \dots & \dots & \dots & \dots \\ \dots & \dots & \dots & \dots & \dots & \dots & \dots \\ 1 & x_1^b & (x_1^b)^2 & x_2^b & (x_2^b)^2 & \dots & (x_N^b)^2 \\ 1 & x_1^b & (x_1^b)^2 & x_2^b & (x_2^b)^2 & \dots & (x_N^b)^2 \end{bmatrix}^{-1} \begin{bmatrix} PQ_1^1 & PQ_1^2 & \dots & PQ_1^N \\ PQ_2^1 & PQ_2^1 & \dots & PQ_2^N \\ PQ_3^1 & PQ_3^1 & \dots & PQ_3^N \\ \dots & \dots & \dots & \dots \\ \dots & \dots & \dots & \dots \\ PQ_{2N}^1 & PQ_{2N}^2 & \dots & PQ_{2N}^N \\ PQ_{2N+1}^1 & PQ_{2N+1}^2 & \dots & PQ_{2N+1}^N \end{bmatrix}$$

...Equation 5.2

Therefore using MathCad 8 Professional¹⁷, Equation 5.2 was used to calculate each quadratic constant. An example of such a calculation is illustrated using Design 3.7 in Appendix 10.

5.6.4 Newton-Raphson Solution Procedure

A new estimate of the optimum levels of damping was made using the response from the $2N + 1$ analyses. These often could give a better indication of the optimum damping levels at each floor. Using the new levels of damping and the quadratic constants from the quasi-structural model, a new estimate of the quasi-structural response could be calculated again using Equation 5.1. The error between the new quasi-structural response and the known optimum structural response was calculated. Approximately three or four Newton-Raphson iterations were then performed each using a better estimate of the additional damping, in order to continually reduce the error and eventually calculate the optimum levels of damping at each floor. This procedure is described briefly, as adapted from work by Scarry²⁴ It is again exemplified by the calculation of the optimum levels of damping for Design 3.7 in Appendix 10, which also illustrates the accuracy of the procedure.

Let the initial estimate of the optimum significant structural parameters (damping levels at each floor) be described by:

$$\underline{x}_0 = \begin{bmatrix} x_1 \\ x_2 \\ \cdot \\ \cdot \\ x_N \end{bmatrix} \quad \dots \text{Equation 5.4}$$

The quasi-structural parameters were calculated using Equation 5.1 with the new optimum levels of additional damping, \underline{x}_0 , and the quadratic constants calculated for the quasi-structural model. Comparing these with the known optimum structural response parameters, the square of the error is calculated numerically by:

$$E^2 = \sum_{i=1}^N (PM_i - PQ_i)^2 \quad \dots \text{Equation 5.5}$$

where E^2 = square of the error between the quasi-structural response parameters and optimum structural response parameters

If \underline{x}_0 is considered to be symbolically equal to \underline{x}_k , therefore in terms of x_1, x_2, \dots not numerical values, then symbolically E^2 can be expanded to:

$$E^2 = \sum_{i=1}^N (PM_i - C^i - A_1^i x_1 - B_1^i x_1^2 - \dots - A_N^i x_N - B_N^i x_N^2)^2 \quad \dots \text{Equation 5.6}$$

Differentiating this with respect to \underline{x}_k :

$$\underline{F}(x) = \frac{\partial E^2}{\partial \underline{x}_k} = \underline{0} \quad \dots \text{Equation 5.7}$$

where: $\underline{F}(x)$ = function defining the differential of the error function

therefore:

$$\underline{F}(x) = \begin{bmatrix} f_1(x) \\ f_2(x) \\ \cdot \\ \cdot \\ f_N(x) \end{bmatrix} = \begin{bmatrix} \frac{\partial E^2}{\partial x_1} \\ \frac{\partial E^2}{\partial x_2} \\ \cdot \\ \cdot \\ \frac{\partial E^2}{\partial x_N} \end{bmatrix} = \underline{0} \quad \dots \text{Equation 5.8}$$

Thus a better estimate of the optimum damping at each level is given by:

$$\underline{x}_{n+1} = \underline{x}_n - [J](\underline{x}_n)^{-1} \underline{F}(\underline{x}_n) \quad \dots \text{Equation 5.9}$$

where J is the Jacobian Matrix, defined by:

$$J(x) = \begin{bmatrix} \frac{\partial f_1(x)}{\partial x_1} & \frac{\partial f_1(x)}{\partial x_2} & \dots & \frac{\partial f_1(x)}{\partial x_N} \\ \frac{\partial f_2(x)}{\partial x_1} & \frac{\partial f_2(x)}{\partial x_2} & \dots & \frac{\partial f_2(x)}{\partial x_N} \\ \dots & \dots & \dots & \dots \\ \frac{\partial f_N(x)}{\partial x_1} & \frac{\partial f_N(x)}{\partial x_2} & \dots & \frac{\partial f_N(x)}{\partial x_N} \end{bmatrix} \quad \dots \text{Equation 5.10}$$

This procedure was set up in MathCad 8¹⁷, from which the optimum damping levels were usually obtained after three to four iterations. In some cases the initial estimate of the damping levels was not accurate enough to cause convergence to a sensible solution. When it was apparent that convergence had not occurred, a new initial estimate of the optimum damping levels was attempted with a smaller error and the iteration procedure repeated until convergence occurred. The solution was then checked using an analysis in SAP with the optimum levels of additional damping calculated to ensure that the average response to the near field earthquakes was in fact equal to the optimum response. The results for the retrofit of each seismically isolated structure are presented in Chapter 6.

5.7 Summary

In describing the modelling of multi-storey seismically isolated structures, it has been shown that the unretrofitted response of each isolation system for the multi-storey buildings is similar to the response of the structures modelled with a rigid superstructure. The unretrofitted responses show that the generic structures will need to be retrofitted in order to control, not only isolator deformations, but also deformations of the superstructure in response to near field earthquakes. It was proposed to use additional damping in the superstructure to retrofit each of the buildings. Thus to find optimum levels of additional damping for each storey, system identification was proposed, the procedure for which has been described.

Chapter 6.

Retrofit of Multi-Storey Seismically Isolated Buildings

6.1 Introduction

Having modelled the multi-storey seismically isolated buildings without any additional damping, the need to retrofit both the base and the superstructure of each building was apparent. The seven three storey seismically isolated buildings were initially retrofitted with each of the three forms of damping at the base, viscous damping with velocity exponents of 1.0 and 0.5, and friction damping. Consequently, as this was not adequate to control displacements in the superstructure, additional damping was added between the base and first floor, and first and second floors of the superstructure. Viscous damping with a velocity exponent of 0.5, which was found to be optimal for the majority of the rigid seismically isolated structures based on near field base shear response, was used to retrofit the isolation system of each multi-storey building. The three different forms of additional damping were attempted in the superstructure of each building. This enabled the different forms of additional damping in the superstructure to be compared. The optimum levels of damping were calculated so that the average ductility of each floor was reduced to a maximum of 2.0 in response to the near field earthquakes, with damping levels calculated using the system identification procedure. The various retrofits were compared using base shear, variability, damping forces and floor spectra in order to find the most effective form of additional damping.

One six storey structure was retrofitted with the optimum form of damping found for the three storey structures. The objective was to determine how many levels required additional damping compared to the three storey structure, and whether the level of damping required at the base remained consistent with the levels of damping used for the buildings modelled with rigid and three storey superstructures.

6.2 Response of the Three Storey Buildings Retrofitted at the Base

6.2.1 Deformations at Each Floor for Various Forms of Additional Damping

Each of the three storey buildings was retrofitted using the optimal damping level for each of the three forms of additional damping calculated for the corresponding rigid seismically isolated structure. These damping levels are given in Table 6.1. In Figure 6.1, the displacements of levels one, two and three are shown in terms of ductilities given on the top horizontal axis, while the displacement of the base is given on the bottom axis. These are shown for the unretrofitted buildings and the buildings retrofitted at the base using each of the three forms of damping. A response with additional friction damping was not given for Design 3.1 as the level of damping required exceeded the maximum level attempted of $\mu = 0.15$ as shown in Table 6.1. Similarly, there was no response for Design 10 with additional pure viscous damping.

Table 6.1: Optimum Levels of Damping at the Base from Rigid Superstructure Models

Design	Optimum Damping Levels		
	Viscous Damping (%)		Friction Damping, μ ()
	Exp. = 1.0	Exp. = 0.5	
1	0.333	0.239	> 0.150
2	0.173	0.154	0.120
5	0.218	0.173	0.130
7	0.128	0.113	0.080
10	> 0.205	0.153	0.105
12	0.098	0.090	0.080
15	0.137	0.120	0.090

The results in Figure 6.1 illustrate that the average near field displacement was reduced to the maximum allowable level for each form of damping, however, there was still a soft storey failure in the first level of the superstructure. Adding the average near field deformations at each floor, an addition which can be graphically approximated from Figure 6.1, show that the optimum forms of damping found from the rigid superstructure models based on the near field base shear result in the smallest or close to the smallest total deformations. In most cases this

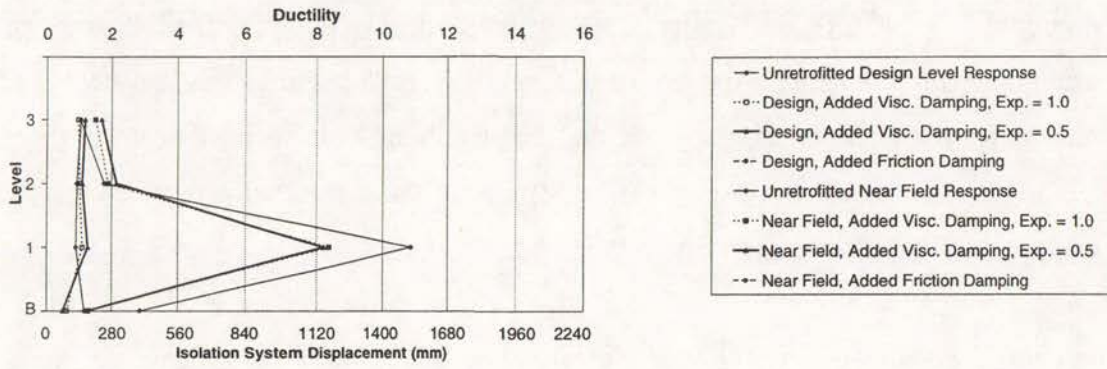
corresponds to smallest deformations at the first floor. The optimum forms of damping used are given in bold in Table 6.1. For example, the optimum form of damping for Design 5 was viscous damping with a velocity exponent of 0.5, and Figure 6.1 shows that the near field displacements for this form of damping are the smaller than those using the other forms. Figure 6.1 also shows that the majority of the structures were optimally retrofitted using viscous damping with a velocity exponent of 0.5.

The comparative magnitude of the total deformations tends to be consistent with the magnitude of the base shears for the various forms of retrofit. For example there was a comparatively large difference between the near field base shear using pure viscous damping and viscous damping with a velocity exponent of 0.5 for Design 15 as shown on Figure 4.16. Figure 6.1 shows that there also a comparatively large difference in inter-storey displacements between these forms of damping for Design 3.15. Similarly, there is a relatively small difference between the base shears using viscous damping with a velocity exponent of 0.5 and friction damping for Design 15. Consequently, it is difficult to determine visually in Figure 6.1 which has the smallest sum of the displacements at each floor between these two forms of damping. Although the inter-storey displacements are non-linear and sometimes irregular in response to earthquake time histories, therefore there are some small exceptions to the trends discussed above, base shear was shown to be a good indicator of performance for the various retrofits.

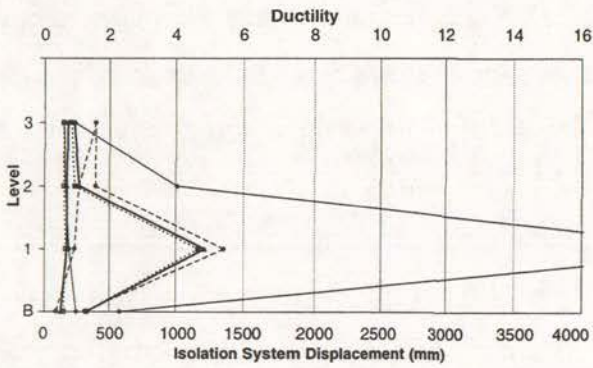
6.2.2 Acceleration Spectra at each Floor

To determine the effect of additional damping at the isolation level on the accelerations at each floor of the superstructure, acceleration spectra for Design 3.7 in response to El Centro were plotted at each floor, as shown in Figure 6.2. It can be seen that using additional pure viscous damping at the base of the structure there is a small increase in response for periods between approximately 0.3 and 1.2 seconds. The increase in accelerations is larger using additional viscous damping with a velocity exponent of 0.5, but much larger using additional friction damping. This may follow as, for the design response, pure viscous damping was found to be optimum form of additional damping. However for Design 3.1 which was optimally retrofitted using additional viscous damping with a velocity exponent of 0.5, it was found that additional pure viscous damping again resulted in the lowest magnitude

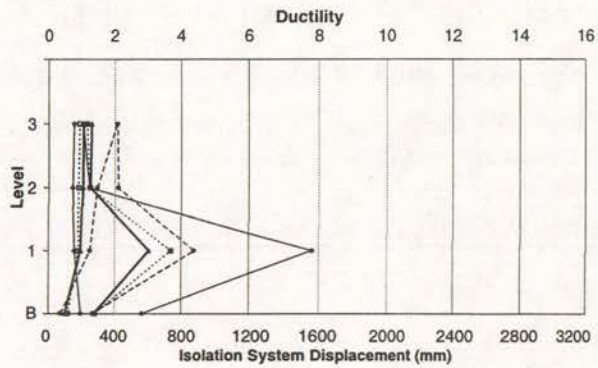
Design 3.1



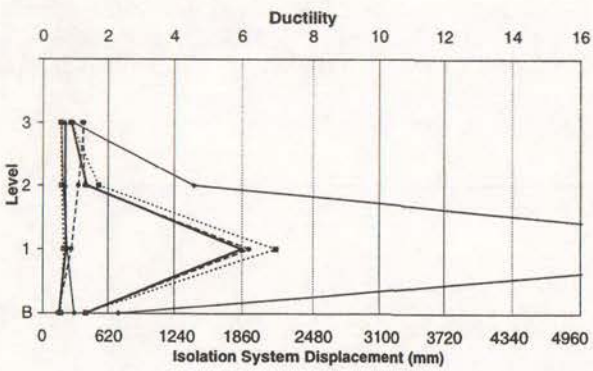
Design 3.2



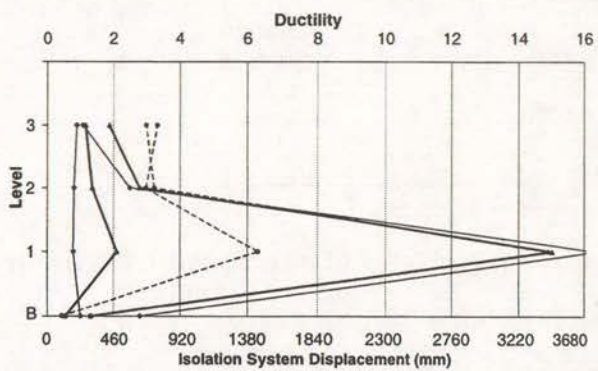
Design 3.5



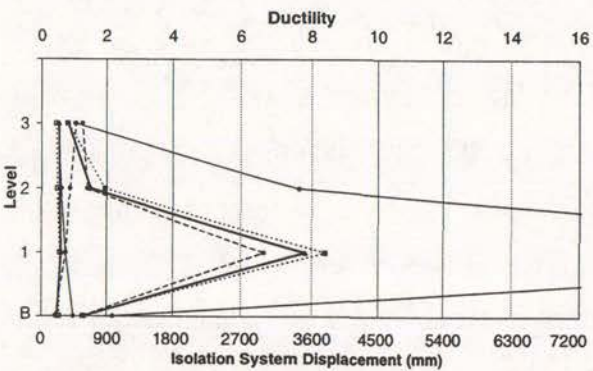
Design 3.7



Design 3.10



Design 3.12



Design 3.15

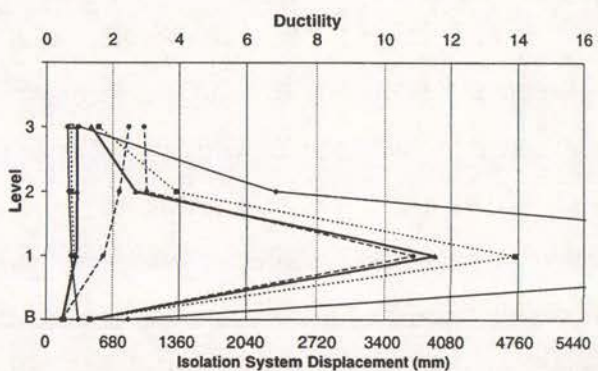


Figure 6.1: Base Retrofitted Response of Three Storey Seismically Isolated Structures

Design 3.1

Design 3.7

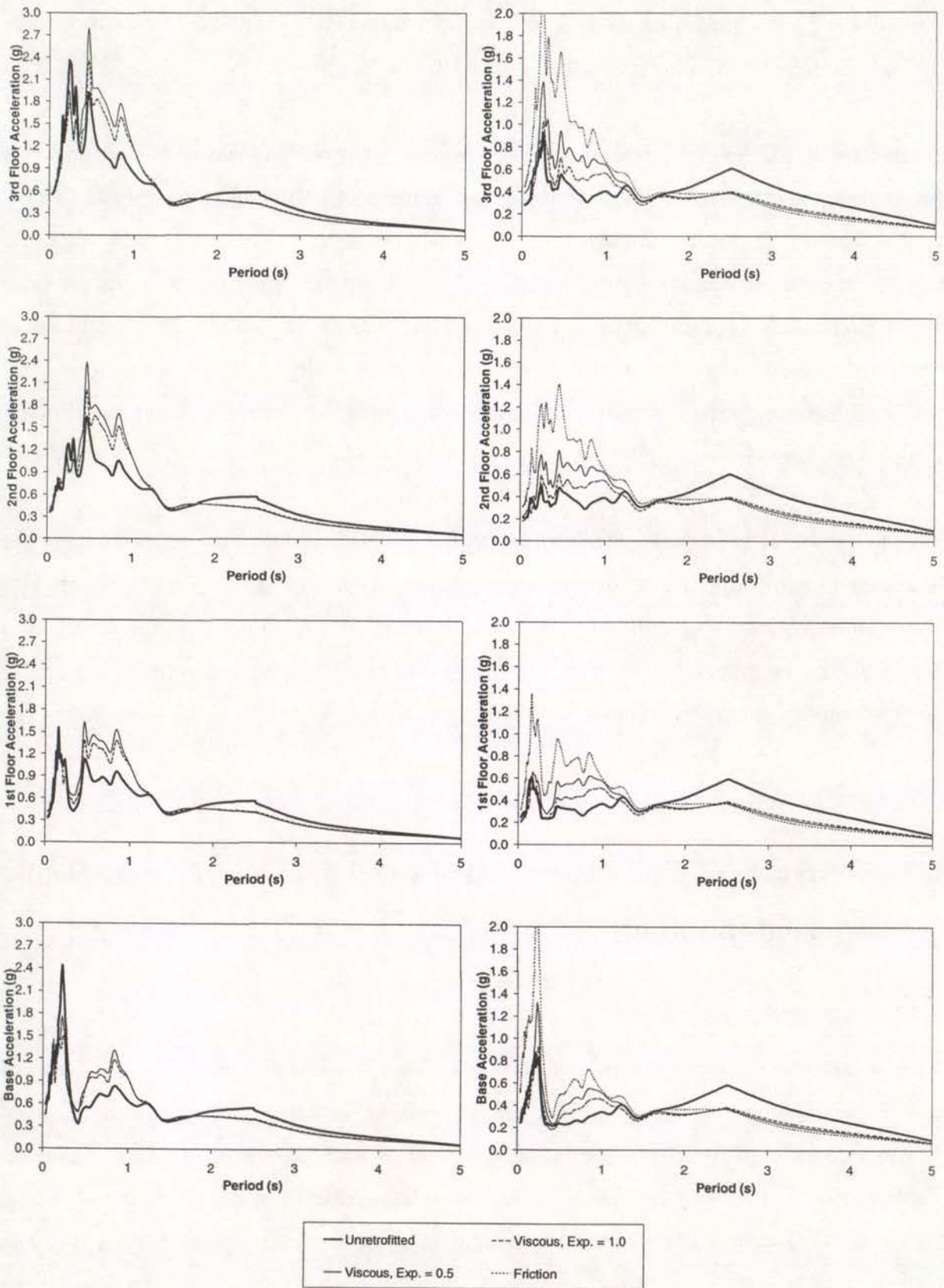


Figure 6.2: El Centro Acceleration Response Spectra at each Floor for Designs 3.1 and 3.7 Retrofitted at the Base

acceleration spectra at each floor. Therefore for both of these structures, regardless of the type of damping found to be optimal in terms of minimising design level base shear, pure viscous damping resulted in the smallest increase in accelerations.

An increase in acceleration response at certain periods is not likely to cause structural damage but is likely to cause damage to some non structural items of a building which vibrate at these natural periods. Therefore, although this damage will not cause a structure to collapse, it may increase the cost of reinstating the building after a design level earthquake. Again there needed to be a compromise between design level response and mitigating the effects of near field earthquakes. It was considered appropriate to have a slightly larger increase in non-structural damage during a design level earthquake if this was required to allow the building to at least withstand a near field event.

Although it was shown that some non structural items were likely to experience more damage as a result of retrofitting the building for near field ground motion, the response for items with long natural periods was reduced. Therefore, if there are important non-structural items contained in a seismically isolated building they may be able to be individually isolated in order to protect them from damage. Floor spectra for the design level earthquakes are investigated further in Section 6.3.7.

6.3 Response of Fully Retrofitting the Three Storey Seismically Isolated Buildings

6.3.1 Introduction

Viscous damping with a velocity exponent of 0.5, which was found to be optimum in terms of near field response for retrofitting the majority of the generic rigid seismically isolated structures, was used to retrofit the isolation system of each generic three storey building. Three forms of additional damping were used to reduce deformations in the first and second floors of the superstructures, so that the maximum average ductility of each floor was less than or equal to 2.0. The optimum levels of damping in each storey and at the base, were calculated using the system identification procedure set out in Section 5.5.

6.3.2 Optimum Levels of Damping

The optimum level of additional damping for each structure, at each floor, is presented in Table 6.2. More precisely, the level of additional viscous damping at the base, with a velocity exponent of 0.5, and the levels of each of the three forms of additional damping added to the superstructure are given. For the two forms of viscous damping, the levels are given in terms of the damping constant divided by the total weight of the structure, while the friction damping is given in terms of the friction coefficient. For three of the seven structures additional damping was required in only the first floor, while the other structures also required it in the second floor. This was consistent for all forms of damping.

Table 6.2: Optimum Levels of Damping at each Floor for Three Storey Seismically Isolated Structures

Design	Base Damping c/W (s/m)	Form of Damping in Superstructure	Level 1 Damping c/W (s/m), μ (%)	Level 2 Damping c/W (s/m), μ (%)	Level 2 Damping c/W (s/m), μ (%)
3.1	0.231	Viscous, Exp = 1.0	1.780	0.324	0
	0.231	Viscous, Exp = 0.5	0.364	0.081	0
	0.231	Friction	0.090	0.020	0
3.2	0.147	Viscous, Exp = 1.0	0.930	0	0
	0.147	Viscous, Exp = 0.5	0.202	0	0
	0.141	Friction	0.044	0	0
3.5	0.173	Viscous, Exp = 1.0	0.445	0	0
	0.167	Viscous, Exp = 0.5	0.121	0	0
	0.167	Friction	0.025	0	0
3.7	0.108	Viscous, Exp = 1.0	1.254	0	0
	0.108	Viscous, Exp = 0.5	0.243	0	0
	0.108	Friction	0.053	0	0
3.10	0.154	Viscous, Exp = 1.0	3.276	0.809	0
	0.149	Viscous, Exp = 0.5	0.445	0.121	0
	0.149	Friction	0.079	0.023	0
3.12	0.090	Viscous, Exp = 1.0	1.577	0.121	0
	0.090	Viscous, Exp = 0.5	0.283	0.040	0
	0.090	Friction	0.062	0.003	0
3.15	0.115	Viscous, Exp = 1.0	2.589	0.647	0
	0.111	Viscous, Exp = 0.5	0.405	0.121	0
	0.111	Friction	0.075	0.021	0

The level of damping required using pure viscous damping is up to 80% of the critical level in Design 10, which is unrealistically high. For the same structure, using a velocity exponent of 0.5, a damping constant equivalent to 11% of the critical pure viscous damping level was required. Similar, differences were found for the other structures. The large differences are

shown in Table 6.2. For the isolation systems the difference between the two forms of viscous damping was not nearly as large, as can be seen in Table 4.2. It is believed, although not fully tested, that the reason for such a large difference is due to the floors being modelled to deform in shear with no post yield stiffness, in contrast with the isolation systems which have been modelled with some post yield stiffness.

Therefore, for most of the generic models pure viscous damping was not an effective form of retrofit, thus the optimum form of damping is either viscous damping with a velocity exponent of 0.5 or friction damping. To compare each form of damping the displacements and forces in each of the buildings were investigated.

6.3.3 Average Deformations at each Floor

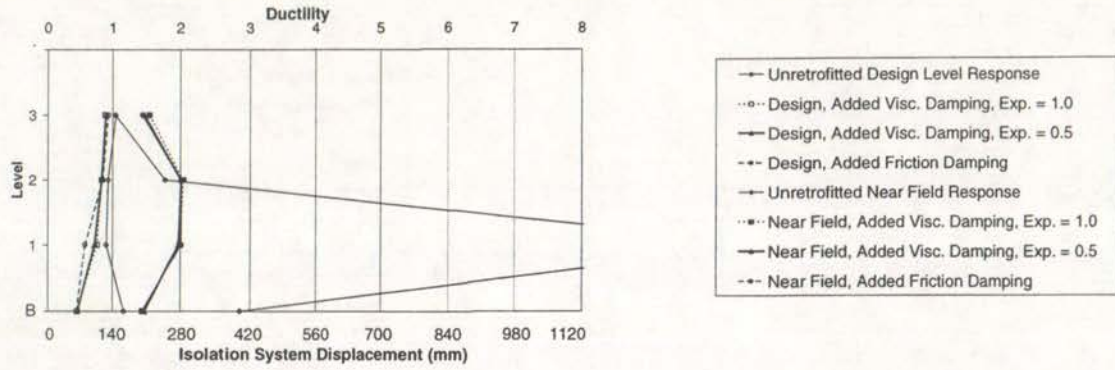
Figure 6.3 illustrates the design and near field displacement responses of each building after each storey has been retrofitted. The displacement of the isolation system is shown on the bottom horizontal axis of each plot, while the ductility of each floor in the superstructure is shown on the top axis. The various forms of damping shown correspond to the forms of damping used to retrofit the superstructure. As the average near field displacement response served as the basis for retrofit, it follows that the floors with additional damping, given as non zero in Table 6.1, have the same response (within 5%) for each form of damping. In some cases there was variation between the different forms of damping for the floors which did not require retrofitting.

Considering the design level earthquakes, Figure 6.3 shows that there is a generally zero to 20% reduction in the deformations of each floor after retrofit, while isolator displacements are reduced by a larger amount up to 50 to 60%. It may be considered beneficial to decrease deformations in each floor of the superstructure in response to design level earthquakes, however, it is later shown that the consequence of reducing deformations is an increase in accelerations at each floor.

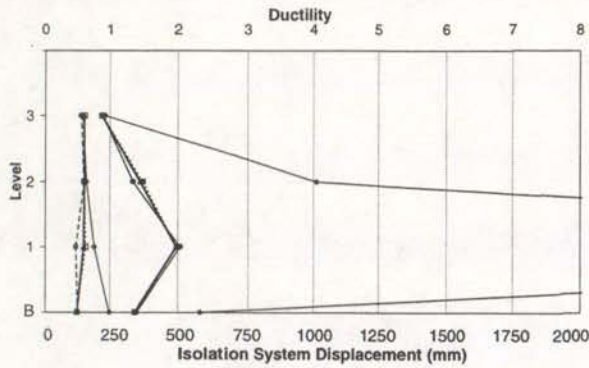
6.3.4 Storey Shear Forces

The difference between the various forms of damping was more apparent when comparing the column shear and the damping forces for each form of additional damping in the

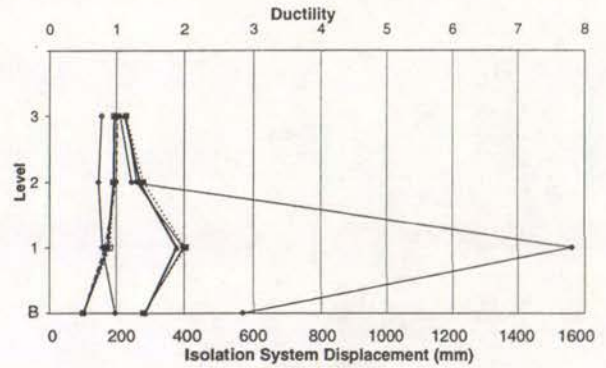
Design 3.1



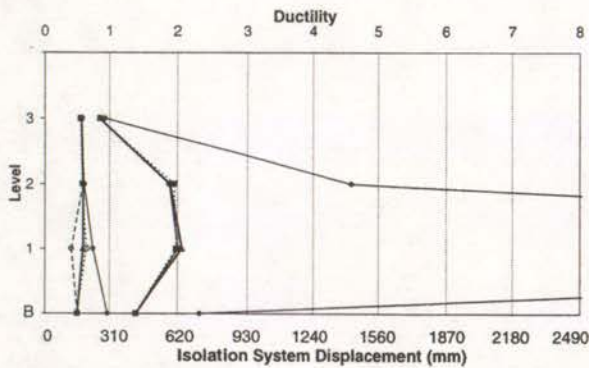
Design 3.2



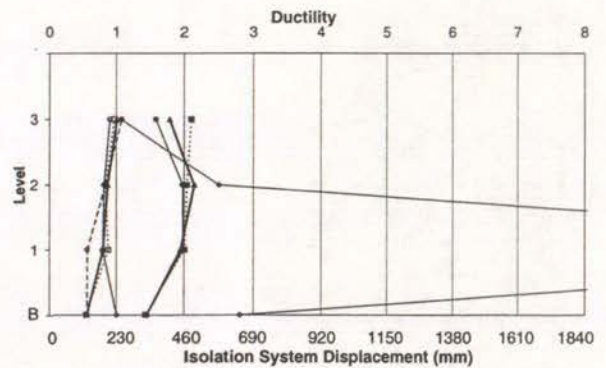
Design 3.5



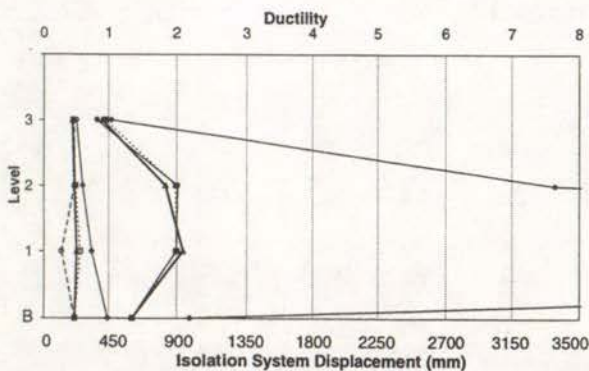
Design 3.7



Design 3.10



Design 3.12



Design 3.15

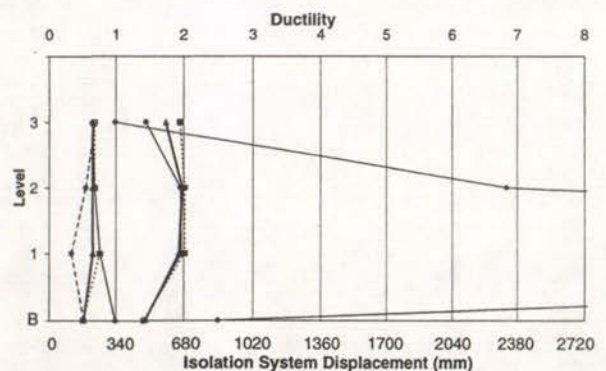
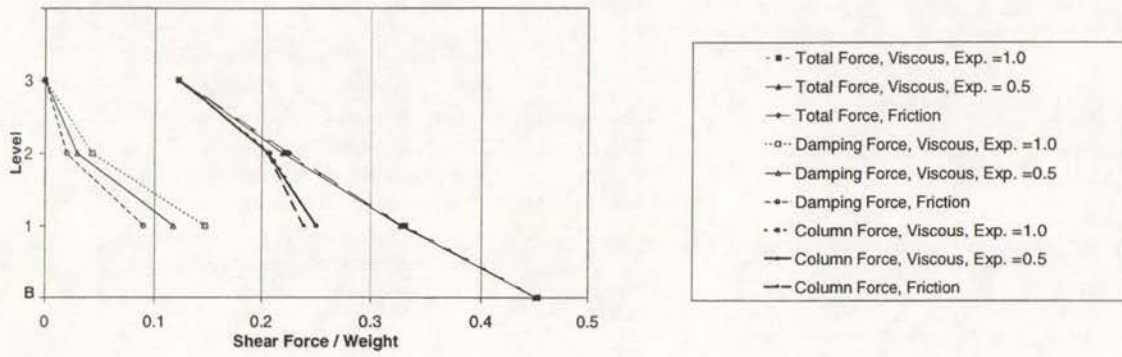
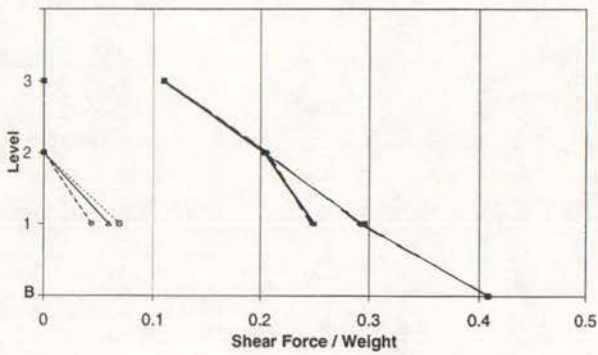


Figure 6.3: Deformations of the Three Storey Seismically Isolated Structures after Retrofitting the Superstructure

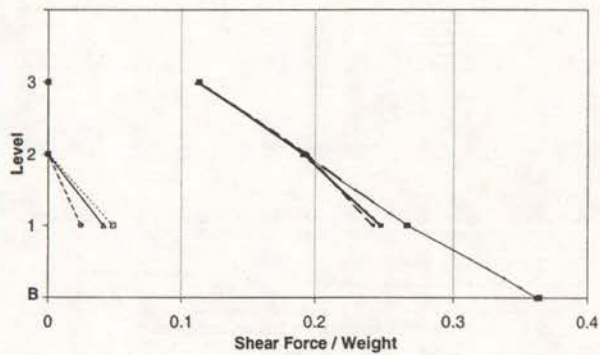
Design 3.1



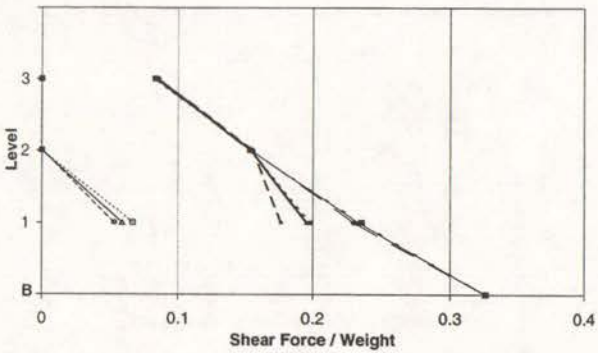
Design 3.2



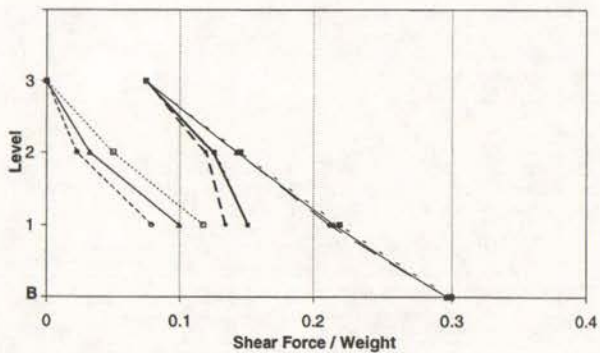
Design 3.5



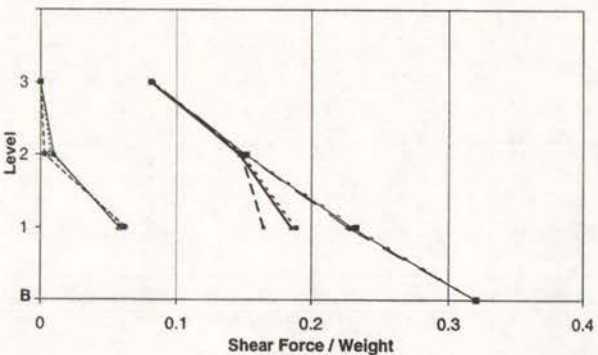
Design 3.7



Design 3.10



Design 3.12



Design 3.15

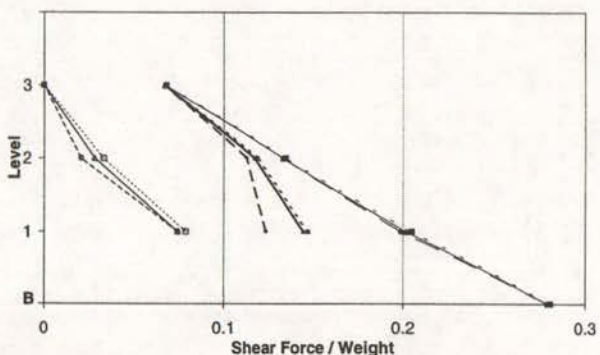


Figure 6.4: Near Field Shear Forces in Three Storey Seismically Isolated Structures

superstructure. Figure 6.4 shows the average near field inter-storey shear forces in each of the structures retrofitted with the various forms of damping. Each plot shows the maximum damping forces, maximum column forces and the maximum total inter-storey shear forces at all levels. The damping force and isolator force have not been given at the isolator level as the same form of damping was used to retrofit the isolation system of all structures even though different forms of damping were used in the superstructure. This was in order to focus on comparisons of different forms of additional damping in the superstructure.

Figure 6.4 shows that the average maximum inter-storey shears are the same for each of the three forms of damping, however, the individual column forces and damping forces differ. In each building retrofitted with friction damping, the average maximum damping force at a given level is the lower than for additional viscous damping. The same applies to the column forces. However, using friction damping, the average sum of the maximum damping and column forces is equal to the average total force at each level. In contrast, using viscous damping the average sum of the two forces is greater than the total force for the both forms of viscous damping. This implies that the maximum viscous damping forces must be out of phase with the maximum column shear forces.

Time histories for the column shear forces, additional damping forces and total shear forces in response to Rinaldi, for Design 7 at level one, are presented in Figure 6.5. Figure 6.5a shows the response of the structure retrofitted using viscous damping with a velocity exponent equal to 1.0. For this earthquake the maximum damping force appears to be largely adding to the maximum column force to give the maximum total force. In contrast, Figure 6.6a shows that the maximum column force is approximately equal to the maximum total shear force for the Sylmar Hospital response, therefore the damping forces must be largely out of phase with the maximum column shear forces. This demonstrates that the response of the building with additional damping can be quite dependent on the earthquake record. Figures 6.5b and 6.6b show the responses of Rinaldi and Sylmar Hospital respectively using additional viscous damping with a velocity exponent of 0.5. These figures show that the difference between the column shear and total shear forces is slightly larger than using pure viscous damping. The response of the friction damped structure is shown in Figures 6.5c and 6.6c. It illustrates that there is direct addition of damping forces to column shear forces using friction damping, thus the maximum total shear force is significantly larger than the column shear force. However,

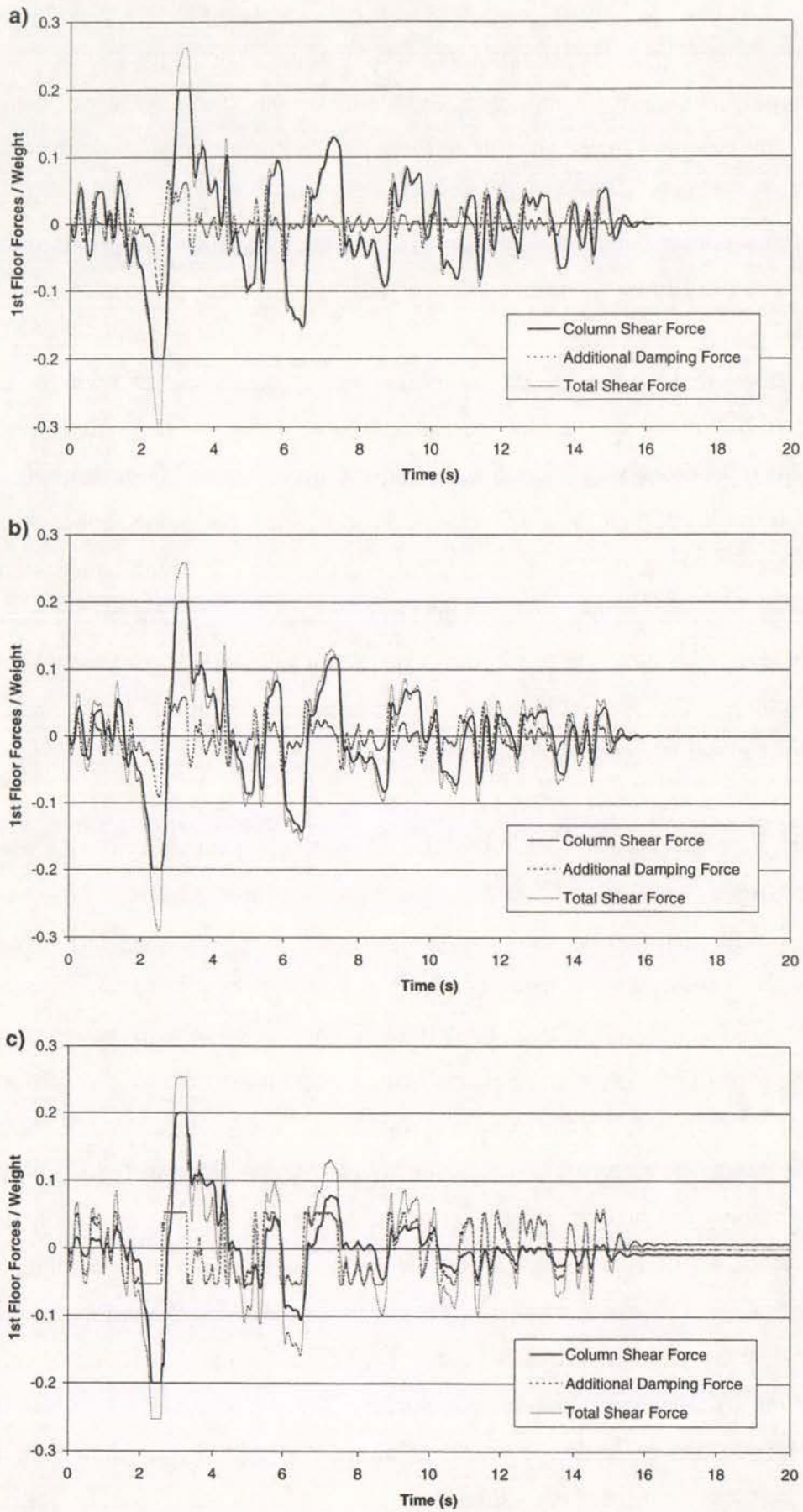


Figure 6.5: Rinaldi Shear Force Time Histories for Design 3.7 with each Form of Damping

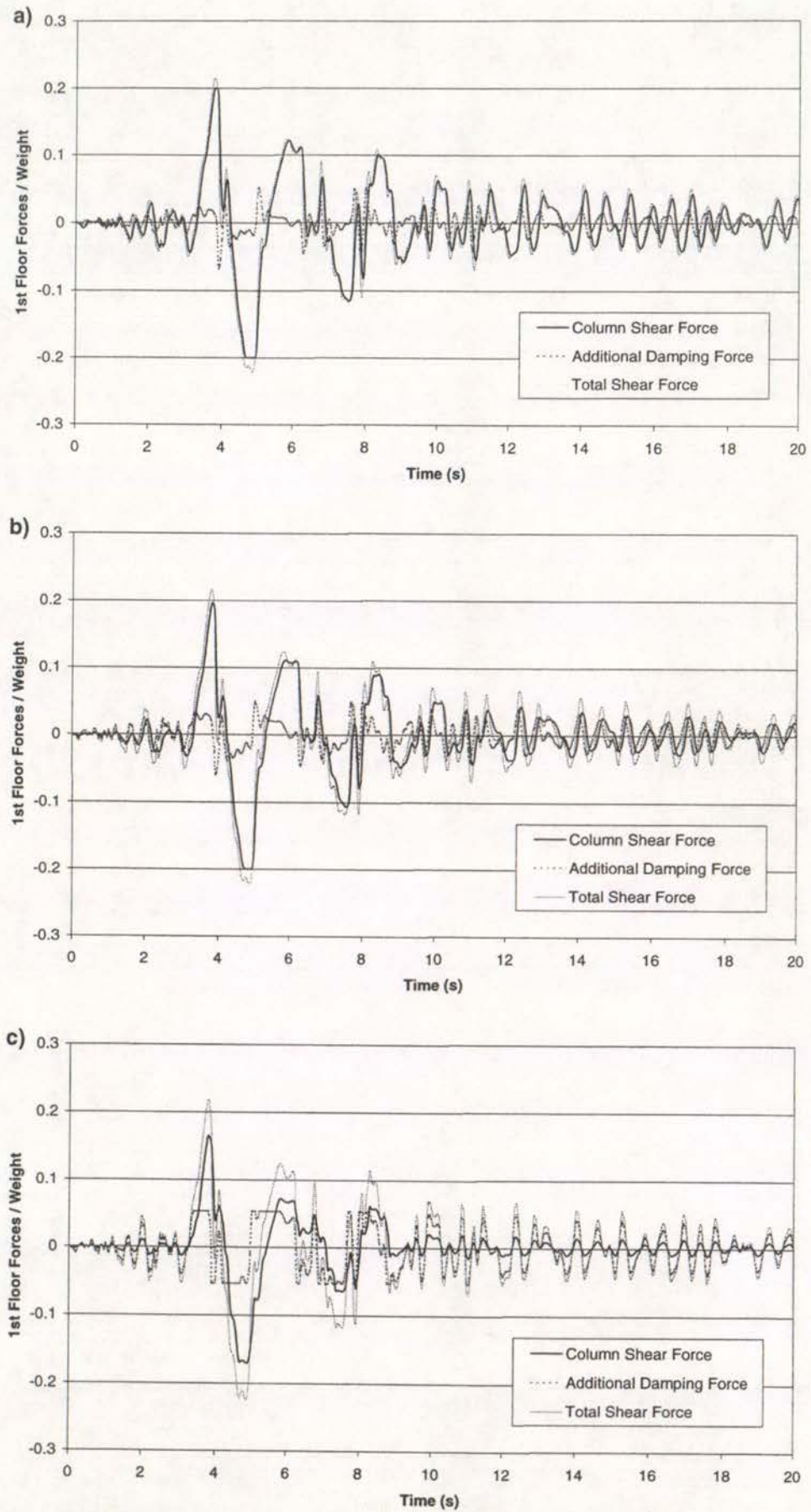


Figure 6.6: Sylmar Shear Force Time Histories for Design 3.7 with each Form of Damping

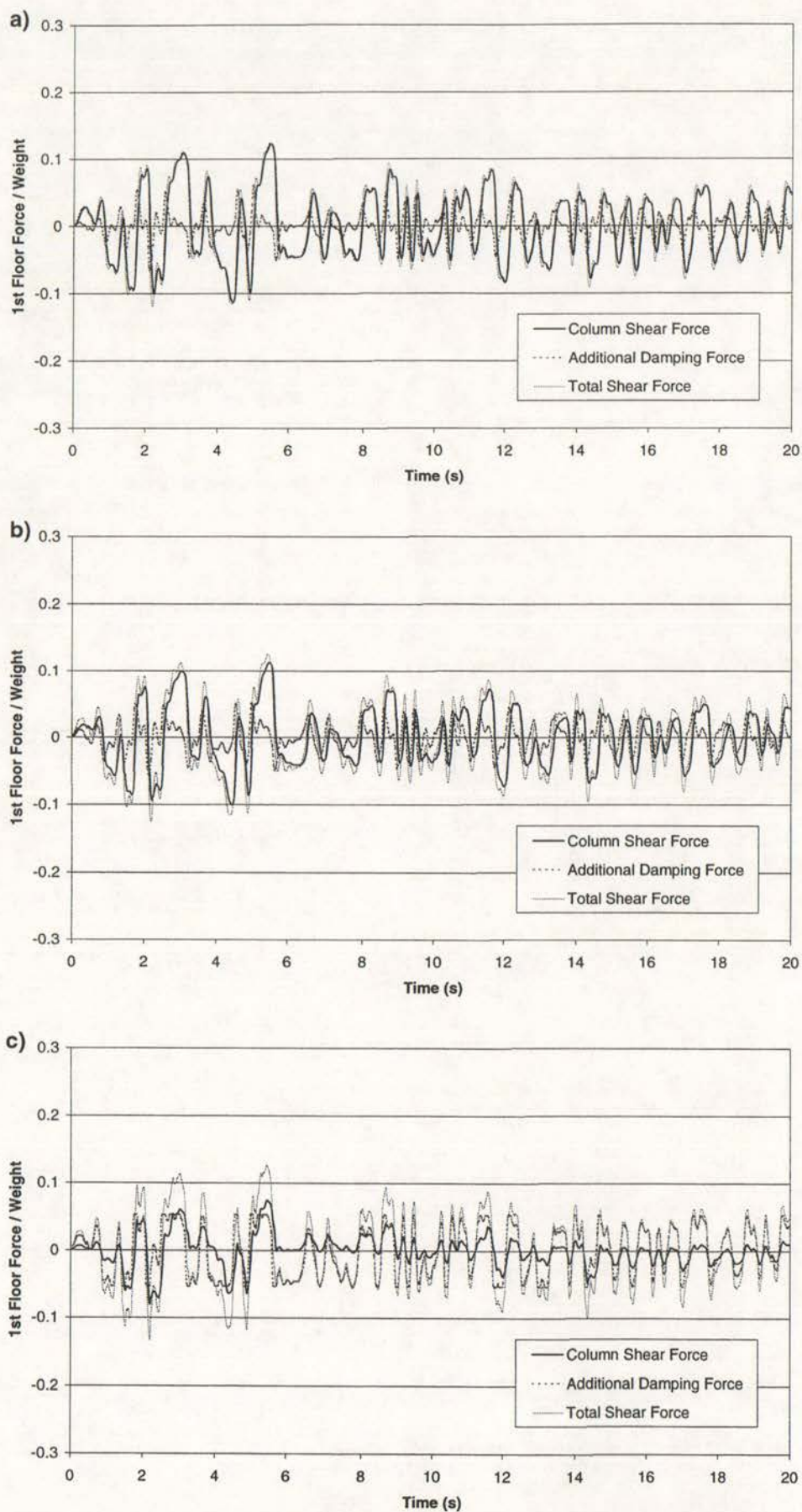


Figure 6.7: El Centro Shear Force Time Histories for Design 3.7 with each Form of Damping

the total shear force for the friction damped buildings is approximately the same as that for the viscous damped buildings, therefore the forces have been partially transferred from the columns into the dampers. The effect of this transfer of forces is discussed in Section 6.3.5.

The storey shear forces for the design level earthquakes are represented in Figure 6.7 using the response to El Centro. Pure viscous damping is the most effective form of retrofit in terms of this design level response as the maximum column shear forces are almost identical to the maximum total shear forces indicating that the damping forces at these maxima are approximately equal to zero, as shown in Figure 6.7a. Therefore the impact of additional viscous damping in response to this level earthquake is small. There is little change in the response using viscous damping with a velocity exponent of 0.5. In contrast, the total shear force due to additional friction damping, shown in Figure 6.7c, is significantly larger than the column shears. As with the near field earthquakes large portions of the column shear forces have been transferred into the dampers.

6.3.5 Axial Forces due to Additional Damping

The damping has been modelled as shear elements in the superstructure of the three storey seismically isolated buildings, however, it is likely that it will have to be implemented as part of a diagonally braced framing system. Figure 6.8 shows an example of a diagonally braced frame in a three storey building.

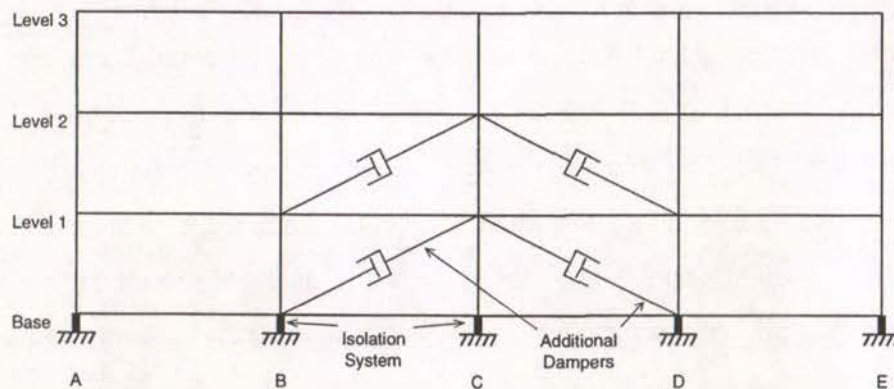


Figure 6.8: Example of Three Storey Building with Additional Damping in the Superstructure.

This building illustrates one possible configuration for applying additional damping to the first and second levels. The building assumes a 2:1 ratio of bay width to storey height. Using

this configuration the horizontal component of the force in each of the dampers acts to reduce the lateral displacements. However, the vertical components of the damping forces at a given level, cause additional axial forces to be induced in the columns or isolator bearings of the level below. For the configuration shown, the vertical components in the central column will oppose each other resulting in no axial forces in the columns assuming the forces in both dampers at a given floor are equal. However, the axial forces in columns B and D will be significant.

For a numerical example the forces in Design 1, which has the largest damping forces as shown in Figure 6.4, are assumed. The damping force divided by the total weight in the first and second storeys is approximately equal to 0.12 and 0.03 respectively. Assuming these are resisted by two perimeter frames, one of which is shown in Figure 6.8, then the corresponding forces in each frame is 0.06 and 0.015 respectively. As there are two dampers at each level then the horizontal components of the forces in each damper are equal to 0.03 and 0.0075 those in the first and second floors respectively. Assuming the horizontal component of the force divided by the total weight in each damper at the second floor is 0.0075, the maximum damping axial force in first floor columns B and D using the 2:1 ratio of height to width is 0.00375. Similarly, if the horizontal component of each of the forces in each damper at the first floor is 0.03, the additional axial force divided by the total weight of the building in the isolator bearing at columns B and D is 0.015. The total additional axial force due to damping in the bearings is equal to the sum of the first and second floor forces, which is equal to 0.01875 times the total weight of the building. If each of the perimeter frames carry 12.5% of the axial load in the building, based on a structure with perimeter frames at either side of the building and three equally spaced interior frames, then the axial force divided by the total weight in columns B and D is 0.03125 at the base. Thus the additional axial load in the isolator bearings is 60% of the static axial compression force and can act in either in tension or compression. This is a significant amount, therefore if additional damping was used to retrofit the superstructure of a isolated building a detailed frame and section analysis would be required to ensure that the columns and bearings could withstand the additional axial forces.

The influence of axial forces highlights one of the deficiencies of additional friction damping in the superstructure. The maximum damping forces using friction damping occur at the same time as the maximum lateral deformations in the columns, inducing combined bending and axial actions. In contrast, with viscous damping the axial forces in the columns tend to be

slightly larger, however, as exemplified in Figures 6.5 to 6.7 the maximum damping forces tend to occur when the forces and deformations in the columns are small, therefore combined actions are minimised.

Another possible way of retrofitting the superstructure of a multi-storey seismically isolated building, is to increase the relative stiffness and strength of the columns at the levels in which the failure is occurring. An increase in stiffness would transfer deformations into other floors and an increase in strength would increase the hysteretic area of the column and thus the effective damping. The additional strength and stiffness would not be part of a cross braced framing system therefore additional axial loads would not be an issue. However, the problem with column modifications is that it is likely to be time consuming and require severe disruption to operations of a building in order to implement. Investigation of a building with a different distribution of stiffness and strength was undertaken in the analysis of the William Clayton building to follow.

6.3.6 Variability between Individual Earthquake Responses

Each level has been retrofitted so that the average displacement response has a ductility equal to 2.0 or less in response to the near field earthquakes. If all the near field earthquakes had caused the superstructure yield at each level, then the average shear force in the columns should be equal to the yield force. It was observed that the column shear forces in Figure 6.4 were often less than the yield forces, particularly for the structures retrofitted with friction damping. This implies that the some of the earthquakes were not causing the structures to yield at all levels. Since the average displacement is equal to a ductility of two, then some of the earthquakes were causing extremely high inter-storey deformations. The variability between the different earthquakes was investigated using the coefficient of variations for the design and near field displacement response at each floor, as shown in Figure 6.9.

Figure 6.9 illustrates that at level one, the coefficient of variation for the buildings retrofitted with friction damping is much larger in response to the near field earthquakes than for both forms of viscous damping. In contrast, at the upper floors there tended to be more variation in the buildings when retrofitted with viscous damping. In general, however, additional friction damping had a more variable near field displacement response. In terms of the design level

earthquakes, the variation was clearly larger for the friction damped structure. The two forms of viscous damping had similar responses. Therefore additional viscous damping appears to be a more appropriate retrofit than friction damping, as it is less sensitive to the type of earthquake. This sensitivity is especially important when a structure being retrofitted is located in a region where there have been few, if any, near field earthquakes recorded in the past.

6.3.7 Acceleration Floor Spectra for Various Forms of Additional Damping

The consequence of additional damping in the superstructure was calculated for the design level earthquakes in terms of acceleration response of each floor using five percent damped acceleration floor spectra. The El Centro floor spectra for Design 7, calculated using SAP, are presented in Figure 6.10. It can be seen that the responses with the various forms of additional damping in the superstructure are almost identical. The response at short periods, between zero and 0.3 seconds, of the retrofitted building was approximately the same as the response of the unretrofitted building. For periods between 0.3 and 1.2 seconds the response of the retrofitted building was larger at each floor than the response of the unretrofitted building, with up to a 100% increase in accelerations. In contrast, the response at each floor for periods greater than 1.2 seconds was less than the unretrofitted response.

The other design level earthquakes, using viscous damping with a velocity exponent of 0.5, show similar trends in Figures 6.8 and 6.9. There was commonly a similar response at short periods, an increase for the mid-range periods, and a decrease in response at longer periods when damping is added to the structure. The magnitude of the change in response differs between the various earthquake records. The Bucharest earthquake shows almost no increase in response at any period, while Joshua Tree has over a 100% increase at certain periods. There is typically a 50% increase in acceleration response at each floor for a period range between 0.3 and 1.5 seconds.

Comparing Figures 6.10 and 6.11 with Figure 6.2, using additional viscous damping with a velocity exponent of 0.5, shows that the response of the building with additional damping exclusively at the isolation level is very similar to the response with additional damping throughout the structure. Therefore, the increase in response due to additional damping is

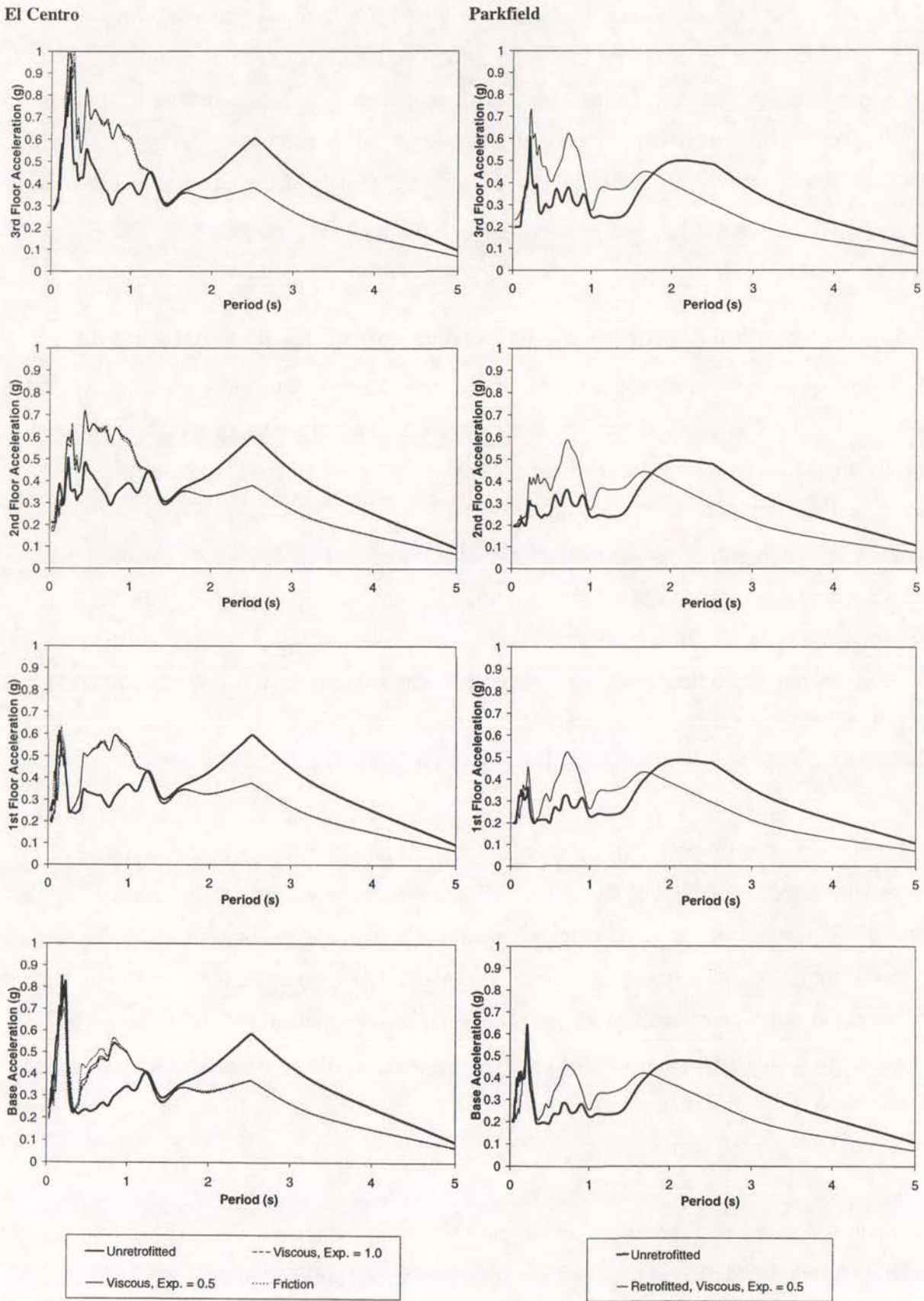


Figure 6.10: El Centro and Parkfield Acceleration Response Spectra at each Floor for Design 3.7

Bucharest

Joshua Tree

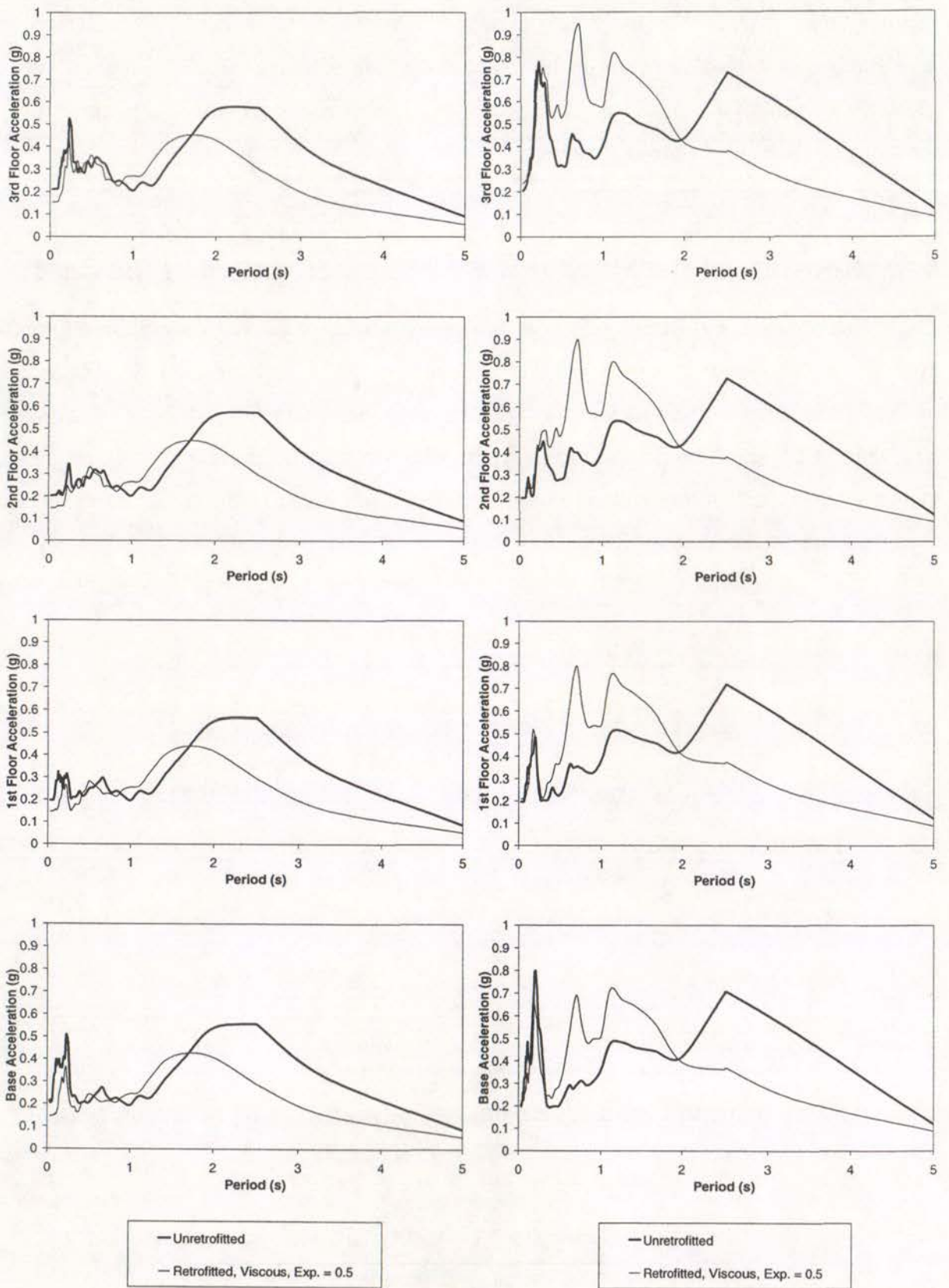


Figure 6.11: Bucharest and Joshua Tree Acceleration Response Spectra at each Floor for Design 3.7

almost entirely dependent on the additional damping in the base and has little dependence on the additional damping in the superstructure. Therefore although a 50% increase in accelerations was typical in each of the structures retrofitted using viscous damping with a velocity exponent of 0.5, this could be expected to be decreased to around 30% by retrofitting the structures with pure viscous damping.

6.4 Response of the Six Storey Building Retrofitted at the Base

The six storey building, Design 6.7, was initially retrofitted at the base using the optimum level of viscous damping, with a velocity exponent of 0.5, found for the isolation system modelled with a rigid superstructure. As with the three storey structure, although the average near field response of the isolation system was close to the maximum allowable response, there remained a soft storey failure in the first floor, as shown in Figure 6.12. As expected, the superstructure needed retrofitting.

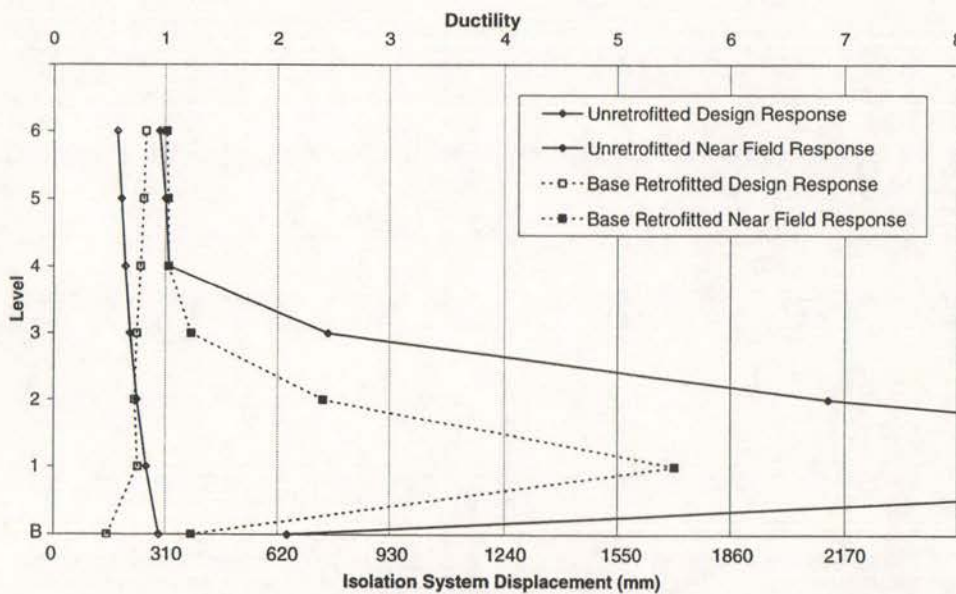


Figure 6.12: Unretrofitted and Base Retrofitted Response of Six Storey Seismically Isolated Building

Table 6.3: Additional Damping for each Level of Six Storey Structure

Additional Viscous Damping, Exponent = 0.5, c/W (s/m)						
Base	Level 1	Level 2	Level 3	Level 4	Level 5	Level 6
0.103	0.236	0.078	0	0	0	0

6.5 Retrofit of the Superstructure for the Six Storey Building

6.5.1 Optimum Levels of Damping

One form of damping, additional viscous damping with a velocity exponent of 0.5, was used to retrofit the superstructure of the six storey building. System identification was used to find the optimum levels at each floor. The results for Design 6.7 are presented in Table 6.3, which can be compared with the results of Design 3.7 in Table 6.2 and rigid structure in Table 6.1. Damping levels are given in terms of damping constants divided by the total weight of the structure.

6.5.2 Average Deformations at each Floor

The average inter-storey design level and near field deformations at each floor after retrofit are given in Figure 6.13. The lower floors have been reduced to a maximum average ductility approximately equal to 2.0, while the upper floors have ductilities less than 2.0. A soft storey failure was prevented. This response is similar to the response of the three storey buildings as shown in Figure 6.3.

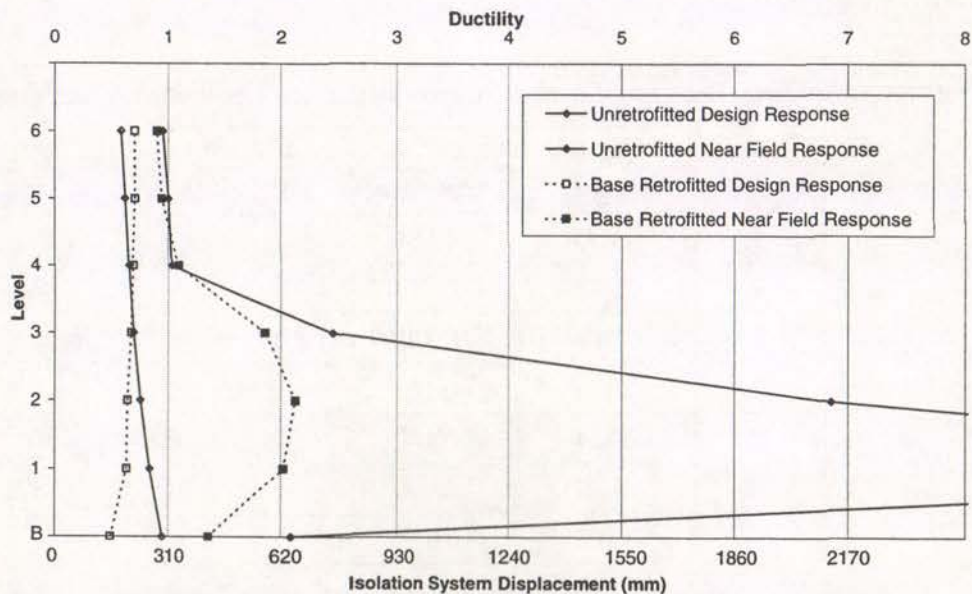


Figure 6.13: Deformation of Six Storey Seismically Isolated Building

6.6 Comparison of Retrofits for the Multi-Storey Buildings

It was shown that the three storey structures, retrofitted with the optimum levels of three forms of additional damping at the base, had deformations in the superstructure comparable to the relative base shear responses for each different type of additional damping. Therefore using the near field base shear response in a rigid superstructure model was generally able to find the most effective form of additional damping at the base.

Table 6.4 gives the level of additional damping required in the isolation system of each structure modelled with a rigid superstructure compared with the three storey seismically isolated buildings and the single six storey building. It is based on the isolation systems retrofitted using viscous damping with a velocity exponent equal to 0.5. This table shows that there is little difference between the damping levels, with the three storey buildings having zero to 10% decrease in the level of additional damping required at the base, compared to the rigid structures. The six storey building has a similar decrease in the level of damping compared to the three storey building. The small decrease in the level of additional damping required at the base can be accounted for by the yielding of the columns in the superstructure, which dissipates some energy. The small differences in the damping levels for the multi-storey buildings imply that Figure 4.18 can be used reasonably effectively to estimate the optimum level of damping required at the base of any seismically isolated building.

Table 6.4: Additional Damping Level at Base of Rigid and Three Storey Buildings

Design	Viscous Damping, Exp.= 0.5, c/W (s/m)		
	Rigid	Three Storey	Six Storey
1	0.239	0.231	
2	0.147	0.147	
5	0.173	0.167	
7	0.113	0.108	0.103
10	0.154	0.149	
12	0.090	0.090	
15	0.120	0.111	

Similar levels of damping were also found optimal in the three and six storey superstructures of Designs 3.7 and 6.7 respectively. The levels of additional damping at the first floor were approximately the same. These damping levels, in terms of the damping constant divided by

the total weight of the structure, were equal to 0.243 and 0.236 respectively. A small amount of extra damping required in the second floor of the six storey structure to prevent the soft storey failure.

6.7 Effect of Retrofitting Multi-Storey Seismically Isolated Buildings on the Response to Small Earthquakes

6.7.1 Reduction in Acceleration Response

The acceleration above which occupants become aware of an earthquake is commonly considered to be 0.02 g. Therefore, for Design 7 with modelled with rigid superstructure, El Centro and Parkfield were scaled by 0.042 and 0.050 respectively so that the base shear divided by the total weight was equal to 0.04. This was just below the yield force divided by the total weight for the isolation system of 0.041. The maximum accelerations were expected to be approximately 0.04 g respectively, twice the maximum felt accelerations. It was considered likely that the additional viscous damping retrofit would be able to reduce the base shears in response to these small earthquakes and reduce accelerations to levels which could not be felt by occupants.

The acceleration response of the unretrofitted three storey seismically isolated structure with Design 7 isolation system properties was equal to 0.040 and 0.074 g for El Centro and Parkfield respectively. After retrofitting the three storey building, using additional viscous damping with a velocity exponent of 0.5, the El Centro and Parkfield acceleration responses were 0.017 and 0.040 g respectively. Therefore, the accelerations were about 50% of their unretrofitted levels in response to both ground motions.

6.7.2 Acceleration Spectra at each Floor for Small Earthquakes

The effect of retrofitting the three storey seismically isolated structure, Design 3.7, for the small earthquakes was calculated in terms of acceleration floor spectra. Figure 6.14 shows 5% damped acceleration floor spectra for both earthquakes prior to retrofitting and after the optimal retrofit using viscous damping with a velocity exponent of 0.5. The figure shows that when the structure is retrofitted with additional viscous damping the El Centro response is

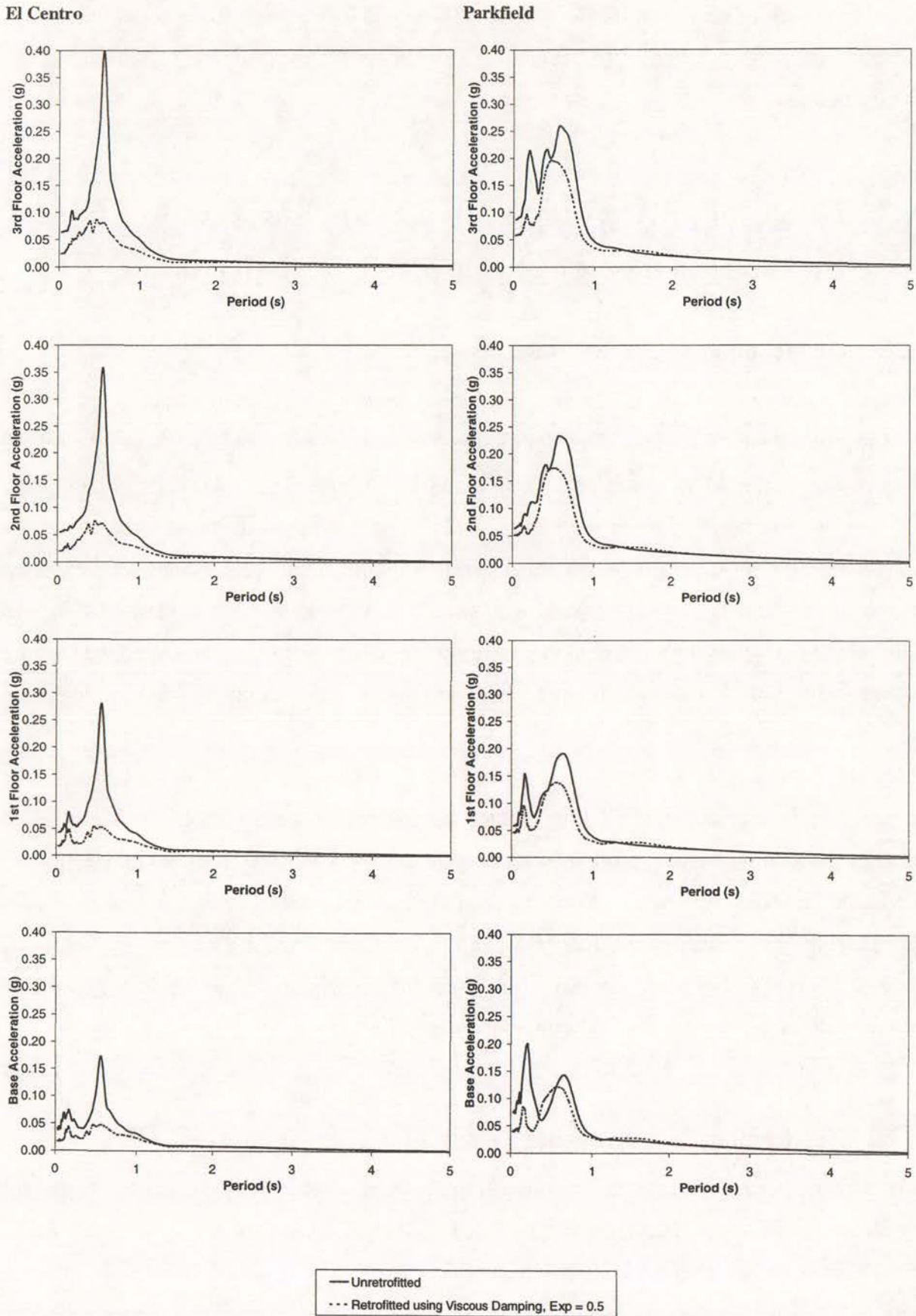


Figure 6.14: Acceleration Floor Spectra for the Small Earthquakes

reduced by up to 80% at a period around 0.5 seconds for the top floor. Typically the accelerations are reduced by 50% for periods between zero and 1.0 seconds. The additional damping is less effective in response to Parkfield although there is a considerable reduction in accelerations at short periods.

6.8 Summary of Results for Retrofitting of Multi-Storey Seismically Isolated Buildings

Retrofitting the isolation systems of the generic multi-storey buildings, although it was able to limit the isolator deformations to the maximum allowable level, did not mitigate the soft storey failure in the superstructures. The smallest responses in the superstructures were found using those forms of damping initially found to result in the lowest base shears during retrofit of the rigid seismically isolated structures. Consequently, viscous damping with a velocity exponent of 0.5 was considered the most effective form of damping for the majority of the structures in terms of near field response. For the design level earthquakes pure viscous damping was found to be less damaging, particularly in terms of acceleration floor spectra.

The three forms of damping in the superstructure, the optimum levels of which were found using system identification, were able to reduce the displacement of each floor to the maximum allowable displacement. The amount of pure viscous damping required in some of the structures was up to 80% of critical viscous damping, making it an inappropriate form of additional damping for these structures. In contrast, the levels using viscous damping with a velocity exponent of 0.5 were much lower. Thus two forms of additional viscous damping were focused on; viscous damping with a velocity exponent of 0.5 and friction damping.

Comparing the average near field damping, column shear and total shear forces at each level in the buildings, initially demonstrated that friction damping was perhaps more effective than viscous damping effective as the damping forces were smallest. The difference in forces between using friction damping and viscous damping with a velocity exponent of 0.5 was typically 10 to 20%. Thus, when considering axial forces in the columns, because the maximum damping forces were partially out of phase with the maximum displacements, using viscous damping was considered more effective. The displacement variations showed that viscous damping would be more appropriate as it is less sensitive to different earthquake

records, particular for the design response, compared to friction damping. Therefore overall, viscous damping with a velocity exponent of 0.5 was found to be most effective.

Floor spectra for the various forms of damping in the superstructure showed that accelerations were almost entirely independent of the different forms of damping in the superstructure, but were mostly dependent on the level and type of additional damping in the isolation system of the seismically isolated buildings.

It was shown that additional viscous damping was also able to reduce the response to small earthquakes that tend to vibrate a structure at levels which do not cause the isolation systems to yield. Additional damping should increase in the comfort of the building during an earthquake of this magnitude.

Chapter 7.

Retrofit of the William Clayton Building using Additional Damping

7.1 Introduction

It has been shown conceptually in previous chapters that additional damping could be used to retrofit each of the generic seismically isolated structures for near field ground motion. The concepts developed were now applied to a model of a real structure, the William Clayton building, to determine whether it too can be retrofitted using additional damping.

The William Clayton Building in Wellington, as shown in Figure 7.1²⁶, was the first seismically isolated building in the world¹⁹ and is now considered vulnerable to near field earthquakes. It is located not only in a potentially active seismic region, but is also within 200 metres of an active fault. However it was designed before the effects of large near field earthquakes on structures were fully appreciated⁷. The William Clayton building was designed for a maximum isolation system displacement of 150 mm which, if exceeded, causes the structure to impact on adjacent retaining walls and other boundaries. It is now expected that a near field earthquake is likely to cause the isolation system to exceed its maximum allowable displacement and result in damage to the superstructure of the building and adjacent retaining walls.

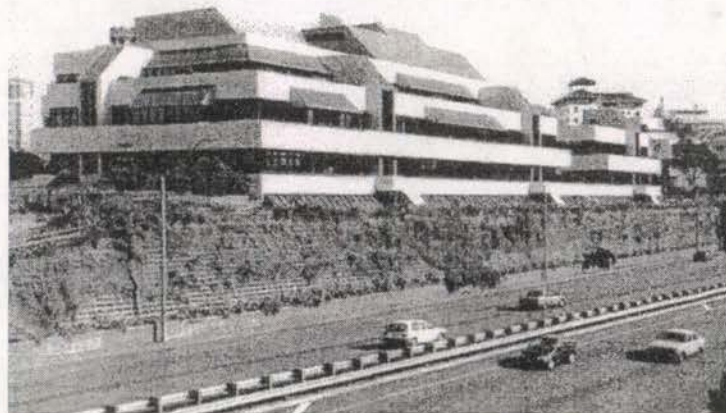


Figure 7.1: William Clayton Building²⁶

The William Clayton building is a four storey reinforced concrete structure, as described by Megget¹⁹. The plan dimensions of the building are 97 by 40 metres and the first level has a height of 5.0 m, while the other floors have a height of 4.0 m. The columns extend 0.7m below the centreline of the beams at the base of the building where they are supported by lead rubber bearings. As the performance of seismic isolation was relatively unproven at the time of construction, the William Clayton building was designed with ductile joints and detailed so that it could behave as a beam hinging mechanism in case forces in various parts of the structure exceeded their elastic limits.

In this thesis a numerical model of the structure was used to calculate the building's response to near field earthquakes and determine whether additional damping was feasible for controlling this response without compromising its performance during a design level event. A typical frame of the building, in the transverse plane, was initially modelled as an isolation system with a rigid superstructure in SAP, later referred to as the "rigid model". The rigid model is comparable to the generic rigid models. It was used to find an appropriate magnitude near field response and determine whether additional damping would be able to limit the near field displacements of the isolation system. The frame of the building was then modelled as a four storey frame similar to that modelled in Drain 2D¹³ during the original design of the structure in 1979¹⁹, as illustrated in Figure 7.2.

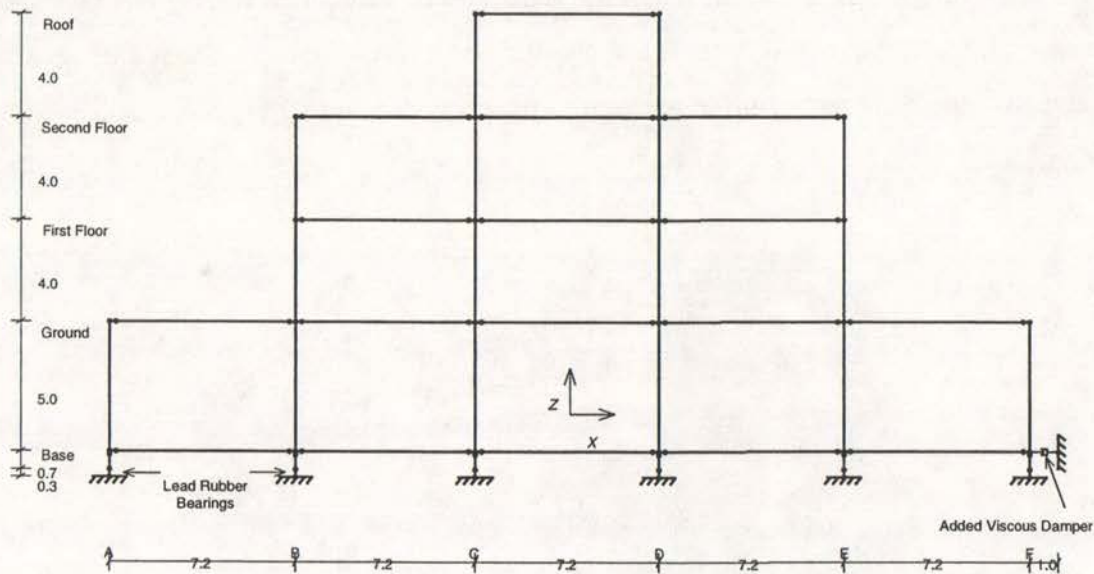


Figure 7.2: Multi-Storey Model of the William Clayton Building

The four storey model incorporated beam and column properties and beam plastic hinging to obtain a time history response almost identical to the original design response. It was able to be used to determine the effects of any proposed retrofit of the isolation system on the superstructure of the building, and determine whether additional damping was required in the superstructure as was the case with the generic buildings.

7.2 Modelling of the William Clayton Building with a Rigid Superstructure

7.2.1 Description of the Rigid Model

The mass of the transverse frame for the William Clayton building, equal to 982 tonnes, was confined to one node and the isolation system was modelled as a plastic shear element between the node and the ground, similar to its generic counterpart shown in Figure 2.1. The properties of the isolation system were representative of the six lead rubber bearings in the given frame. The initial stiffness of an individual lead rubber bearing was equal to 10000 kN/m, the post yield stiffness ratio was equal to 0.25 and yield force was equal to 100 kN, as stated by Megget¹⁹. Therefore, to represent six bearings, the properties were defined by an initial stiffness of 60000 kN/m, post yield stiffness ratio of 0.25 and yield force of 600 kN. As with the generic structures the isolation system was designed to act only in shear in the global "x" direction. Also like the generic structures, damping was assumed to be provided by the hysteretic deformations of the bilinear isolation system.

For the original design of the William Clayton Building it was found that El Centro record scaled by a factor of 1.5 had a maximum response of 107 mm using the four storey frame. Subsequently, the maximum isolation system displacement of the rigid SAP model in response to El Centro, using the same scale factor, was equal to 121 mm. This was larger than the original response as the rigid SAP model had less inherent damping than the four storey frame. Later analyses using a four storey model show that the original Drain 2D and SAP responses are almost identical.

The corresponding maximum base shear divided by the weight for the rigid SAP model was equal to 0.235. Using the initial stiffness and yield force for the six lead rubber bearings, the

yield displacement of the isolation system was equal to 10 mm, giving a ductility equal to 12.1. Consequently, the design effective stiffness of the isolation system was calculated, using Equation 2.4, as 18720 kN/m. The design effective period, using Equation 2.1a, was equal to 1.44 seconds. Using Equations 2.5 and 2.6 the equivalent viscous damping of the system was equal to 11.6%.

7.2.2 Earthquakes Records and their Corresponding Scale Factors

The same time histories for the design level and near field records, used for the generic structures, were applied to the model of the William Clayton Building. However, new scale factors for each of the records were calculated. Based on an equivalent viscous damping of 11.6%, the design damping coefficient is equal to 1.25 from Table A-16-C in the UBC¹². As the design displacement of the rigid SAP model is known (121 mm), and the effective period is 1.44 s, Equation 2.2 can be rearranged to give:

$$C_{VD} = \frac{4\pi^2}{g} \frac{D_D B_D}{T_D} \quad \dots \text{Equation 7.1}$$

Therefore, Equation 7.1 gives a design seismic coefficient that describes the UBC design spectrum which gives a response equal to the response of the William Clayton building to the El Centro ground motion scaled by a factor of 1.5. This design seismic coefficient was equal to 0.42, compared to 0.64 for the generic structures. The difference accounts for the difference in seismicity for the highly active region of California, to which the generic structures were designed, and the seismicity of the William Clayton building site perceived in the late 1970s. Using the seismic coefficient the acceleration response spectrum was shown for periods greater than approximately 0.6 seconds, as given in Figure 7.3.

The near field factor was equal to 2.0 for the generic structures. Using the same near field factor, the near field seismic coefficient for the William Clayton building was calculated to be 0.84. The resulting William Clayton near field acceleration spectrum is also shown on Figure 7.3.

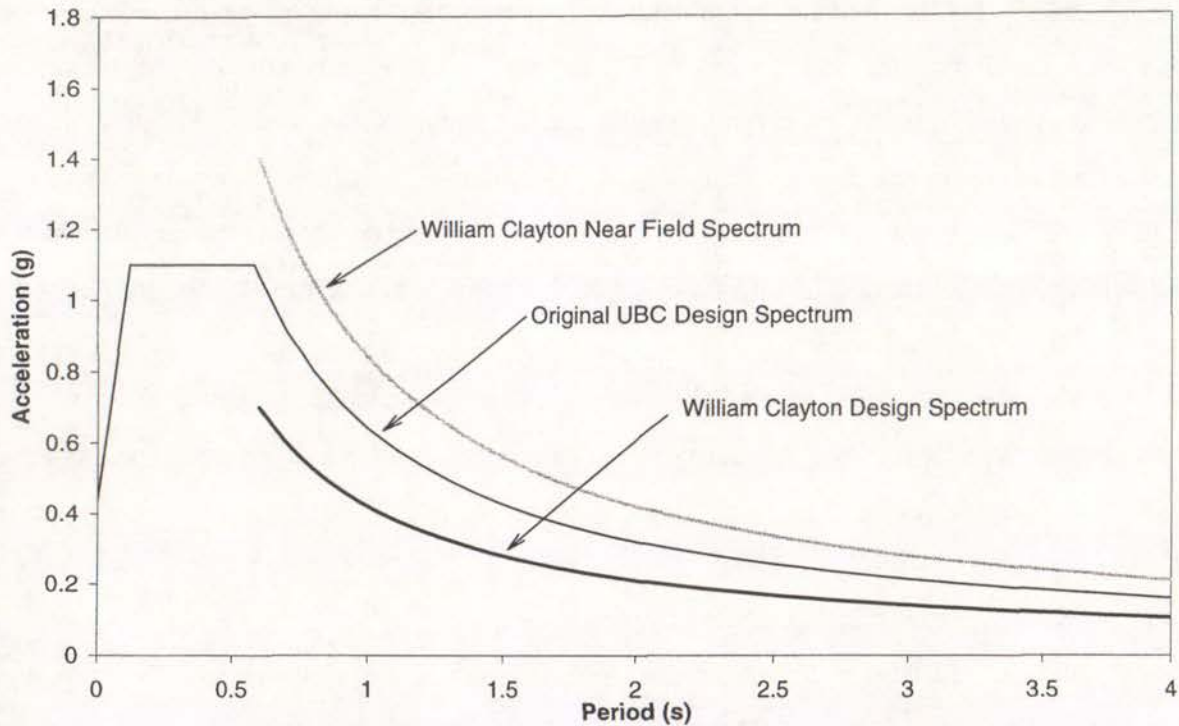


Figure 7.3: Design and Near Field Acceleration Spectra for the William Clayton Building

As discussed the maximum allowable displacement of the isolation system for the William Clayton Building is 150mm. If the maximum allowable displacement had been defined by the UBC using a maximum capable earthquake coefficient of 1.25, as for the generic structures, the maximum allowable displacement for the William Clayton building would have been 166 mm. This was calculated using the procedure set out in Section 2.1.4. The maximum allowable displacement of 150 mm was used for the purposes of retrofit, however the UBC value was useful for discussion and comparison of the William Clayton building with the generic structures.

As the design response of El Centro was equal to 121mm, each of the three other design level earthquakes was scaled so that the displacement response of the isolation system was equal to the El Centro design response. The scale factors for each earthquake is given in Table 7.1.

The near field response was calculated in the same way as for the generic structures. The post yield stiffness was assumed to be the same for displacements larger than the design displacement and the ductility was able to be calculated using an estimate of the near field isolator displacement response. Thus the near field effective stiffness, period and damping were calculated using Equations 2.2, 2.4, 2.5 and 2.6. Substituting the design parameters,

C_{VD} , T_D and B_D , for the near field parameters into Equations 2.1 and 2.2 gave a new estimate of the near field displacement response. By modifying the initial estimate, the maximum displacement was found after several iterations to be equal to 314 mm. This procedure is exemplified in Appendix 3. The near field displacement is 2.6 times larger than the design displacement, within the approximate range of 2.5 to 3.0 calculated for the generic structures. It clearly exceeds the maximum allowable displacement for the structure of 150 mm.

Each of the six near field earthquakes were scaled so that the response of the rigid superstructure model for the William Clayton building, with a 5% tolerance, was equal to 314 mm. The scale factors for each of the design and near field earthquakes are included in Table 7.1.

Two earthquakes, El Centro and Parkfield, were also scaled to represent small earthquakes with a maximum base shear of 0.04 times the total weight of the structure. This is discussed in Section 7.3.6.

Table 7.1: Scale Factors for the William Clayton Building

Design Level Earthquakes	
El Centro	1.50
Parkfield	0.55
Bucharest	0.55
Joshua Tree	0.95
Average	0.89
Near Field Earthquakes	
Northridge (Sim.)	0.50
Rinaldi	0.60
Sylmar Hospital	0.65
Elysian Park	0.90
Luceme	1.20
Imperial Valley	1.25
Average	0.85

7.2.3 Unretrofitted Response

As shown in Tables 7.2 and 7.3 the average displacement and base shear response respectively, of the rigid SAP model, are approximately the same as the corresponding responses calculated using the William Clayton design and near field spectra. Low coefficients of variation indicate little variation in the response between the different earthquakes. When Tables 7.2 and 7.3 are compared to Tables 3.5 and 3.6 it is observed that the response of the rigid William Clayton model does not compare well to any individual generic seismically isolated structure. Interpolation between generic responses was therefore used for later comparisons.

Table 7.2: Displacement Response of William Clayton Modelled with a Rigid Superstructure

Design Displacement (mm)			Near Field Displacement (mm)		
UBC Displacement	Average Earthquake Displacement	Coefficient of Variation	UBC Displacement	Average Earthquake Displacement	Coefficient of Variation
121	122	0.034	314	315	0.021

Table 7.3: Base Shear Response of William Clayton Modelled with a Rigid Superstructure

Design Base Shear / Weight			Near Field Base Shear / Weight		
UBC Base Shear	Average Earthquake Base Shear	Coefficient of Variation	UBC Base Shear	Average Earthquake Base Shear	Coefficient of Variation
0.225	0.229	0.028	0.517	0.518	0.019

7.2.4 Retrofit of William Clayton Building Modelled with a Rigid Superstructure

7.2.4.1 Application of Additional Damping

In order to reduce the near field displacements of the isolation system to the maximum allowable level, two forms of viscous damping with velocity exponents equal to 1.0 and 0.5 respectively, and friction damping were separately added to the isolation system. The procedure for adding the various forms of damping was described in Sections 4.2.2.1 and 4.2.2.2. Damping coefficients of 0.045, 0.089, 0.178, 0.267 and 0.356 were investigated, corresponding to pure viscous damping levels of 5, 10, 20, 30 and 40% of critical viscous damping. The constants were calculated using Equation 4.2, based on the total weight of 982

tonnes and design effective stiffness of 18720 kN/m. Friction damping was applied with friction coefficients equal to 0.02, 0.05, 0.10 and 0.15, based on the total weight of the structure.

7.2.4.2 Average Results of Retrofit

The average displacement and base shear response of the structure, for both design level and near field earthquakes, retrofitted with each form of damping, is presented in Figure 7.4. As with other similar figures such as shown in Figure 4.4, the average design response is described by the set of curves on the left while the near field response is described by the curves on the right. Each curve represents a different form of damping and points on each curve indicate increasing levels of damping when following the curves from left to right. This figure shows the near field base shear response for corresponding levels of additional damping at which the near field displacement response is reduced to the maximum allowable displacements, equal to 150 mm and 166 mm. The level of damping and also the reduction in the design and near field displacements and base shears, compared to the original responses are presented in Table 7.4. Responses are based on an average response for the individual design level and near field earthquakes. In Table 7.4 additional viscous damping is given in terms of the damping constant divided by the total weight of the structure and friction damping is given in terms of the friction coefficient. This table is based on a maximum displacement of 150 mm. The damping and reduction in responses for the structure based on a maximum displacement of 166 mm is given in Table 7.5.

7.2.5 Optimum Response and Comparisons with Generic Structures

As shown in Table 7.4, viscous damping with a velocity exponent of 0.5 had the smallest near field base shear response, averaged over the various earthquakes. This is consistent with the majority of the generic structures. The base shear was defined at the levels for each form of damping resulting in a near field displacement equal to the maximum allowable displacement of 150 mm. The near field base shears using the other forms of damping were within 5% of this optimum base shear at the maximum displacement. As with the majority of the generic structures, the design level earthquakes had the lowest base shear using pure viscous damping. Due to the similarity between the various forms of damping all three were used in attempts to retrofit the four storey model of the William Clayton building.

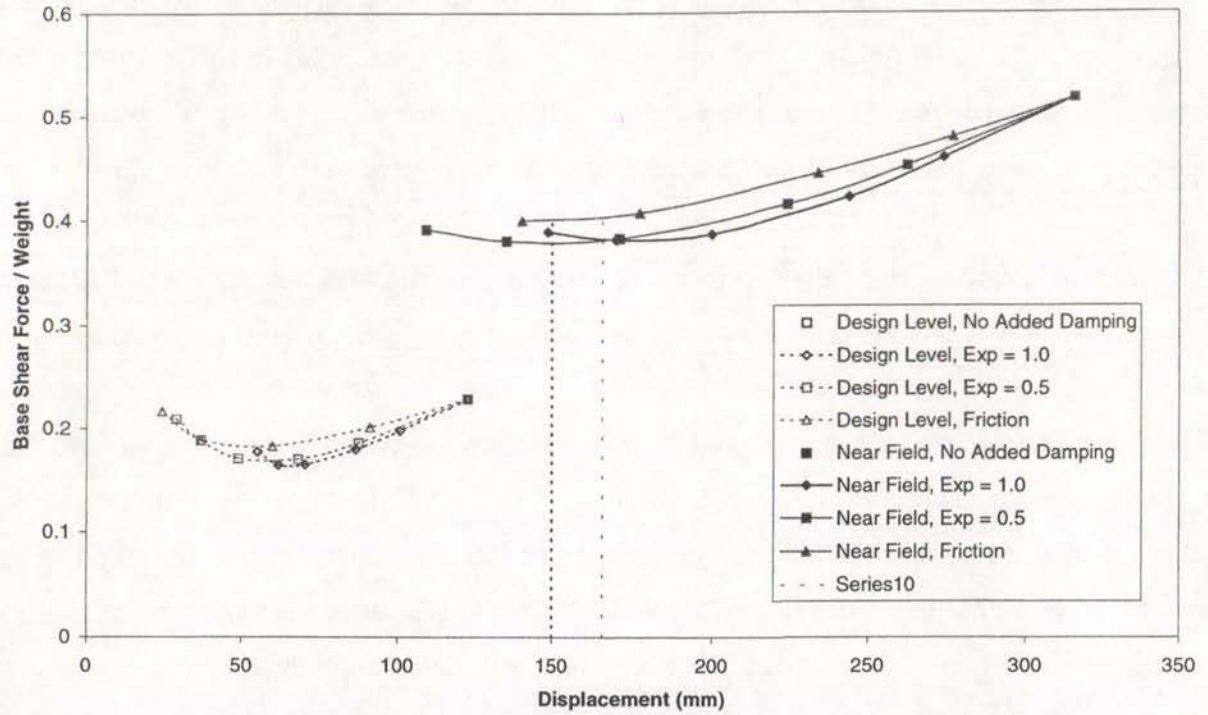


Figure 7.4: Average Design and Near Field Response of Isolation System Retrofitted with Three Forms of Damping

Table 7.4: Reduction in Average Response of Isolation System Using Optimal Damping Level Based on Maximum Displacement of 150 mm

Damping Type	Damping c/W (s/m) μ ()	Design		Near Field	
		Displacement (%)	Base Shear (%)	Displacement (%)	Base Shear (%)
Viscous, Exp. = 1.0	0.356	55	23	52	24
Viscous, Exp. = 0.5	0.320	63	21	52	27
Friction	0.140	75	10	52	23

Table 7.5: Reduction in Average Response of Isolation System Using Optimum Damping Level Based on a Maximum Displacement of 166 mm

Damping Type	Damping c/W (s/m) μ ()	Design		Near Field	
		Displacement (%)	Base Shear (%)	Displacement (%)	Base Shear (%)
Viscous, Exp. = 1.0	0.285	51	28	47	26
Viscous, Exp. = 0.5	0.187	67	21	47	26
Friction	0.120	75	15	47	22

The response of the rigid SAP model appears to follow the trends found for the generic structures. Depending on the size of the maximum displacement relative to the unretrofitted near field displacement different forms of damping are optimal. This can be illustrated in Figure 7.4. For purposes of comparison with the rigid generic structures, a maximum displacement of 166 mm is more appropriate, as this is what would have been required by the UBC. At this displacement the two forms of viscous damping had the same near field base shear response, but the design response was still optimal using pure viscous damping.

Using Figure 4.18 which enables a prediction to be made based on the generic structures, the optimum level of damping for the isolation system of the William Clayton building is 22% using viscous damping with a velocity exponent of 0.5. Therefore the predicted damping constant divided by the total weight is equal to 0.196. The level of viscous damping, with a velocity exponent of 0.5, required to reduce the near field displacement to the 166 mm maximum displacement is 0.187, in terms of the damping constant divided by the total weight of the structure. Therefore the value predicted using the generic structures is within 5% of the actual value for the William Clayton building. Differences can be attributed to non-linearity not accounted for in the linear prediction plots and different in bilinear post yield stiffness ratio, which is equal to 0.25 for the William Clayton building compared with 0.02 used in the structures represented in Figure 4.18. The relative magnitude of both the design and near field acceleration spectra for the William Clayton building was 34% smaller than the spectra used in calculating the response of the generic structures, based on the relative seismic coefficients. However, the relative difference between the design level, maximum allowable and near field responses was the same for the William Clayton building and the generic structures. Hence, the William Clayton building modelled with a rigid superstructure behaved as predicted from results of the generic structures.

7.3 Analysis and Retrofit of a Multi-Storey Model of the William Clayton Building

7.3.1 Overview

A full two dimensional multi-storey numerical model of a section of the William Clayton Building was constructed in SAP in order to determine the effects of near field ground motion

on the superstructure of the building. The model was based on the Drain 2D¹³ model using in the original design of the structure¹⁹. Comparisons were made with the original analysis output from the El Centro time history²⁰, and also the published design of the structure¹⁹, to test the integrity of the SAP model.

The results using the rigid superstructure model suggested that additional damping can be used to control isolator deformations. However, as the near field base shear force was higher than the design base shear, it was expected that deformations larger than the design deformations would be incurred in the superstructure. The effectiveness of the various possible retrofits was investigated in terms of acceleration floor spectra and variability between the various earthquakes. The response of the retrofitted structure was also calculated for small earthquakes, which tend to cause the building to vibrate without yielding the isolation system.

7.3.2 SAP Model

7.3.2.1 Dimensions of the Structure

The full multi-storey model of a transverse frame of the William Clayton Building is shown in Figure 7.2. The dimensions and properties of the model were chosen to represent properties of the real structure as in the initial time history analysis in Drain 2D²⁰. All nodes in the model are free to translate in the “x” and “z” directions and also free to rotate about the “y” axis, except the nodes connected to the ground which are fully fixed, and those above the isolation system which cannot translate in the “z” direction.

7.3.2.2 Modelling of Beams and Columns

Each beam and column is modelled with rigid end zones of 0.25 metres at either end, measured from the centreline of the adjacent columns or beams. The rigid end zones in the beams have generally been modelled as short stiff beam or column elements respectively. This enabled plastic hinges to be modelled at the end of the rigid end zones. The plastic hinges were modelled as zero length non-linear links with a high stiffness in the degrees of freedom that deform in shear and a bilinear stiffness for the rotational degree of freedom. The initial rotational stiffness was calculated to be 100 times the stiffness of the corresponding

beam and column, therefore its deformation was negligible prior to hinge yielding. The rotational stiffness of a beam can be calculated using Equation 7.2, from conventional beam bending theory and is used to calculate the rotational stiffness of the hinges in Table 7.6.

$$k_{\theta} = \frac{4EI}{l} \quad \dots \text{Equation 7.2}$$

where: k_{θ} = rotational stiffness of beam

E = elastic modulus

I = moment of inertia

l = length of beam between rigid ends

In the original analysis the beams and columns were assumed to have a post yield stiffness ratio of 0.02. Therefore, as the stiffness of the hinges were assumed to be 100 times the stiffness of the corresponding beams and columns the post yield stiffness ratio was equal to 0.0002 to obtain a similar model in SAP. This modelling process is verified in Section 7.3.3 and was shown to give almost identical results. The original Drain 2D analysis assumed slightly different yield moments in the plastic hinges for positive and negative rotations. As SAP could not easily model different yield moments in the two directions and the difference between the yield moments was small, the average was used for modelling in SAP.

Table 7.6: Beam and Column Properties

Elements	Area (m ²)	Moment of Inertia (m ⁴)	Shear Area (m ²)	Hinges	
				Rotational Stiffness (x10 ⁶ kNm)	Yield Moment (kN)
Base Beams	0.660	0.0300	0.440	45.1	1050
Ground Beams	0.710	0.0400	0.470	60.2	1200
1st Floor Beams	0.660	0.0300	0.440	45.1	815
2nd Floor Beams	0.610	0.0200	0.400	29.9	475
Roof Beams	0.610	0.0200	0.400	29.9	475
Columns	0.640	0.0341	0.426	-	-
Base Columns	0.640	0.0341	0.426	763.8	1500
Rigid Ends	100	10	100	-	-

The properties of the beams and columns are presented in Table 7.6. The elastic modulus for all elements is equal to 25.2 GPa, Poisson's ratio is equal to 0.3 and the post yield stiffness of the beam and column hinges is equal to 0.0002 as stated above.

7.3.2.3 Modelling of Isolation System

The isolator bearings were modelled as non-linear links that only deform in shear, therefore the small axial deformations in the bearings have not been modelled. The shear properties have been defined as bilinear with an initial stiffness of 10000 kN/m, a post yield stiffness ratio of 0.25 and a yield force of 100 kN. There are six of these bearings on the frame modelled, as shown in Figure 7.2.

7.3.2.4 Seismic Weight

The total weight of the building frame is 9633 kN corresponding to a total mass of 982 tonnes. This is distributed between each of the floors as shown in Table 7.7. Assuming a rigid diaphragm at each floor, the nodes located at the intersection of the beams and columns on a given level, have been constrained so that the displacements in the "x" direction are equal. Subsequently, the mass is concentrated at one node on each floor corresponding to the node intersecting with column C, as labelled on Figure 7.2.

Table 7.7: Mass at each Floor

Level	Mass (tonnes)
Base	260
Ground	287
1st Floor	161
2nd Floor	161
Roof	113

7.3.2.5 Damping

The original analysis of the William Clayton Building was modelled in Drain 2D using viscous damping in the form of Rayleigh damping⁵. This can be written in terms of a mass proportionality constant, and a stiffness proportionality constant, as in Equation 7.3.

$$C = \alpha M + \beta K \quad \dots \text{Equation 7.3}$$

where: α = mass proportionality constant

β = stiffness proportionality constant

In the original model of the William Clayton building²⁰, the mass proportionality constant, α , was equal to 0.1639 associated with the mass at each level. For each beam and column element in the superstructure the stiffness proportionality constant, β , was equal to 0.00249. The stiffness constant for the isolators, however, was assumed to be equal to zero.

SAP does not model damping in the this way, instead damping is defined in terms of a fraction of critical viscous damping in each mode. It is possible to convert the Rayleigh damping into equivalent viscous damping using the natural period of each elastic mode in the structure. The procedure is outlined by Clough and Penzien⁵. For any given mode, i , the modal damping in terms of the natural frequency, ω_i , is given in Equation 7.4.

$$\xi_i = \frac{\alpha}{2\omega_i} + \frac{\beta\omega_i}{2} \quad \dots \text{Equation 7.4}$$

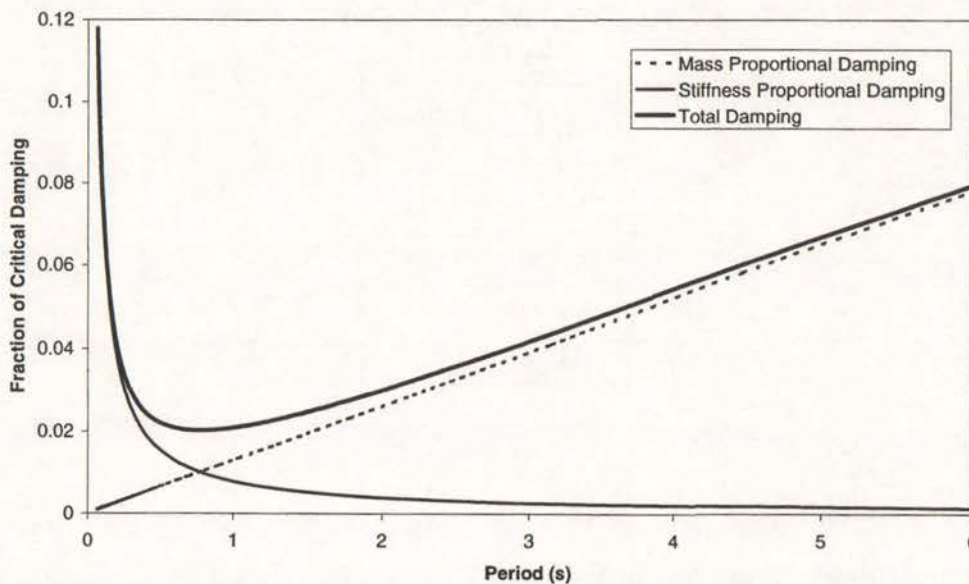


Figure 7.5: Mass and Stiffness Proportional Damping

Graphically Equation 7.4 is plotted in Figure 7.5, using α and β as in the original model of the William Clayton building. Modal damping assumes the same mass and stiffness proportionality constants are used for all elements in the structure, but the original analysis of the William Clayton building had no stiffness proportional damping in the isolation system. It can be shown that this has little effect on the model. Figure 7.5 illustrates that at long periods, the stiffness proportional damping is small and the effective damping is almost entirely dependent on the mass proportional damping. Therefore, as the period of vibration associated with an isolation system tends to be relatively long, it is was expected that the stiffness proportional damping would be small and have little effect on the solution. Similarly, at short periods the stiffness proportional damping is high. Therefore, the higher modes, which account for much of the deformation in the superstructure, were expected to have damping approximately proportional to the stiffness, as in the generic structures.

The original Drain 2D model assumed that the effective stiffness of the isolation system was based on its initial elastic stiffness. Using this assumption, from a modal analysis in SAP it was found that the first mode effective period, which was evident from the modeshapes, had a natural period of 0.91 seconds and was effectively an isolation system deformation mode. Therefore it can be seen in Figure 7.5 that at this period, the stiffness proportional damping is approximately 0.8%. As this is small, particularly compared to the design equivalent viscous damping of 11.6%, modelling it as non-zero will have little effect on the response of the building.

Table 7.8: Modal Damping

Mode	Natural Period (s)	Modal Damping (%)
1	0.907	2.0
2	0.312	2.9
3	0.161	5.1
4	0.114	7.0
5	0.070	11.3

Therefore using the proportionality constants from the Drain 2D analysis and the natural frequency for each mode from a modal analysis in SAP, the damping in each mode was calculated. The natural period calculated for the first five elastic modes, which largely act in

the translational “x” direction, are given in Table 7.8 along with the corresponding modal damping. The other modes are non-linear modes which have small participation in the response, therefore, the damping in these modes was nominally assumed to be equal to 11% the same as for Mode 5.

7.3.3 Comparison of Drain 2DX and SAP

As the original analysis of the William Clayton Building was performed using Drain 2D and the retrofit of the structure was to be performed in SAP, a comparison of the two packages was required to ensure that modelling was comparable. A portal frame model was constructed in both Drain 2DX, a newer version of Drain 2D, and SAP with the properties shown in Figure 7.6. The frame is pinned at the base with plastic hinges at the joints at either end of the beam.

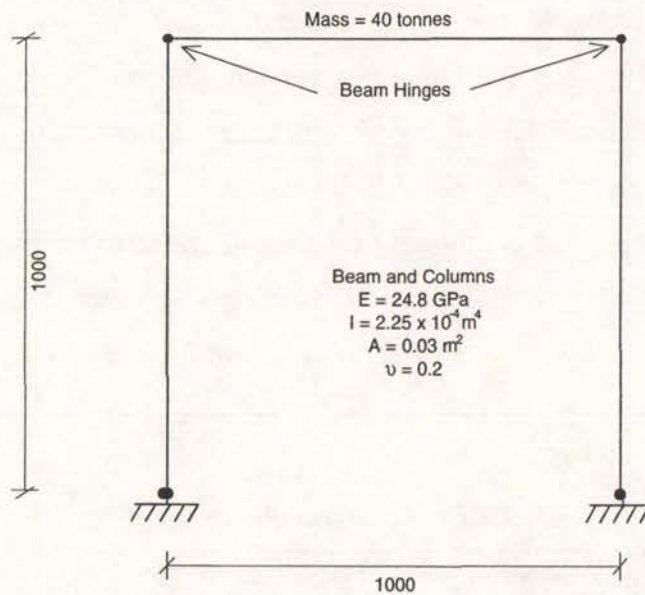


Figure 7.6: Portal Frame used for Comparison of Drain 2DX and SAP

The hinges were modelled in SAP as zero length non-linear links at the intersection of the beam and columns, with bilinear properties as described in Section 7.3.2.2. The hinges were modelled in Drain 2DX as beam hinges with a post yield stiffness equal to 0.02, effectively the same as the SAP model. The damping in SAP was modelled at five percent modal damping in the elastic and non-linear modes. The same level of damping was modelled in Drain with α equal to 2.167 and β equal to 0. Figure 7.7 shows that the time histories for the Drain 2DX and SAP analyses were almost identical, which indicates the solution techniques

for the two non linear analyses are comparable, as is the modelling of the damping and the plastic hinges in the frame.

The displacement time history calculated in SAP for the base and roof levels of the William Clayton building in response to El Centro, compared to the original response calculated in Drain 2D²⁰, are given in Figures 7.8 and 7.9. They illustrate that the responses of the base and the roof calculated in SAP are similar to the responses calculated by Drain 2D, with less than 10% variation at any time. There are a number of possible sources for the small variation. Slight differences in the yield moments between SAP and Drain 2D can probably account for much of the variation, but other sources include differences in the time history iteration technique, treatment of damping, plastic hinge formation and the different time increments used in the analysis.

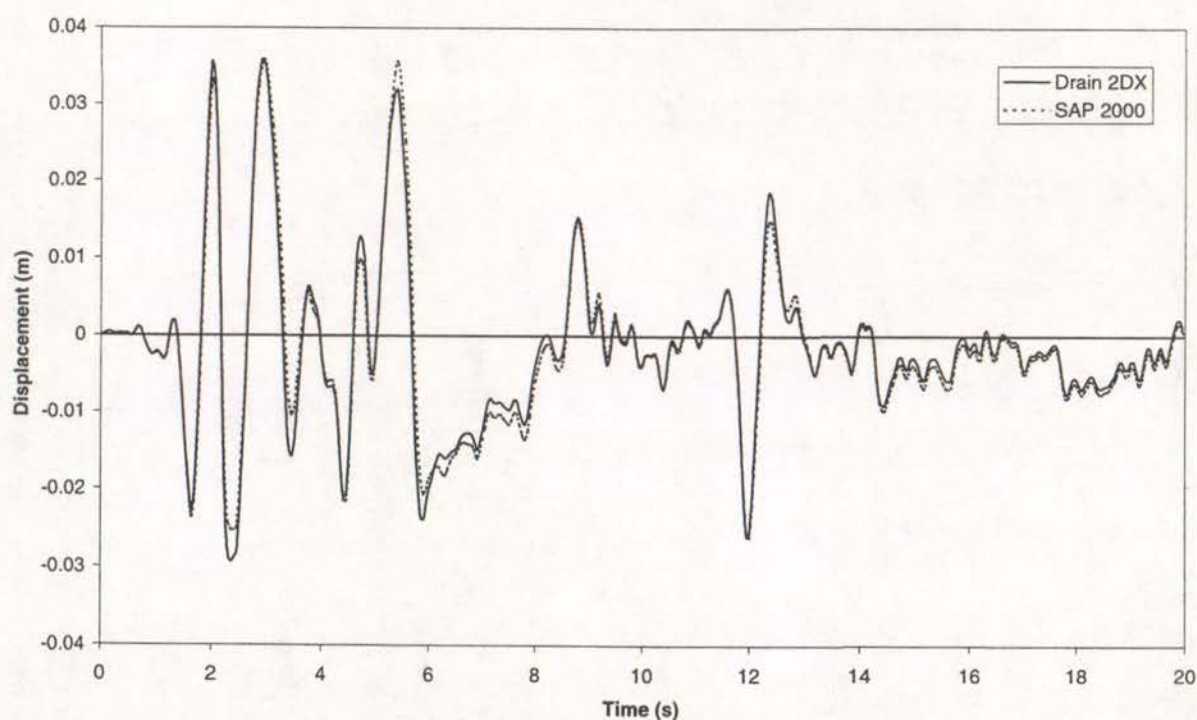


Figure 7.7: One Bay Portal Frame used to Verify SAP Model

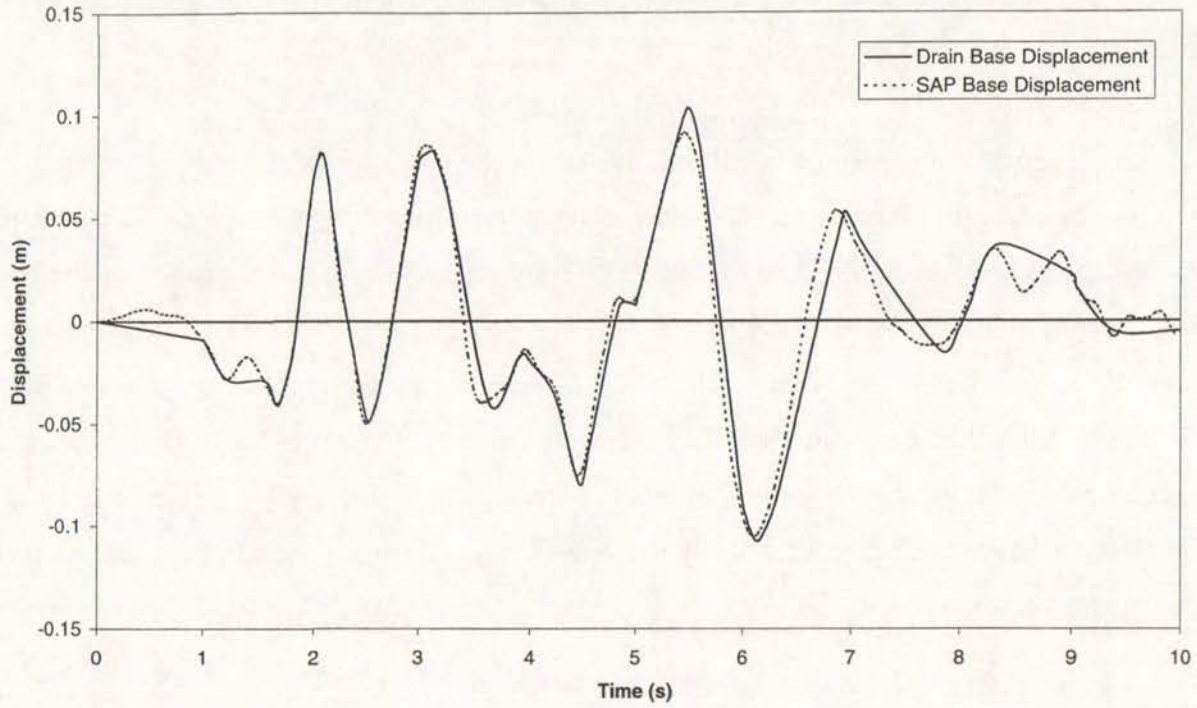


Figure 7.8: El Centro Base Displacement Time History for William Clayton Building

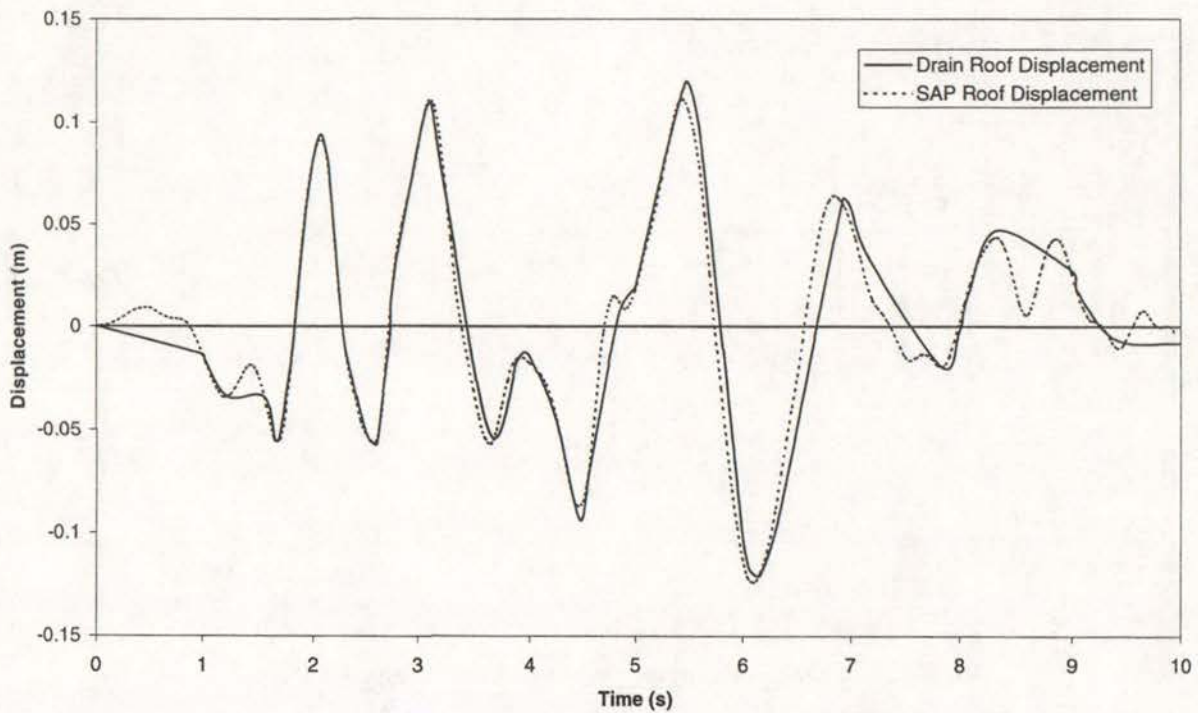


Figure 7.9: El Centro Roof Displacement Time History for William Clayton Building

7.3.4 Response of Unretrofitted Building

The frame of the William Clayton Building, as shown in Figure 7.2, was analysed using the four design level earthquakes and the six near field earthquakes. The magnitude of the earthquakes was scaled using the same factors as the building modelled with a rigid superstructure, given in Table 7.1. The maximum inter-storey displacements at each level, averaged over the various earthquake responses, for the different design level and near field earthquakes respectively are presented in Table 7.9. Comparisons with the rigid structure at the base are also given. The displacements illustrate that the response of the base was reduced when the superstructure was added to the model, due to additional damping contained in the superstructure of the building. The coefficients of variation have also increased with the modelling of the superstructure, however as for the generic structures this is a largely a function of the scaling, in that they were scaled to the unretrofitted rigid SAP model response.

The average displacement of the isolation system in response to the near field earthquakes is 82% greater than the maximum allowable response, thus retrofit of the isolation system is required. However, unlike the generic structures analysed in Chapter 5, there was no indication of a soft storey failure in response to the near field earthquakes. The near field inter-storey displacements in the superstructure were only two to three times the design response.

Table 7.9: Inter-storey Displacements for Unretrofitted William Clayton Building

Level	Design Displacement (mm)		Near Field Displacement (mm)	
	Average	Coefficient of Variation	Average	Coefficient of Variation
Base	108	0.015	273	0.059
Ground	4.68	0.063	10.92	0.062
1	2.54	0.187	8.36	0.050
2	2.10	0.212	5.92	0.057
Roof	1.52	0.219	3.92	0.158

7.3.5 Retrofit of the William Clayton Building

7.3.5.1 Average Response at the Base

In an attempt to control the isolator deformations, additional damping was provided at the base of the William Clayton Building. The same levels of additional damping were used as in the rigid superstructure model:

1. Viscous damping with damping constants corresponding to levels of 5, 10, 20, 30 and 40% of critical damping using damping exponents equal to 0.5 and 1.0; and
2. Friction damping with friction coefficients equal to 0.02, 0.05, 0.10 and 0.15.

The response of the base of the structure with each of these various levels of additional damping is shown in Figure 7.10. As with other plots of this nature the design response is represented by the set of curves on the left while the near field response is represented by the curves on the right. Each curve represents a different form of damping and the points indicate increasing levels of damping, as described previously. The maximum displacement of 150 mm is shown and was used to find the appropriate levels of damping for retrofitting.

Figure 7.10 is very similar to Figure 7.4 for the rigid superstructure model, however, the reduction in displacements when including the superstructure in the SAP model is also evident in Figure 7.10. As a result smaller levels of damping are required to limit the near field displacements to the maximum allowable displacement. At the maximum displacement of 150 mm both forms of viscous damping have the same near field base shear response. However additional pure viscous damping has a better design response in terms of a lower design level base shear. Friction damping is again least effective. Optimum retrofit results for each form of damping are summarised in Table 7.10 where displacement and base shears are given in terms of reduction in the unretrofitted response.

Table 7.10: Reduction in Average Response of Isolation System Using Optimal Retrofit

Form of Damping	Damping Level c/W (s/m) $\mu ()$	Design Level		Near Field	
		Displacement (%)	Base Shear (%)	Displacement (%)	Base Shear (%)
Visc. Exp. = 1.0	0.320	47	19	45	21
Visc. Exp. = 0.5	0.205	56	11	45	21
Friction	0.110	67	0	45	18

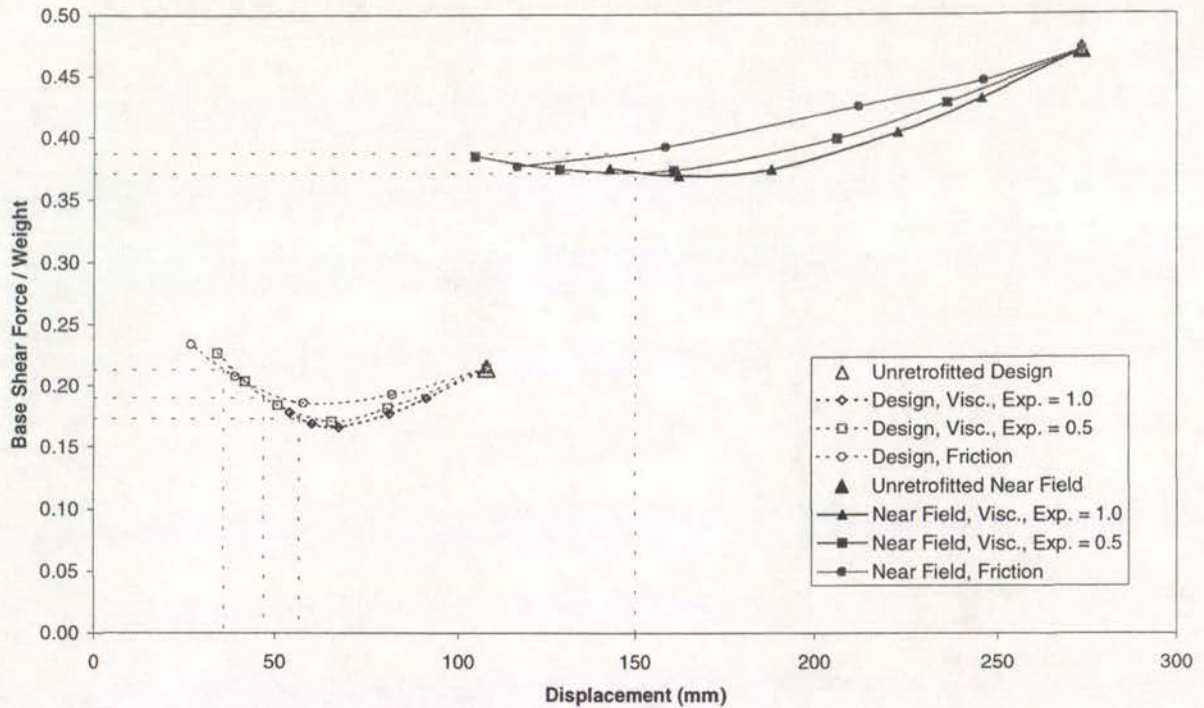


Figure 7.10: Average Design and Near Field Response of Isolation System Retrofitted with Three Forms of Damping

7.3.5.2 Average Displacement of the Superstructure with Optimal Retrofits

For the generic structures, the displacement ductility of each floor was plotted. These ductilities were readily calculated from the inter-storey displacements as the columns were modelled to deform in shear. However, for the William Clayton building with plastic deformations provided by rotation of the beam hinges, it was more difficult to get a direct measure of the inter-storey ductilities. The ductility of each floor was calculated by performing a pushover analysis of the superstructure for the William Clayton building, and using this to plot base shear versus top floor displacement, as shown in Figure 7.11. The relative forces applied at each floor for the pushover analysis were calculated using Equation 2.8, as defined by the UBC. The initial stiffness and post yield stiffness are shown in Figure 7.11 from which the top floor yield displacement was estimated at to 42 mm. Assuming a yield displacement of each floor proportional to height, the top floor displacement was used to calculate the yield displacement at each floor and subsequent inter-storey yield displacements. Plots of base shear versus displacements at each floor confirmed that the above assumption was valid. The equivalent static forces used in the pushover

analysis and resulting inter-storey yield displacements calculated at each floor are given in Table 7.11.

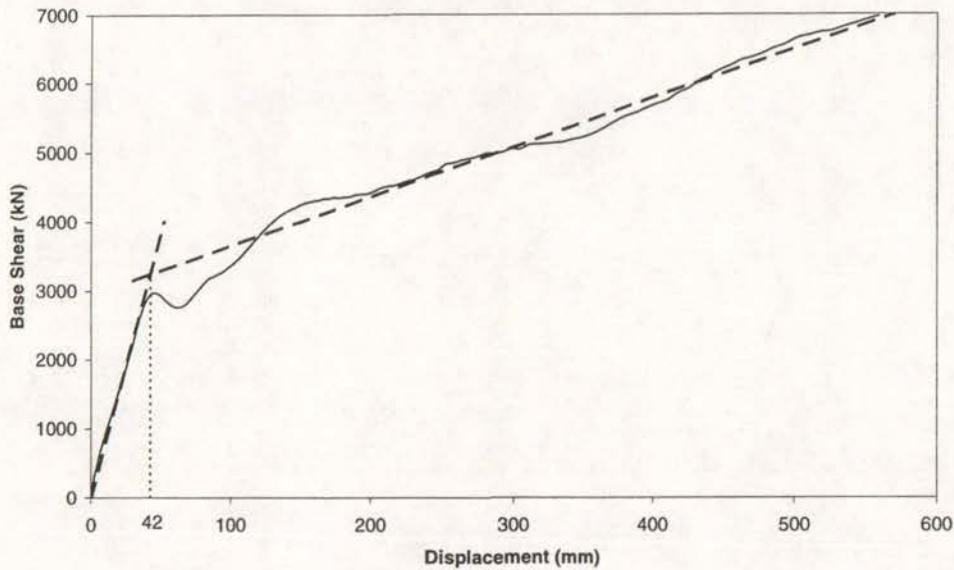


Figure 7.11: Force Displacement Relationship for Pushover of William Clayton Building

Table 7.11: Results of Pushover Analysis for William Clayton Building

Level	Weight (kN)	Height (m)	Relative Equivalent Static Force (kN)	Interstorey Yield Displacement (mm)
Base	2550	0	0	
Ground	2820	5	0.208	12.35
2	1580	9	0.210	9.88
3	1580	13	0.303	9.88
Roof	1110	17	0.279	9.88
Total	9640		1.00	42.0

The average design level and near field inter-storey displacements for each floor of the William Clayton building, retrofitted with each of the three forms of damping at their optimum levels, are presented in Figure 7.12. The inter-storey ductility of each floor above the base is given by the top horizontal axis while the displacement of the isolation system in millimetres is given on the bottom axis. It should be noted that the maximum inter-storey displacements between the various floors in this figure did not necessarily occur at the same time for a given earthquake record. Figure 7.12 shows that the ductility of each floor with any form of additional damping is less than one, therefore there is no need to retrofit the

superstructure of the William Clayton building, as was required in the generic structures. Although there is some yielding in the plastic hinges at certain levels of the superstructure, these do not result in large inelastic deformations at each level.

The two forms of viscous damping have a similar near field response in the superstructure, as shown in Figure 7.12, resulting from equal base shears. In contrast, the deformations with friction damping are slightly larger at each floor corresponding to a larger base shear. The design level earthquakes show that the superstructure displacements using additional viscous damping are smaller than the unretrofitted displacements, while the deformations have been increased using additional friction damping, again corresponding to the relative size of the base shear for each structure. Therefore, Figure 7.12 suggests that the viscous damping is more effective than friction damping. At this stage it is difficult to differentiate between the two forms of viscous damping.

7.3.5.3 Variation in Response between Earthquakes

Figure 7.13 shows the coefficient of variation for the displacement response at each level with various forms of additional damping at their optimum levels. It was difficult to differentiate between the various forms of damping in terms of variations for the William Clayton building. This is unlike the retrofits for the generic structures, where it was found that additional friction damping caused the largest variation in response between the three additional forms of damping. However, Figure 7.13 shows that the variation increases near the top of the structure, where it can be shown that the largest inelastic deformations are found. In the generic structures, the larger variation in deformations tended to be in the lower floors, once again where the largest inelastic deformations are found. In general the coefficients of variation tend to be of similar magnitude to those found in the generic structures.

7.3.5.4 Individual Earthquake Response at the Base

The earthquake record exhibiting the least favourable near field response for this building is Elysian Park. It can be interpolated from Figure 7.14 that for this ground motion the maximum near field displacement using additional pure viscous damping with a damping

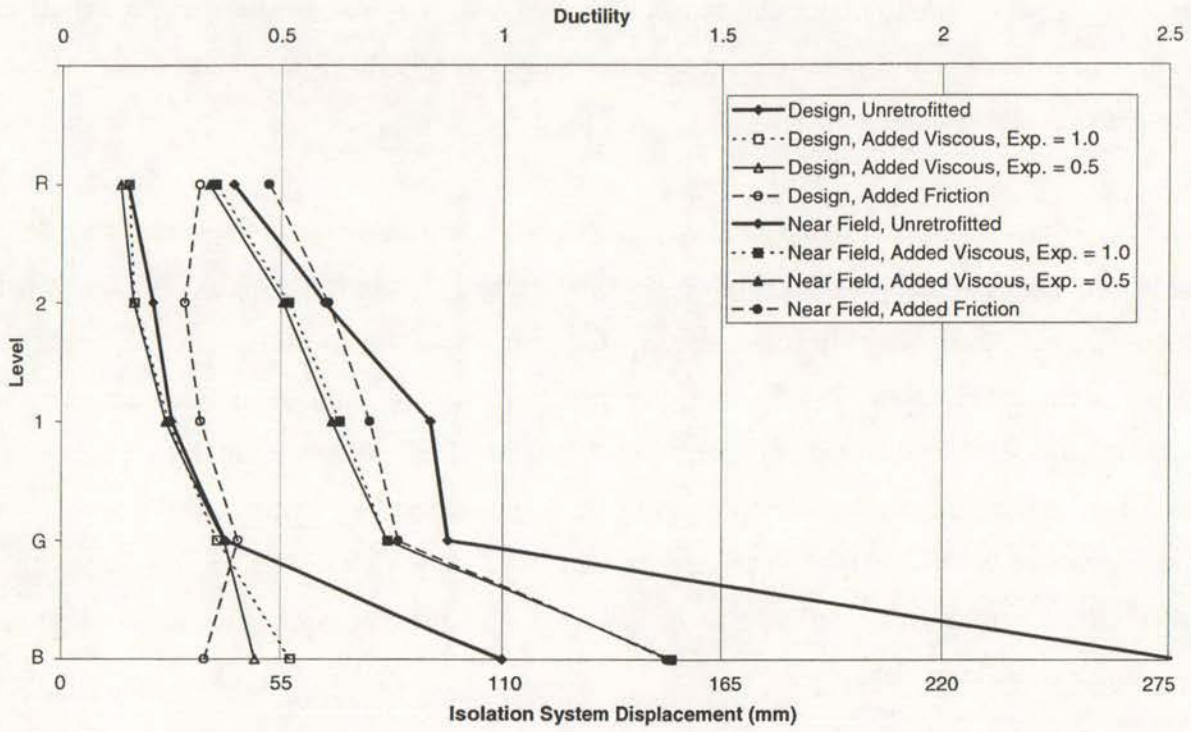


Figure 7.12: Average Displacement of Each Floor

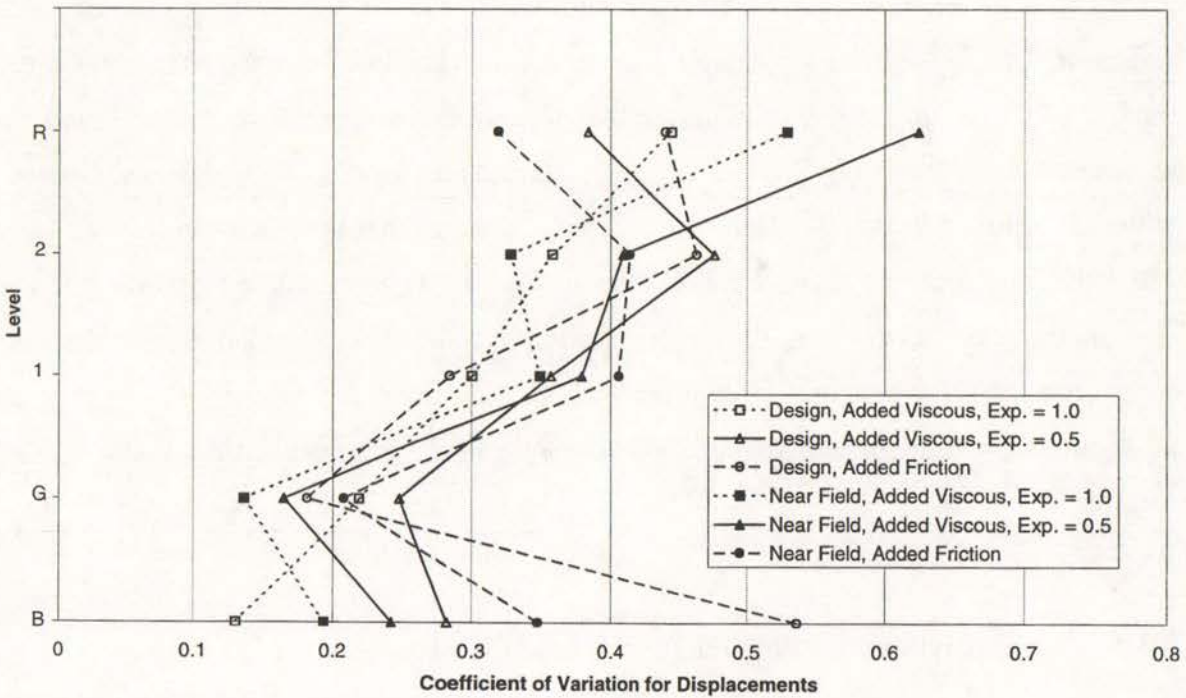


Figure 7.13: Coefficients of Variation for Displacements of Each Floor

constant of 0.32 would be approximately 180 mm, assuming no buffer or retaining walls existed to prevent such a displacement. Therefore, additional damage would be expected in the superstructure when the maximum displacement was exceeded. It can be seen that this worst case response is approximately equal to the average plus one standard deviation response. Therefore, it may have be desirable to increase the level of additional damping to prevent pounding based on the average plus one standard deviation response. However, this would result in a higher base shear for the design level earthquakes. Using near field displacements, averaged over the various earthquake responses as the basis for retrofit, was considered a good compromise between attempting to limit near field displacements while causing minimal impact to the design response.

The Sylmar Hospital record was used by Zhou³⁵ for the basis of retrofitting the William Clayton Building using hysteretic damping. Figure 7.14 shows that most favourable near field response was obtained using the Sylmar Hospital ground motion compared to the other records. This might suggest that it is not conservative to use this record. However, Zhou based the study on an unscaled Sylmar Hospital record, where as a scale factor of 0.65 was used to modify the amplitude of ground motion in this thesis. Ultimately, the two studies are likely to be comparable.

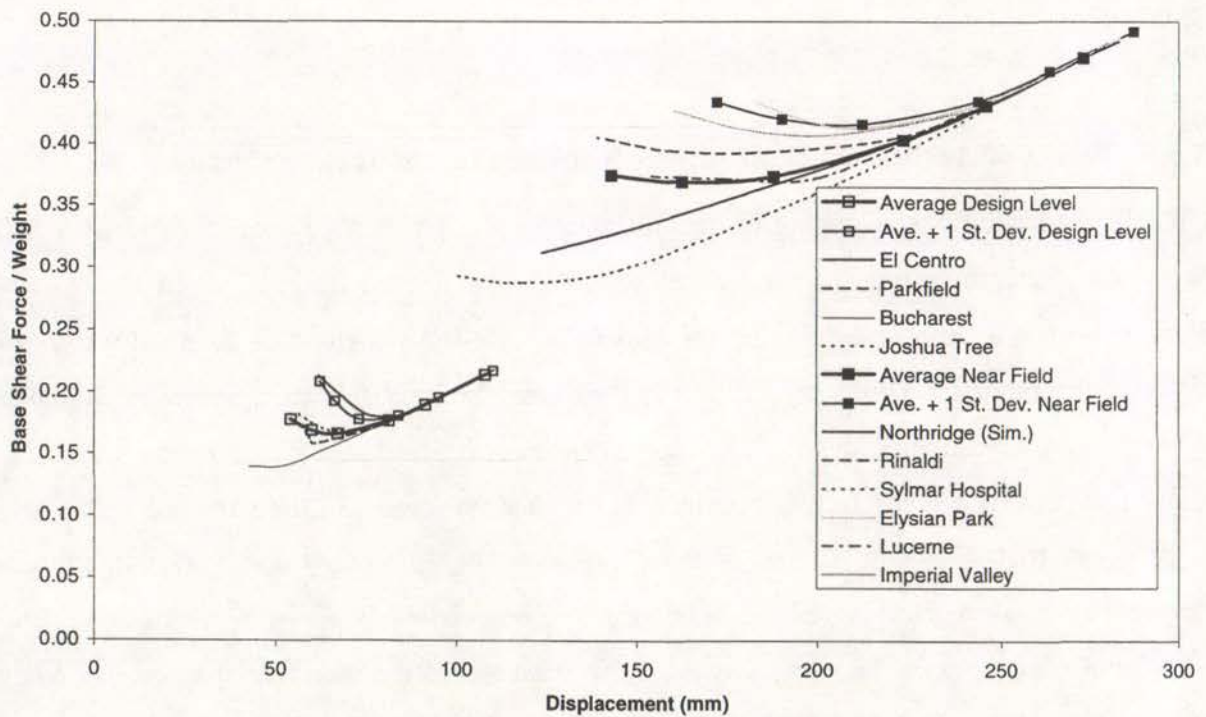


Figure 7.14: Individual Earthquake Response at the Base for Various Levels of Pure Viscous Damping

7.3.5.5 Acceleration Floor Spectra

In order to investigate the effects of retrofitting the William Clayton building on the non structural components and occupants of the building in response to the design level earthquakes, acceleration spectra were plotted for each floor. Figure 7.15 uses El Centro to illustrate that the spectra at each floor, for the building retrofitted with any form of additional damping, exceed the unretrofitted spectra at periods between approximately 0.3 and 1.2 seconds. For longer periods the response is actually reduced. The smallest increase in the acceleration spectra is at the base and gets progressively larger at higher levels of the building.

There is a considerable difference between the various forms of damping particularly at the short periods. The magnitude of the acceleration spectra for the building retrofitted with pure viscous damping is less than 50% of the spectra for the friction damped building at periods with the largest response. Using pure viscous damping the increase in acceleration is typically a maximum of 40 to 50% at each floor. The acceleration spectra for each design level earthquake are compared in Figure 7.16, showing that similar trends are evident, with pure viscous damping having the smallest increase in response for each records. As such, the floor spectra confirm that pure viscous damping is the most effective form of retrofit for this building.

7.3.6 Effect of Additional Damping in Response to Small Earthquakes

The effect of additional damping on the response of the William Clayton building to small earthquakes was investigated using acceleration spectra at each floor. The El Centro and Parkfield records were scaled so that the maximum base shear divided by the total weight of the structure modelled with a rigid superstructure was equal to 0.040 to represent earthquakes which cause the isolation system to vibrate elastically. The scale factors were 0.040 and 0.032 respectively. The resulting accelerations for the full model of the structure at the base were equal to 0.0234 and 0.0164 g in response to the El Centro and Parkfield records respectively. Thus damping in the superstructure reduced each of these responses. After additional pure viscous damping was added to the base of the structure the corresponding accelerations were equal to 0.0112 and 0.0135 g respectively. Therefore there was a further decrease, equal to approximately 50% for the El Centro record and 20% for the Parkfield

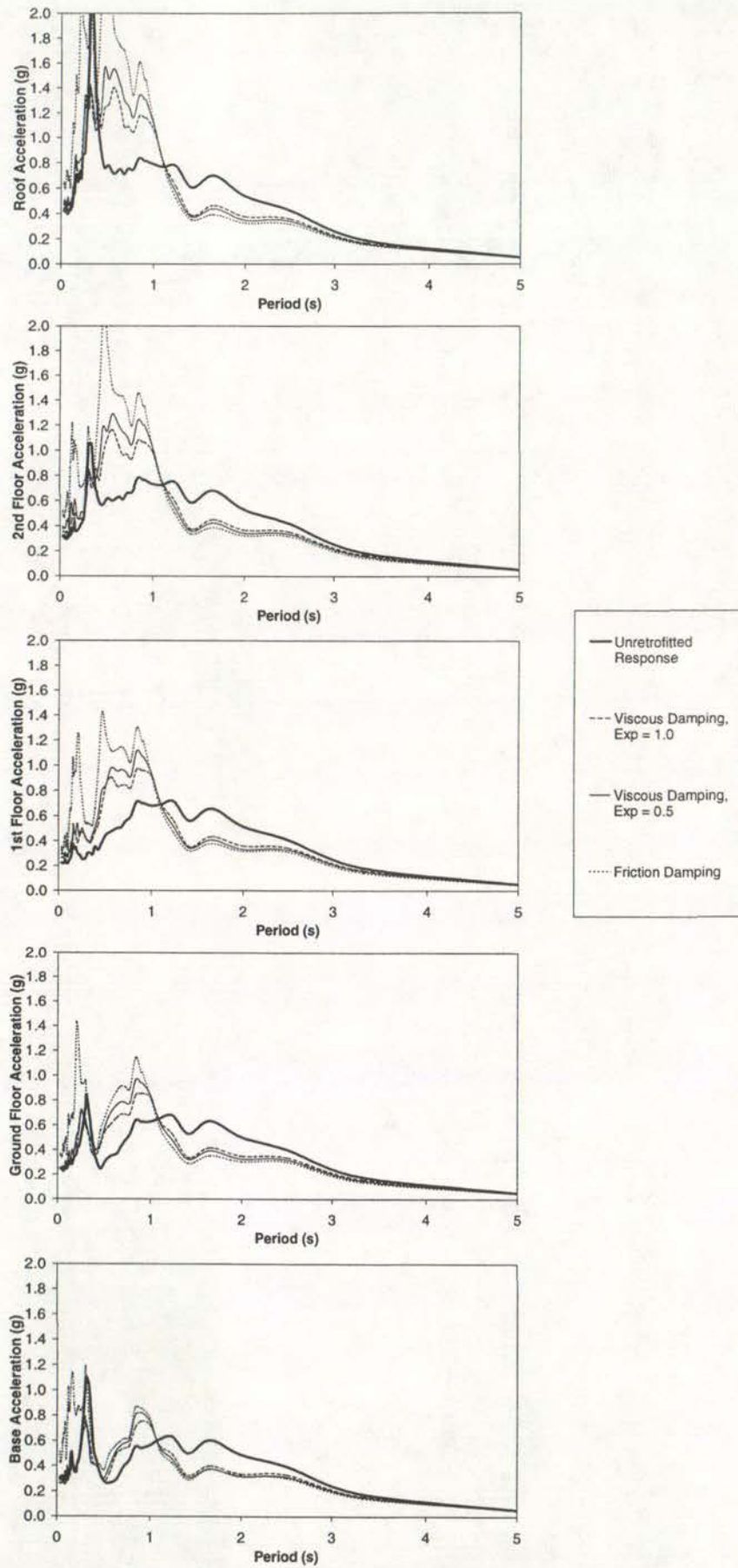
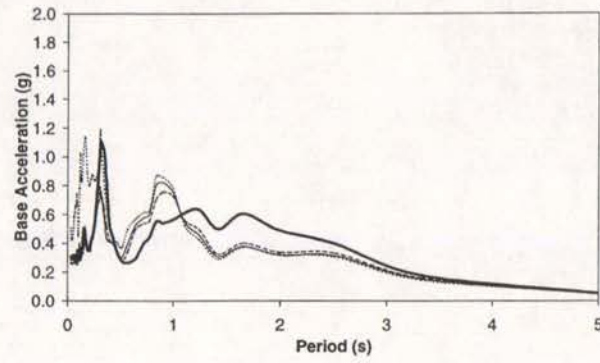
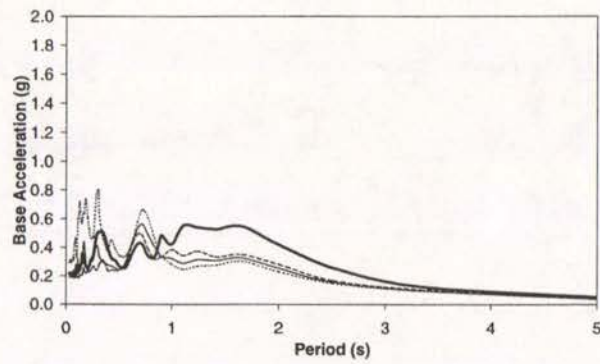


Figure 7.15: El Centro Floor Acceleration Spectra

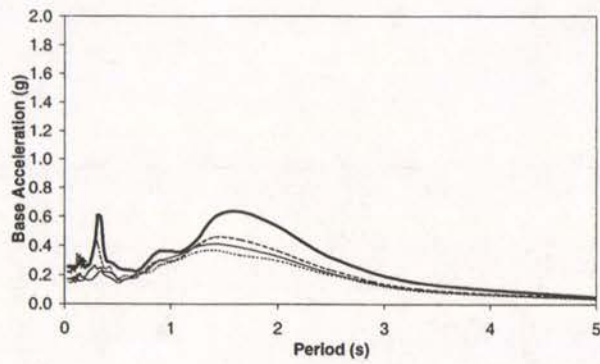
El Centro



Parkfield



Bucharest



Joshua Tree

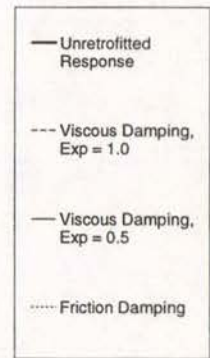
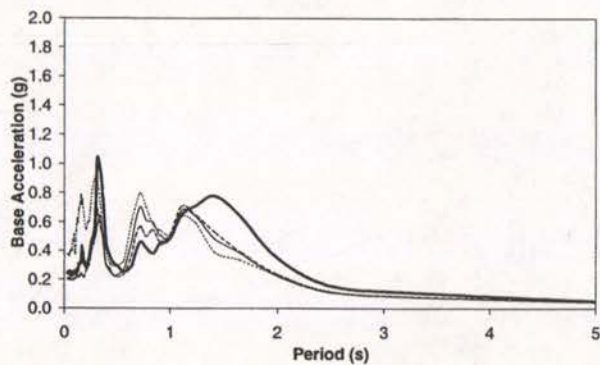


Figure 7.16: Acceleration Spectra at the Base Level for Design Level Earthquakes

response. At the top floor the unretrofitted accelerations were 0.0456 and 0.258 g respectively, while after adding pure viscous damping to the base, the top floor accelerations were 0.0242 and 0.0256 g. Again there was a 50% decrease in the El Centro acceleration, but no change in the Parkfield response.

The acceleration floor spectra for the El Centro response at each level, before and after retrofit with additional pure viscous damping, are shown in Figure 7.17. The additional damping reduces the response at all levels for both the El Centro and Parkfield records. The maximum reduction was 70% at the top floor in response to El Centro, at a period of approximately 0.9 seconds. Therefore it was shown that additional damping was not only able to control the response of the William Clayton building to near field earthquakes, but also reduce the accelerations in response to small magnitude earthquakes.

7.4 Optimal Retrofit for the William Clayton Building

Additional pure viscous damping, applied at the base, has been shown in previous sections to be the most effective form of additional damping. The impact on the design response is relatively small and the performance of the superstructure during a near field event is within its structural capacity. Taylor devices, designed particularly for incorporation into seismic isolation, are able to be supplied for a range of forces from approximately 500 kN to 10,000 kN³¹. The maximum force in the damper, in response to the near field earthquakes is 2590 kN during the Rinaldi ground motion time history, taken from the analysis in SAP. Therefore a series of dampers placed in the crawl space of the isolation system for each transverse frame of the William Clayton building, collectively able to at least generate this force would be appropriate for retrofitting the structure. The optimal damping constant for the additional viscous damping is equal to 0.320 s/m times the weight of the structure. Therefore the damping constant required in the frame is 3080 kNs/m, which can be provided by the manufacturer using these specifications. The dampers will need to be arranged to ensure the combination of their forces does not induce torsional moments in the building.

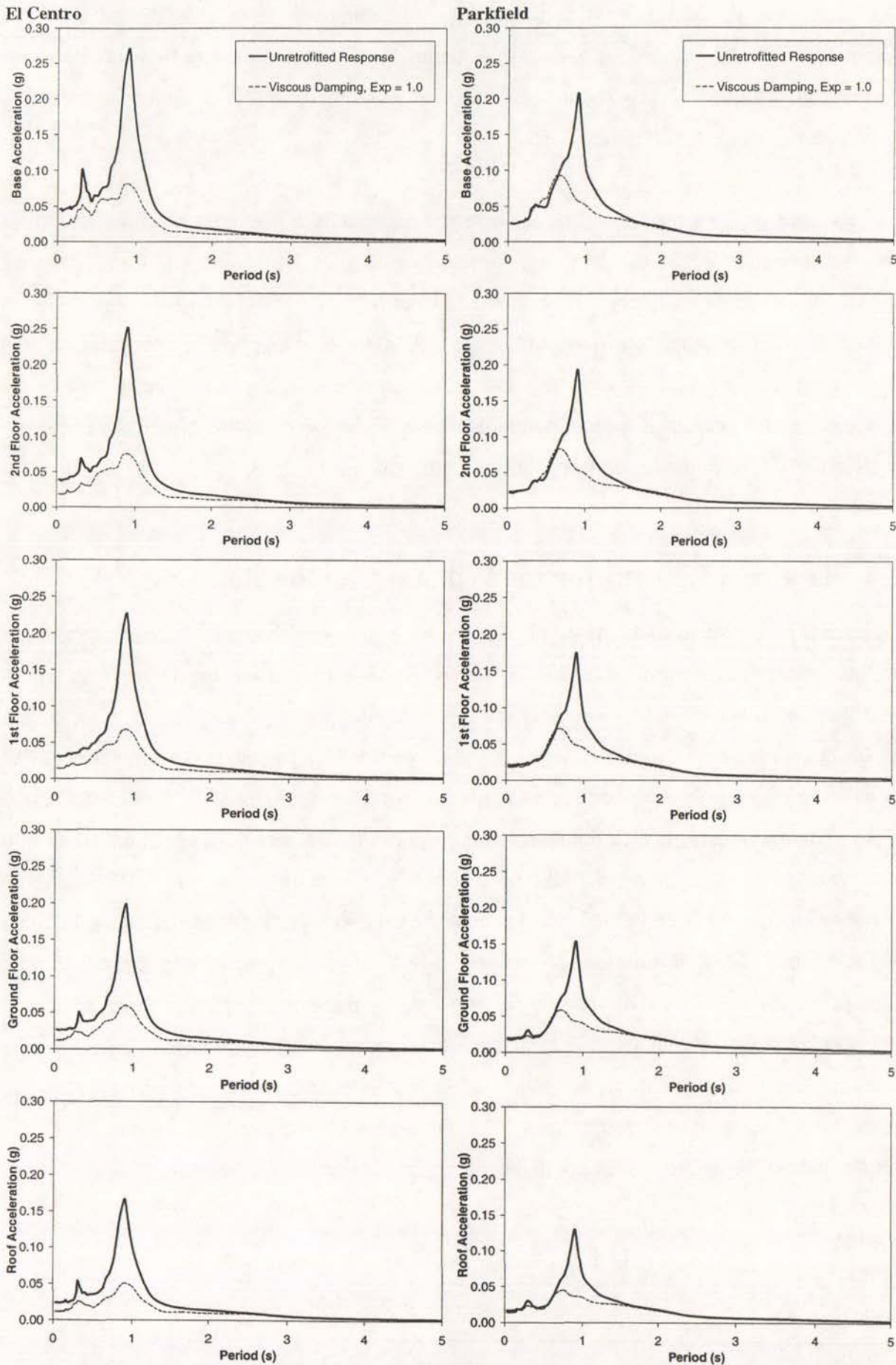


Figure 7.17: Small El Centro and Parkfield Accn. Floor Spectra Before and After Retrofit

7.5 Summary and Comparisons with the Generic Structures

A typical transverse frame of the William Clayton building, modelled as an isolation system with rigid superstructure, performed as predicted by the response of the generic structures. The unretrofitted near field response was 2.6 times the design response within the range found for the generic structures. After retrofitting the isolation system the level of damping found to limit the near field displacement response to the maximum allowable displacement was as predicted by the generic structures. Furthermore, the optimum forms of damping for the design level and near field responses respectively were also as expected from the results of retrofitting the generic isolation systems.

A model of the four storey transverse frame, typical in the William Clayton building, was able to give a response in SAP almost identical to the original design response of the structure modelled in Drain 2D. When additional damping was added to the isolation system, the response of the isolation system for the four storey model was comparable to the response using the rigid superstructure and the response of the generic structures. The most effective form of additional damping, in terms of near field base shears for the multi-storey William Clayton model, was either form of viscous damping. The design base shear remained smallest using pure viscous damping. Differentiation between the two forms of viscous damping was made using the response of the superstructure. Unlike the generic structures it was found that the variation between individual earthquake responses was no greater for any form of damping, thus it was unable to be used for differentiation. However, as with the generic structures, the acceleration floor spectra were increased by adding damping to each structure, but minimally increased using pure viscous damping. Therefore, it was quite clear that pure viscous damping was the most effective form of additional damping at the base the William Clayton building.

As the superstructures of the generic buildings were modelled with the same stiffness at each level, and the stiffness was not evenly distributed between each level of the William Clayton building, the response of the superstructures were quite different. The even distribution of stiffness caused a soft storey failure in the first storey of each of the generic structures when subject to near field earthquakes. In the William Clayton building the deformations in response to the near field earthquakes were more uniform up the structure and with the relatively small size of the deformations, no retrofit was needed in the superstructure. A large

number of beams and columns in the model of the William Clayton building meant that there was inherently more redundancy in the structure compared to the generic structures modelled with a single column at each floor. This resulted in smaller overall deformations. As damping was modelled as entirely stiffness proportional in the generic structures and largely proportional to stiffness in the William Clayton building, a different distribution of stiffness also equated to a different distribution of damping which did not help to control the soft storey deformation in the generic structures. The beam and column hinges in the William Clayton building were also modelled with a post yield stiffness of 0.02, which although small, helped to prevent large deformations in the structure compared to zero post yield stiffness modelled in the generic structures. Generic structures, more representative of the properties of the William Clayton building, may have been modelled with a stiffness distribution proportional to the height of each floor and some post yield stiffness.

The response of the William Clayton Building to the small magnitude earthquakes, which tended to cause the isolation system of the structures to vibrate elastically, was similar to the response of the three storey generic structure. The optimal retrofits for the two structures were able to reduce the response of small earthquakes by typically 50%. This is an added benefit of additional viscous damping, which will increase comfort for the occupants of the buildings during small, non damaging earthquakes.

The results from the William Clayton building confirm, that viscous damping is generally more effective than friction or hysteretic damping for retrofitting seismically isolated structures as shown in the modelling of the generic structures. Only if an extremely large level of damping was required to retrofit an isolation system would friction damping become more effective, in which case the accelerations in the superstructure would be large and a feasible retrofit using additional damping would be doubtful.

For the William Clayton building a series of pure viscous dampers such as Taylor devices, located at the isolation layer on each transverse frame, able to generate a force of 2600 kN with a damping constant of 3080 kNs/m is optimal. The damping could be provided by either one, two or several dampers with combined properties equal to those described above.

Chapter 8.

Conclusions

8.1 Design and Modelling of Seismically Isolated Buildings

A number of generic seismically isolated structures were designed using the 1997 Uniform Building Code (UBC). They were considered typical of those designed in the past without consideration of the possible effects of near field earthquakes. Six near field records taken from past earthquakes were found to exhibit forward directivity ground motion and were considered appropriate for modelling the effects of near field earthquakes. The records were characterised by large magnitude ground motions and a low frequency pulse. Their response spectra were similar to the UBC near field spectrum.

8.2 Retrofit of the Generic Seismically Isolated Buildings for Near Field Earthquakes

8.2.1 Identification of Suitable Passive Control Devices.

Additional viscous damping, with velocity exponents equal to 0.5 and 1.0, and additional friction damping each limited the near field displacements of the isolation systems to the maximum allowable levels. Hysteretic buffers and mass tuned damping were not effective in reducing the near field isolator displacements.

8.2.2 Optimum Form of Additional Damping using Design Level Response

For the majority of the generic seismically isolated buildings additional pure viscous damping in the isolation system of the buildings resulted in the lowest design level base shear response. In remaining buildings viscous damping with a velocity exponent of 0.5 was found to be optimal. Levels of damping were defined as the levels required to limit the near field displacements to the maximum allowable displacements. The difference in various retrofits was related to the properties on the isolation systems.

Where additional damping was required in the superstructure of seismically isolated buildings, viscous damping had a smaller impact on the design level response compared to friction damping.

Adding damping to the isolation system of the seismically isolated buildings increased acceleration floor spectra. This increase was smallest using additional pure viscous damping, with typically a 30% increase in accelerations at periods between 0.3 and 1.5 seconds.

8.2.3 Optimum Form of Additional Damping using Near Field Response

In the majority of the generic seismically isolated structures viscous damping with a velocity exponent of 0.5 was the most effective form of additional damping in the isolation system in terms of reducing the near field base shears. For certain buildings pure viscous damping resulted in a lower near field base shear, while in the remaining buildings friction damping gave the lowest base shear.

The generic seismically isolated structures had a soft storey failure in the superstructure of the isolation system. In most cases this was optimally retrofitted using additional viscous damping with a velocity exponent of 0.5. Since additional damping must be implemented in the superstructure as part of a diagonal framing system, additional axial forces were induced in the columns and bearings of the seismically isolated buildings. The magnitude of these forces was considered to be manageable, however a frame and section analysis of the columns would be required in order to ensure that the strength of the columns were adequate. A form of additional viscous damping was favoured over friction damping, because when using viscous damping the additional axial forces are out of phase with the maximum lateral deformations in the columns.

8.2.4 Compromise Between Optimum Design Level and Near Field Responses

Optimum forms of additional damping, based on design response, were generally different to those using near field response. Therefore some compromise needed to be made between the two responses. The design base shear was increased by typically 5 to 10% using the optimum form of damping calculated based on the near field response. Similarly, the near field base shear was typically increased by 5 to 10% using the optimum design level retrofit. As design

level earthquakes were considered to be more common, it was appropriate to optimise the design level response and allow a slightly larger than the optimal near field base shear. Thus additional pure viscous damping was the optimum form of retrofit for the majority of the seismically isolated buildings.

Even with the most effective form of retrofit found in terms of the design response, there was a small increase in accelerations which is likely to cause additional non-structural damage in the buildings. The level of this damage was considered acceptable.

It was found that the effectiveness of the various forms of additional damping was dependent on the relative unretrofitted near field response to the maximum allowable response. For the relative levels modelled using the generic structures, viscous damping was found to be the most effective form of retrofit. Additional friction damping would only be more effective than viscous damping in retrofitting a seismically isolated building if a large reduction in near field response was required. The required reduction in the isolator displacements would need to be considerably larger than those modelled in this thesis. For such a large modification in isolator displacements, damage in the superstructure of the building would be increased by a considerable amount. Friction damping is considered to be the most effective form of hysteretic damping. Although not modelled, it is expected that a form of additional hysteretic damping, other than friction damping, would be no more effective than the forms of damping modelled.

8.2.5 Effect of Additional Damping on Response to Small Earthquakes

Additional pure viscous damping in the isolation system was able to reduce the response of the generic seismically isolated structures during small earthquakes. The accelerations felt by occupants of the buildings during this level of earthquake were reduced by up to 50%.

8.3 Retrofit of William Clayton Building

A typical transverse frame of the seismically isolated William Clayton building was found to be vulnerable to near field earthquakes. It was found that the displacement of the isolation system could be reduced to the maximum allowable displacement using levels of damping as predicted by the generic buildings. The optimum form of additional damping in the isolation

system was pure viscous damping. This most effectively minimised both design level and near field base shears. Comparisons of acceleration floor spectra before and after retrofit were consistent with those for the generic structures, as was the response to small earthquakes.

There was no soft storey failure in the superstructure of the William Clayton building in response to near field ground motion. The near field inter-storey ductility of the superstructure was found to be less than one at each level. This meant that no additional damping was required to retrofit the superstructure.

The proposed optimum retrofit for the typical transverse frame of the William Clayton building is a series of pure viscous dampers with combined properties which are able to supply a maximum damping force of 2600 kN, with a damping constant of 3080 kNs/m.

8.4 Future Work

The structural implications of near field earthquakes have been discussed comprehensively in this thesis, from which a proposal for the retrofit of the William Clayton building and other generic structures has been calculated. However proposing these retrofits relied on certain assumptions in the seismology surrounding each building. In calculating initial design level and near field responses, this study relied on the comparative acceleration spectra for these earthquakes as defined by the provisions in the UBC.

There is no historical record of near field earthquakes in New Zealand and the ground motions induced by near field earthquakes tend to be dependent on a number of regional and directional effects. Therefore it is difficult to define with any certainty the magnitude of near field ground motion which can be expected at a site such as that of the William Clayton building in Wellington. Investigations need to be undertaken to predict expected fault rupture mechanisms and the resulting ground motion for critical regions in New Zealand close to active faults. Models have been used in the past to predict the rupture of an existing fault in California¹⁰, therefore perhaps similar models could be used for faults in New Zealand.

References

1. Andriono, T., and A. J. Carr, 1991. **A Simplified Earthquake Resistant Design Method for Base Isolated Multistorey Structures**. Bulletin of the New Zealand National Society for Earthquake Engineering. Vol 24: pp. 238-250.
2. Bertero, V. V., S. A. Mahin, and R. A. Herrera, 1978. **Aseismic design Implications of Near-Fault San Fernando Earthquake Records**. Earthquake Engineering and Structural Dynamics. Vol 6: pp. 31-42.
3. Buckle, I. G., 2000. **Passive Control of Structures for Seismic Loads**. Proceedings of the 12th World Conference on Earthquake Engineering (CD Rom), Auckland.
4. Chandra, R., M. Masand, S. K. Nandi, C. P. Tripathi, R. Pall, and A. Pall, 2000. **Friction Dampers for Seismic Control of La Gardenia Towers South City, Gurgaon, India**. Proceedings of the 12th World Conference in Earthquake Engineering (CD Rom), Auckland.
5. Clough, R. W., and J. Penzien, 1993. **Dynamics of Structures (Second Ed.)**. McGraw Hill Book Co., Singapore.
6. Computers and Structures Inc., 1998. **SAP 2000 - Three Dimensional Static and Dynamic Finite Element Analysis and Design of Structures - Analysis Reference**. Computers and Structures, Inc, Berkeley.
7. Davidson, B. J., L. M. Megget, and W. Chan, 1998. **The Re-Analysis of the Base Isolated William Clayton Building to Near Source Earthquakes**. Proceedings of the New Zealand Society for Earthquake Engineering Annual Conference, Wairakei.
8. Davidson, B. J., and T. W. Robertson, 1991. **Dynamic Absorbers for a Vibrating Staircase**. Proceedings of the IPENZ Annual Conference, Wellington. pp. 233-241.

9. Hall, J. F., 1998. **Seismic Response of Steel Frame Buildings to Near Source Ground Motions**. Earthquake Engineering and Structural Dynamics. Vol 27: pp. 1445-1464.
10. Hall, J. F., T. H. Heaton, M. W. Halling, and D. J. Wald, 1995. **Near Source Ground Motion and its Effects on Flexible Buildings**. Earthquake Spectra. Vol 11: pp. 569-605.
11. Institute of Crustal Studies - University of California (Santa Barbara), 2000. **The Strong Motion Database**. Webpage, <http://smdb.crustal.ucsb.edu/>.
12. International Conference of Building Officials, 1997. **1997 Uniform Building Code**. International Conference of Building Officials.
13. Kanaan, A. E., and G. H. Powell, 1973. **Drain-2D, A General Purpose Computer Program for Dynamic Analysis of Inelastic Plane Structures**. Earthquake Engineering Research Centre, Berkeley, California.
14. Kelly, J. M., 1999. **The Role of Damping in Seismic Isolation**. Earthquake Engineering and Structural Dynamics. Vol 28: pp. 3-20.
15. Makris, N., 1997. **Rigidity-Plasticity-Viscosity: Can Electrorheological Dampers Protect Base-Isolated Structures from Near-Source Ground Motions**. Earthquake Engineering and Structural Dynamics. Vol 26: pp. 571-591.
16. Makris, N., and S. Chang, 1998. **Effect of Damping Mechanisms on the Response of Seismically Isolated Structures**. PEER Report, University of California, Berkeley. Vol 06.
17. Mathsoft Inc., 1998. **MathCad 8 Professional**. U.S.A.
18. McVerry, G. H., 1997. **Near-Fault Earthquake Records and Implications for Design Motions**. Proceeding of the New Zealand Society for Earthquake Engineering Annual Conference, Wairakei. pp. 88-95.

19. Megget, L. M., 1979. **Analysis and Design of a Base-Isolated Reinforced Concrete Frame Building**. Bulletin of the New Zealand National Society for Earthquake Engineering. Vol 11: pp. 245-254.
20. Megget, L. M., 1979. **Drain 2D Analysis Output - William Clayton Building**. Vogel Computer Centre.
21. Mockle (Ed), J. P., 1996. **Northridge Earthquake of Jan 17 1994 - Reconnaissance Report**. Earthquake Spectra. Vol 2.
22. Pall, R., G. Gauthier, S. Delisle, and A. Pall, 2000. **Friction Dampers for Seismic Upgrade of Quebec Police Headquarters, Montreal**. Proceedings of the 12th World Conference in Earthquake Engineering (CD Rom), Auckland.
23. Robinson, W. H., 1999. **Products**. Web page, www.robinson-seismic.co.nz/products.
24. Scarry, J. M., 1983. **A System Identification Method for Structural Engineering Applications**. Department of Civil Engineering, Auckland.
25. Skinner, R. I., and G. H. McVerry, 1995. **Seismic Isolators for Ground Motions with Large Displacements and Velocities**. 11th World Earthquake Engineering Conference, Acapulco, Mexico.
26. Skinner, R. I., W. H. Robinson, and G. H. McVerry, 1993. **An Introduction to Seismic Isolation**. John Wiley & Sons Ltd, Chichester.
27. Somerville, P., 1997. **The Characteristics and Quantification of Near Fault Ground Motion**. NCEER Technical Report. Vol 97: pp. 293-318.
28. Somerville, P., 2000. **Seismic Hazard Evaluation**. Proceedings of the 12th Annual Conference on Earthquake Engineering (CD Rom), Auckland.

29. Soong, T. T., and J. B F Spencer, 2000. **Active, Semi-Active and Hybrid Control of Structures**. Proceedings of the 12th World Conference on Earthquake Engineering (CD Rom), Auckland.
30. Takashi, N., S. Tetsuo, N. Arihide, S. Hitoshi, and I. Satoru, 2000. **Study on Earthquake Response Characteristics of Base-Isolated Building using the Friction Dampers with Coned Disc Springs**. Proceedings of the 12th World Conference in Earthquake Engineering (CD Rom), Auckland.
31. Taylor Devices Inc., 1999. **Taylor Devices Seismic Dampers and Seismic Protection Products**. Web page, www.taylordevices.com/.
32. Timoshenko, S., D. H. Young, and W. Weaver, 1974. **Vibration Problems in Engineering**. Wiley & Sons Inc., New York.
33. van de Vorstenbosch, G., A. W. Charleson, and W. H. Robinson, 1999. **A Survey of Seismically Isolated Structures in New Zealand**. Proceedings of the New Zealand Society for Earthquake Engineering Annual Conference, Rotorua. pp. 72-75.
34. Zayas, V. A., and S. S. Low, 2000. **Seismic Isolation for Strong Near Field Motions**. Proceedings of the 12th World Conference on Earthquake Engineering (CD Rom), Auckland.
35. Zhou, J. X., J. W. Cousins, and W. H. Robinson, 2000. **Using a Lead-Based Damper to Increase Near-Source Ground Motion Resisting Capacity of Existing Base-Isolated Buildings**. Proceedings of the 12th World Conference in Earthquake Engineering (CD Rom), Auckland.

Appendices

Appendix 1 Ground and Site Parameters for Design of Generic Seismically Isolated Structures

Design Parameters

- The soil profile type (Table 16-J)¹² is S_d corresponding to a stiff soil site. This closely resembles the intermediate soil type in the New Zealand Loadings Code.
- The seismic zone is zone 4 corresponding to areas of high seismicity such as California (Figure 16.2)¹².
- Seismic zone factor, Z , is 0.40 (Table 16-I).
- The near source factors, N_a (Table 16-T)¹² and N_v (Table 16-T)¹², are both 1.0 for earthquakes capable of large magnitude events with the fault source greater than 15 km from the site.
- The seismic coefficients $C_{AD} = 0.44 N_a$ (Table 16-Q)¹² and $C_{VD} = 0.64 * N_v$ (Table 16-R) are 0.44 and 0.64 respectively.
- The seismic importance factor, I (Table 16-K), has been taken as 1.00 as for a standard occupancy structure.

Maximum Capable Earthquake Parameters

- The maximum capable earthquake coefficient, $M_M = 1.25$ (Table A-16-D).
- The maximum seismic coefficients C_{AM} (Table A-16-F)¹² and C_{VM} (Table A-16-G) are 0.61 and 0.80 respectively.

Near Field Parameters

- The near field factors N_A and N_v are equal to 1.5 and 2.0 respectively.
- The near field seismic coefficients C_{ANF} and C_{VNF} (Table A-16-F)¹² and (Table A-16-G) are 0.66 and 1.28 respectively.

Appendix 2 Example for Design of a Bilinear Isolation System, Design 7, from an Effective Linear System

Assume Seismic Weight (W) **10000 kN**

Ground Properties (Refer Appendix 2)

Occupancy Category (I, I_p)	1.00	1.00
Soil Profile Type	S_d	
Seismic Zone	4	
Seismic Zone Factor (Z)	0.4	
Zone 4 Near Source Factor (N_a, N_v)	1.00	1.00
Non Near Field Seismic Coefficients (C_a, C_v)	0.44	0.64

Isolation System Properties - Assuming Bilinear Isolation System

Estimate of Initial Stiffness (k_0)	257500 kN/m (Suggested first guess of $10W/m$)	←
Estimate of Yield Force (F_y)	409 kN (Suggested first guess of $0.05W$)	←
Assign Post Yield Stiffness Ratio (α)	0.02	

Design Displacement

Estimate Design Displacement (D_D)	311 mm (Equal to Design Disp. From Linear Design)
Calculate Yield displacement	1.588 mm (Calc. from Init. Stiff. and Yield Force)
Calculate Ductility (μ)	195.8

Calculation of Effective Stiffnesses (Refer Equation 2.4)

Maximum Isolator Stiffness (k_{Dmax})	6439 kN/m
Minimum Isolator Stiffness (k_{Dmin})	6439 kN/m (Assuming $k_{min} = k_{max}$)

Check effective period and damping equal to design values. If not, modify initial stiffness and yield force.

Calculation of Equivalent Viscous Damping in the Isolation System

R	0.199 (Refer Equation 2.5)	
Equivalent Viscous Damping (β_D)	12.7 % (Refer Equation 2.6)	→
Effective Damping Coefficient (B_D)	1.28 (From UBC Table A16C)	

Calculate Effective Period

Period (T_D)	2.500 s (Refer Equation 2.1a)	→
------------------	--------------------------------------	---

Check Design Displacement

Isolator Design Seismic Coefficients (C_{vD})	0.64 (From UBC Table 16R)
Design Displacement (D_D)	311 mm (Refer Equation 2.2)

Check isolation system displacement equal to linear design isolation system displacement

Design Base Shear Force

Base Shear (V_b) **2000 kN** (Refer Equation 2.3)

Check design base shear equal to linear design base shear

Appendix 3 Calculation of the Near Field Response for a Bilinear Isolation System, Design 7

Assume Seismic Weight (W)	10000 kN	
<u>Ground Properties</u> (Refer Appendix 2)		
Occupancy Category (I_p)	1.00	1.00
Soil Profile Type	S_d	
Seismic Zone	4	
Seismic Zone Factor (Z)	0.4	
Zone 4 Near Source Factor (N_a, N_v)	1.50	2.00
Near Field Seismic Coefficients (C_a, C_v)	0.66	1.28

Isolation System Properties - Assuming Bilinear Isolation System

Initial Stiffness (k_0)	257500 kN/m
Yield Force (F_y)	409 kN
Post Yield Stiffness Ratio (α)	0.02

Near Field Displacement

Estimate Near Field Displacement (D_{NF})	834 mm (Estimate 2.5 times design displacement)
Calculate Yield displacement	1.588 mm (Calc. from Init. Stiff. and Yield Force)
Calculate Ductility (μ)	525.1

Calculation of Effective Stiffnesses (Refer Equation 2.4)

Maximum Isolator Stiffness (k_{NFmax})	5631 kN/m
Minimum Isolator Stiffness (k_{NFmin})	5631 kN/m (Assuming $k_{min} = k_{max}$)

Check Near Field Displacement calculated equal to estimated displacement. If not, modify estimated displacement.

Calculation of Equivalent Viscous Damping in the Isolation System

R	0.085 (Refer Equation 2.5)
Equivalent Viscous Damping (β_{NF})	5.4 % (Refer Equation 2.6)
Effective Damping Coefficient (B_{NF})	1.02 (From UBC Table A16C)

Calculate Effective Period

Period (T_{NF})	2.673 s (Refer Equation 2.1a)
---------------------	-------------------------------

Check Near Field Displacement

Isolator Near Field Seismic Coefficient (C_{vNF})	1.28 (From UBC Table A16G)
Near Field Displacement (D_{NF})	834 mm (Refer Equation 2.2)

Near Field Base Shear Force

Base Shear (V_b)	4694 kN (Refer Equation 2.3)
----------------------	------------------------------

Appendix 4 UBC Isolation System Properties in Response to the Near Field Spectrum

Design Number	Effective Period (s)	Post Yield Stiffness Ratio	Equivalent Viscous Damping	Effective Stiffness / Weight (/m)	Initial Stiffness / Weight (/m)	Post Yield Stiffness / Weight (/m)	Yield Force / Weight	Ductility	Design Displacement (mm)	Design Force / Weight
1	1.83	0.02	14.7	1.199	46.00	0.920	0.124	161.4	435	0.521
2	2.14	0.02	5.4	0.879	40.20	0.804	0.051	523.7	667	0.587
3	2.14	0.10	5.5	0.876	7.99	0.799	0.057	93.5	668	0.585
4	2.15	0.20	5.8	0.871	3.95	0.790	0.067	39.1	664	0.578
5	2.33	0.02	11.5	0.740	30.30	0.606	0.081	221.3	593	0.439
6	2.36	0.10	12.5	0.722	5.76	0.576	0.095	35.5	587	0.424
7	2.67	0.02	5.4	0.563	25.75	0.515	0.041	525.1	834	0.469
8	2.68	0.10	5.5	0.561	5.12	0.512	0.046	94.0	835	0.469
9	2.69	0.20	5.7	0.558	2.53	0.506	0.054	39.2	830	0.463
10	3.05	0.02	14.9	0.432	16.50	0.330	0.075	159.0	719	0.311
11	3.15	0.10	17.8	0.406	2.87	0.287	0.092	21.7	700	0.284
12	3.10	0.02	2.8	0.418	20.00	0.400	0.022	1080.0	1161	0.485
13	3.10	0.10	2.8	0.418	4.00	0.400	0.024	195.7	1161	0.485
14	3.11	0.20	2.8	0.417	1.99	0.399	0.027	85.5	1162	0.485
15	3.31	0.02	7.5	0.367	16.20	0.324	0.042	367.4	957	0.352
16	3.32	0.10	7.8	0.364	3.19	0.319	0.048	63.6	953	0.347
17	3.35	0.20	8.3	0.359	1.55	0.310	0.058	25.4	943	0.338

Appendix 5 Calculation of Column Stiffness for the Three Storey Superstructure

Assuming the total weight of the superstructure is 10,000 kN, then the weight of each floor of the 3 storey building is $10,000 / 4 = 2500$ kN. This corresponds to a mass of 255 tonnes per floor.

Matlab Formulation

Note: 1) Many of the symbols used in Matlab procedure below have been changed so that they are consistent with those used in development of the procedure in Section 4.4.4.2, as it is not possible to write some symbols; such as Greek symbols, superscripts and subscripts, in Matlab.

Using the procedure developed in Section 2.4.3:

```
» M=diag([255,255,255])
```

M =

255	0	0
0	255	0
0	0	255

```
» k=[2 -1 0; -1 2 -1; 0 -1 1]
```

k =

2	-1	0
-1	2	-1
0	-1	1

```
» [phi,w^2/Ks]=eig(k,M)
```

phi =

0.591009	0.736976	0.327985
-0.736976	0.327985	0.591009
0.327985	-0.591009	0.736976

$w^2/K_s =$

0.0127333	0	0
0	0.0060979	0
0	0	0.0007767

For the first mode:

$w^2/K_s = 0.0007767$

Since: $T = 0.4$ seconds
 $\Rightarrow w^2 = 246.74$ (rad/s)

Therefore:

$$K_s = 317673 \text{ (kN/m)}$$

Dividing by the total weight of the superstructure:

$$K_s = 31.7673 W \text{ (/m)}$$

Appendix 6 Frequencies and Mode Shapes for Three and Six Storey Superstructures

Three Storey Structure

Mode	1	2	3
Natural Period	0.40	0.14	0.10
Natural Frequency	15.7	44.0	63.6
ϕ_1	0.45	-1.25	1.80
ϕ_2	0.80	-0.55	-2.25
ϕ_3	1.00	1.00	1.00

Six Storey Structure

Mode	1	2	3	4	5	6
Natural Period	0.80	0.27	0.17	0.13	0.11	0.10
Natural Frequency	7.9	23.1	37.0	48.8	57.7	63.3
ϕ_1	0.24	-0.71	1.14	-1.50	1.77	-1.94
ϕ_2	0.47	-1.06	0.81	0.36	-2.01	3.44
ϕ_3	0.67	-0.88	-0.56	1.41	0.51	-4.15
ϕ_4	0.83	-0.26	-1.21	-0.70	1.43	3.91
ϕ_5	0.94	0.50	-0.29	-1.24	-2.14	-2.77
ϕ_6	1.00	1.00	1.00	1.00	1.00	1.00

Appendix 7 Calculation of Modal Damping in Three Storey Superstructure

The mass matrix, stiffness matrix, mode shapes and frequencies are taken from Appendix 6.

Matlab Results for Calculation of the Damping Constant

Note: 1) Many of the symbols in Matlab procedure below have been changed so that they are consistent with those used in development of the procedure in Section 4.4.4, as it is not possible to write some symbols; such as Greek symbols, superscripts and subscripts, in Matlab.

```
» c=[2 -1 0; -1 2 -1; 0 -1 1]
```

```
c =
```

```
    2    -1     0
   -1     2    -1
    0    -1     1
```

```
»  $\phi_1 = \phi(:,3)$ 
```

```
 $\phi_1 =$ 
```

```
    0.328
    0.5910
    0.7370
```

(Note: This is actually column three of the $[\phi]$ matrix but corresponds to the first mode)

```
»  $K_s = 317673$ ;
```

```
»  $\omega_1 = \text{sqrt}((\omega^2/K_s)(3,3)*K_s)$ 
```

```
 $\omega_1 =$ 
```

```
    15.7080
```

```
»  $\xi = 0.05$ ;
```

```
»  $M_1 = \phi_1' * M * \phi_1$ 
```

```
 $M_1 =$ 
```

```
    255.0000
```

```
»  $c_1 = \phi_1' * c * \phi_1$ 
```

```
 $c_1 =$ 
```

```
    0.1981
```

```
»  $C_s = 2 * \xi * \omega_1 * M_1 / c_1$ 
```

```
 $C_s =$ 
```

```
    2022.36
```

Dividing by the total weight of the system:

$$C_s = 0.2202 W \text{ (s/m)}$$

Appendix 8 Modal Damping for Three and Six Storey Superstructures

Three Storey Structure

Mode	1	2	3
Fraction Of Critical Damping	0.050	0.140	0.202

Six Storey Structure

Mode	1	2	3	4	5	6
Fraction Of Critical Damping	0.050	0.147	0.236	0.310	0.367	0.402

Appendix 9 Effective Damping Check in SAP 2000 Models

A rigid base three storey superstructure, with no isolation system, was subject to a cyclic load to test the damping in the system.

From theory of single degree of freedom systems⁵, equation of motion for a system with a forced vibration is:

$$m\ddot{u} + c\dot{u} + ku = -mA\omega^2 \sin \omega t \quad \dots\text{Equation A9.1}$$

and the steady state response is:

$$u(t) = \frac{A}{m} \beta^2 D \sin(\omega t - \theta) \quad \dots\text{Equation A9.2}$$

where the Dynamic Amplification factor, D , is:

$$D = \frac{1}{\sqrt{(1 - \beta^2)^2 + (2\xi\beta)^2}} \quad \dots\text{Equation A9.3}$$

where: β = ratio of forced frequency to undamped natural frequency of structure

For a multi degree of system the formulation is the similar. The equation of motion is:

$$[M] \ddot{\underline{u}} + [C] \dot{\underline{u}} + [K] \underline{u} = -[M] \underline{r} A \omega^2 \sin \omega t \quad \dots\text{Equation A9.4}$$

where:

$$\underline{r} = \begin{bmatrix} 1 \\ 1 \\ 1 \\ \cdot \\ 1 \end{bmatrix}_{n \times 1} \quad \dots\text{Equation A9.5}$$

For a given mode, i , assuming the forcing frequency is close to but not equal to the natural frequency of the given mode therefore the influence of the other modes is negligible, the response is described by:

$$\underline{u}_i = \underline{\phi}_i \frac{L_i A}{M_i} \beta_i^2 D_i \sin(\omega t - \vartheta) \quad \dots \text{Equation A9.6}$$

where D_i is as given in Equation A9.3 using β and ξ for the mode, i , and L_i and M_i are:

$$L_i = \underline{\phi}_i^T [M] \underline{x} \quad \dots \text{Equation A9.7}$$

$$M_i = \underline{\phi}_i^T [M] \underline{\phi}_i \quad \dots \text{Equation A9.8}$$

Similarly:

$$u_{i \max} = \underline{\phi}_i \frac{L_i A}{M_i} \beta_i^2 D_i \quad \dots \text{Equation A9.9}$$

The first mode natural frequency of the three storey superstructure was 15.71 rad/s as given in Appendix 6. A cyclic vibration with a forcing frequency, ω , of 16.00 rad/s was applied to the superstructure, therefore $\beta_1 = 1.0186$. The amplitude $A\omega^2$ was 1 m/s², therefore $A=0.0039063$ m. The modeshape for the first mode is given in Appendix 6.

The maximum expected response of the system at steady state can be calculated using the first mode. $L_1 = 422.27$ using Equation A8.7 and $M_1 = 255.00$ using Equation A9.8. ξ_1 was initially defined as 0.05, consequently $D_1 = 9.21$ using Equation A8.3. , Therefore:

$$\underline{u}_{1 \max} = \begin{bmatrix} 0.0203 \\ 0.0365 \\ 0.0456 \end{bmatrix}$$

The actual response of the system from SAP 2000 was:

$$\underline{u}_{\max} = \begin{bmatrix} 0.0203 \\ 0.0367 \\ 0.0459 \end{bmatrix}$$

Therefore the results show that the damping is correct and that the response is equal to the first mode response.

Appendix 10 Example for Calculation of Optimum Levels of Damping using System Identification

The optimum levels of damping in each level of a three storey base isolated structures have been calculated using the system identification procedure. The building, Design 3.7, was retrofitted using viscous damping with a velocity exponent of 0.5 which is given in terms of the percentage of critical viscous damping. Additional damping was required at the base and first floor only. The MathCad 8 formulation for the system identification procedure is shown below.

Development of Quasi Structural Model

Optimum Structural Response Parameters

$$(pm1 \ pm2) := (430.0000000 \ 12.5915643)$$

$$pm := (pm1 \ pm2)$$

$$pm = (430 \ 12.5915643)$$

Significant Structural Parameters

$$\begin{bmatrix} xb1 & xb2 \\ xu1 & xu2 \\ xl1 & xl2 \end{bmatrix} := \begin{bmatrix} 21 & 7 \\ 22 & 9 \\ 20 & 5 \end{bmatrix}$$

Quasi Structural Response Parameters

$$\begin{bmatrix} pq11 & pq12 \\ pq21 & pq22 \\ pq31 & pq32 \\ pq41 & pq42 \\ pq51 & pq52 \end{bmatrix} := \begin{bmatrix} 431.7024833 & 11.6431090 \\ 421.5954667 & 11.5476450 \\ 442.0692333 & 11.7483347 \\ 432.3729500 & 9.7449735 \\ 430.4662167 & 14.7116580 \end{bmatrix}$$

Calculation of Quadratic Coefficients

$$\begin{bmatrix} 1 & xb1 & xb1^2 & xb2 & xb2^2 \\ 1 & xu1 & xu1^2 & xb2 & xb2^2 \\ 1 & xl1 & xl1^2 & xb2 & xb2^2 \\ 1 & xb1 & xb1^2 & xu2 & xu2^2 \\ 1 & xb1 & xb1^2 & xl2 & xl2^2 \end{bmatrix} = \begin{bmatrix} 1 & 21 & 441 & 7 & 49 \\ 1 & 22 & 484 & 7 & 49 \\ 1 & 20 & 400 & 7 & 49 \\ 1 & 21 & 441 & 9 & 81 \\ 1 & 21 & 441 & 5 & 25 \end{bmatrix}$$

$$\begin{bmatrix} c1 & c2 \\ a11 & a12 \\ b11 & b12 \\ a21 & a22 \\ b21 & b22 \end{bmatrix} := \begin{bmatrix} 1 & xb1 & xb1^2 & xb2 & xb2^2 \\ 1 & xu1 & xu1^2 & xb2 & xb2^2 \\ 1 & xl1 & xl1^2 & xb2 & xb2^2 \\ 1 & xb1 & xb1^2 & xu2 & xu2^2 \\ 1 & xb1 & xb1^2 & xl2 & xl2^2 \end{bmatrix}^{-1} \begin{bmatrix} pq11 & pq12 \\ pq21 & pq22 \\ pq31 & pq32 \\ pq41 & pq42 \\ pq51 & pq52 \end{bmatrix}$$

$$\begin{bmatrix} c1 & c2 \\ a11 & a12 \\ b11 & b12 \\ a21 & a22 \\ b21 & b22 \end{bmatrix} = \begin{bmatrix} 697.145939638 & 31.763286262 \\ -15.6912847 & -0.30534055 \\ 0.1298667 & 0.00488085 \\ 1.46683315 & -3.28989475 \\ -0.070724987 & 0.146301687 \end{bmatrix}$$

Newton Raphson Solution Procedure

Iteration Number 1

Estimate of Optimum Significant Structural Parameters

$$\begin{bmatrix} x_1 \\ x_2 \end{bmatrix} := \begin{bmatrix} 21 \\ 7 \end{bmatrix} \quad x_0 := \begin{bmatrix} x_1 \\ x_2 \end{bmatrix} \quad x_0 = \begin{bmatrix} 21 \\ 7 \end{bmatrix}$$

Criterion Function

$$pq1 := c1 + (x1 \cdot a11 + x1^2 \cdot b11) + (x2 \cdot a21 + x2^2 \cdot b21)$$

$$pq2 := c2 + (x1 \cdot a12 + x1^2 \cdot b12) + (x2 \cdot a22 + x2^2 \cdot b22)$$

$$pq := \begin{bmatrix} pq1 \\ pq2 \end{bmatrix} \quad pq = \begin{bmatrix} 431.7024833 \\ 11.643109 \end{bmatrix}$$

$$Esq := (pm1 - pq1)^2 + (pm2 - pq2)^2 \quad Esq = 3.7980168429$$

$$Esq \rightarrow (pm1 - c1 - x1 \cdot a11 - x1^2 \cdot b11 - x2 \cdot a21 - x2^2 \cdot b21)^2 + (pm2 - c2 - x1 \cdot a12 - x1^2 \cdot b12 - x2 \cdot a22 - x2^2 \cdot b22)^2$$

Minimising:

$$\frac{d}{dx1} Esq \rightarrow (2 \cdot pm1 - 2 \cdot c1 - 2 \cdot x1 \cdot a11 - 2 \cdot x1^2 \cdot b11 - 2 \cdot x2 \cdot a21 - 2 \cdot x2^2 \cdot b21) \cdot (-a11 - 2 \cdot x1 \cdot b11) + (2 \cdot pm2 - 2 \cdot c2 - 2 \cdot x1 \cdot a12 - 2 \cdot x1^2 \cdot b12 - 2 \cdot x2 \cdot a22 - 2 \cdot x2^2 \cdot b22) \cdot (-a12 - 2 \cdot x1 \cdot b12)$$

$$f1 := (2 \cdot pm1 - 2 \cdot c1 - 2 \cdot x1 \cdot a11 - 2 \cdot x1^2 \cdot b11 - 2 \cdot x2 \cdot a21 - 2 \cdot x2^2 \cdot b21) \cdot (-a11 - 2 \cdot x1 \cdot b11) + (2 \cdot pm2 - 2 \cdot c2 - 2 \cdot x1 \cdot a12 - 2 \cdot x1^2 \cdot b12 - 2 \cdot x2 \cdot a22 - 2 \cdot x2^2 \cdot b22) \cdot (-a12 - 2 \cdot x1 \cdot b12)$$

$$\frac{d}{dx2} Esq \rightarrow (2 \cdot pm1 - 2 \cdot c1 - 2 \cdot x1 \cdot a11 - 2 \cdot x1^2 \cdot b11 - 2 \cdot x2 \cdot a21 - 2 \cdot x2^2 \cdot b21) \cdot (-a21 - 2 \cdot x2 \cdot b21) + (2 \cdot pm2 - 2 \cdot c2 - 2 \cdot x1 \cdot a12 - 2 \cdot x1^2 \cdot b12 - 2 \cdot x2 \cdot a22 - 2 \cdot x2^2 \cdot b22) \cdot (-a22 - 2 \cdot x2 \cdot b22)$$

$$f2 := (2 \cdot pm1 - 2 \cdot c1 - 2 \cdot x1 \cdot a11 - 2 \cdot x1^2 \cdot b11 - 2 \cdot x2 \cdot a21 - 2 \cdot x2^2 \cdot b21) \cdot (-a21 - 2 \cdot x2 \cdot b21) + (2 \cdot pm2 - 2 \cdot c2 - 2 \cdot x1 \cdot a12 - 2 \cdot x1^2 \cdot b12 - 2 \cdot x2 \cdot a22 - 2 \cdot x2^2 \cdot b22) \cdot (-a22 - 2 \cdot x2 \cdot b22)$$

$$f := \begin{bmatrix} f1 \\ f2 \end{bmatrix} \quad f = \begin{bmatrix} -34.665900515 \\ 3.9784299191 \end{bmatrix}$$

Jacobian Matrix

$$\frac{d}{dx1} f1 \rightarrow (-2 \cdot a11 - 4 \cdot x1 \cdot b11) \cdot (-a11 - 2 \cdot x1 \cdot b11) - (4 \cdot pm1 - 4 \cdot c1 - 4 \cdot x1 \cdot a11 - 4 \cdot x1^2 \cdot b11 - 4 \cdot x2 \cdot a21 - 4 \cdot x2^2 \cdot b21) \cdot b11 + (-2 \cdot a12 - 4 \cdot x1 \cdot b12) \cdot (-a12 - 2 \cdot x1 \cdot b12) - (4 \cdot pm2 - 4 \cdot c2 - 4 \cdot x1 \cdot a12 - 4 \cdot x1^2 \cdot b12 - 4 \cdot x2 \cdot a22 - 4 \cdot x2^2 \cdot b22) \cdot b12$$

$$j11 := (-2 \cdot a11 - 4 \cdot x1 \cdot b11) \cdot (-a11 - 2 \cdot x1 \cdot b11) - (4 \cdot pm1 - 4 \cdot c1 - 4 \cdot x1 \cdot a11 - 4 \cdot x1^2 \cdot b11 - 4 \cdot x2 \cdot a21 - 4 \cdot x2^2 \cdot b21) \cdot b11 + (-2 \cdot a12 - 4 \cdot x1 \cdot b12) \cdot (-a12 - 2 \cdot x1 \cdot b12) - (4 \cdot pm2 - 4 \cdot c2 - 4 \cdot x1 \cdot a12 - 4 \cdot x1^2 \cdot b12 - 4 \cdot x2 \cdot a22 - 4 \cdot x2^2 \cdot b22) \cdot b12$$

$$\frac{d}{dx2} f1 \rightarrow (-2 \cdot a21 - 4 \cdot x2 \cdot b21) \cdot (-a11 - 2 \cdot x1 \cdot b11) + (-2 \cdot a22 - 4 \cdot x2 \cdot b22) \cdot (-a12 - 2 \cdot x1 \cdot b12)$$

$$j12 := (-2 \cdot a21 - 4 \cdot x2 \cdot b21) \cdot (-a11 - 2 \cdot x1 \cdot b11) + (-2 \cdot a22 - 4 \cdot x2 \cdot b22) \cdot (-a12 - 2 \cdot x1 \cdot b12)$$

$$\frac{d}{dx1} f2 \rightarrow (-2 \cdot a11 - 4 \cdot x1 \cdot b11) \cdot (-a21 - 2 \cdot x2 \cdot b21) + (-2 \cdot a12 - 4 \cdot x1 \cdot b12) \cdot (-a22 - 2 \cdot x2 \cdot b22)$$

$$j21 := (-2 \cdot a11 - 4 \cdot x1 \cdot b11) \cdot (-a21 - 2 \cdot x2 \cdot b21) + (-2 \cdot a12 - 4 \cdot x1 \cdot b12) \cdot (-a22 - 2 \cdot x2 \cdot b22)$$

$$\frac{d}{dx2} f2 \rightarrow (-2 \cdot a21 - 4 \cdot x2 \cdot b21) \cdot (-a21 - 2 \cdot x2 \cdot b21) - (4 \cdot pm1 - 4 \cdot c1 - 4 \cdot x1 \cdot a11 - 4 \cdot x1^2 \cdot b11 - 4 \cdot x2 \cdot a21 - 4 \cdot x2^2 \cdot b21) \cdot b21 + (-2 \cdot a22 - 4 \cdot x2 \cdot b22) \cdot (-a22 - 2 \cdot x2 \cdot b22) - (4 \cdot pm2 - 4 \cdot c2 - 4 \cdot x1 \cdot a12 - 4 \cdot x1^2 \cdot b12 - 4 \cdot x2 \cdot a22 - 4 \cdot x2^2 \cdot b22) \cdot b22$$

$$j22 := (-2 \cdot a21 - 4 \cdot x2 \cdot b21) \cdot (-a21 - 2 \cdot x2 \cdot b21) - (4 \cdot pm1 - 4 \cdot c1 - 4 \cdot x1 \cdot a11 - 4 \cdot x1^2 \cdot b11 - 4 \cdot x2 \cdot a21 - 4 \cdot x2^2 \cdot b21) \cdot b21 + (-2 \cdot a22 - 4 \cdot x2 \cdot b22) \cdot (-a22 - 2 \cdot x2 \cdot b22) - (4 \cdot pm2 - 4 \cdot c2 - 4 \cdot x1 \cdot a12 - 4 \cdot x1^2 \cdot b12 - 4 \cdot x2 \cdot a22 - 4 \cdot x2^2 \cdot b22) \cdot b22$$

$$J := \begin{bmatrix} j11 & j12 \\ j21 & j22 \end{bmatrix} \quad J = \begin{bmatrix} 210.4735640532 & -9.5103125326 \\ -9.5103125326 & 2.5012734659 \end{bmatrix}$$

$$J^{-1} = \begin{bmatrix} 0.0057367882 & 0.0218123484 \\ 0.0218123484 & 0.4827310037 \end{bmatrix}$$

$$x_1 := x_0 - J^{-1} \cdot f$$

$$x_0 = \begin{bmatrix} 21 \\ 7 \end{bmatrix} \quad x_1 = \begin{bmatrix} 21.1120920281 \\ 5.8356332328 \end{bmatrix} \quad \begin{bmatrix} x1 \\ x2 \end{bmatrix} := x_1$$

Check Criterion Function Converging:

$$pq1 := c1 + (x1 \cdot a11 + x1^2 \cdot b11) + (x2 \cdot a21 + x2^2 \cdot b21)$$

$$pq2 := c2 + (x1 \cdot a12 + x1^2 \cdot b12) + (x2 \cdot a22 + x2^2 \cdot b22)$$

$$pq := \begin{bmatrix} pq1 \\ pq2 \end{bmatrix} \quad pq = \begin{bmatrix} 429.9057223939 \\ 13.2760315703 \end{bmatrix} \quad \text{OK}$$

$$Esq := (pm1 - pq1)^2 + (pm2 - pq2)^2$$

$$Esq = 0.4773837112$$

$$Esq \rightarrow (pm1 - c1 - x1 \cdot a11 - x1^2 \cdot b11 - x2 \cdot a21 - x2^2 \cdot b21)^2 + (pm2 - c2 - x1 \cdot a12 - x1^2 \cdot b12 - x2 \cdot a22 - x2^2 \cdot b22)^2$$

Iteration Number 2

$$\frac{d}{dx1} Esq \rightarrow (2 \cdot pm1 - 2 \cdot c1 - 2 \cdot x1 \cdot a11 - 2 \cdot x1^2 \cdot b11 - 2 \cdot x2 \cdot a21 - 2 \cdot x2^2 \cdot b21) \cdot (-a11 - 2 \cdot x1 \cdot b11) + (2 \cdot pm2 - 2 \cdot c2 - 2 \cdot x1 \cdot a12 - 2 \cdot x1^2 \cdot b12 - 2 \cdot x2 \cdot a22 - 2 \cdot x2^2 \cdot b22) \cdot (-a12 - 2 \cdot x1 \cdot b12)$$

$$f1 := (2 \cdot pm1 - 2 \cdot c1 - 2 \cdot x1 \cdot a11 - 2 \cdot x1^2 \cdot b11 - 2 \cdot x2 \cdot a21 - 2 \cdot x2^2 \cdot b21) \cdot (-a11 - 2 \cdot x1 \cdot b11) + (2 \cdot pm2 - 2 \cdot c2 - 2 \cdot x1 \cdot a12 - 2 \cdot x1^2 \cdot b12 - 2 \cdot x2 \cdot a22 - 2 \cdot x2^2 \cdot b22) \cdot (-a12 - 2 \cdot x1 \cdot b12)$$

$$\frac{d}{dx2} Esq \rightarrow (2 \cdot pm1 - 2 \cdot c1 - 2 \cdot x1 \cdot a11 - 2 \cdot x1^2 \cdot b11 - 2 \cdot x2 \cdot a21 - 2 \cdot x2^2 \cdot b21) \cdot (-a21 - 2 \cdot x2 \cdot b21) + (2 \cdot pm2 - 2 \cdot c2 - 2 \cdot x1 \cdot a12 - 2 \cdot x1^2 \cdot b12 - 2 \cdot x2 \cdot a22 - 2 \cdot x2^2 \cdot b22) \cdot (-a22 - 2 \cdot x2 \cdot b22)$$

$$f2 := (2 \cdot pm1 - 2 \cdot c1 - 2 \cdot x1 \cdot a11 - 2 \cdot x1^2 \cdot b11 - 2 \cdot x2 \cdot a21 - 2 \cdot x2^2 \cdot b21) \cdot (-a21 - 2 \cdot x2 \cdot b21) + (2 \cdot pm2 - 2 \cdot c2 - 2 \cdot x1 \cdot a12 - 2 \cdot x1^2 \cdot b12 - 2 \cdot x2 \cdot a22 - 2 \cdot x2^2 \cdot b22) \cdot (-a22 - 2 \cdot x2 \cdot b22)$$

$$x_2 := x_1 - J^{-1} \cdot f$$

$$x_1 = \begin{bmatrix} 21.1120920281 \\ 5.8356332328 \end{bmatrix} \quad x_2 = \begin{bmatrix} 21.1279029533 \\ 6.2334054947 \end{bmatrix} \quad \begin{bmatrix} x1 \\ x2 \end{bmatrix} := x_2$$

Check Criterion Function Converging:

$$pq1 := c1 + (x1 \cdot a11 + x1^2 \cdot b11) + (x2 \cdot a21 + x2^2 \cdot b21)$$

$$pq2 := c2 + (x1 \cdot a12 + x1^2 \cdot b12) + (x2 \cdot a22 + x2^2 \cdot b22)$$

$$pq := \begin{bmatrix} pq1 \\ pq2 \end{bmatrix} \quad pq = \begin{bmatrix} 429.988294636 \\ 12.6681893995 \end{bmatrix}$$

$$Esq := (pm1 - pq1)^2 + (pm2 - pq2)^2$$

$$Esq = 0.0060084214$$

$$Esq \rightarrow (pm1 - c1 - x1 \cdot a11 - x1^2 \cdot b11 - x2 \cdot a21 - x2^2 \cdot b21)^2 + (pm2 - c2 - x1 \cdot a12 - x1^2 \cdot b12 - x2 \cdot a22 - x2^2 \cdot b22)^2$$

Iteration Number 3

$$x_3 := x_2 - J^{-1} \cdot f$$

$$x_2 = \begin{bmatrix} 21.1279029533 \\ 6.2334054947 \end{bmatrix} \quad x_3 = \begin{bmatrix} 21.1297139101 \\ 6.2849765489 \end{bmatrix} \quad \begin{bmatrix} x1 \\ x2 \end{bmatrix} := x_3$$

Check Criterion Function Converging:

$$pq1 := c1 + (x1 \cdot a11 + x1^2 \cdot b11) + (x2 \cdot a21 + x2^2 \cdot b21)$$

$$pq2 := c2 + (x1 \cdot a12 + x1^2 \cdot b12) + (x2 \cdot a22 + x2^2 \cdot b22)$$

check:

$$pq := \begin{bmatrix} pq1 \\ pq2 \end{bmatrix} \quad pq = \begin{bmatrix} 429.9998037284 \\ 12.5927969603 \end{bmatrix} \quad \text{OK}$$

$$Esq := (pm1 - pq1)^2 + (pm2 - pq2)^2$$

$$Esq = 0.000001558$$

For further information contact:

Department of Civil and Resource Engineering, School of Engineering
The University of Auckland, Private Bag 92019, Auckland, New Zealand
Telephone: 64-9-373 7599 ext. 8166 or 5715 Facsimile: 64-9-373 7462